Electrostatic Interaction for High Performance Waterborne Coatings

MAIALEN ARGAIZ TAMAYO

SUPERVISORS: PROF. RADMILA TOMOVSKA

DR. MIREN AGIRRE

TESIS DOCTORAL FEBRERO 2022

eman ta zabal zazu

Universidad del País Vasco

Euskal Herriko Unibertsitatea

Electrostatic Interaction for High Performance Waterborne Coatings

Maialen Argaiz Tamayo

Supervised by: **Prof. Radmila Tomovska**

Dr. Miren Aguirre

Chemical Engineering Group

University of the Basque Country UPV/EHU

Donostia-San Sebastián

2022

Aitona eta amona

Acknowledgements – Eskerrak

I would like to express my sincere gratitude to my supervisors Radmila Tomovska and Miren Aguirre for their patience and guidance. This work could never have been achieved without their support. Working under their supervision was a great opportunity for to grow as a chemist and person.

I would like to gratefully thank Dr. Silfredo Bohorquez who provided me the opportunity to join their team as intern and for their support during these four months in Allnex. I would like to thank other members of Allnex for their support and their assistance in paint applications.

I would like to acknowledge the financial support of Industrial Liaison Program in Polymerization in Dispersed Media.

Abstract

Sustainable development is one of the great challenges of the 21st century. Without any doubt, this complex issue must be addressed at many different levels, including producing environmentally friendly waterborne films. However, many industrial polymer production processes relay still on the use of organic solvents, which contributes to increase emission of volatile organic compounds (VOC). Along with environmental concerns, the stringent environmental standards for VOCs emission have been a driving force for replacing processes that use solvents by cleaner water-based ones. Nevertheless, the water-based polymers still present lower mechanical performance than their solvent-based counter products. While from the polymer solution, the films formed after solvent evaporation are perfectly continuous, the film formation process from polymer aqueous dispersions (latexes) is much complex. The polymer chains are enclosed within submicron particles that during the water evaporation have to join through polymer chains interdiffusion. The worst mechanical performance and considerable water sensitivity of waterborne films is directly related to the film formation process and usually is responsible for the lower performance of the films, which slow down the replacement of the solvent-borne coatings by the water-borne ones on the market.

Reinforcement of the soft polymer films by inducing inter-particle physical bonding was an alternative approach towards the improvement on the performance of waterborne coatings.

Among other physical interactions, complexes formed through ionic bonds were highly interesting, owing to the relatively high-energy required to break a single bond. Thus, the main objective of this work was to induce inter-chain or inter-particle ionic complexation in polymer dispersions to produce waterborne coatings and to investigate their effect on the final performance of the polymer film.

To shed a bit of light on the ionic complexation process in oppositely charged latex blends and the ionic bonding effect on the performance of the resulting films, in this work, oppositely charged polymer particles were synthesized by one- (batch) or a two-step (semibatch) emulsion polymerization process of the basic coating formulation made of BA/MMA in 50/50 wt. ratio. The anionic charges were introduced using functional monomers, such as NaSS and IA, whereas DMAEMA and styrenic DABCO salt (DABCO) were employed to introduce cationic charges.

The effect of ionic inter-particle complexation on the final mechanical performance was first investigated, blending NaSS and DMAEMA containing latexes considering two parameters: the surface charge density and the number of particles. Modest improvement for ionic complex material was observed despite the overall level of chain interdiffussion degree (seen by FRET technique) was lower than for the reference material. Regarding the water resistance of the materials, as a general trend, the reference blends showed higher water absorption than the ionic complex materials likely due to the neutralization of the ionic species in the last.

While denser ionic network was achieved owed to the more efficient particle packaging reached by blending oppositely charged particles with different sizes that contributed to increase

the probability of the ionic complexation, further improvement of the film's properties was also achieved, introducing functional monomers containing two charges per molecule (IA and DABCO) within the BA/MMA polymer chains. By more efficient particle packaging, the increased contact between large/small particles contribute to the increase of the ionic bonding points, reinforcing the inter-particle complexes as seen in the tensile test and water uptake tests. Furthermore, introducing functional monomers containing two charges per molecule contribute to increase the ionic bonding points for reinforcing the inter-particle complexes.

The possibility of producing and complexing emulsifier-free cationic waterborne dispersions using a homemade cationic monomer DABCO, characterized with two charges per molecule was investigated. Waterborne dispersions, stabilized by DABCO cationic monomer were synthetized in the absence of emulsifier by seeded semibatch emulsion polymerization process, varying DABCO content and achieving high solids content. Stiffer and less flexible, but less water resistant materials were obtained by increasing the DABCO concentration, likely due to denser reinforcing network created by the polymer chains rich in rigid DABCO, as it was observed in TEM images (honeycomb structure). Afterwards, the ionic complexation of emulsifier-free DABCO dispersions with emulsifier-free NaSS was studied, in which no important differences in mechanical strength of the blend films were detected between non-dialyzed and dialyzed ones, whereas their presence affected slightly the water resistance. Nevertheless, improvements by means of mechanical test and water resistance test could be observed for one of the prepared sample set, likely due to the ionic complex formed.

Finally, the effect of ionic complex in clear- and pigmented-coats performance when blending oppositely charged dispersions was analysed. In the first part of this work, the possibility of using anionic latexes synthetized with two types of polymerizable surfactants (Latemul PD-104 and Hitenil AR-10), with and without addition of MAA functional monomer as potential binders was examined. In the second part, the ionic complexation effect on paint performance when using synthetized anionic resins and commercial cationic resin blend as binders in the formulation was investigated, achieving as a general trend slight improvement in hardness while the other properties were not affected compared to the reference ones.

Laburpena

Garapen iraunkorra XXI. mendeko erronka handietako bat da. Zalantzarik gabe, gai konplexu hau hainbat mailatan jorratu behar da, besteak beste, ingurumena errespetatzen duten uretan oinarritutako filmak sintetizatuz. Tradizionalki, disolbatzailetan oinarritutako filmak merkatua menperatu dute, era berean konposatu organiko hegazkorren (KOH) emisioak areagotuz, eta ondorioz ingurumena kaltetuz. Ingurumen-kezkarekin batera, KOH-en isurketa ekiditeko ingurumen-arau zorrotzak direla eta, uretan oinarritutako filmak merkatuan lerratzen hasi dira. Hala ere, hauek aurkezten dituzten propietateak ahulagoak dira orokorrean. Disolbatzaileetan oinarritutako estalduren kasuan, disolbatzailea lurruntzean kohesio handiko filmak lortzen diren bitartean, uretan oinarritutako dispertsioetatik (latexak) filma eratzeko prozesua askoz konplexuagoa da. Polimero-kateek nanopartikulak osatzen dituzte, eta ura lurruntzean, partikula desberdinetan dauden kateek elkarren artean interdifunditzen dute, katramilatuz eta azkenik film koherente bat lortuz. Orokorrean, uretan oinarritutako filmen propietate mekanikoak baxuagoak eta uraren sentikortasun handia, filmaren eraketa-prozesuarekin erlazionatuta dago. Guzti honek, merkatuan disolbatzaileetan oinarritatuko estalduren ordezkatzea moteltzen duelarik.

Uretan oinarritutako estalduren propietateak hobetzeko aukeretako bat partikulen arteko lotura fisikoen bidez filmak indartzea izan da. Interakzio fisikoen artean, lotura ionikoen bidez

sortutako konplexuak oso interesgarriak ziruditen, lotura bakar bat hausteko behar den energia nahiko altua delako. Beraz, lan honen helburu nagusia uretan oinarritutako estaldurak eratzea da dispertsio partikulen arteko eta partikula osatzen duten kateen arteko konplexazio ionikoa sortuz, eta konplexazio honek filmaren propietateetan duen eragina sakonki ikertzea.

Konplexazio ionikoaren prozesua eta ondorioz, filmen lotura ionikoen efektua ikertzeko, lan honetan, positiboki eta negatiboki kargatutako polimero-partikulak sintetizatu ziren emultsio polimerizazioz, prozesu ez-jarraitu edo erdi-jarraituen bitartez. Lan honetan, BA/MMA monomeroak erabili dira 50/50 pisuan latexen formulazio orokor bezala. Karga ionikoak monomero funtzionalak erabiliz inkorporatu ziren, alde batetik karga anionikoak NaSS eta IA monomeroekin, eta DMAEMA eta DABCO estireniko gatza (DABCO) bestetik karga kationikoak sortzeko.

Lehenik, NaSS eta DMAEMA inkorporatuta dituzten dispertsioekin eratutako filmen arteko konplexazio ionikoa aztertu zen. Nahasketa hauek burutzeko bi parametro hartu ziren kontuan, alde batetik gainazaleko karga-dentsitatea eta bestetik, partikula kopurua. Konplexatutako materialetan kateen arteko difusio-maila (FRET teknikaren bidez analizatuta) erreferentziazko materialetan baino txikiagoa izan arren, propietate mekanikoetan hobekuntza xumea sumatu zen. Materialen urarekiko erresistentziari dagokionez, joera orokor gisa, erreferentziazko nahasteek, konplexatutako materialak baino ur-xurgapen handiagoa erakutsi zuten, espezie ionikoen neutralizazioaren ondorioz.

Tamaina ezberdineko polimero partikulak nahastean, partikulen egitura trinkoagoa lortzen da eta joera hau are eta gehiago hobetzen da kontrako karga duten partikulak nahasteagatik, konplexazio ionikoaren probabilitatea areagotu eta filmaren propietateak hobetzea lortu baitzen. Gainera, filmaren propietateak haratago hobetu ziren, molekula bakoitzeko bi karga dituzten monomero funtzionalak (IA eta DABCO) BA/MMA polimero kateen barnean inkorporatuz. Partikula handien/txikien arteko kontaktua handiagotzeak, lotura ionikoen puntuak areagotzea eragin zuen, egitura trinkoagoa sortuz eta konplexu ionikoa indartuz, trakzio-probetan eta ur testetan ikusi bezala. Gainera, molekula bakoitzeko bi karga dituzten monomero funtzionalak inkorporatzeak, lotura ioniko puntuak handitzea eragin zuen partikulen arteko konplexuak haratago indartuz.

Emultsionatzailerik gabeko ur-dispertsio kationikoak sintetizatzeko eta konplexatzeko aukera ikertu zen, molekula bakoitzeko bi karga dituen DABCO monomero kationiko bat erabiliz. Emultsionatzailearen ezean, DABCO monomero kationikoz egonkortutako ur dispertsioak sintetizatu ziren emultsio polimerizazio prozesu erdi-jarraituaren bitartez, DABCO kontzentrazio ezberdinak erabiliz eta solido-eduki handia lortuz. Material zurrunagoak, baina urarekiko erresistentzia gutxiagokoak lortu ziren, DABCO kontzentrazioarekin txikitzen zihoan heinean. Ondoren, emultsionatzailerik gabeko DABCO dispertsioen konplexazio ionikoa emultsionatzailerik gabeko NaSS partikulekin ikertu zen, non ez ziren desberdintasun nabarmenak detektatu propietate mekanikoei dagokionez nahaste ez-dializatuen eta dializatuen artean. Urarekiko erresistentziari dagokionez, berriz, desberdintasunak nabariagoak izan ziren. Bestalde, konplexatutako zenbait materialetan hobekuntza nabarmenak ikusi ziren propietate

mekanikoei eta urarekiko erresistentziari begira, ziurrenik sortutako konplexu ionikoaren ondorioz.

Azkenik, konplexu ionikoaren eragina formulaturiko pinturetan aztertu zen. Lan honen lehen zatian, bi emultsifikatzaile polimerizagarri (Latemul PD-104 eta Hitenol AR-10) eta MAA monomero funtzionala gehituta eta gehitu gabe sintetizatutako latex anionikoak aglutinatzaile gisa erabiltzeko aukera aztertu zen. Bigarren zatian, konplexazio ionikoaren efektua pinturaren propietateetan ikertu zen, formulazioan aglutinatzaile gisa sintetizatutako erretxina anionikoa eta erretxina kationiko komertzialaren nahastea erabiltzean. Erreferentziarekin alderatuta hobekuntza txikia lortu zen gogortasunari dagokionez, gainerako propietateetan hobekuntzarik detektatu ez zen bitartean.

Table of Contents

List of Acronyms

2-MEP	2-(Methacryloyloxy)ethyl phosphate
AA	Acrylic acid
AAEMA	Aceto acetoxy ethyl methacrylate
AIBA	2,2′-azobis(2-methylpropionamidine) dihydrochloride
AFM	Atomic Force Microscopy
$AgNO_3$	Silver nitrate
AsAc	Ascorbic acid
BA	Butyl acrylate
BdG	Butyl diglycol
BG	Butyl glycol
CHDF	Capilary Hydrodynamic Fractionation
D_2O	Deuterium oxide
dp	Average particle diameter
DABCO	1,4-diazabicyclo[2.2.2]octane
DATB	Dodecyltrimethylammonium bromide
DFT	Density Functional Theory
DLS	Dynamic Light Scattering
DMAEMA	2-(dimethylamino)ethyl methacrylate
DMC	Methacrylate ethyl trimethyl ammonium chloride
DMF	Dimethylformamide
DMSO	Dimethyl sulfoxide
DSC	Differential Scanning Calorimetry
EDL	Electric Double Layer
FF7	Brugolitte FF7
F.M	Functional monomer

FRET	Fluorescence Resonance Energy Transfer
GPC	Gel Permeation Chromatography
H_2O	Water
H-bond	Hydrogen bond
HCl	Hydrochloric acid
IA	Itaconic acid
KOH	Potassium hydroxide
KPS	Potassium persulfate
MAA	Methacrylic acid
mbm	Mol based on main monomers
MEPE	Metallo supramolecular coordination polyelectrolytes
MFFT	Minimum Film Formation Temperature
MMA	Methyl methacrylate
Mw	Weight average molar mass
Na^+	Sodium cation
NaOH	Sodium hydroxide
NH_4^+	Ammonium cation
NH_4OH	Ammonium hydroxide
NNP-A	[1-(4-nitrophenyl)-2pyrrolidinmethyl]-acrylate
NMR	Nuclear Magnetic Resonance
NaSS	Sodium styrene sulphonate
NR_3	Amine group
$NR_4^+X^-$	Ammonium group
PEO	Poly(ethylene oxide)
Phe-MMA	(9-phenanthryl)methyl methacrylate
PPO	Poly(propylene oxide)
PSD	Particle Size Distribution
PVOH	Polyvinyl alcohol
PVP	Polyvinylpyrrolidone
COOH	Carboxylic acid group

S	Styrene
SANS	Small-Angle Neutron Scattering
s.c.	Solids Content
SDS	Sodium Dodecyl Sulfate
SEC	Size Exclusion Chromatography
SO_3H	Sulfonic acid group
SO_4^{2-}	Sulfate
TBHP	Tert-butyl hydroperoxide
TEM	Transmission Electron Microscopy
Tex	Texanol
THF	Tetrahydrofuran
VAc	Vinyl acetate
Vc	Critical volume fraction
VOC	Volatile Organic Compounds
w/o	Water/organic phase
wbm	Weight based on main monomers
wbp	Weight based on polymer
WHPH	Waterborne dispersion free-isocyanate polyurethane
wt	Total weight
ZnO	Zinc oxide

List of Symbols

a_s	Parking area
Đ	Molar mass dispersity
ε_0	Permittivity
$F_{el.}$	Electrostatic Force
ID	Fluorescence decay profile
L	Length
pKa	-log (Disassociation constant)
q_1	Charge 1
q_2	Charge 2
ϕ_{ET}	Quantum efficiency of energy transfer
r	radius
R_{F0}	Föster distance
T	Temperature
T_g	Glass transition temperature
t	Time
τ_D^0	Donor fluorescence lifetime
w (t)	Rate of energy transfer
λ_D	Debye length

Chapter 1. Introduction

1.1. Waterborne coatings and paints

The global market of coatings and paints based on polymers is projected to grow substantially over the period of 2020-2027 owing to the worldwide increasing demand of these products from the construction and automotive sectors for instance.[1,2] Coatings are defined as clear-coat materials that can be found in liquid, paste or powder form, while paints are defined as pigmented products that form opaque dried films when applied to a substrate (ISO 4618). In other words, a paint is a coating enriched with different additives. The main function of these products are on the one hand to ensure the desire appearance, and on the other to protect the surface of the substrate against corrosion or chemical attacks.[3]

In general, paints consist of a polymeric binder, pigments, additives and solvent.[4,5] The binder is formed by a polymeric resin, which forms a matrix to hold the rest of the components together. The polymeric binder is crucial as it imparts adhesion and has a great impact on the final mechanical and barrier properties.[4] Pigments that form the discontinuous phase, provide additional or improved properties to the coating.[6] Pigments can be divided in two categories: functional and extender. Functional pigments are responsible for the colour and opacity of the material, whereas the extenders are used to lower the price of the product by increasing the volume of a given coating.[5] The addition of small amounts of additives (dispersing agent,

coalescence agent, defoamer, thickener…) can greatly improve the physical properties and performance of the material, such as the appearance, hardness, adhesion, corrosion protection or storage stability.[7] All these ingredients are dispersed in a continuous media, which can be organic solvent or water.[5]

Traditionally, coatings have been produced by solution polymerization using high amounts of organic solvents that increases substantially the released amount of volatile organic compounds (VOC) of the product in the atmosphere. Along with the environmental concerns, the stringent environmental standards for emission of VOCs have been a driving force for the replacement of processes that use solvents by cleaner water based ones, namely waterborne coatings.[8–10] In waterborne coatings, the continuous phase is water, meaning that low VOC or even VOC free materials could be obtained.[8–10] The main production method of waterborne polymers is emulsion polymerization.

1.2. Emulsion Polymerization

The polymeric dispersions, often called latexes, are produced by free radical emulsion polymerization in which the monomer is dispersed in the aqueous continuous phase by means of surfactants and it is polymerized producing polymer nanoparticles with an average diameter between 80-300 nm. This technique offers not only environmentally friendly products, but also efficient heat removal. Namely, free radical polymerization is an exothermic process and the water as continuous phase provides a great medium for heat transfer, owing to its low viscosity

and high specific capacity. The main distinctive feature of this process is that it is possible to produce high molecular weight polymer at a high reaction rate owing to radical compartmentalization.[11,12]

The understanding of emulsion process is a key factor for the design of products with tailored properties. The properties of these products are determined by various factors, such as the formulation (monomers, initiator, surfactant, buffer, chain transfer agent and crosslinker) and the process variables (type of reactor, temperature, feeding strategies). The type of process operation (batch, semibatch and continuous) has also a strong impact on the course of the polymerization and product properties. Generally, batch process is applied to polymerize monomers with similar reactivities and low heat generation rate, while semibatch process is more widely used since it offers ability to control the heat transfer during polymerization and the monomer concentration in the reactor, achieving better control of nucleation process and copolymer composition.[11] On the other hand, continuous process is employed for high volume production of emulsion polymers.

In a batch process, monomers, water and emulsifier are charged in the reactor, except the initiator. In most of the formulations, the concentration of surface active species is above their critical micellar concentration, therefore, micelles are created in the system once monomer droplets are stabilized and aqueous media is saturated.[11,13] These micelles are swollen with monomer. The initiation takes place by decomposition of radicals using either thermal or redox initiators. Typically, radicals are formed in the aqueous media, but as they are too hydrophilic

to enter directly into the micelles, they react with the monomer present in the aqueous media forming oligoradicals. These oligoradicals propagate until a point in which they become hydrophobic enough to enter into micelles. Once a radical enters into the micelle, it propagates fast, forming precursor particles. This mechanism is known as heterogeneous nucleation and is characteristic for monomers with low water solubility, as styrene (S).[11] However, in absence of micelles or in case of monomer with higher water solubility, as acrylic acid (AA) and methacrylic acid (MAA) the concentration of these species in water increases. In such case, the oligoradicals grow fast and become insoluble in water. Consequently, the growing chains precipitate in the aqueous phase and the emulsifier present in water is absorbed stabilizing the surface of the precipitate chains and forming a precursor polymer particle. The remaining hydrophilic monomer diffuse fast into the organic phase. This nucleation mechanism is known as homogeneous nucleation.[11] The growth of these precursor polymer particles leads to mature polymer particles. Through the monomer diffusion, the polymerization proceeds and the latex particles become larger and monomer droplets become smaller until they disappear. In the last stages of the polymerization, the monomer inside the polymer particles is consumed.

1.3. Film formation process for waterborne coatings

When the polymer aqueous dispersions made of polymers with glass transition temperature (T_g) lower than room temperature are dried under standard atmospheric conditions, a continuous polymer film is obtained. Nevertheless, films cast from waterborne dispersions still present worst mechanical performance than the solvent-based films. Thus, to

understand what is the main limitation of the films cast from waterborne polymers and which the future challenges are, it is critical to analyse how the latex is transformed into a final film, since the film formation process from waterborne dispersions is completely different than from solvent-based ones. In solvent-borne polymers, a coherent polymer film is obtained through two drying stages. Firstly, the majority of the solvent is evaporated, followed by diffusive evaporation of the remaining solvent which lead to the entanglement of the polymer chains into a tight network.[14] The process is illustrated in Figure 1.1.

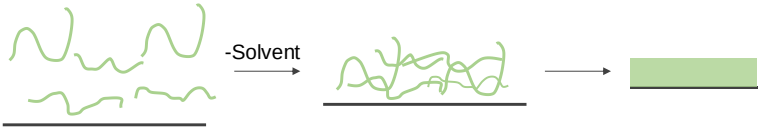

Figure 1.1. Formation of continuous film in solvent-borne polymers.

On the contrary, drying of waterborne dispersions in order to form a coherent polymer film is split in three main steps (Figure 1.2): (I) Water evaporation and ordering of particles, (II) Particle deformation and (III) Coalescence and interdiffusion of polymer chains at particle-particle interfaces. Eventually, film forming steps can overlap. Waterborne dispersion drying process strongly influence the final performance of the polymer film.[15,16] In the following paragraphs, each of these stages will be briefly described.

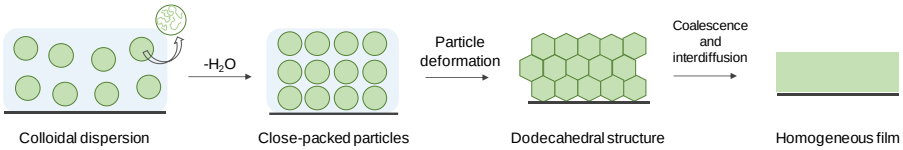

Figure 1.2. Formation of a continuous film from a waterborne colloidal dispersion.

Once the waterborne dispersion is applied onto a substrate, first, the water is evaporated. As water evaporates, the polymer particles get closer to each other up to a point in which they are very close to each other forming a close-packed array with water filled interstices.[17] When the particles are close enough, the water interstitial evaporates and the particles are deformed owing to Van der Waals and capillary forces. This stage is defined by densely packed array in which particles are deformed, but still discrete particles retain their identity.[15,17] At this stage, the film becomes transparent due to the close up of the void spaces. This transition happens above the minimum film formation temperature (MFFT), which corresponds to the lower temperature require to achieve optical transparency. If the temperature at which the dispersion is dried is higher than the MFFT, a cloudy and cracked film is obtained avoiding the deformation process.[16]

The last step is given by the coalescence of the polymer particles, where particle's boundaries disappear reducing the total interfacial area, followed by polymer chains interdiffusion through particle-particle interface. A proper formation of a coherent film is not achieved until the polymer chains from neighbouring particles interdiffused across the particles boundaries, where original particles are no longer distinguishable (Figure 1.3). This last transition occurs above T_g of the polymer.[15,18] It was found that the maximum material's strength is achieved when the interpenetration of the polymer chains is comparable to their radius of gyration.[15]

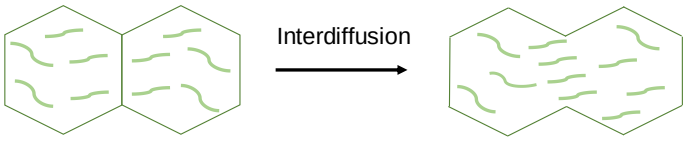

Figure 1.3. Schematic view of polymer chain diffusion between neighbour particles.

From the above discussion, it can be summarized that essentially two requirements are needed for a coherent and strong polymer film. While soft polymer is required for a proper deformation and polymer diffusion, tough polymer is needed to provide the desire mechanical strength.[15,18] These conflicting demands are responsible for lower mechanical performance of the waterborne polymer films and for slowing down the replacement of the solvent-borne coatings by the waterborne ones on the market.

Several approaches have been studied to reinforce the mechanical strength of waterborne coatings, based on either enhancing the diffusion of hard polymer chains or giving additional functionalities to the soft polymer chains. On the one hand, the diffusion of polymer chains can be promoted by addition of plasticizers, which are extensively used in industry.[5,19–21] Incorporation of coalescence agents, initially to soft polymer particles provides the formation of coherent and continuous films. Typically, during film formation process, water together with these compounds are evaporated acquiring hard and non-tacky material.[19,20] Despite traditional coalescent agents, which increase the VOC content in the dispersions, efforts have been devoted to design low VOC dispersions without compromising mechanical performance. As an example, the use of water for an effective hydroplasticization has been reported for certain polymer types.[22,23] Alternatively, diffusivity requirements can be satisfied by blending low T_g and high T_g

polymer latexes[24,25] or developing multiphase systems that combine hard and soft polymer domains within the same polymer particle.[26] In both cases, while hard polymer provides mechanical strength, the soft fraction allows proper polymer chain mobility in order to complete the film formation process. Likewise, in some works polymer nanocomposites with inorganic fillers are combined to obtain improvements in mechanical strength of the final product.[27]

On the other hand, additional functionalities can be introduced to a soft polymer to induce either chemical crosslinking or physical interactions.[28–30] Although chemical crosslinking is widely used in industry, it presents some drawbacks because of the use of toxic chemicals (as isocyanates, aziridines and carbodiimmides) in the self-crosslinking reactions, which put these methods under scrutiny.[5,28,31] Formation of physical (non-covalent) networks (through host-guest interactions, metal-ligand binding, π-π stacking, hydrogen or ionic bonding) appear as an suitable alternative to the chemical crosslinking.[29,30,32]

So far, the use of host-guest interactions has emerged as a new tool for the formation of fibre networks. For example, Dong et al. showed a monomer which had the host moiety in one of the ends of the chains and the guest moiety in the other side.[33] Linear supramolecular polymer chains self-assembled forming a three dimensional (3D) fibre network. These materials showed temperature and pH responsiveness. On the other hand, metal supramolecular coordination polyelectrolytes (MEPEs) have come out as a promising alternative for the fabrication of electrochromic materials showing high performance and fabrication efficiency. These materials gained great interest owing to their potential applications in antiglare mirrors and glasses,

protective eyewear and smart windows for automobiles and buildings.[34–37] A series of MEPEs have been studied based on the redox metal ions Fe, Ru, Co, Ni, Zn, Cu or Pt and ligands such as 1,4- bis(2,2′:6′,2″-terpyridine-4′-yl)benzene (BTPY).[38,39] Nevertheless, approaching towards the topic of interest of this work, a polymeric material with increase mechanical strength and healability has been recently reported. These properties were attributed to the non-covalent π-π stacking interactions between the pyrenyl end-groups of a polyamide and the polyimide chain.[40]

Effect of hydrogen bonding (H-bonding) on reinforcing particle-particle interface has been demonstrated. In one of the reported investigations, the presence of carboxylic groups (-COOH) in styrene-butadiene particles shell led to the formation of H-bonds reinforcing the particle-particle interface.[32] Moreover, recently, it was shown that blend films between an acrylic dispersion containing pyrrolidone groups and tannic acid led to a physical network formed by hydrogen bonding. The polymer film showed improvement in the elastic modulus of the polymeric films, however the network did not hinder the water absorption of the film.[41] These studies demonstrated the positive effect of hydrogen interactions in industrial applications as adhesives and coatings. However, if the energy strength of a single H-bonding is analysed, it can be observed that a lower value (1-167 kJ mol^{-1}) than for other non-covalent interactions as a single ionic bond (50-250 kJ mol^{-1}) has been reported.[42–44] Generally, an energy between 1-167 kJ mol^{-1} is required to break a single hydrogen bond formed between a donor group (alcohol, amine, carboxylic acid and primary amine groups) and an acceptor one (alkyl fluoride, ether, alcohol, amine, ester, carboxylic acid, amide and aldehyde, ketone groups). However, stronger linkage could be also formed using double, triple, or even cuadruple H-bonds, achieving higher

strengths.[45] Thus, the reported improvements together with the energy strength information not only for H-bond, but for ionic interactions, made us think on the effect of the ionic complex formation via single or even, double ionic bond in this work.

Up to now, several works have been published in which the efficiency of ionic interactions between oppositely charged polymers have been demonstrated for different applications, mostly biomedical.[46–49] Focusing on the works developed in the area of polymer dispersions, formation of ionic hydrogen supramolecular network was reported by mixing ammonium moieties coming from isocyanate-free water-dispersable polyurethane dispersion and adipic and citric acid organic molecules, which contain carboxylic acid groups.[50] The resulting material presented enhanced mechanical properties and exhibit self-healing ability. The formation of a percolating ionic network between a dispersion containing MAA (40% solids content, s.c.) and zinc oxide (ZnO) nanoparticles, resulting in a polymer film with improved storage and elastic modulus was reported.[51] Likewise, it was demonstrated that the addition of zinc oxide/potassium hydroxide (ZnO/KOH) inorganic material into a waterborne dispersion containing MAA functional monomer (F.M) (45% s.c.) lead to the formation of an ionic network improving the elastic modulus of the resulting material.[52]

Taking all these works into consideration, it becomes clear that inter-chain or inter-particle ionic complexation of waterborne polymers may be an efficient tool to improve the final performance of the polymer films. In order to understand the basics of the ionic bonding, a

description about this physical (non-covalent) interactions and their physical meaning will be briefly presented in the following section.

1.4. Ionic bonding

Ionic bonding is the electrostatic attraction between negatively charged and positively charged atoms (Figure 1.4).[53,54] Electrons movement from one specie to another cause the formation of species with overall electrical charges. Such species are called ions. While the species with overall negative charge are defined as anions, the ones with overall positive charge are known as cations.

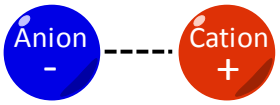

Figure 1.4. Schematic view of ionic bonding between anion and cation atoms.

Ions can be classified depending on the amount of atoms involved in the system, in monoatomic, as Br^- and Na^+, or may consist of two different atoms, as $SO_4^{2-}$and NH_4^+. Additionally, ions may contain more than a few atoms as $HOC_6H_4CO_2^-$ and $(C_4H_9)_4N^+$ or consist of many atoms forming the well-known polyions, which constituted the disassociate part of a polyelectrolyte. In this case, polyelectrolytes may be natural, as protein and nucleic acids, or synthetic, as poly(acrylic acid) or poly(diallyldimethylammonium chloride).[55]

1.4.1. Origin of interfacial charge

The majority of solid surfaces in aqueous solutions acquire some type of electrical charge. Although addition of ionically charged colloids and electrolyte solutions affect colloids stability, the presence of these charged species provide different benefits as it is explain later. Interfaces may become electrically charged by several mechanisms as listed bellow.[53,56]

(1) Preferential solubilization of surface ions, where electrical charges are provided when crystalline materials are sparingly soluble in aqueous media. For instance silver iodide crystals.

(2) Direct ionization of surface groups, where materials containing functional groups are fully ionized and one of the formed ion is bonded chemically to the material (Figure 1.5). Materials which can undergo this mechanism are metal oxides and many polymer latexes containing functional groups like carboxylic and sulfonic acids (-COOH, -SO_3H), amino groups (-NR_3, R=H or an organic group) and quaternary ammonium groups ($-NR_4^+X^-$). The degree of the induced ionization is determined by the pH of the medium and the strength of the acid/base group, which is defined by its disassociation constant (pKa for acids and pKb for basics). Thus, for weak bases and acids as carboxylic and amine groups, their molecular and ionic state is defined by their pKa. Strong acids as sulfonates and sulfuric acid esters present relatively low pKa (around 1) that suppress the possibility of showing these species in their molecular state since the pH of the medium should be lower than 1. Likewise, quaternary ammonium salts show pH independency, offering cationic charged species in the whole pH range.

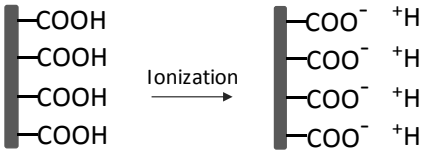

Figure 1.5. Schematic view for ionization of carboxylic acid containing surface.[56]

(3) Substitution of surface ions, where minerals, clays and oxide compounds suffer from isomorphous substitution, meaning that one atom is replaced by another one with a lower valence. For instance, a silicon atom with a valence of +4 in clay might be substitute by aluminium with a valence of +3, resulting in a surface with a negative charge.

(4) Specific ion absorption, where surfaces do not bring charged species, but they are able to adsorb species that provide the expected charge behaviour. For example, the adsorption of ionic surfactant into polymer surfaces is of great relevance in emulsion polymerization technique. In such case, adsorption of anionic surfactant give a negatively charge surface, while cationic surfactant provides a positively charge surface.

(5) Charge deriving from specific surface structure, where structures as kaolinite clay mineral with a chemical composition of $Al_2Si_2O_5(OH)_4$ are cleavage, producing anionic and cationic charged surfaces.

In this work, direct ionization mechanism will be used to obtain electrically charged polymer particles. In order to understand the importance of the formation of charged surfaces

and their activity in colloidal systems, the basics of electrostatic theory is presented in the following section.

1.4.2. Electrostatic theory

The electrostatic interaction is described by Coulomb´s law,[54] which considers the attraction of a cation and anion atom. This law describes mathematically the electrostatic force ($F_{el.}$) between opposite charges (q_1 and q_2) in vacuum. According to this law, $F_{el.}$ is directly proportional to the number of charges around the particles (q_1 and q_2) and inversely proportional to the distance between particles (r), as shown in equation 1.1. For two charges of opposite sign, F_{el} will be negative, thus the interaction will be attractive, while for charges of equal sign, $F_{el.}$ will be positive forming a repulsive interaction (Figure 1.6).

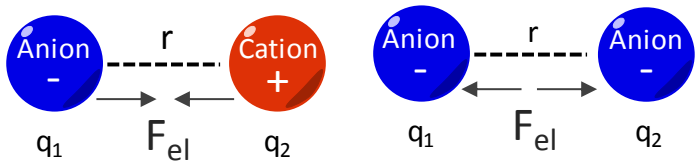

(a) (b)

Figure 1.6. Schematic representation of Coulomb´s law for (a) attractive interactions and (b) repulsive interactions.

$$F_{el.} = \frac{q_1 q_2}{4\pi\varepsilon_0} \cdot \frac{1}{r^2} \quad \text{(eq. 1.1)}$$

However, Coulomb´s law can be just applied for an isolated specie, while in a real situation all the ions involve in the system should be considered. For instance, the presence of charged

particles with the same or different surface sign, polyelectrolytes and free ions present in solution. Thus, in order to apply Coulomb´s law to the electrolytes and colloids solutions, Boltzmann´s distribution should be taken into account which describes the counter ions needed to balance the charge of the surface. The region of excess of the opposite sign in the vicinity of a charged surface is described as the ionic environment or charge cloud. In colloids science, the Debye-Huckel theory is applied to determine the ionic environment around polymer particles, known as electrical double layer (EDL).[53,56,57] This concept is illustrated in Figure 1.7, where a particle possess evenly distributed charges that are balanced by the total opposite charge, the counterions in the EDL. These counterions are distributed with a gradient of concentration starting from the surface, which decreases with the distance from the particle center and decays through the bulk. The thickness of this EDL is characterized by the Debye length.

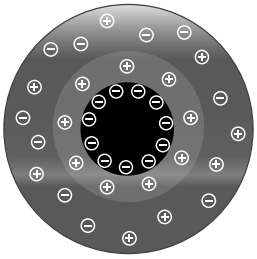

Figure 1.7. Schematic view of electric double layer (EDL) in colloid system.

In a colloidal system, particles with the same charge repel each other upon approaching, owing to the EDL. Van der Waals forces tend to make contact between particles at very short distances. These forces, especially repulsive forces coming from EDL are sensitive to parameters such as number of charges around the particles, electrolyte concentration and pH and the

valence of ions involve in the system. Thus, the increase of any of these parameters might diminish the thickness of the EDL, destabilizing the system.

The control of the mentioned parameters is a key point since blending of oppositely charged particles will strongly affect the balance of the repulsive and attractive forces, likely shifting the balance to attractive ones, therefore, destabilizing the blended system. This means that the selection of the ionic species and the incorporation of these species onto the polymer particles is one of the most important factors that control the parameters affecting the EDL. Hence, in the following paragraphs the most common monomers used in emulsion polymerization as well as the different ionic species will be discussed.

1.5. Common monomers and functional monomers used in emulsion polymerization

Waterborne dispersions are produced using a wide range of monomers depending on the end use application.[11] Vinyl acetate (VAc) show a T_g of 30 °C, meaning that a brittle material will be formed when a VAc homopolymer is dried at room temperature (25 °C). Additionally, it may suffer from hydrolysis once the film is in contact with moisture areas and alkaline substrates as masonry, being inefficient for exterior applications. An alternative use for exterior decorative paints is the copolymerization of VAc with n-butyl acrylate (BA), ethylene or VeoVa (a vinyl ester of versaric acid), which not only allows a proper film formation due to the reduce in the T_g of the film, but also improves the water sensitivity and alkali resistance owing to the higher hydrophobicity of these compounds.[58]

Styrene (S) containing polymers offer water resistance due to its hydrophobicity. However, it provides formation of rigid particles which do not allow good film formation at room temperature owing to its high T_g (100 °C). This is why addition of softer monomers as butadiene and acrylates, significantly improves the film formation process. In fact, styrene-butadiene copolymers are produced varying their ratios in order to balance the performance of the material. While high content of S will produce tough and durable material, low content will produce more flexible and sticky material. However, polymers containing S are not very used for exterior applications owing to their poor resistant to ultraviolet light due to the aromatic rings, leading to the degradation of the coating once it is exposed to sunlight for instance.[59]

Acrylic polymer family, which consists of esters of acrylate and methacrylate, is widely used in coating industry due to the ability to tune the glass transition temperature (T_g), hydrophobicity properties and morphology design at a relatively low cost.[59] Varying the composition of monomers that show unlike T_g, they cover a wide range of application areas, as adhesives (T_g = -60°C - -25 °C), decorative paints (T_g = 10 - 40 °C) and general industrials coatings (T_g = 35 - 40 °C). Contrary to poly(vinyl acetate) and poly(styrene), waterborne acrylic systems are commonly used for exterior applications owing to their resistant to ultraviolet degradation and low water sensitivity. The most common monomers of this family are methyl methacrylate (MMA) and BA, which show T_g values of 106 °C and -56 °C, respectively.[59] For a common decorative paint formulation, BA/MMA (1/1 weight ratio) is polymerized. Owing to the characteristic that acrylic monomers show and specially the well-studied BA/MMA

combination, these two acrylic monomers were selected as the main monomers to polymerize by emulsion polymerization.

Regarding the ionic species, in the last decades, two main pathways have been used to incorporate these species onto waterborne polymer particles synthesized by emulsion polymerization: (1) ionic initiators, monomers and polymerizable emulsifiers that are able to covalently bond onto polymer particles; or (2) ionic species that adsorb onto polymer particles, as surfactants. In this work, attention has been focused on the incorporation of ionic monomers (functional monomers). For example, in the literature, it has been demonstrated that functional monomer's incorporation into a BA/MMA system provides not only colloidal stabilization[60,61], but also improves mechanical performance.[62,63] However, there are some works in which have been demonstrated that the addition of functional ionic monomers affects negatively the water sensitivity.[63,64]

The most common anionic monomers to synthetized anionically charged polymer particles are the ones containing carboxylic groups,[65,66,67] phosphates[68] and sulphonates,[66,69,70] while cationically charged polymer particles have been polymerized using cationic monomers, mainly containing amine groups.[71,72]

1.5.1. Anionic functional monomers

Carboxylic acid containing monomers are widely used in waterborne dispersions. The most common acids used are AA, MAA and itaconic acid (IA). The main differences between MAA

and AA with IA is their chemical structure, the first two owe one carboxylic group per molecule, whereas IA contains two carboxylic groups (see Figure 1.8). The deprotonation of the carboxylic group leads to a strong charge repulsion in waterborne dispersions, stabilizing efficiently the colloidal system. As mentioned in the ionic bonding section, the extent of the ionization at different pH values can be characterized by measuring the pKa. While AA and MAA show a unique pka around 4.25 and 4.5, respectively, IA presents two pKas (3.85 and 5.45).[73] This means that at pH lower than their respective pKa values, the acid losses its ionic state. However, at pH higher than pKa, the acids are found in a disassociated state, providing ionic character and stabilizing the polymer particles.[66] It is postulated that the partition of the mentioned anionic monomers between the water phase, the organic phase and the interface between aqueous/organic phase (w/o) is strongly dependent on the pH of the medium, the reactivity ratios and the polymerization process (batch or semibatch). On the one hand, the partition coefficient strongly depends on the degree of ionization as at low pH, these species are in its molecular state or non-dissociated formed, while at higher pH than their pKa, the carboxylic groups are in their ionic state, increasing the affinity to water.[74,75] On the other hand, higher water solubility of the functional monomers might also contribute to lower incorporation into the main monomers as larger amount of oligomers are polymerized in aqueous phase.[73]

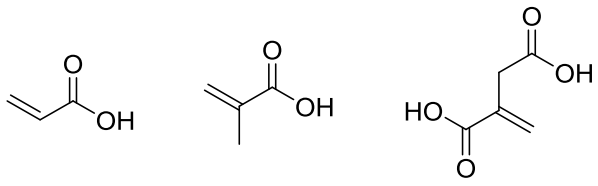

(a) (b) (c)

Figure 1.8. Chemical structure for (a) acrylic acid, (b) methacrylic acid and (c) itaconic acid anionic functional monomer.

The addition of a phosphate monomer as SIPOMER PAM100 (Figure 1.9) into BA/MMA/MAA/AAEMA latex did not have an effect on kinetics, while the gel fraction increased with phosphate monomer content.[76] In addition, the copolymerization of a monomer containing phosphate group (as 2-(Methacryloyloxy)ethyl phosphate, 2-MEP) with BA/MMA have been also studied (Figure 1.9), obtaining 50-60% incorporation of 2-MEP onto particles, and the remaining species were found in the aqueous phase.[68]

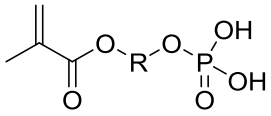

Figure 1.9. Chemical structure for SIPOMER PAM100.

As for sulfonates, recently, NaSS (Figure 1.10) copolymerization with BA and MMA in free radical emulsion polymerization was deeply studied by S. Bilgin et al.[63] They reported an emulsifier-free seeded semibatch emulsion polymerization process for high incorporation of NaSS (60%) onto the polymer particles, while the remaining species were found in the aqueous phase.

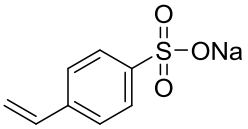

Figure 1.10. Chemical structure for sodium styrene sulfonate.

While carboxylic groups might be interesting due to their ionic/molecular state control by a simple pH change, the high incorporation of phosphonate methacrylate monomers and NaSS makes these groups highly attractive for producing charged particles with high surface charge density. The performance of the materials containing the described functionalities was also examined in order to have a broader view. It was showed that the presence of MAA copolymerized with BA had a low effect on gel content, but significant effect on the film properties: stronger films measured from creep tests and increase peel and tack adhesion.[74] Furthermore, increased viscosity of paint formulation was reported owing to AA or MAA in copolymerization with BA/MMA system.[60] Nevertheless, it was demonstrated that the polymer films containing carboxylic acid groups presented significant water sensitivity.[64] On the other hand, the established chemical interactions between the phosphate groups with the metal surface enhanced the adhesion properties of the film toward the substrate. Additionally, it was found that the presence of phosphate functional groups not only impart strong adhesion, but also anticorrosion properties and scrub resistance.[68,76,77] In the case of NaSS incorporation into BA/MMA, owing to the presence of the phenyl group on NaSS chemical structure, the mechanical properties of the polymeric films were considerably improved. However, the water up-take increased sharply with NaSS concentration up to a point in which the integrity of the polymer film was lost, due to the large amount of water-soluble oligomers.[63]

1.5.2. Cationic functional monomers

During the last decades, attention have been focused on the synthesis of cationic latexes by emulsion polymerization[72,78] owing to the promising applications in the preparation of organic-inorganic composite materials, self-assemblies and biomedical materials.[79,80] The first studies in the open literature of cationically charged particles were published in 1970s by Breitenbatch et. al.[81,79] They showed the emulsion copolymerization of S and VAc in the presence of 2,2′-azobis(2-methylpropionamidine) dihydrochloride (AIBA) cationic initiator.

There are mainly two different types of cationic monomers: pH dependent or pH independent ones. On the one hand, weak amines can be found, and their cationic state depends on the pH. On the other hand, there are the quaternary ammonium salts, which are strong bases, and do not have pH dependency, offering cationic charged species in the whole pH range. Some common examples of these two main families are illustrated in Figure 1.11.

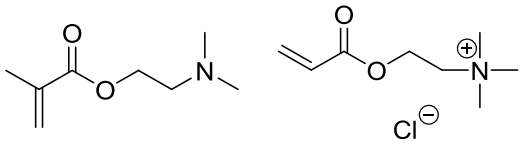

(a) (b)

Figure 1.11. Chemical structure for cationic monomers (a) 2-(dimethylamino)ethyl methacrylate (b) [2-(Acryloyloxy)ethyl]trimethylammonium chloride.

Regarding the cationic dispersions synthetized using pH dependent cationic monomers, in most of the cases lower solids content than 25% have been reported.[82–85] Even though, Sakoia et al. reached high solids content (49%), obtaining an emulsifier-free cationic latex using 2-

(dimethylamino)ethyl methacrylate (DMAEMA) as the cationic monomer[86], they reported that the number of particles were not reproducible. As for pH independent monomers, low solids content latex were reported as well.[87,88] Nonetheless, Liu et al. reported the copolymerization of styrene with 1,2-dimethyl-5-vinylpyridinium methyl sulfate and 1-ethyl 2-methyl 5-vinylpyridinium bromide reaching 30-35% solids contents.[89] Thus, tertiary amine groups ionic/molecular state may be controlled, but not ammonium group ones, which should be taken into consideration for selection of the cationic monomer for future studies.

Unfortunately, industrial applications of these latexes as coatings and adhesives have scarcely been studied in the literature, mainly due to the low solids content for such application. There are several examples in patent literature, where cationic latexes were used as binders for decorative coating application,[90,91] nevertheless, stabilized with conventional surfactants. Rheenen et al. designed a coating containing cationic latex binder that exhibited enhance adhesion to anionic substrates together with stain blocking properties.[90] The cationic latex was synthetized by using amine-functional, ethylenically unsaturated monomers and non-ionic or cationic surfactant. Sheetz et al. prepared stable paints containing a cationic binder which show desirable adhesives properties[91]. The cationic functionally was obtained with an acid protonated amine or a quaternary ammonium functionality, and the particles were stabilized by non-ionic or amphoteric surfactants. Moreover, a water based cationic epoxy ester type binder was reported to give very good corrosion properties.[92] Cationically stabilized epoxy resins were obtained in two-step process: first, aromatic or aliphatic epoxide reacted with an aliphatic amine

to form the epoxy-amine, which are neutralized and further reacted with an epoxy in aqueous dispersion.

To sum up, the works performed employing functional monomers exhibit overall improve colloidal stability as well as enhance mechanical performance of the polymer films. However, clearly, the presence of these species increased the water sensitivity of the materials, limiting their use in exterior applications, which will be one of the main challenges of this work.

1.6. Motivation and objective of the thesis

In light of the foregoing, it can be summarized that the mechanical strength of waterborne coatings might be greatly improved by introducing interactions between the individual particles within the polymer films, such as non-covalent or physical interactions. Clearly, complexes formed through ionic bonds are highly interesting, owing to the relatively high-energy required to break a single bond. In waterborne dispersions, two approaches might be used to induce ionic complexation. On the one hand, blending of oppositely charged particles with water soluble molecules or polymer chains, and on the other hand, blending of oppositely charged dispersions. In any of the cases, ionically charged polymer particles or even polymer chains should be designed.

Therefore, the main objective of this work is to induce inter-chain or inter-particle ionic complexation in polymer dispersions for production of waterborne coatings and to investigate their effect on the final performance of the polymer film.

For this purpose, a conventional coating formulation made of BA/MMA in 50/50 weight ratio was used through this study, in which the anionic charges were introduced by use of functional monomers, such as NaSS and IA, whereas DMAEMA and styrenic DABCO salt (DABCO) were employed to introduce cationic charges.

The interest for IA and DMAEMA functional monomers comes from the pH dependence of their charged state, which may help to control their protonated state when blending with pH independent or low pKa species. Furthermore, IA was selected owing to the presence of two carboxylic groups present within the molecule. NaSS was selected due to the high incorporation of this monomer into BA/MMA, affecting positively the performance of the polymer film. DABCO cationic monomer was chosen owing to its chemical structure, where two cationic charges per molecule were presented.

1.7. Outline of the thesis

The content of this thesis is divided in 7 chapters being the first one a brief introduction and the motivation of this work.

In **Chapter 2**, BA/MMA latexes were copolymerized with functional monomers such as NaSS and DMAEMA by emulsion polymerization. Blends were prepared and the effect of ionic inter-particle complexation on the final mechanical and water absorption performance was investigated. The extent of chain interdiffusion was analysed by Fluorescence Resonance Energy Transfer (FRET).

Chapter 3 describes the synthesis of BA/MMA latexes using again NaSS and DMAEMA as ionic monomers, but particles with different sizes were prepared. The effect that the particle size may have in the inter-particle complexation together with the particle packed efficiency were investigated.

In **Chapter 4**, BA/MMA latexes were synthesized using functional monomers with two charges per molecule in order to increase the surface charge density without increasing of the quantity of the functional monomer. The effect of ionic complexation on the final performance of the polymer film was examined.

In **Chapter 5,** emulsifier-free emulsion polymerization of BA/MMA stabilized with DABCO cationic monomer is described. The effect of the cationic monomer concentration on kinetics and final performance of the film was studied. Finally, blends between emulsifier-free DABCO and NaSS were performed in order to investigate the final performance of the polymer films.

Chapter 6 has been developed in collaboration with Allnex Company (The Netherlands) under the supervision of Dr. Silfredo Bohorquez. In this chapter the effect of electrostatic interactions on paints performance was examined.

Finally, in **Chapter 7** the most relevant conclusions of this thesis are summarized.

At the beginning of the manuscript, the **Acronyms** and **Symbols** are listed. A detailed description of the main experimental procedures as latex synthesis, latex characterization techniques, polymer films characterization and the characterization and application methods of

the clear- and pigmented-coats are given in **Appendix I** and **Appendix II**. In **Appendix III**, the most important aspects of FRET analysis are described. In **Appendix VI** the surface analysed performed by Atomic Force Microscopy (AFM) for Chapter 3 can be found and in **Appendix V**, DABCO monomer synthesis and features are presented. Finally, in **Appendix VI** some of the results obtained during the internship in Allnex Company are summarized.

1.8. References

(1) Research, G. V. Paints & Coatings Market Size, Share & Trends Analysis Report By Product (Powdered, Solvent-Borne), By Material (Acrylic, Epoxy), By Application (Architectural & Decorative, Non Architectural), And Segment Forecasts, 2020 - 2027; 2020.

(2) Paints & Coatings Market by Resin (Acrylic, Alkyd, Epoxy, Polyurethane, Polyester), Technology (Waterborne, Solventborne, Powder), Application (Architectural [Residential, Non-Residential], Industrial), and Region - Global Forecasts to 2024; 2019.

(3) Goldschmidt, A.; Streitberger, H.-J. *BASF Handbook Basics of Coating Technology*, Network.; Hannover, Germany, 2007.

(4) Karger-Kocsis, J. *Paints, Coatings and Solvents*; 1994; Vol. 51. https://doi.org/10.1016/0266-3538(94)90094-9.

(5) Müller, B.; Poth, U. *Coatings Formulation: An International Textbook*; Vincentz Network: Hannover, Germany, 2011.

(6) Alvarez, V.; Paulis, M. Effect of Acrylic Binder Type and Calcium Carbonate Filler Amount on the Properties of Paint-like Blends. *Prog. Org. Coatings* **2017**, *112* (May), 210–218. https://doi.org/10.1016/j.porgcoat.2017.07.023.

(7) Heilen, W. *Additives for Waterborne Coatings*; 2014.

(8) European Commission. *Screening Study to Identify Reductions in VOC Emissions Due to the Restrictions in the VOC Content of Products*; Brussels, 2002.

(9) Directive 2004/42/CE of the european parliament and of the council. *Official Journal of the European Union*; 2004.

(10) Sherman, J.; Chin, B.; Huibers, P. D. T.; Garcia-Valls, R.; Hatton, T. A. Solvent Replacement for Green Processing. *Environ. Health Perspect.* **1998**, *106*, 253–271.

(11) Barandiaran, M. J., De la Cal, J. C., Asua, J. M. *Polymer Reaction Engineering*; J.M.Asua, Ed.; Blackwell: Oxford, 2007.

(12) Asua, J. M. Emulsion Polymerization: From Fundamental Mechanisms to Process Developments. *J. Polym. Sci. Part A Polym. Chem.* **2004**, *42* (5), 1025–1041. https://doi.org/https://doi.org/10.1002/pola.11096.

(13) Thickett, S. C.; Gilbert, R. G. Emulsion Polymerization: State of the Art in Kinetics and Mechanisms. *Polymer (Guildf).* **2007**, *48* (24), 6965–6991. https://doi.org/10.1016/j.polymer.2007.09.031.

(14) Swartz, N. A.; Clare, T. L. Understanding the Differences in Film Formation Mechanisms of Two Comparable Solvent Based and Water-Borne Coatings on Bronze Substrates by Electrochemical Impedance Spectroscopy. *Electrochim. Acta* **2012**, *62*, 199–206. https://doi.org/10.1016/j.electacta.2011.12.015.

(15) Keddie, J. L.; Routh, A. F. *Fundamental of Latex Film Formation*; Springer laboratory: Netherlands, 2010.

(16) Winnik, M. . Latex Film Formation. *Polym. News* **1977**, *3* (4), 194–203. https://doi.org/10.1016/S1359-0294(97)80026-X.

(17) Steward, P. A.; Hearn, J.; Wilkinson, M. C. An Overview of Polymer Latex Film Formation and Properties. *Adv. Colloid Interface Sci.* **2000**, *86* (3), 195–267. https://doi.org/10.1016/S0001-8686(99)00037-8.

(18) Keddie, J. L. Film Formation of Latex. *Mater. Sci. Eng.* **1997**, *21* (97), 101–170.

(19) Schroeder, W. F.; Liu, Y.; Tomba, J. P.; Soleimani, M.; Lau, W.; Winnik, M. A. Effect of a Coalescing Aid on the Earliest Stages of Polymer Diffusion in Poly(Butyl Acrylate-Co-Methyl Methacrylate) Latex Films. *Polymer (Guildf).* **2011**, *52* (18), 3984–3993. https://doi.org/10.1016/j.polymer.2011.06.028.

(20) Barbosa, J. V.; Veludo, E.; Moniz, J.; Mendes, A.; Magalhães, F. D.; Bastos, M. M. S. M. Low VOC Self-Crosslinking Waterborne Acrylic Coatings Incorporating Fatty Acid Derivatives. *Prog. Org. Coatings* **2013**, *76* (11), 1691–1696. https://doi.org/10.1016/j.porgcoat.2013.07.016.

(21) Jiang, S.; Van Dyk, A.; Maurice, A.; Bohling, J.; Fasano, D.; Brownell, S. Design Colloidal Particle Morphology and Self-Assembly for Coating Applications. *Chem. Soc. Rev.* **2017**, *46* (12), 3792–3807. https://doi.org/10.1039/c6cs00807k.

(22) Tsavalas, J. G.; Sundberg, D. C. Hydroplasticization of Polymers: Model Predictions and Application to Emulsion Polymers. *Langmuir* **2010**, *26* (10), 6960–6966. https://doi.org/10.1021/la904211e.

(23) Dron, S. M.; Paulis, M. Tracking Hydroplasticization by Dsc: Movement of Water Domains Bound to Poly(Meth)Acrylates during Latex Film Formation. *Polymers (Basel).* **2020**, *12* (11), 1–19. https://doi.org/10.3390/polym12112500.

(24) Feng, J.; Winnik, M. A.; Shivers, R. R.; Clubb, B. Polymer Blend Latex Films: Morphology and Transparency. *Macromolecules* **1995**, *28* (23), 7671–7682. https://doi.org/10.1021/ma00127a013.

(25) Akhmatskaya, E.; Asua, J. M. Dynamic Modeling of the Morphology of Latex Particles with in Situ Formation of Graft Copolymer. *J. Polym. Sci. Part A Polym. Chem.* **2012**, *50* (7), 1383–1393. https://doi.org/10.1002/pola.25904.

(26) Limousin, E.; Ballard, N.; Asua, J. M. Soft Core–Hard Shell Latex Particles for Mechanically Strong VOC-Free Polymer Films. *J. Appl. Polym. Sci.* **2019**, *136* (23), 1–12. https://doi.org/10.1002/app.47608.

(27) Crosby, A. J.; Lee, J.-Y. Polymer Nanocomposites: The "Nano" Effect on Mechanical Properties. *Polym. Rev.* **2007**, *47* (2), 217–229. https://doi.org/10.1080/15583720701271278.

(28) Tillet, G.; Boutevin, B.; Ameduri, B. Chemical Reactions of Polymer Crosslinking and Post-Crosslinking at Room and Medium Temperature. *Prog. Polym. Sci.* **2011**, *36* (2), 191–217. https://doi.org/10.1016/j.progpolymsci.2010.08.003.

(29) Lehn, J.-M. Supramolecular Polymer Chemistry - Scope and Perspective. *Polym. Int.* **2002**, *51* (10), 825–839. https://doi.org/10.1002/pi.852.

(30) Savyasachi, A. J.; Kotova, O.; Shanmugaraju, S.; Bradberry, S. J.; Ó'Máille, G. M.; Gunnlaugsson, T. Supramolecular Chemistry: A Toolkit for Soft Functional Materials and Organic Particles. *Chem* **2017**, *3* (5), 764–811. https://doi.org/10.1016/j.chempr.2017.10.006.

(31) Lorke, S.; Müller, U.; Meissl, R.; Brüggemann, O. Covalent Cross-Linking of Polymers at Room Temperature. *Int. J. Adhes. Adhes.* **2019**, *91*, 150–159. https://doi.org/10.1016/j.ijadhadh.2019.03.011.

(32) Richard, J.; Maquet, J. Dynamic Micromechanical Investigations into Particle/Particle Interfaces in Latex Films. *Polymer (Guildf).* **1992**, *33* (19), 4164–4173. https://doi.org/10.1016/0032-3861(92)90622-4.

(33) Dong, S.; Luo, Y.; Yan, X.; Zheng, B.; Ding, X.; Yu, Y.; Ma, Z.; Zhao, Q.; Huang, F. A Dual-Responsive Supramolecular Polymer Gel Formed by Crown Ether Based Molecular Recognition. *Angew. Chemie - Int. Ed.* **2011**, *50* (8), 1905–1909. https://doi.org/10.1002/anie.201006999.

(34) Pai, S.; Moos, M.; Schreck, M. H.; Lambert, C.; Kurth, D. G. Green-to-Red Electrochromic Fe(II) Metallo-Supramolecular Polyelectrolytes Self-Assembled from Fluorescent 2,6-Bis(2-Pyridyl)Pyrimidine Bithiophene. *Inorg. Chem.* **2017**, *56* (3), 1418–1432. https://doi.org/10.1021/acs.inorgchem.6b02496.

(35) Niklasson, G. A.; Granqvist, C. G. Electrochromics for Smart Windows: Thin Films of Tungsten Oxide and Nickel Oxide, and Devices Based on These. *J. Mater. Chem.* **2007**, *17* (2), 127–156. https://doi.org/10.1039/b612174h.

(36) Han, F. S.; Higuchi, M.; Kurth, D. G. Metallo-Supramolecular Polymers Based on Functionalized Bis-Terpyridines as Novel Electrochromic Materials. *Adv. Mater.* **2007**, *19* (22), 3928–3931. https://doi.org/10.1002/adma.200700931.

(37) Higuchi, M. Stimuli-Responsive Metallo-Supramolecular Polymer Films: Design, Synthesis and Device Fabrication. *J. Mater. Chem. C* **2014**, *2* (44), 9331–9341. https://doi.org/10.1039/c4tc00689e.

(38) Hu, C. W.; Sato, T.; Zhang, J.; Moriyama, S.; Higuchi, M. Multi-Colour Electrochromic Properties of Fe/Ru-Based Bimetallo- Supramolecular Polymers. *J. Mater. Chem. C* **2013**, *1* (21), 3408–3413. https://doi.org/10.1039/c3tc30440j.

(39) Hossain, M. D.; Sato, T.; Higuchi, M. A Green Copper-Based Metallo-Supramolecular Polymer: Synthesis, Structure, and Electrochromic Properties. *Chem. - An Asian J.* **2013**, *8* (1), 76–79. https://doi.org/10.1002/asia.201200668.

(40) Burattini, S.; Colquhoun, H. M.; Fox, J. D.; Friedmann, D.; Greenland, B. W.; Harris, P. J. F.; Hayes, W.; MacKay, M. E.; Rowan, S. J. A Self-Repairing, Supramolecular Polymer System: Healability as a Consequence of Donor-Acceptor π-π Stacking Interactions. *Chem. Commun.* **2009**, No. 44, 6717–6719. https://doi.org/10.1039/b910648k.

(41) Jiménez, N.; Ballard, N.; Asua, J. M. Hydrogen Bond-Directed Formation of Stiff Polymer Films Using Naturally Occurring Polyphenols. *Macromolecules* **2019**, *52* (24), 9724–9734. https://doi.org/10.1021/acs.macromol.9b01694.

(42) Faul, C. F. J.; Antonietti, M. Ionic Self-Assembly: Facile Synthesis of Supramolecular Materials. *Adv. Mater.* **2003**, *15* (9), 673–683. https://doi.org/10.1002/adma.200300379.

(43) Vapaavuori, J.; Bazuin, C. G.; Priimagi, A. Supramolecular Design Principles for Efficient Photoresponsive Polymer–Azobenzene Complexes. *J. Mater. Chem. C* **2018**, *6* (9), 2168–2188. https://doi.org/10.1039/c7tc05005d.

(44) Gastone Gilli and Paola Gillli. *The Nature of the Hydrogen Bond*; Oxford University Press: New York, 2009.

(45) Wilson, A. J. Non-Covalent Polymer Assembly Using Arrays of Hydrogen-Bonds. *Soft Matter* **2007**, *3* (4), 409–425. https://doi.org/10.1039/b612566b.

(46) Han, L.; Mao, Z.; Wuliyasu, H.; Wu, J.; Gong, X.; Yang, Y.; Gao, C. Modulating the Structure and Properties of Poly(Sodium 4-Styrenesulfonate)/ Poly(Diallyldimethylammonium Chloride) Multilayers with Concentrated Salt Solutions. *Langmuir* **2012**, *28* (1), 193–199. https://doi.org/10.1021/la2040533.

(47) Izumrudov, V. A.; Kharlampieva, E.; Sukhishvili, S. A. Multilayers of a Globular Protein and a Weak Polyacid: Role of Polyacid Ionization in Growth and Decomposition in Salt Solutions. *Biomacromolecules* **2005**, *6* (3), 1782–1788. https://doi.org/10.1021/bm050096v.

(48) Schneider, A.; Vodouhe, C.; Ludovic, R.; Francius, G.; Le Guen, E.; Schaaf, P.; Voegel, J.-C.; Frisch, B.; Picart, C. Multifunctional Polyelectrolyte Multilayer Films: Combining Mechanical Resistance, Biodegradability and Bioactivity. *Biomacromolecules* **2007**, *8* (1), 139–145. https://doi.org/10.1021/bm060765k.

(49) Chluba, J.; Voegel, J.-C.; Decher, G.; Erbacher, P.; Schaaf, P.; Ogier, J. Peptide Hormone Covalently Bound to Polyelectrolytes and Embedded into Multilayer Architectures Conserving Full Biological Activity. *Biomacromolecules* **2001**, *2* (3), 800–805. https://doi.org/10.1021/bm015529i.

(50) Bossion, A.; Olazabal, I.; Aguirresarobe, R. H.; Marina, S.; Martín, J.; Irusta, L.; Taton, D.; Sardon, H. Synthesis of Self-Healable Waterborne Isocyanate-Free Poly(Hydroxyurethane)-Based Supramolecular Networks by Ionic Interactions. *Polym. Chem.* **2019**, *10* (21), 2723–2733. https://doi.org/10.1039/c9py00439d.

(51) Pinprayoon, O.; Groves, R.; Lovell, P. A.; Tungchaiwattana, S.; Saunders, B. R. Polymer Films Prepared Using Ionically Crosslinked Soft Core-Shell Nanoparticles: A New Class of Nanostructured Ionomers. *Soft Matter* **2011**, *7* (1), 247–257. https://doi.org/10.1039/c0sm00447b.

(52) Musa, M. S.; Milani, A. H.; Shaw, P.; Simpson, G.; Lovell, P. A.; Eaves, E.; Hodson, N.; Saunders, B. R. Tuning the Modulus of Nanostructured Ionomer Films of Core-Shell Nanoparticles Based on Poly(: N -Butyl Acrylate). *Soft Matter* **2016**, *12* (39), 8112–8123. https://doi.org/10.1039/c6sm01563h.

(53) Myers, D. *Surfaces, Interfaces, and Colloids*; John Wiley & Sons: New York, 1999.

(54) Pauling, L. The Nature of the Chemical Bond and the Structure of Molecules and Crystals: An Introduction to Modern Structural Chemistry. *Journal of the American Chemical Society*. New York 1960, pp 4121–4121. https://doi.org/10.1021/ja01500a088.

(55) Nagasawa, M. *Physical Chemistry of Polyelectrolyte Solutions*; John Wiley & Sons, 2015; Vol. 53.

(56) Masliyah, J. H.; Bhattacharjee, S. *Electrokinetic and Colloid Transport Phenomena*; 2005. https://doi.org/10.1002/0471799742.

(57) Ohshima, Hiroyuki & Furusawa, K. *Electrical Phenomena at Interfaces: Fundamentals, Measurements and Applications*; Taylor & Francis.

(58) Cordeiro, C. F. Vinyl Acetate Polymers. *Van Nostrand's Encycl. Chem.* **2005**, *44* (14), 1–29. https://doi.org/10.1002/0471740039.vec2622.

(59) Satas, D.; Tracton, A. A.; Rafanelli, A. J. *Coatings Technology Handbook, Second Edition*; 2002; Vol. 124. https://doi.org/10.1115/1.1446069.

(60) Jose.M.Asua. *Polymeric Dispersions: Principles and Applications*; Springer Science and Business: Spain, 1996.

(61) Polpanich, D.; Tangboriboonrat, P.; Elaïssari, A. The Effect of Acrylic Acid Amount on the Colloidal Properties of Polystyrene Latex. *Colloid Polym. Sci.* **2005**, *284* (2), 183–191. https://doi.org/10.1007/s00396-005-1366-6.

(62) Qie, L.; Dub, M. A. The Influence of Butyl Acrylate/Methyl Methacrylate/2-Hydroxy Ethyl Methacrylate/Acrylic Acid Latex Properties on Pressure Sensitive Adhesive Performance. *Int. J. Adhes. Adhes.* **2010**, *30* (7), 654–664. https://doi.org/10.1016/j.ijadhadh.2010.07.002.

(63) Bilgin, S.; Tomovska, R.; Asua, J. M. Effect of Ionic Monomer Concentration on Latex and Film Properties for Surfactant-Free High Solids Content Polymer Dispersions. *Eur. Polym. J.* **2017**, *93*, 480–494. https://doi.org/10.1016/j.eurpolymj.2017.06.029.

(64) González, E.; Paulis, M.; Barandiaran, M. J. Effect of Controlled Length Acrylic Acid-Based Electrosteric Stabilizers on Latex Film Properties. *Eur. Polym. J.* **2014**, *59*, 122–128. https://doi.org/10.1016/j.eurpolymj.2014.07.023.

(65) Ceska, G. W. The Effect of Carboxylic Monomers on Surfactant-free Emulsion Copolymerization. *J. Appl. Polym. Sci.* **1974**, *18* (2), 427–437. https://doi.org/10.1002/app.1974.070180210.

(66) Guillaume, J. L.; Pichot, C.; Guillot, J. Emulsifier-free Emulsion Copolymerization of Styrene and Butyl Acrylate. I. Kinetic Studies in the Absence of Surfactant. *J. Polym. Sci. Part A Polym. Chem.* **1990**, *28* (1), 119–136. https://doi.org/10.1002/pola.1990.080280109.

(67) Kang, K.; Kan, C.; Du, Y.; Li, Y.; Liu, D. Control of Particle Size and Its Distribution in Soapfree Emulsion Copolymerization of MMA-EA-AA. *Acta Polym. Sin.* **2004**, No. 4, 580–584.

(68) Gaboyard, M.; Jeanmaire, T.; Pichot, C.; Hervaud, Y.; Boutevin, B. Seeded Semicontinuous Emulsion Copolymerization of Methyl Methacrylate, Butyl Acrylate, and Phosphonated Methacrylates: Kinetics and Morphology. *J. Polym. Sci. Part A Polym. Chem.* **2003**, *41* (16), 2469–2480. https://doi.org/10.1002/pola.10784.

(69) Liu, L. J.; Krieger, I. Emulsifier-Free Emulsion Polymerization With Ionic Comonomer. *J. Polym. Sci. A1.* **1981**, *19* (11), 3013–3026. https://doi.org/10.1002/pol.1981.170191133.

(70) Bilgin, S.; Tomovska, R.; Asua, J. M. Surfactant-Free High Solids Content Polymer Dispersions. *Polymer (Guildf).* **2017**, *117*, 64–75. https://doi.org/10.1016/j.polymer.2017.04.014.

(71) Sauzedde, F.; Ganachaud, F.; Elaïssari, A.; Pichot, C. Emulsifier-free Emulsion Copolymerization of Styrene with Two Different Amino-containing Monomers: II. Surface and Colloidal Characterization. *J. Appl. Polym. Sci.* **1997**, *65* (12), 2331–2342. https://doi.org/10.1002/(sici)1097-4628(19970919)65:12<2331::aid-app7>3.3.co;2-p.

(72) Dziomkina, N. V.; Hempenius, M. A.; Vancso, G. J. Synthesis of Cationic Core-Shell Latex Particles. *Eur. Polym. J.* **2006**, *42* (1), 81–91. https://doi.org/10.1016/j.eurpolymj.2005.07.015.

(73) Oliveira, M. P.; Giordani, D. S.; Santos, A. M. The Role of Itaconic and Fumaric Acid in the Emulsion Copolymerization of Methyl Methacrylate and N-Butyl Acrylate. *Eur. Polym. J.* **2006**, *42* (5), 1196–1205. https://doi.org/10.1016/j.eurpolymj.2005.11.016.

(74) Koh, A. Y. C.; Mange, S.; Bothe, M.; Leyrer, R. J.; Gilbert, R. G. The Influence of Copolymerization with Methacrylic Acid on Poly(Butyl Acrylate) Film Properties. *Polymer (Guildf).* **2006**, *47* (4), 1159–1165. https://doi.org/10.1016/j.polymer.2005.12.053.

(75) Santos, A. M.; Guillot, J.; McKenna, T. F. Partitioning of Styrene, Butyl Acrylate and Methacrylic Acid in Emulsion Systems. *Chem. Eng. Sci.* **1998**, *53* (12), 2143–2151. https://doi.org/10.1016/S0009-2509(98)00031-1.

(76) González, I.; Mestach, D.; Leiza, J. R.; Asua, J. M. Adhesion Enhancement in Waterborne Acrylic Latex Binders Synthesized with Phosphate Methacrylate Monomers. *Prog. Org. Coatings* **2008**, *61* (1), 38–44. https://doi.org/10.1016/j.porgcoat.2007.09.012.

(77) Chimenti, S.; Vega, J. M.; García-Lecina, E.; Grande, H. J.; Paulis, M.; Leiza, J. R. In-Situ Phosphatization and Enhanced Corrosion Properties of Films Made of Phosphate Functionalized Nanoparticles. *React. Funct. Polym.* **2019**, *143* (April), 104334. https://doi.org/10.1016/j.reactfunctpolym.2019.104334.

(78) Zou, D.; Li, X. F.; Zhu, X. L.; Kong, X. Z. Preparation of Cationic Latexes of Poly(Styrene-Co-Butyl Acrylate) and Their Properties Evolution in Latex Dilution. *Chinese J. Polym. Sci. (English Ed.* **2012**, *30* (2), 278–286. https://doi.org/10.1007/s10118-012-1113-7.

(79) Ramos, J.; Forcada, J.; Hidalgo-Alvarez, R. Cationic Polymer Nanoparticles and Nanogels: From Synthesis to Biotechnological Applications. *Chem. Rev.* **2014**, *114* (1), 367–428. https://doi.org/10.1021/cr3002643.

(80) Fulda, K. U.; Kampes, A.; Krasemann, L.; Tieke, B. Self-Assembled Mono- and Multilayers of Monodisperse Cationic and Anionic Latex Particles. *Thin Solid Films* **1998**, *327–329* (1–2), 752–757. https://doi.org/10.1016/S0040-6090(98)00780-9.

(81) BREITENBACH JW; KUCHNER K; FRITZE H; TARNOWIECKI H. Emulsion Polymerisation of Styrene and Vinyl Acetate. *Brit Polym. J* **1970**, *2* (1–2), 13–17.

(82) Alince, B.; Inoue, M.; Robertson, A. A. Latex–Fiber Interaction and Paper Reinforcement. *J. Appl. Polym. Sci.* **1976**, *20* (8), 2209–2219. https://doi.org/10.1002/app.1976.070200815.

(83) Alince, B.; Inoue, M.; Robertson, A. A. Cationic Latex Interaction with Pulp Fibers. I. Deposition of Styrene-butadiene Latex Having Quaternized Amino Groups. *J. Appl. Polym. Sci.* **1979**, *23* (2), 539–548. https://doi.org/10.1002/app.1979.070230224.

(84) Tamai, H.; Hamada, A.; Suzawa, T. Deposition of Cationic Polystyrene Latex on Fibers. *J. Colloid Interface Sci.* **1982**, *88* (2), 378–384.

(85) Ohtsuka, Y.; Kawaguchi, H.; Hayashi, S. Preparation and Characterization of Cationic Copolymer Latex. 2. Copolymerization of Styrene with 4-Vinylpyridine in an Emulsifier-Free Aqueous Medium. *Polymer (Guildf).* **1981**, *22* (5), 658–662. https://doi.org/10.1016/0032-3861(81)90357-8.

(86) Sakota, K.; Okaya, T. Preparation of Cationic Polystyrene Latexes in the Absence of Emulsifiers. *J. Appl. Polym. Sci.* **1976**, *20* (7), 1725–1733. https://doi.org/10.1002/app.1976.070200701.

(87) van Streun, K. H.; Belt, W. J.; Piet, P.; German, A. L. Synthesis, Purification and Characterization of Cationic Latices Produced by the Emulsion Copolymerization of Styrene with 3-(Methacrylamidinopropyl)Trimethylammonium Chloride. *Eur. Polym. J.* **1991**, *27* (9), 931–938. https://doi.org/10.1016/0014-3057(91)90036-N.

(88) Xu, Z.; Yi, C.; Cheng, S.; Zhang, J. Emulsifier-Free Emulsion Copolymerization of Styrene and Butyl Acrylate with Cationic Comonomer. *J. Appl. Polym. Sci.* **1997**, No. October 1996, 1–9.

(89) Liu, L. J.; Krieger, I. Emulsifier-Free Emulsion Polymerization With Cationic Comonomer. *J. Polym. Sci. A1.* **1981**, *19* (11), 3013–3026. https://doi.org/10.1002/pol.1981.170191133.

(90) Rheenen, Van; Ralph, P. Cationic Latex Paint Composition, US5312863A, 1994.

(91) Sheetz, D.P & Mich, M. Latex Composition Having Improved Adhesion, 1972.

(92) Paar, Willibald; Feola, Roland; Gmoser, J. Aqueous Binders Based on Epoxy Resins. US 2002/0091195A1, 2002.

Chapter 2. Ionic inter-particle complexation using functional monomers with one charge per molecule

2.1. Introduction

As pointed out in Chapter 1, the performance of waterborne coatings is critically affected by the film formation process, in which the individual polymer particles must join within a continuous film. Consequently, the waterborne polymers present lower performance than their solvent borne counter-polymers. To increase the performance of the waterborne dispersions, in this work waterborne polymer films were reinforced by the formed physical network through ionic interactions.

In this line, Tiggelman et al. blended two oppositely charged waterborne polymer latexes made of BA/MMA, using either small amount of AA or DMAEMA as anionic and cationic functional monomers, respectively, with 30% s.c.[1] It was shown that by a simple acid–base proton transfer, an ionic crosslinking was induced, which significantly influenced the film properties. Thus, by increasing the ionic content, the adhesion energy of the films to the substrates decreased, whereas, their water sensitivity increased. However, the ionic complexation process was not deeply studied, neither the effect of important parameters onto

the complexation, such as pH, surface charge density or particle size. On the other hand, the increased water sensitivity indicates presence of higher number of free, non-complexed ions.

To shed a bit of light on the ionic complexation process in oppositely charged latex blends and the ionic bonding effect on the performance of the resulting films, in this work, oppositely charged polymer particles were synthesized by a two-step emulsion polymerization process using a basic coating formulation made of BA and MMA in 50/50 wt. ratio. NaSS and DMAEMA ionic functional monomers were used in small amounts (1-3% with respect to B/MMA weight) to produce charged particles. The possibility of ionic bonds formation between the selected opposite ionic monomers was studied by means of Density Functional Theory (DFT) calculations. Furthermore, in order to get an insight on the effect of ionic bonding onto the interdifussion ability of the polymer chains during film formation process, direct energy transfer (ET) was monitored in films prepared from polymer particles labelled with (9-phenanthryl) methyl methacrylate (Phe-MMA) as the donor and 1-(4-nitrophenyl)-2-pyrrolidinmentyl]-acrylate (NNP-A)[2] as the acceptor by FRET technique.

2.2. Experimental part

2.2.1. Materials

The materials are given in Appendix I.

2.2.2. Computational details

All geometry optimizations were carried out within DFT using the M062X functional[3] combined with the 6-31+G(d,p) basis set.[4] To confirm that the optimized structures were minima or transition states on the potential energy surfaces, frequency calculations were performed at the same level of theory. These frequencies were then used to evaluate the zero-point vibrational energy and the thermal corrections, at T = 298.15 K, in the harmonic oscillator approximation. Single-point calculations using the 6-311++G(2df,2p) basis set[5] were performed on the optimized structures in order to refine the electronic energy. All the calculations were carried out with the Gaussian 16 suite of programs.[6]

2.2.3. Synthesis of waterborne polymer latex

Ionically charged waterborne polymer latexes were synthesized by a two-step seeded semibatch emulsion polymerization process. A typical acrylic formulation, 50/50 BA/MMA was used and two different functional monomers were chosen to give the ionic character to the latexes. NaSS (Chapter 1, Figure 1.10) was used as the anionic functional monomer, which was incorporated onto BA/MMA polymer particles following the synthesis procedures reported by Bilgin et al.[7] DMAEMA was selected as cationic monomer (Chapter 1, Figure 1.11) due to its pH dependency, which might help to control the amine protonated state as mentioned in Chapter 1.

Initially a seed with BA/MMA (50/50 wt%) at 10% s.c. for anionically charged system and 20% for cationic one was prepared. Formulations for the seed synthesis of anionically and cationically charged latexes are shown in Appendix I, Table I.1.

In a second step, the seed was grown by semibatch emulsion copolymerization. The ratio between the main monomers BA and MMA was maintained 1/1 by weight. The functional monomers content (NaSS and DMAEMA) was varied between 1% and 3% with respect to the main monomers (BA and MMA) amount in weight (wbm%). In these processes, tert-butyl hydroperoxide/ascorbic acid (TBHP/AsAc) were used as redox initiators. Schematic view of these processes is illustrated in Scheme 2.1. Description of these processes as well as formulations are shown in Appendix I, Table I.2. These polymer dispersions were named as NaSS1 (when 1 wbm% NaSS was used), NaSS3 (when using 3 wbm%), DMAEMA1 (when employing 1% DMAEMA) and DMAEMA3 (when 3 wbm% DMAEMA was used).

	Initial charge	**Feeding**	**Initial charge**	**Feeding**
NaSS1 **NaSS3**	BA/MMA NaSS	1. AsAc 2. TBHP	Seed (10% s.c.)	1. BA/MMA 2. AsAc/NaSS 3. TBHP

	1st step	2nd step	
t_0	Seed	Semibatch	t_{final}

	Initial charge	**Feeding**	**Initial charge**	**Feeding**
DMAEMA1 **DMAEMA3**	Surfactant	1. BA/MMA 2.AsAc/DMAEMA 3. TBHP	Seed (20% s.c.)	1. BA/MMA 2.AsAc/DMAEMA 3. TBHP

Scheme 2.1. Scheme for ionically charged polymer particles synthesis.

In order to carry out FRET analysis, a fluorescent dye donor and acceptor molecule have to be covalently linked into the polymer backbone.[8,9] Phe-MMA donor molecule was added to BA/MMA monomers preemulsion for anionically charged latex (NaSS1 -FRET), while NNP-A

acceptor dye molecule to BA/MMA monomers preemulsion for cationically charged latex (DMAEMA1-FRET). Both latexes were covalently labelled with 1 mol% of fluorescent dye based on major monomers (BA/MMA). For the sake of comparison, the latexes were synthesized following the same procedure as the one described above, but this time reactions were performed in 100 mL reactors. For more details, check Appendix III.

2.2.4. Latex characterization

The conversion was calculated gravimetrically and the evolution and final particle size of the latexes was measured by dynamic light scattering (DLS). The gel fraction was determined by Soxhlet extraction, using tetrahydrofuran (THF) as the solvent. The molar masses of the soluble fraction of polymers was determined by Size Exclusion Chromatography/Gel Permeation Chromatography (SEC/GPC). Finally, incorporation of functional monomer, surface charge density and ionic monomer fraction participating in the formation of water-soluble species were experimentally determined by titration. A detailed description of the characterization methods is provided in Appendix II.

2.2.5. Blends preparation and film formation

To minimize the effect of water-soluble compounds during the ionic interaction between the oppositely charged polymer particles, the latexes were dialyzed eliminating the water-soluble species together with the non-ionic surfactant from the waterborne latex. Conductivity of water was followed until a value around 2 $\mu S\ cm^{-1}$ was achieved, which corresponds to the

deionized water conductivity. The main characteristic of NaSS specie is its relatively low pKa (around 1),[7] while pka of poly(DMAEMA) is around 7.5.[10] This means that when the pH is below 7.5 all the ionic species are in their cationic and anionic state favouring the formation of the ionic network between oppositely charged polymer particles, whereas when the pH is higher than 7.5, the DMAEMA molecules are in their molecular form avoiding interactions between the oppositely charged ionic groups (Figure 2.1).

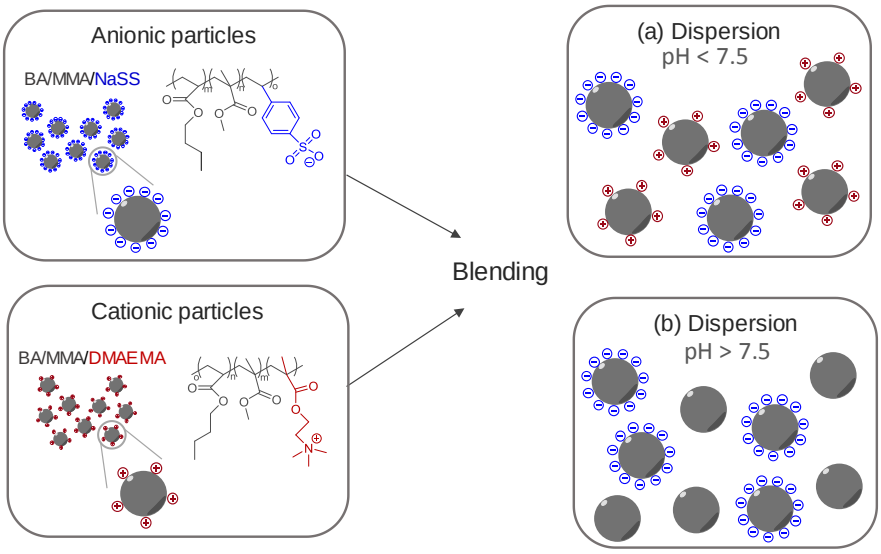

Figure 2.1. Schematic representation of the blends between NaSS and DMAEMA functionalized latex.

The blends were first prepared by mixing both latexes based on the equal number of opposite charges. Blends were first performed between 1% and 3% ionic monomer containing latexes (Blend C1-1 and Blend C3-3, respectively) to study the effect of density charge on the final performance of the films. As the incorporation of the NaSS into polymer particles is higher than incorporation of DMAEMA (these results are presented in Table 2.3), more amount of

DMAEMA containing latex was added to the blends in order to obtain equal number of oppositely charge species. Furthermore, blends between NaSS1 latex and DMAEMA3 one (Blend C1-3) were also prepared since both latex present similar surface charge density values, 16 μC cm^{-2} and 19 μC cm^{-2}, respectively, as shown in Table 2.1, and therefore, in this case clearer effect of ionic bonding was expected to be observed. A summary of the prepared blends is shown in Table 2.1.

The effect of the ionic network might be screened in case of Blend C1-1 and Blend C3-3 owing to the high amount of cationic species added to the blend. Therefore, in order to increase the ionic bonding points of 1% and 3% systems, blends were also performed based on the equal number of opposite particles (Blend P1-1 and Blend P3-3, respectively). As NaSS1 and NaSS3 containing latex show higher particle size (Table 2.3) than DMAEMA1 and DMAEMA3 ones, greater amount of NaSS latex was added to these blends. Moreover, blends between NaSS1 and DMAEMA3 latex (Blend P1-3) were also employed to further investigate the effect of blending particles with similar density charge. A summary of these blends is presented in Table 2.1.

Table 2.1. Receipt of polymer blends preparation.

	Surface charge density ($\mu C\ cm^{-2}$)			**Number of particles ($Np\ L^{-1}$)**		
Latex (mL)	Blend C1-1	Blend C3-3	Blend C1-3	Blend P1- 1	Blend P3-3	Blend P1-3
NaSS1	3	-	5	5	-	5
NaSS3	-	3	-	-	5	-
DMAEMA1	5	-	-	4	-	-
DMAEMA3	-	5	4	-	3	4

Thus, blends were named as Blend C and Blend P indicating whether the blends were performed considering the surface charge density (Blend C) or the number of particles (Blend P). The numbers refer to the concentration of each latex used (NaSS containing latex-DMAEMA containing latex).

The blends prepared at pH> 7.5, will be used as the reference material due to the lack of ionic interaction at this pH. To control the pH of these blends ammonium hydroxide (NH_4OH) and sodium hydroxide (NaOH) solutions were used. The main difference between these two solutions is the volatility of ammonia (NH_3). Since NH_4OH is a weak base, an equilibrium exists between the ammonium cation (NH_4^+) and the NH_3 in the aqueous solution as presented in equation 2.1.[9,11]

$$NH_4^+\ (aq.) + OH^-(aq.)\ \leftrightarrow\ NH_3\ (g) \uparrow + H_2O\ (l) \quad \text{(eq. 2.1)}$$

As NH_3 is a volatile compound, during the drying process NH_3 will evaporate, shifting the equilibrium to the right side and decreasing the concentration of NH_4OH in the medium.[9] The

effect of the NH_3 evaporation leads to a drop in the pH and therefore, the tertiary amine groups presented in the DMAEMA specie turned into protonated state. On the contrary, sodium hydroxide is a non-volatile specie. This means that once sodium hydroxide (NaOH) solution (pH 11) is added to the blend, the pH of this solution will remain constant, around 9, allowing the preparation of reference films and avoiding ionic interactions.

In all the cases, the basic solutions were added to the cationically charged latexes while stirring. Once the pH of the DMAEMA containing latex was above 7.5, the anionically charged latex was added forming the blend. Blends were mixed for two hours before casting the films. The blends were cast into silicon molds and they were let drying for 7 days at 23 ± 2 °C and 55 ± 5% relative humidity.

Dye labelled latexes were blended following the same methodology. Blends were performed employing NaSS1-FRET and DMAEMA1-FRET containing latex at different pHs (pH< 7.5 and pH> 7.5). Blending was prepared considering the two parameters mentioned before: surface charge density and number of particles. After mixing for 2 hours, a few drops of each blend were casted into glass substrates. Films were allowed to dry at standard conditions (23 ± 2 °C and 55 ± 5% relative humidity). The time at which both films appeared dry and transparent was taken as time zero (t_0) for FRET experiments. The polymer interdifussion process was monitored following the evolution of the fluorescent decay profile $I_D(t)$. The results are given in terms of the quantum efficiency energy transfer (ϕ_{ET}), which is related to the fraction of molecular mixing in a system of labeled particles and it is defined as equation 2.2[12–14]:

$$\Phi_{ET}(t) = 1 - \frac{\int_0^\infty I_D(t)dt}{I_D^0(t)\,dt} \quad \text{(eq.2.2)}$$

where $\int_0^\infty I_D(t)dt$ refers to the integrated area under the normalized decay profile and $I_D^0(t)\,dt$ is defined as the donor decay profile of the film containing donor fluorescence molecule (τ_D^0). More details can be found in Appendix III.

2.2.6. Polymer film characterization

The thermal characterization of the blend polymer films was carried out by differential scanning calorimetry (DSC). The mechanical properties of the original (NaSS1, NaSS3, DMAEMA1 and DMAEMA3) and blend polymer films were determined by tensile test and the water sensitivity of the blend polymer films was analysed in terms of water uptake tests and water contact angle (WCA) measurements. The interdifussion ability of the blend polymer chains during film formation process was monitored using FRET. The detailed description of these methods is provided in Appendix II.

2.3. Results and discussion

2.3.1. Theoretical calculations

Before studying the formation of the ionic network in the polymer film, one important point was to ensure that the interactions between the opposite charges of NaSS and DMAEMA were energetically favoured over their corresponding counterions. Hence, DFT calculations were performed to study the interactions between the NaSS and DMAEMA ionic monomers in terms

of binding energy. The estimated binding energy of ΔE = -109.16 kcal mol^{-1} is ascribed to the electrostatic interaction between the negatively charged sulfonate moiety of NaSS and the positively charged amino moiety of DMAEMA, reinforced by a H-bonding interaction established between the protonated DMAEMA and one oxygen atom of NaSS (Figure 2.2). The hydrogen bond shows a short H···O bond (1.361 Å) and an almost planar N-H···O angle (177°), which suggest a rather strong interaction. This result indicates that the ionic complexation is feasible in the selected ionic monomers systems.

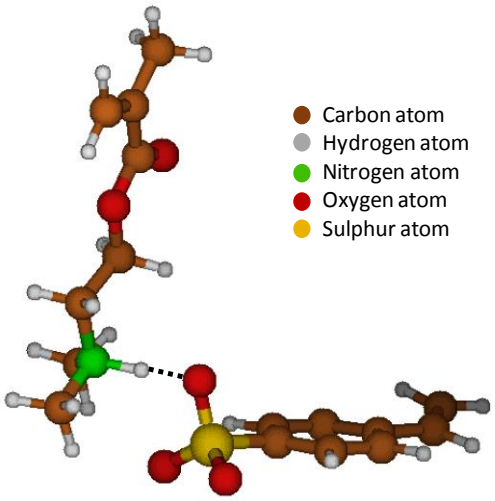

Figure 2.2. Geometrical feature of NaSS and DMAEMA ionic monomers in water.

2.3.2. Overview of latex characteristics

The charged latexes were synthesized by a two-step seeded semicontinuous emulsion polymerization in presence of 1-3% of ionic monomer based of the weight of main monomers

(BA/MMA). In case of NaSS, emulsifier-free polymer latex were obtained, whereas in case of DMAEMA, non-ionic surfactant was used to improve the colloidal stability of the resulting latex.

Table 2.2 summarizes the results for the seed latexes. Complete conversion was obtained at the end of the polymerization for both dispersions, reaching values above 97%. Average particle size was similar for both latexes, 140 nm.

Table 2.2. Summary for the seed latex characteristics.

Latex	Conversion (%)	d_P (nm)
NaSS	98	140 ± 2
DMAEMA	97	140 ± 3

The time evolution of the monomer conversion (instantaneous and overall) in the second step of the synthesis of both latexes in presence of different amount of ionic monomers is presented in Figure 2.3. Almost full conversion was achieved at the end of the polymerization process in all cases. The instantaneous conversions were high along the reactions, indicating very low monomer concentration in the reactor during the syntheses. In both cases, no significant effect of ionic monomer concentration on the reaction kinetics was observed.

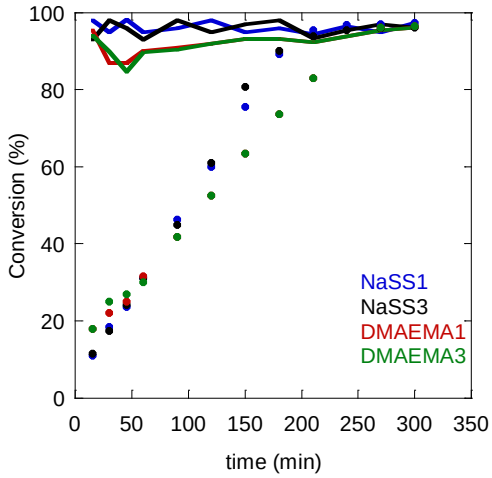

Figure 2.3. Monomer conversion evolution for latexes containing NaSS and DMAEMA functional monomers. The continuous line represents the instantaneous conversion, while the dots the overall conversion.

The main characteristics of the polymer latexes are presented in Table 2.3. Regarding the average particle size (dp), by increasing the content of ionic monomer from 1% to 3%, the average particle size increased, for both anionic and cationic latex. Similar behaviour was reported for the case of NaSS[7], which occurs due to increasing of the ionic strength in the latex, screening the stabilization effect of the ionic groups incorporated onto polymer particles.

Table 2.3. Average particle size, surface incorporation of ionic monomer and fraction of ionic monomer participating as water-soluble species measurements for anionically and cationically charge latex.

Latex	d_P (nm)	Surface incorporation (ionic monomer %)	Surface charge density ($\mu C\ cm^{-2}$)	Fraction of ionic monomer in water - soluble species (ionic monomer %)
NaSS1	275 ± 5	70 ± 6	16 ± 2	30 ± 2
NaSS3	300 ± 4	52 ± 3	36 ± 4	35 ± 3
DMAEMA1	240 ± 5	33 ± 4	9 ± 2	42 ± 10
DMAEMA3	250 ± 2	19 ± 4	19 ± 3	45 ± 10

It can be seen in Table 2.3 that the quantity of ionic species incorporated onto polymer particles increased with the ionic monomers concentration. According to Sevilay et al.,[7] this effect was attributed to the increased ionic strength in the system that shifted the absorption equilibrium towards polymer particles, which also explained why no significant difference on quantity of oligoradicals in aqueous phase was observed with increasing ionic monomer concentration. NaSS was incorporated importantly more than the DMAEMA monomer, which is also in agreement with previous works reported using cationic monomers.[15] Furthermore, as it may be observed from Table 2.3, in case of the cationic monomer, higher fraction of functional monomer participated in the formation of water-soluble species. It is worth mentioning that this amount may be slightly underestimated, due to the decreased solubility of oligomers containing DMAEMA units at neutral pH, at which the phases were separated during the procedure of determination of ionic monomer fraction participating in the formation of water-soluble species.

For both latexes, the incorporated quantity of ionic monomers increased with their concentration, and consequently the surface charge density increased as well. The effect is more pronounced for NaSS.

The polymer microstructure was analysed by determining the insoluble part of the polymer in THF (gel content) and the molar mass of the soluble part of the polymer. As observed in Table 2.4 the gel content for the anionically charged polymers was above 50%, while it was above 30% when DMAEMA was employed. The high values obtained could be attributed to the presence of ionic species, which are not soluble in organic solvents since in seeded semibatch emulsion polymerizations of BA/MMA, the formation of crosslinked structures is almost negligible (< 5 wt%).[16] Nevertheless, there might be a contribution of branching and crosslinking reactions in these latexes since it is well known that TBHP initiator is efficient in hydrogen abstraction.[7] The soluble fraction of the polymer was analysed by SEC/GPC and as expected, low molecular weights were measured in all the cases as it is shown in Table 2.4. The molar masses of the anionic latexes where lower than the cationic ones due to the larger amount of gel content, in which the larger molar masses were incorporated. The polydispersity index values are in the range of the ones normally obtained in the BA/MMA emulsion polymerizations.

Table 2.4. Microstructure of the charged polymers.

Latex	Gel content (%)	M_w (kDa)	Đ
NaSS1	53 ± 2	304	2.5
NaSS3	55 ± 1	260	2.4
DMAEMA1	40 ± 2	350	2.0
DMAEMA3	30 ± 1	400	2.1

2.4. Polymer film performance

Polymer particles functionalized with 1% and 3% of NaSS and DMAEMA were blended at two different pHs. In the first set of blends, the ionic interactions between the particles were promoted by keeping the pH below 7.5, at which, both types of polymer particles were charged. The second set of blends was prepared at pH above the pKa of the cationic functional group of DMAEMA monomer (pH> 7.5), which ensures its neutral state, avoiding ionic interactions between the particles. The blends obtained at pH> 7.5 were considered as reference material. Furthermore, the blending process was based either on the same surface charge density (Blends C1-1, C3-3 and C1-3) or on the same number of particles (Blends P1-1, P3-3 and P1-3) in both latexes. The films were prepared from the blended latexes. As shown in Figure 2.4 and Figure 2.5, homogeneous and transparent films were obtained in all the cases.

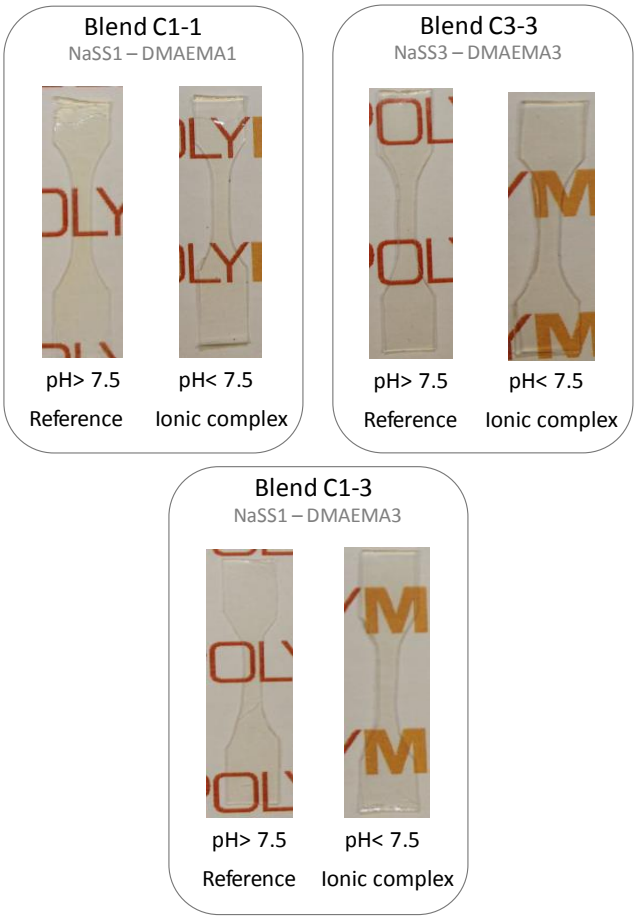

Figure 2.4. Appearance of the polymer blend films obtained based on equal number of opposite charges.

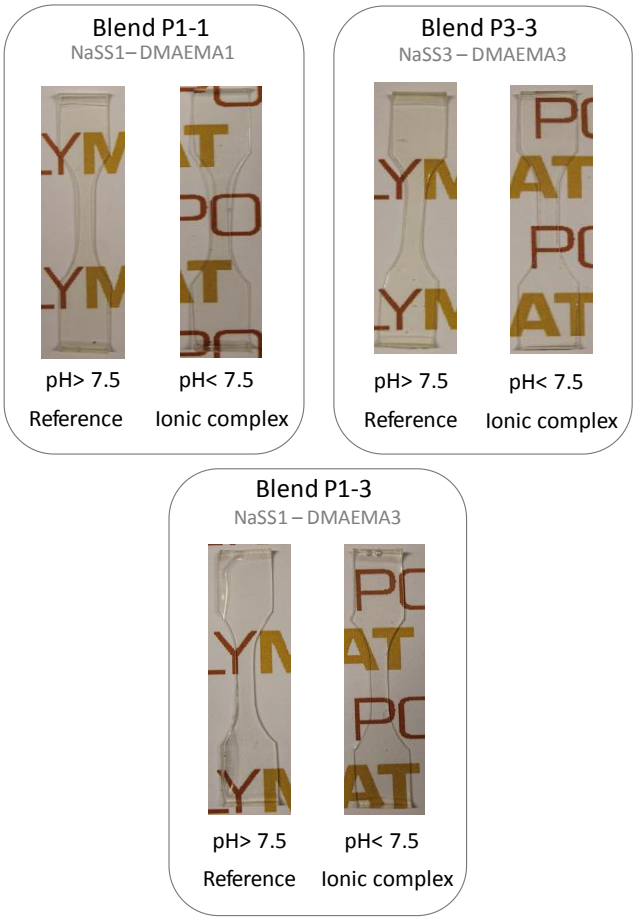

Figure 2.5. Appearance of the polymer blend films obtained based on equal number of opposite particles.

Similar T_g values of the reference and ionic complex materials were observed, in a range of 18 – 20 °C, indicating that there is no important effect of the ionic complexation on the T_g of the resulting polymer blends, probably because the main monomers in the both blended polymers were the same (BA/MMA in 50/50 wt. ratio).

Recently, the relation between the surface charge density and surface wetting properties of polymer film was demonstrated in plasma treated polymer films, that recovered the hydrophobicity due to a decrease of the surface charge density.[17] This means that in case of ionic complexation, the neutralization of the surface charges within the polymer films might affect the wetting properties. Therefore, the change of the water contact angles (WCA) of the ionic complexed films with respect to reference film could be a solid suggestion of the established ionic complexes. In Table 2.5, WCA of the ionic complexes and reference films are shown. Lower WCA for reference films than for the ionic complexes was observed in all cases, probably owing to the presence of free ionic species that increase the hydrophilicity of the reference polymer films. In all the cases, the WCA of the ionic complex materials was above 90°, which means that the films after establishing ionic interactions, were hydrophobic.

Table 2.5. Contact angle measurements for reference and ionic complex films.

Blend system		Water Contact Angle (°)
Blend C1-1	Reference	64 ± 4
	Ionic complex	90 ± 3
Blend C3-3	Reference	64 ± 2
	Ionic complex	87 ± 3
Blend C1-3	Reference	76 ± 2
	Ionic complex	90 ± 1
Blend P1-1	Reference	78 ± 1
	Ionic complex	87 ± 2
Blend P3-3	Reference	86 ± 3
	Ionic complex	94 ± 4
Blend P1-3	Reference	74 ± 1
	Ionic complex	91 ± 1

The stress-strain curves of the dialyzed original films (NaSS1, NaSS3, DMAEMA1 and DMAEMA3) were first examined as shown in Figure 2.6. Anionically charged polymers with NaSS produced much more mechanically resistant film, with higher Young modulus and lower elongation at break than the cationically charged films with DMAEMA. When the functional monomer quantity was increased, slightly enhanced properties can be observed, especially elongation at break, resulting in much more flexible films.

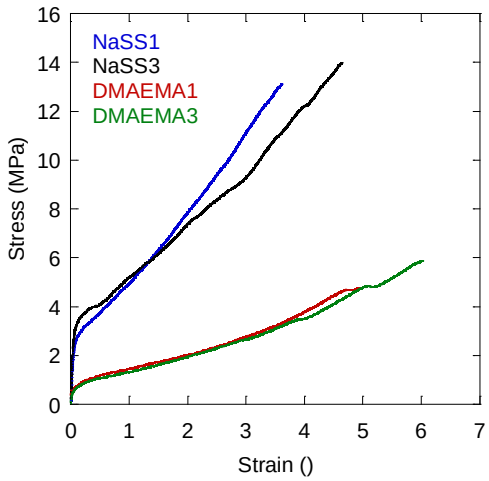

Figure 2.6. Stress-strain curves for NaSS1, NaSS3, DMAEMA1 and DMAEMA3 original films.

The stress-strain plots of the blend polymer films prepared from the blends with the same surface charge density, at different pHs are represented in Figure 2.7a, whereas Figure 2.7b shows the tensile curves of the blend films prepared with equal number of oppositely charged particles. The mechanical properties determined from the stress-strain curves are presented in Table 2.6 and Table 2.7.

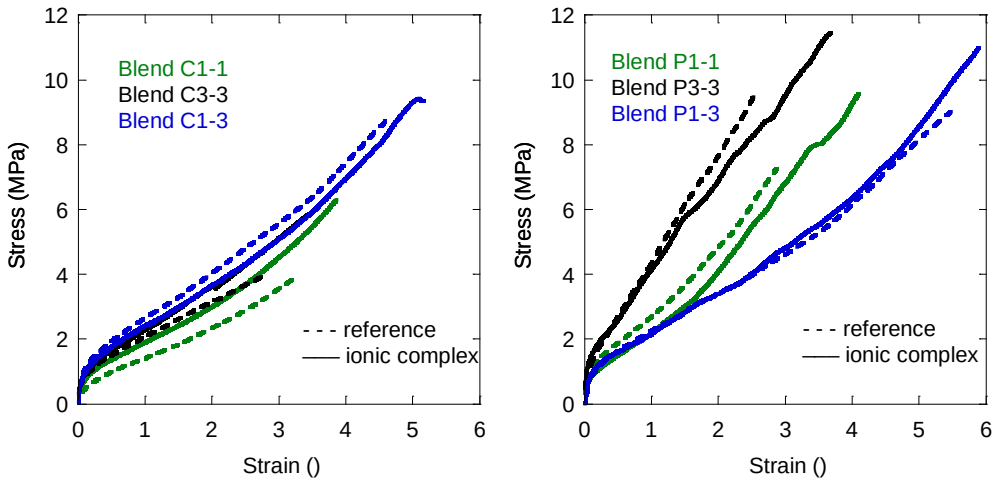

Figure 2.7. Mechanical properties measured at macroscopic level between oppositely charged polymer particles blends performed based on (a) surface charge density and (b) number of particles and at different pH. The dash lines represents the reference latex (pH> 7.5) while the continuous lines the ionic complex (pH< 7.5).

Table 2.6. Mechanical properties of the polymer blends performed at different surface charge density and pH, related to the stress-strain plots represented in Figure 2.7a.

Blend		Young´s modulus (MPa)	Elongation at break	Ultimate strength (MPa)	Toughness (MPa)
C1-1	Reference	3 ± 2	3.7 ± 1.0	4.5 ± 1.1	7.1 ± 1.1
	Ionic complex	4 ± 1	3.8 ± 1.1	6.1 ± 0.6	12.1 ± 1.6
C3-3	Reference	5 ± 1	3.1 ± 0.7	3.9 ± 0.2	7.1 ± 1.8
	Ionic complex	6 ± 2	3.5 ± 0.4	5.8 ± 0.4	11.3 ± 1.7
C1-3	Reference	5 ± 2	4.6 ± 0.9	8.7 ± 0.5	21.5 ± 1.7
	Ionic complex	5 ± 1	5.2 ± 1.0	9.5 ± 1.3	24.4 ± 1.5

Table 2.7. Mechanical properties of the polymer blends performed at different surface charge density and pH, related to the stress-strain plots represented in Figure 2.7b.

Blend		Young´s modulus (MPa)	Elongation at break	Ultimate strength (MPa)	Toughness (MPa)
P1-1	Reference	8 ± 1	3.1 ± 0.3	7.4 ± 0.7	11.9 ± 2.8
	Ionic complex	6 ± 1	3.8 ± 0.5	9.1 ± 2.3	18.5 ± 4.1
P3-3	Reference	16 ± 2	2.4 ± 0.2	8.3 ± 1.2	12.1 ± 2.3
	Ionic complex	14 ± 2	3.7 ± 0.5	11.1 ± 1.4	22.8 ± 1.6
P1-3	Reference	5 ± 1	5.4 ± 0.2	9.4 ± 0.5	25.1 ± 3.6
	Ionic complex	4 ± 1	5.7 ± 0.2	10.9 ± 0.4	28.3 ± 1.6

When blending soft (DMAEMA) and hard (NaSS) polymers, properties of the blend materials in between both components are expected. As observed in Figure 2.7 all the blends (ionic complex ones) were in between their corresponding original films (Figure 2.6), meaning that the established ionic bonding might not be sufficient for improving the hard properties shown by NaSS containing latexes.

In Figure 2.7a, where Blends C1-1, C3-3 and C1-3 are presented, slightly higher Young's modules, ultimate strength and toughness, with a clearly higher elongation at break (Table 2.6) were obtained for the ionic complexed systems, which may be directly related to the ionic bonding effect. This effect is similar for Blends C1-1 and C3-3, indicating that the higher surface density in the last one did not affected additionally the ionic complexation and the properties. Probably, this is a consequence of the addition of higher amount of cationic latex (due to the lower incorporation of cationic monomer) in both cases, which places space limitation to the complexation process. It is worth mentioning that the ionic bonding was established during film

formation, where agitation is avoided and particles containing DMAEMA likely tend to group together due to the larger number. To check this, Blend C1-3 was prepared by blending the NaSS1 latex (275 nm, 17 μC cm^{-2}) with DMAEMA3 latex (250 nm, 19 μC cm^{-2}), with similar particle sizes and charge densities. As it can be observed in Figure 2.7a, there is no improvement effect observed for the ionic complex. The slightly better properties of C1-3 with respect to C1-1 and C3-3 blends are likely result on the higher content of NaSS latex (Table 2.1), which presents mechanically more resistant films (Figure 2.6).

Similar effect of ionic bonding was observed for Blends P1-1, P3-3 and P1-3 (Figure 2.7b), in terms of slightly higher ultimate strength, toughness and elongation at break values (Table 2.7). However, a small drop in Young modulus was observed in this set of the blends after the complexation. This effect is stronger for Blend P3-3 than for Blend P1-1, probably due to the higher surface charge density of the blended particles (Table 2.3). Even though equal number of opposite particles were incorporated into the blends, likely due to their difference in the surface charge density, the observed effects are rather modest. Moreover, the tensile characteristic of the Blend P1-3, prepared by employing NaSS1 latex (275 nm, 16 μC cm^{-2}) and DMAEMA3 latex (250 nm, 19 μC cm^{-2}), which allow blending of similar particle number with similar particle charge, again resulted in modest improvement of the properties (Table 2.7).

Taking into consideration the particle systems blended in this work, ionic complexation might occur at two levels. When particles with opposite charges approach each other during film formation, the ionic complexation might occur either in the first step of particle packaging (inter-

particle complexation, Figure 2.8a) or in the second step when the chain interdiffusion occurs (inter-chain complexation, Figure 2.8b). In the former case, the formation of inter-particle ionic complexes would prevent the chain interdiffusion.

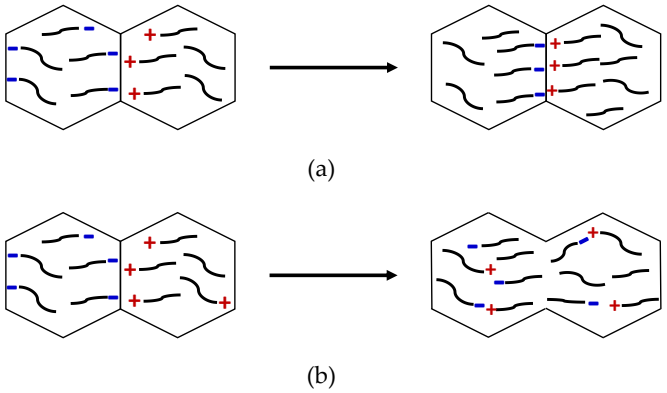

Figure 2.8. Schematic view of ionic complexation step at (a) inter-particle level and (b) inter-chain level.

Few techniques have been developed to quantitatively measure the polymer chain diffusion in latex films. The most actively used methods are Small-Angle Neutron Scattering (SANS) and FRET.[18] Although the SANS technique is appropriate for measuring the interdiffusion over distances comparable with the particle size, it is not adequate for measuring at shorter distances, hence, in this work FRET technique was chosen.[19,20] For that aim, dye labelled charged polymer latexes were prepared with similar properties (conversion, particle size, incorporation, surface density, gel content and molar masses) to the unlabelled polymer latex. Details for the characteristics can be found in Table 2.8.

Table 2.8. Characteristics of labelled dye anionically and cationically charged latexes.

Latex/Characterization	NaSS1-FRET	DMAEMA1-FRET
Conversion (%)	97	93
dp (nm)	255 ± 5	245 ± 5
Surface incorporation (F.M %)	75 ± 2	29 ± 1
Surface charge density (μC cm^{-2})	18 ± 2	8 ± 1
Insoluble polymer (%)	51 ± 1	40 ± 5
Mw (kDa)	280 ± 10	310 ± 25
Đ	2.5	1.6

The influence of the complexation process on the polymer chain diffusion was examined following the extent of energy transfer in newly formed polymer films from the blends of NaSS1-FRET and DMAEMA1-FRET (Blend C1-1 and Blend P1-1). Figure 2.9 compares the evolution of quantum efficiency energy transfer (Φ_{ET}) over time for both polymer films, ionic complex (pH< 7.5) and reference material (pH> 7.5). As observed, in both cases (Figure 2.9a and Figure 2.9b), Φ_{ET} values were maintained almost constant throughout the time, being much lower for the ionic complexed material.

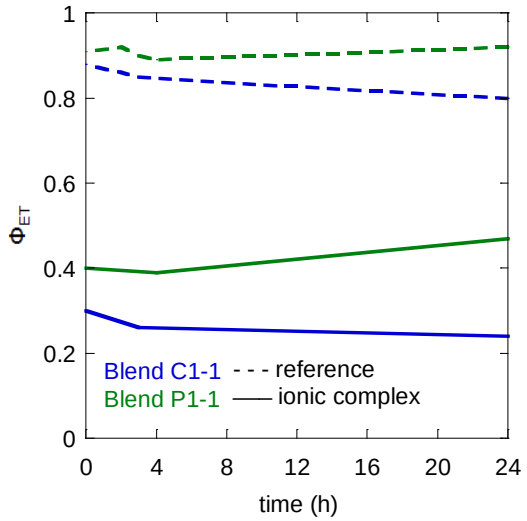

Figure 2.9. Evolution of quantum efficiency energy transfer for Blend C1-1 and P1-1 during blending of oppositely charged polymer particles blends performed at different pH. The dash lines represents the reference latex (pH>7.5) while the continuous lines the ionic complex (pH<7.5).

These results show that at the present drying conditions, in case of ionic complexed material (pH< 7.5), the interdiffusion of polymer chains between neighbouring particles was significantly lower. This effect was attributed to the presence of inter-particles ionic bonds, which created a network of bonded polymer chains rich in ionic monomer units. This ionic network conveys flexibility to the complexed films, as observed in tensile tests results. However, it simultaneously prevents the chain interdiffusion, accounted for the modestly enhanced mechanical properties.

By comparison of reference and ionic complex material, one may observe that the blend prepared with equal particle sizes (Blend P1-1) present higher chain interdiffusion degree than the blend with equal surface charge densities (Blend C1-1). This is an indication of less ionic

complexes established in case of Blend P1-1, which clearly explains the lowest effect on mechanical properties, observed in Figure 2.7.

For practical application of waterborne polymer coatings, their sensitivity to water is an essential characteristic. Usually, the presence of ionic species within the polymer films, from either the surfactant, ionic monomers or other components, increases their water sensitivity. For instance, it was shown that hydrophilic block copolymers containing AA in the shell, presented high water sensitivity.[20] In the work of Tiggelman and coworkers,[1] the main drawback of the material formed by ionic complexation of AA containing particles and DMAEMA ones, was the high water uptake (more than 15%). However, Sevilay et al. have demonstrated that, in case of NaSS stabilized polymer films, this increment occurred sharply in the initial contact with water, after which the water uptake remains constant and usually much lower than the film in which conventional surfactant was employed.[4] The high initial water uptake occurred due to the anionic network formed within the film, which leads to saturation, whereas in the case of conventional surfactants, they formed a hydrophilic pocket able to absorb much larger water quantities.

The water sensitivity of the blends prepared in this study, measured by means of water uptake, are presented in Figure 2.10.

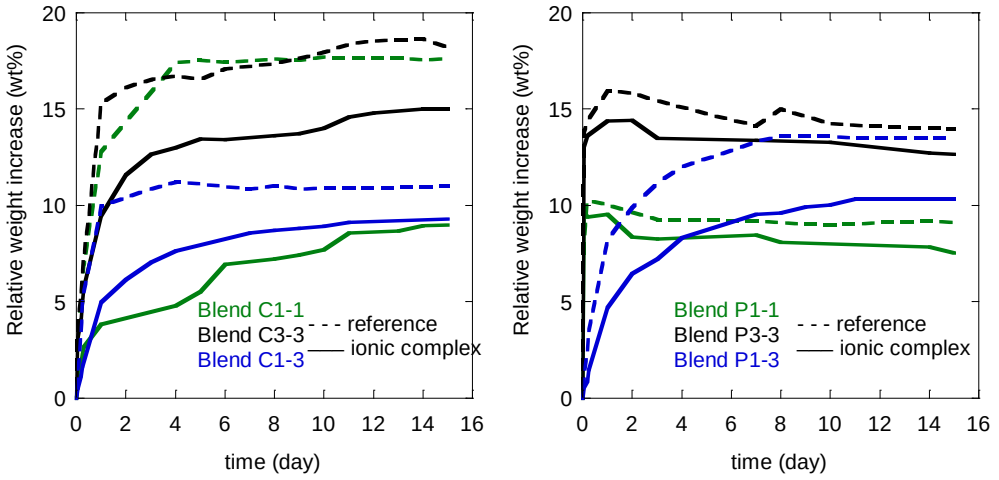

Figure 2.10. Evolution of relative weight increased of blends performed based on (a) surface charge density and (b) number of particles and at different pH. The dash lines represents the reference latex (pH>7.5) while the continuous lines the ionic complex (pH<7.5).

As it can be seen in Figure 2.10a, the reference Blends C1-1 and C3-3 present similar behaviour absorbing up to almost 20 wt% of water, likely due to high sulfonate ions concentration (at pH of preparation of reference blends, the cationic latex is mostly in neutral state). On the other hand, the ionic complex Blends C1-1 and C3-3 presented much lower water uptake, which moreover depends on the surface charge density. Therefore, ionic complex Blend C1-1 absorbs about 8 wt%, importantly less than Blend C3-3 (14 wt%). The drop of water uptake with respect to reference blends is likely due to the ionic complexation process that led to the neutralization of most of the present charges, pointing out that very few free charges are presented in the complex films. In ionic complex Blend C3-3 there is still a high number of free charges, probably due to the mentioned steric hindrance to the complexation reaction. The same

reason is behind the observed slightly higher water uptake of ionic complex Blend C1-3 than the ionic complex Blend C1-1.

The water uptake of the polymer films prepared by blending the same number of particles is shown in Figure 2.10b. The reference and ionic complex Blends P1-1 and P3-3 showed similar water sensitivity during the first hours, being high the amount of water that penetrated within the film (10 wt% and 15 wt%, respectively). Relatively smaller difference between the reference and ionic complex blends is a consequence of the excess free sulfonate charges (the surface charge density of the anionic particles was higher, Table 2.3). However, the water absorption by ionic complex Blends P1-1 and P3-3 dropped after the first two hours, probably owing to the weight loss of the polymer film. Some water-soluble species were dissolved by penetrating the water and desorbing from the film to the water phase. For the blend with much lower difference in density charge, Blend P1-3, clearly, the ionic complex material did not absorb as much water as the reference one during the first hours, probably due to a higher degree of neutralization in this case and less amount of free charges.

In addition, films were dried and weighted before and after their immersion in water to determine the weight loss of the materials. The weight loss (wt%) is referred to the initial weight of the samples (Figure 2.11).

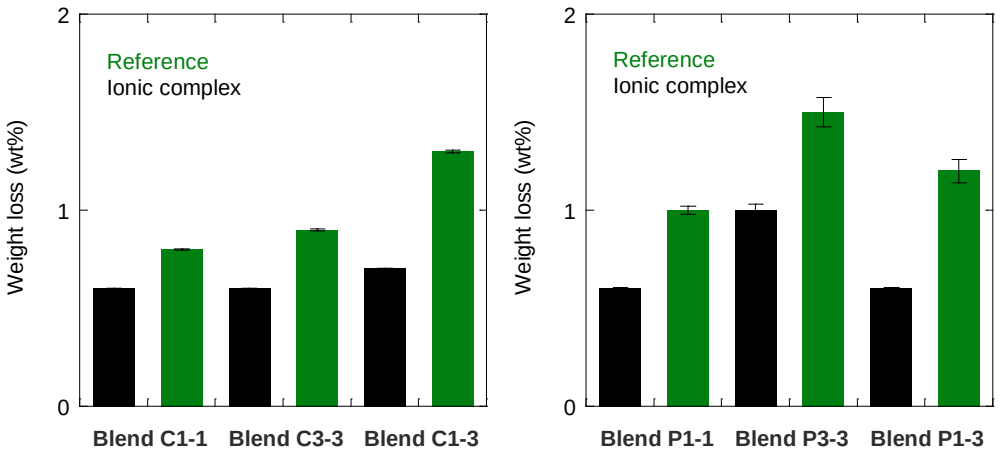

Figure 2.11. Weight loss (wt%) values after water uptake experiments for blend films performed considering (a) surface charge density and (b) number of particles at different pH.

Even though the films were prepared from the same latexes, the reference film contained higher amount of soluble polymer chains. Although dialyzed latexes were used for these blends, polymer chains with higher molecular weight than the membrane cut-off (12000 - 14000 Da) were not eliminated, contributing to the observed weight loss as they may have migrated from the film. It can be said that for Blends C1-1, C3-3 and C1-3, the amount of material lost was small (<1 wt%, <1 wt% and <1.5 wt%, respectively), whereas for Blend P1-1, P3-3 and P1-3, the lost was slightly higher (<1 wt%, <1.5 wt% and <1.5 wt%, respectively). We hypothesize that the difference between reference film and respective ionic complex occurred due to decreased desorption of water-soluble chains from the film to the water phase by the presence of ionic complexes, actuating as physical barriers. The highest difference from respective reference film was observed for ionic complex C1-3 and P1-3, indicating that the extent of ionic bonds for these

blends was higher than for the others, due to the decreased steric limitations to the ionic bonding reactions.

2.5. Conclusions

In this work, ionic complexation between waterborne particles and its effect on the final film performance was studied. The oppositely charged polymer particles were prepared by emulsion polymerization of BA/MMA main monomers in presence of small amount (1-3 %) of either NaSS or DMAEMA ionic monomers. Density functional theory calculations showed that the interaction between main ions of NaSS and DMAEMA was favoured against the interaction with their respective counter ions, providing a fundamental background on the formation of an ionic complexation when mixing oppositely charged polymeric dispersions. The blends were prepared varying two parameters: surface charge density and number of particles.

Mechanical properties tested by tensile measurements showed that the ionic complexed blends, presented slightly better mechanical properties than the reference blend, although the effect was rather modest in all studied combinations. The modest result obtained was attributed to the steric limitation that individual particles have during film formation process, due to differences in number of particles and surface charge densities, along with a lack of agitation. In such conditions, many charges remain free. Nevertheless, the modest enhancement of mechanical properties was kept even in the blends prepared with similar particle size and surface charge density.

Considering these results, FRET technique was used to examine if the ionic bonding occurs at molecular or particle level during blending at both pHs. The results revealed that in the ionic complexed blends, the interdiffusion of polymer chains between neighbouring particles was hindered with respect to reference blend. It was thought that the created network of ionic complexed polymer chains shell around individual polymer particles within the film decreased the overall level of chain interdiffusion, however, it slightly reinforced the film. The reference blend presented enhanced polymer chain mobility, but lower mechanical performance. This means that when ionic network is formed, polymer chains diffusion is affected, and consequently slight mechanical properties improvement is observed.

On the other hand, clearly the reference blends prepared at pH> 7.5 showed higher water absorption compared to the ionic complex blend (pH< 7.5), owing to the lack of neutralization between ionic species in the former. Exception are the films prepared by blending based on the same particle number (P1-1 and P3-3), where the greater surface charge density of NaSS particles is responsible for such high water penetration within blend materials, screening the possible effect of formed ionic interaction. Despite that dialyzed latex were used throughout this study, migration of polymer chains with higher molecular weight than the membrane cut-off (14000 Da) might contribute to the observed weight loss from the polymer blends during water uptake measurements.

The presented inter-particle complex between sulfonate – amine groups containing latexes open a promising approach for reinforcing polymer films cast from water-based polymers.

However, this concept still needs further investigation in order to reinforce the established interactions.

2.6. References

(1) Tiggelman, I.; Hartmann, P. C. Ionic Autocrosslinking of Water-Based Polymer Latices: A New Concept of Acid-Base Interaction Occurring upon Film Formation. *Prog. Org. Coatings* **2010**, *67* (1), 76–83. https://doi.org/10.1016/j.porgcoat.2009.09.018.

(2) Turshatov, A.; Adams, J. A New Monomeric FRET-Acceptor for Polymer Interdiffusion Experiments on Polymer Dispersions. *Polymer (Guildf).* **2007**, *48* (26), 7444–7448. https://doi.org/10.1016/j.polymer.2007.10.023.

(3) Zhao, Y.; Truhlar, D. G. The M06 Suite of Density Functionals for Main Group Thermochemistry, Thermochemical Kinetics, Noncovalent Interactions, Excited States, and Transition Elements: Two New Functionals and Systematic Testing of Four M06-Class Functionals and 12 Other Function. *Theor. Chem. Acc.* **2008**, *120* (1–3), 215–241. https://doi.org/10.1007/s00214-007-0310-x.

(4) Hehre, W. J.; Ditchfield, K.; Pople, J. A. Self-Consistent Molecular Orbital Methods. XII. Further Extensions of Gaussian-Type Basis Sets for Use in Molecular Orbital Studies of Organic Molecules. *J. Chem. Phys.* **1972**, *56* (5), 2257–2261. https://doi.org/10.1063/1.1677527.

(5) Krishnan, R.; Binkley, J. S.; Seeger, R.; Pople, J. A. Self-Consistent Molecular Orbital Methods. XX. A Basis Set for Correlated Wave Functions. *J. Chem. Phys.* **1980**, *72* (1), 650–654. https://doi.org/10.1063/1.438955.

(6) Frisch, M. J.; Trucks, G. W.; Schlegel, H. B.; Scuseria, G. E.; Robb, M. A.; Cheeseman, J. R.; Scalmani, G.; Barone, V.; Petersson, G. A.; Nakatsuji, H.; et al. Gaussian 16, Revision B.01. Wallingford CT 2016.

(7) Bilgin, S.; Tomovska, R.; Asua, J. M. Effect of Ionic Monomer Concentration on Latex and Film Properties for Surfactant-Free High Solids Content Polymer Dispersions. *Eur. Polym. J.* **2017**, *93*, 480–494. https://doi.org/10.1016/j.eurpolymj.2017.06.029.

(8) Zhao, C.-L.; Wang, Y.; Hruska, Z.; Winnik, M. A. Molecular Aspects of Latex Film Formation: An Energy-Transfer Study. *Macromolecules* **1990**, *23* (18), 4082–4087. https://doi.org/10.1021/ma00220a009.

(9) González, E.; Barandiaran, M. J.; Paulis, M. Isolation of the Effect of the Hairy Layer Length on the Mechanical Properties of Waterborne Coatings. *Prog. Org. Coatings* **2015**, *88*, 137–143. https://doi.org/10.1016/j.porgcoat.2015.06.027.

(10) Omer, M.; Khan, M.; Kim, Y. K.; Lee, J. H.; Kang, I.-K.; Park, S.-Y. Biosensor Utilizing a Liquid Crystal/Water Interface Functionalized with Poly(4-Cyanobiphenyl-4'-Oxyundecylacrylate-b-((2-Dimethyl Amino) Ethyl Methacrylate)). *Colloids Surfaces B Biointerfaces* **2014**, *121*, 400–408. https://doi.org/10.1016/j.colsurfb.2014.06.028.

(11) Salentinig, S.; Jackson, P.; Attalla, M. A Computational Study of the Suppression of Ammonia Volatility in Aqueous Systems Using Ionic Additives. *Struct. Chem.* **2014**, *25* (1), 159–168. https://doi.org/10.1007/s11224-013-0263-8.

(12) Wu, J.; Winnik, M. A.; Farwaha, R.; Rademacher, J. Effect of a Water-Soluble Polymer on Polymer Interdiffusion in P(MMA-Co-BA) Latex Films. *Macromol. Chem. Phys.* **2003**, *204* (16), 1933–1940. https://doi.org/10.1002/macp.200350060.

(13) Kobayashi, M.; Rharbi, Y.; Winnik, M. A. Effect of Inorganic Pigments on Polymer Interdiffusion in a Low-Tg Latex Film. *Macromolecules* **2001**, *34* (6), 1855–1863. https://doi.org/10.1021/ma000604n.

(14) Pinenq, P.; Winnik, M. A.; Ernst, B.; Juhué, D. Polymer Diffusion and Mechanical Properties of Films Prepared from Crosslinked Latex Particles. *J. Coatings Technol.* **2000**, *72* (903), 45–61. https://doi.org/10.1007/bf02697987.

(15) Dziomkina, N. V.; Hempenius, M. A.; Vancso, G. J. Synthesis of Cationic Core-Shell Latex Particles. *Eur. Polym. J.* **2006**, *42* (1), 81–91. https://doi.org/10.1016/j.eurpolymj.2005.07.015.

(16) González, I.; Asua, J. M.; Leiza, J. R. The Role of Methyl Methacrylate on Branching and Gel Formation in the Emulsion Copolymerization of BA/MMA. *Polymer (Guildf).* **2007**, *48* (9), 2542–2547. https://doi.org/10.1016/j.polymer.2007.03.015.

(17) Bormashenko, E.; Multanen, V.; Chaniel, G.; Grynyov, R.; Shulzinger, E.; Pogreb, R.; Whyman, G. Phenomenological Model of Wetting Charged Dielectric Surfaces and Its Testing with Plasma-Treated Polymer Films and Inflatable Balloons. *Colloids Surfaces A Physicochem. Eng. Asp.* **2015**, *487*, 162–168. https://doi.org/10.1016/j.colsurfa.2015.09.065.

(18) Kim, K. D.; Sperling, L. H.; Klein, A.; Wignall, G. D. Characterization of Film Formation from Direct Mini-Emulsified Polystyrene Latex Particles via SANS. *Macromolecules* **1993**, *26* (17), 4624–4631. https://doi.org/10.1021/ma00069a032.

(19) Wang, Y.; Zhao, C.; Winnik, M. A. Molecular Diffusion and Latex Film Formation: An Analysis of Direct Nonradiative Energy Transfer Experiments. *J. Chem. Phys.* **1991**, *95* (3), 2143–2153. https://doi.org/10.1063/1.461013.

(20) González, E.; Paulis, M.; Barandiaran, M. J. Effect of Controlled Length Acrylic Acid-Based Electrosteric Stabilizers on Latex Film Properties. *Eur. Polym. J.* **2014**, *59*, 122–128. https://doi.org/10.1016/j.eurpolymj.2014.07.023.

Chapter 3. Effect of particle size and packaging on the ionic inter-particle complexation

3.1. Introduction

In Chapter 2, it has been observed that when blending similar size oppositely charged particles to induce the ionic bonding during film formation, the improvement in the blend properties and performance with respect to the non-ionic bonded reference was modest. It has been hypothesized that there was not sufficient contact between the oppositely charged particles and only few ionic bonds were established, due to poor packaging of the particles. Therefore, the aim of this Chapter is to improve ionic inter-particle complexation, by blending oppositely charged polymer particles with different particle sizes improving particle packaging. In such a way, by favouring the contact between large and small particles at the same time the ionic bonding may increase, creating denser ionic network within the polymer films.

During the past decades, latex blended systems combining hard/soft polymers and large/small particles have attracted increasing attention, owing to the possibility of controlling the dispersion rheology, the film formation and the final film properties.[1–6] Generally, the particle packaging of a bimodal/multimodal PSD latexes improves in comparison to a monodisperse system, offering possibility to increase solids content during synthesis, to lower the viscosity and

the MFFT of the product.[7] Other latex and film properties have been also improved when mixing different size particles, such as good coalesce and hence, improved film formation, block resistance, water uptake and tensile strength.[7,8] Nevertheless, none of the works studied the ionic complexation when blending particles with different sizes.

Despite the great advantages of blending latexes with large and small particles, if the size ratios are not well controlled, unexpected air voids might be created within the film, affecting the final properties. This is why, Kusy developed a model to achieve an optimal particle packaging, minimizing the air voids.[1,9] These calculations provide a great approximation of the minimum volume fraction of the dispersed phase (small particles) to form a continuous phase around the primary particles (large particles) for various size ratios (dp_{large}/dp_{small}). This strategy was followed in the present Chapter in order to increase the probability of the ionic complexation between the oppositely charged particles with different sizes. For that aim, BA/MMA (50/50 wt%) latexes were used, synthesized by batch or semibatch emulsion polymerization, using NaSS and DMAEMA to provide colloidal stability and anionic and cationic charges to the polymer particles, respectively.

3.2. Experimental part

3.2.1. Materials

The materials are given in Appendix I.

3.2.2. Synthesis of ionically charged dispersions

Ionically charged latexes were synthesis by batch and semibatch emulsion copolymerization processes using a typical coating formulation 50/50 BA/MMA by weight. Functional monomers described in Chapter 2 were employed (NaSS as anionic monomer and DMAEMA as cationic one). For this work, three latex containing NaSS anionic monomer were used with an average particle size of 70 nm, 140 nm and 275 nm and another three latexes containing DMAEMA with an average particle size of 140 nm, 240 nm and 250 nm.

All the synthesis processes to produce different latexes are described in Appendix I, more precisely, Table I.1, I.2 and I.3, however, a brief description of these latexes in terms of final solids content and functional monomer amount used is given in Table 3.1.

To widen the portfolio of latexes with different particle sizes, NaSS and DMAEMA seeds (Chapter 2) were used as small size latexes (140 nm NaSS and 140 nm DMAEMA), whereas the large size latexes 275 nm NaSS (indicated as NaSS1 in Chapter 2), 240 nm DMAEMA (named as DMAEMA1 in Chapter 2) and 250 nm DMAEMA (indicated as DMAEMA3 in Chapter 2) were obtained by growing the seeds. Nonetheless, the possibility of producing an anionic latex with much lower size than 140 nm was attractive and this is why a new latex was synthetized following the recipe developed by Pérez-Martinez et al.[10]

All the latexes were synthesized using a two-step seeded semibatch process using a redox initiator system (TBHP/AsAc), except 70 nm NaSS latex, which was synthesized batchwise and

with potassium persulfate (KPS), meaning that KPS species will compete with NaSS sulfonate groups in the ionic bonding.

Table 3.1. Summary of the synthetized latexes.

Latex	dp (nm)	Ionic monomer (wbm%)	s.c. (%)
70 nm NaSS	70	2	30
140 nm NaSS	140	2	10
275 nm NaSS	275	1	50
140 nm DMAEMA	140	3	20
240 nm DMAEMA	240	1	50
250 nm DMAEMA	250	3	50

3.2.3. Latex Characterization

The conversion was calculated gravimetrically and the evolution and final particle size of the latexes was measured by DLS. The gel fraction was determined by Soxhlet extraction, using THF as the solvent. The molar masses of the soluble fraction of polymers was determined by SEC/GPC. Finally, incorporation of functional monomer and surface charge density were experimentally determined by titration. A detailed description of the characterization methods is provided in Appendix II.

3.2.4. Blends and film forming of oppositely charged dispersions

The effect of water-soluble compounds created during copolymerization of respective ionic monomer with BA/MMA on the electrostatic interactions between the oppositely charged

polymer particles was minimized by eliminating these species together with the non-ionic surfactant from the waterborne dispersion. For this purpose, all the dispersions were dialyzed using membranes with a cut-off of 12-14 kDa and following the water conductivity through these dialysis processes until a value around 2 μS cm^{-1} was achieved, which corresponds to the deionized water conductivity.

Blends were performed applying Kusy´s model to the systems,[9] where the necessary content of small particles (dispersed phase) to cover the large particles was defined. The minimum volume fraction of small size latex required to achieve the dispersed phase is defined as the critical volume fraction (Vc) and it is calculated as a function of the size ratio of large to small particles. This model output is graphically represented in Figure 3.1.

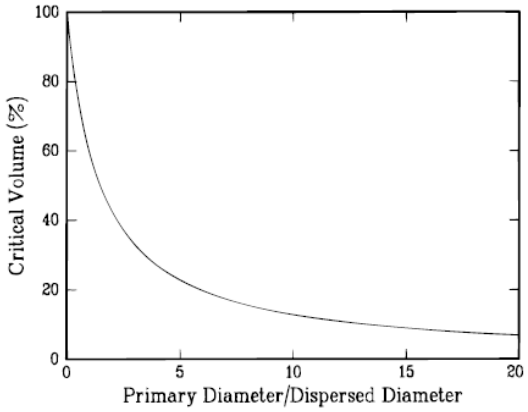

Figure 3.1. Critical volume fraction of small size latex as a function of the size ratio of large to small particles.[1,9]

When large and small soft particles are combined bellow the calculated Vc, means that there are insufficient small particles to form the desire continuous phase surrounding the bigger ones

and therefore, voids will be presented within the polymer film leading to a network with less ionic bonding points than expected. However, blending large/small soft particles above the Vc, much higher amount of small particles would be presented, affecting also negatively the expected ionic structure formed between large and small particles since the excess of small particles with the same charge will be in close contact.

Herein, four blends were prepared by blending oppositely charged dispersions with different particle sizes. Following Kusy's model, small particles content (Vc (%)) was calculated for each of the blend systems as described in Table 3.2. Blends were named by the particle size of the latexes used in each mixture.

Table 3.2. Quantity of each latex in the performed blends.

Latex (%)	Blend 70-240	Blend 140-240	Blend 275-140	Blend 70-250
70 nm NaSS	28	-	-	27
140 nm NaSS	-	43	-	-
275 nm NaSS	-	-	60	-
140 nm DMAEMA	-	-	40	-
240 nm DMAEMA	72	56	-	-
250 nm DMAEMA	-	-	-	73

The blends were prepared following the same procedure described in Chapter 2, meaning that all the blends were performed at two different pH. At pH> 7.5, where most of DMAEMA were in their neutral state avoiding the ionic bonding between the particles (reference material) and at pH< 7.5, where the formation of ionic structure was favoured (ionic complex material).

The pH of these blends were controlled employing NH_4OH and NaOH solutions, denoting that all the blends were prepared under basic pH. Owing to the volatility of NH_3 during film formation, a drop in the pH occurs, allowing the tertiary amine groups presented in the DMAEMA specie to turn into their protonated state.[11] On the contrary, NaOH is a non-volatile specie, implying that the pH of this solution will remain constant, ensuring that no ionic interactions will happen in the reference materials.

In all the cases, NH_4OH and NaOH solutions were added to the cationically charged latexes, ensuring pH was above 7.5 before mixing with the anionically charged latex to form the blend. Blends were mixed for two hours before casting into silicon molds and allowed drying for 7 days at 23 ± 2 °C and 55 ± 5 % relative humidity.

3.2.5. Polymer film characterization

The morphology of polymer films was studied by means of AFM. The thermal characterization of the blend polymer films was carried out by differential scanning calorimetry (DSC). The mechanical properties of the polymer films were determined by tensile test and the water sensitivity of the polymer films was analysed in terms of water uptake tests. The detailed description of these methods is provided in Appendix II.

3.3. Results and discussion

3.3.1. General overview of the latex characteristics

The main characteristics of all polymer latexes, are presented in Table 3.3. The latex characteristics, except 70 nm NaSS, were presented in Chapter 2. In case of 70 nm NaSS, high conversion (99%) was achieved and the gel fraction was above 70%, likely due to the presence of ionic species in the polymer chains, which decreases the solubility of the polymer in THF. The sol molar mass was in the expected range.[12] It can be said, that the observed characteristics of the 70 nm NaSS latex are similar to the other latexes presented in Chapter 2.

Table 3.3. Summary of the main characteristics of the latexes.

Latex	Conversion (%)	s.c. (%)	dp (nm)	Gel content (%)	Mw (kDa)	Đ
70 nm NaSS	99	30	70 ± 1	74 ± 2	144	2.4 ± 0.2

Table 3.4 summarizes the surface charge density values for each of the latexes employed in this work owed to the practical importance of this feature.

Table 3.4. Surface incorporation and surface charge density for each latex.

Latex	Surface incorporation (ionic monomer %)	Surface charge density ($\mu C\ cm^{-2}$)	Surface charge density/particle ($\mu C\ particle^{-1}$)
70 nm NaSS	90 ± 4[a]	14 ± 1	$1.8 \cdot 10^{-9}$
140 nm NaSS[b]	-	-	-
275 nm NaSS	70 ± 6	16 ± 2	$3.8 \cdot 10^{-8}$
140 nm DMAEMA	30 ± 2	4 ± 1	$2.5 \cdot 10^{-9}$
240 nm DMAEMA	33 ± 4	9 ± 2	$1.6 \cdot 10^{-8}$
250 nm DMAEMA	19 ± 4	19 ± 3	$3.7 \cdot 10^{-8}$

[a]Real incorporation of NaSS cannot be calculated owing to the presence of KPS
[b]Experimental error

The surface charge density is calculated taking into consideration the incorporated functional monomer content and the particle size diameter as described in Appendix II. For easier comparison, the surface charge density per particle (surface charge density $particle^{-1}$) values were also calculated and presented in Table 3.4. As expected, 275 nm NaSS and 250 nm DMAEMA latex show the highest values ($3.8 \cdot 10^{-8}$ and $3.7 \cdot 10^{-8}$ $\mu C\ particle^{-1}$, respectively) likely due to the higher functional monomer content incorporated onto particles and the lower number of particles in the system. In case of 70 nm NaSS, the surface charge density/particle decreases to $1.8 \cdot 10^{-9}$, due to the much higher number of particles, whereas 140 nm DMAEMA and 240 nm DMAEMA present lower values per particle ($2.5 \cdot 10^{-9}$ and $1.6 \cdot 10^{-8}$ $\mu C\ particle^{-1}$, respectively) owing to the lower incorporated amount of functional monomer and the higher number of particles. It is worth mentioning that the presence of ionic initiator (KPS) in case of 70 nm NaSS latex makes challenging the calculations of the surface charge densities and introducing

probably some error. On the other hand, regarding 140 nm NaSS, the incorporation and surface charge density could not be calculated owing to experimental errors. Theoretically, the expected surface charge density value was around 10-12 μC cm^{-2}.

3.3.2. Polymer blend film morphology

Two sets of blends were performed, being one set for the reference materials (at pH> 7.5) and the other set for the ionic complex materials (pH< 7.5). Homogeneous and transparent films were obtained in all the cases as shown in Figure 3.2.

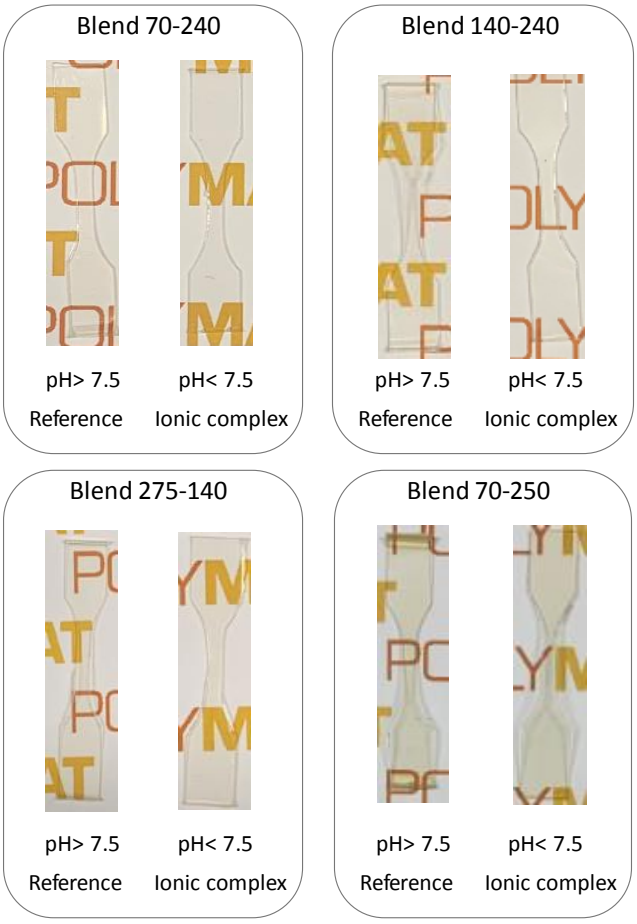

Figure 3.2. Blend polymer film appearance at different pH´s for Blend 70-240, 140-240, 275-140 and 70-250.

The polymer films surface was examined by AFM. Figure 3.3 and Figure 3.4 show representative AFM phase images of Blend 70-240 at 5 μm and 1 μm scale, respectively. AFM images of the other blend films are shown in Appendix IV. Clear distribution of small particles around big particles was observed on the surface of both films. Nevertheless, one can appreciate much smaller neat area of small particles in the ionic complex, which means that the particle

distribution was affected by pH, providing more probability for ionic complexation to happen. Furthermore, as observed in Figure 3.4 where further augmentation of the film surface and of individual particles is presented, the established ionic complexes affected the particle shape, which lost the identity of individual spherical particle, likely due to the multiple ionic bonds established between the large particles and a number of small ones. This occurrence is especially evidenced in Figure 3.5, where under inverted colours, the effect of ionic bonding between the particles on the particle morphology is obvious.

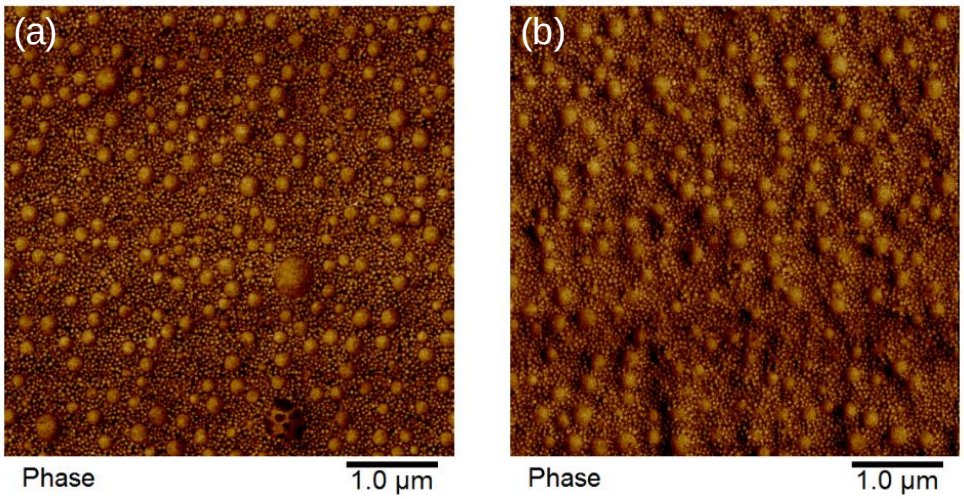

Figure 3.3. AFM air-film interface phase images for Blend 70-240 at 5 µm scale and at different pH´s. (a) refers to the reference material, while (b) refers to the ionic complex one.

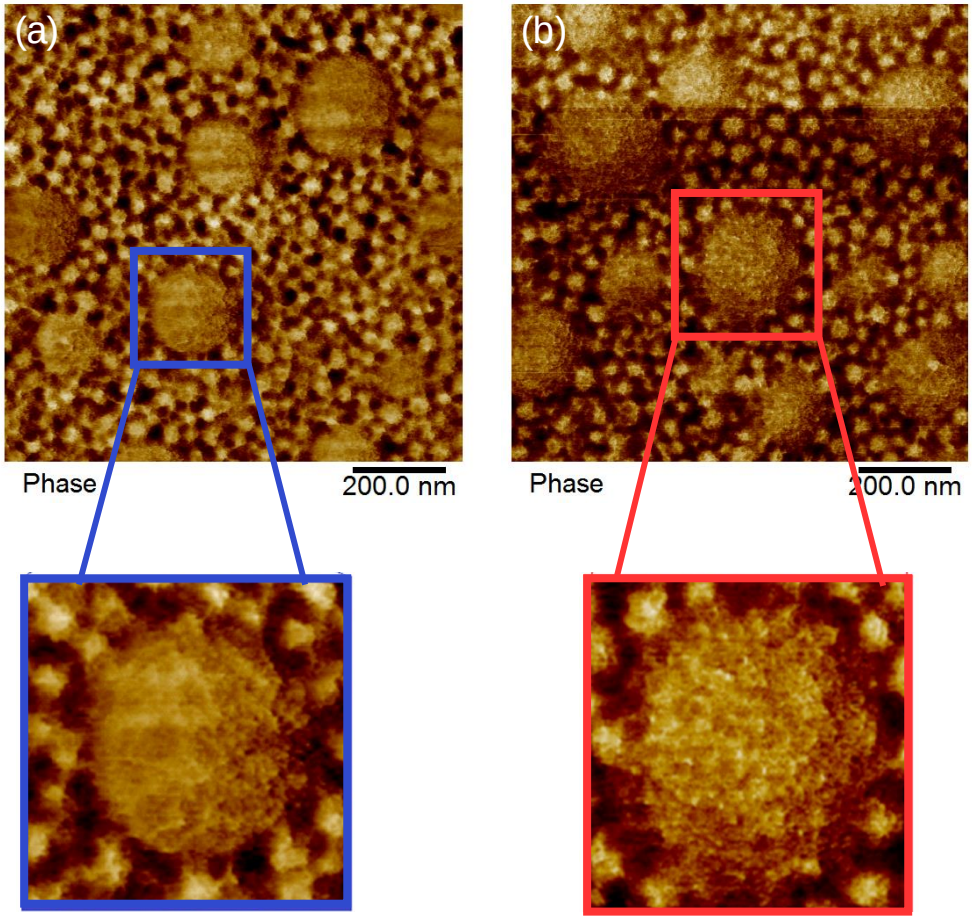

Figure 3.4. AFM air-film interface phase images for Blend 70-240 at 1 μm scale, at different pH´s and magnificated area presenting a single particle: (a) refers to the reference material, while (b) refers to the ionic complex.

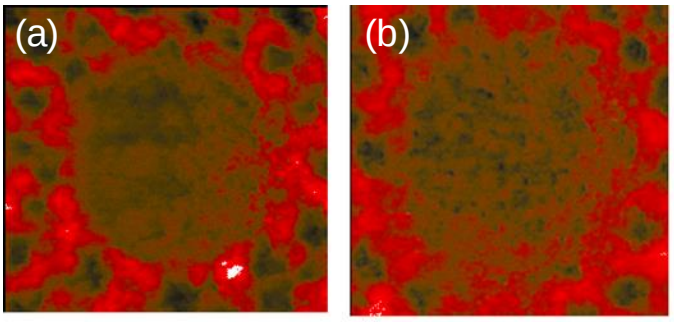

Figure 3.5. AFM air-film interface phase images at 1 μm scale for Blend 70-240 individual particles of (a) reference and (b) ionic complex under inverted colours effect.

3.3.3. Polymer blend film performance

Similar T_g values of the reference and ionic complex materials were observed, in a range of 17 – 20 °C, likely because the main monomers in the both blended polymers were the same (BA/MMA in 50/50 wt. ratio).

Before discussing the different properties of the blends, the total positive and negative charges in each blend were calculated as presented in Table 3.5. A summary of the equations used for determining the neat charge in each of the blends can be found in Appendix II. These calculations offer an approximation of positive and negative charges involve in each of the blended systems. However, it is not straightforward to relate the possible established ionic bond points since the distribution of these charges through the particles' surface and the distribution of these ionically charged particles within the blends are the key point for the formation of ionic bonds. Nevertheless, these values might help understanding some of the results obtained.

Table 3.5. Neat charge calculation for each of the blends.

Blend	Latex	Charge per particle ($\mu C\ particle^{-1}$)	Total charge in the blend (μC)	Experimental neat charge in the blend (μC)[a]	Theoretical neat charge in the blend (μC)[a]
Blend 70-240	70 nm NaSS	$2.2 \cdot 10^{-9}$	$-7.2 \cdot 10^{6}$	$-3.7 \cdot 10^{6}$	-
	240 nm DMAEMA	$1.6 \cdot 10^{-8}$	$+3.5 \cdot 10^{6}$		
Blend[b] 140-240	140 nm NaSS	-	-	-	$+1.3 \cdot 10^{6}$ – $+2.1 \cdot 10^{6}$
	240 nm DMAEMA	$1.6 \cdot 10^{-8}$	$+2.8 \cdot 10^{6}$		
Blend 275-140	275 nm NaSS	$3.8 \cdot 10^{-8}$	$-1.5 \cdot 10^{6}$	$-3.1 \cdot 10^{6}$	-
	140 nm DMAEMA	$2.5 \cdot 10^{-9}$	$+4.6 \cdot 10^{6}$		
Blend 70-250	70 nm NaSS	$2.2 \cdot 10^{-9}$	$-7.1 \cdot 10^{6}$	$-1.8 \cdot 10^{5}$	-
	250 nm DMAEMA	$3.7 \cdot 10^{-8}$	$+7.3 \cdot 10^{6}$		

[a]The positive sign refers to an excess of cationic charges, while the negative sign indicates an excess of negative charges.
[b]Theoretical neat charge in Blend 140-240 was calculated as surface charge density of 140 nm NaSS could not be experimentally calculated.

The stress-strain behaviour of the polymer films cast from the blends at different pH is shown in Figure 3.6 and the mechanical properties related to the stress-strain curves are summarized in Table 3.6.

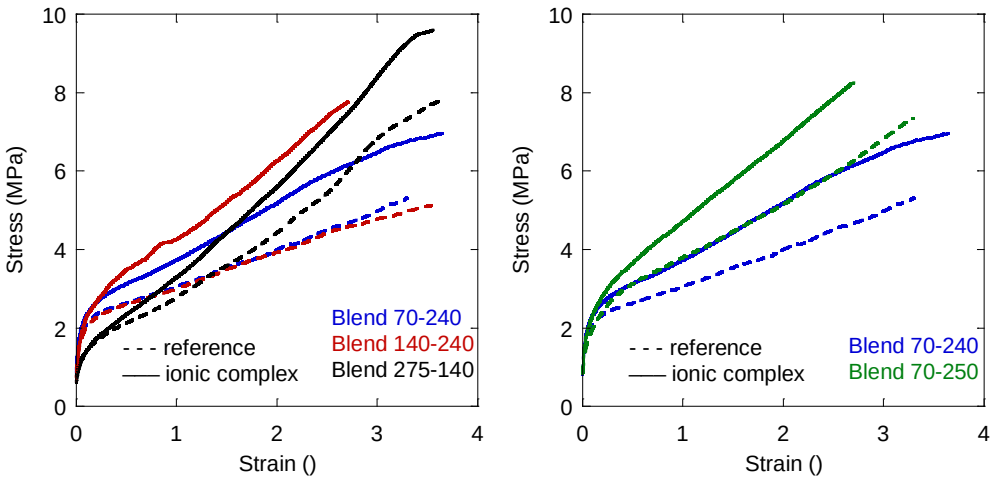

Figure 3.6. The stress-strain behaviour for (a) Blend 70-240, 140-240 and 275-140 and (b) Blend 70-240 and 70-250 at different pH´s. Reference blend films are indicated with discontinuous line, while a continuous line is used for ionic complex blend films.

Table 3.6. Mechanical properties of the polymer blends performed related to the stress-strain plots represented in Figure 3.6.

Blend type		Young´s modulus (MPa)	Elongation at break	Ultimate strength (MPa)	Toughness (MPa)
Blend 70-240	Reference	15 ± 1	3.5 ± 0.2	5.7 ± 0.3	17.7 ± 8.0
	Ionic complex	16 ± 1	3.2 ± 0.6	6.6 ± 0.6	21.8 ± 8.1
Blend 140-240	Reference	13 ± 1	3.2 ± 1.3	5.1 ± 0.7	22.2 ± 8.5
	Ionic complex	16 ± 1	2.7 ± 0.5	7.3 ± 1.4	31.2 ± 7.1
Blend 275-140	Reference	10 ± 1	3.4 ± 0.4	7.4 ± 0.9	26.8 ± 4.7
	Ionic complex	10 ± 1	3.3 ± 0.2	8.3 ± 0.8	28.5 ± 4.3
Blend 70-250	Reference	15 ± 0	3.1 ± 0.2	7.0 ± 0.9	27. 2 ± 4.4
	Ionic complex	17 ± 1	2.4 ± 0.4	7.7 ± 1.1	29.4 ± 1.6

As a general trend, higher Young modulus, ultimate strength and toughness were obtained for ionic complexed materials likely owing to the ionic complexation. The elongation at break drop slightly, which is a characteristic for reinforced systems.[13] This behaviour is opposite than the one observed in previous chapter, where, as main effect of ionic bonding was the increase flexibility. The difference is probably result on the extent of ionic complexation, which is obviously higher in this study, and provided much solid reinforcement. Nevertheless, it is worth mentioning that the present drop in elongation at break is negligible and much lower than expected. Nevertheless, Blend 275-140 does not follow this general behaviour since similar Young modulus and strain at break was obtained for the reference and ionic complex material.

When the size of NaSS latex was varied (Blend 70-240 and Blend 140-240), oppositely than expected (if only the particle size is taken into consideration), the ionic complex Blend 140-240, presents substantially improved ultimate strength and toughness than the reference, while this difference was modest for Blend 70-240 (Table 3.6). This is probably related to less ionic inter-particle bonds formation in the last, affected by few factors. On the one hand, higher neat negative charge in Blend 70-240 than the neat positive charge in Blend 140-240 (Table 3.5), which suggests that there will be more non-neutralized ionic functionalities in the Blend 70-240. On the other hand, as can be observed in AFM images in Figure 3.4, there are still neat polymer areas made only of 70 nm NaSS particles around individual 240 nm DMAEMA, where no ionic bonding was established. These areas are much smaller in the ionic complex of Blend 140-240 (Figure IV.1, Appendix IV). Even though, optimal packing fractions of both latexes were calculated according Kusy's principle[1,9], as their model take into account the ratio between

particles' diameter and not surface area, obviously the fraction of the small particles was overestimated. This effect is larger in case of Blend 70-240 than in Blend 140-240, as observed in AFM images. Regarding the Blend 275-140, slightly lower mechanical resistance improvement was observed after the ionic complexation, likely due to higher neat charge (Table 3.5).

The main difference between Blends 70-240 and 70-250, is the surface charge density of the large DMAEMA particles (240 nm DMAEMA latex is 9 μC cm^{-2} and the one for 250 nm DMAEMA latex is about 19 μC cm^{-2}, see Table 3.4). Both systems present similar improvement of mechanical performance (Table 3.6), despite the much higher neat charge observed for Blend 70-240 (Table 3.5). This is probably a consequence of two contradictory effects. While the larger surface charge density in the Blend 70-250 offers more ions for complexations at the same surface area and less neat charge, Figure IV.3 (Appendix IV) shows that the packaging of the particles seems to be worse than in case of Blend 70-240 (Figure 3.3 and Figure 3.4). Despite neat NaSS polymer areas observed in Blend 70-240, Figure IV.3 in Appendix IV reveals additional presence of groups of DMAEMA polymeric particles in Blend 70-250.

Another important requirement for waterborne coatings is water resistance of the polymer films. As mentioned in Chapter 1 and Chapter 2, the presence of ionic species, including the water-soluble polymer chains, within the film affect negatively the water absorption, lowering the water resistance of the polymer film.[13,14] The established ionic complexes decrease the neat charge present in the system and contribute to a water resistance enhancement.[15] The water uptake results for these polymer blends are presented in Figure 3.7, in which the observed trends

are in accordance to tensile results. The Blends 70-240, 140-240 and 70-250 show increased water resistance compared to the respective reference films, whereas both reference and ionic complex films of Blend 275-140 exhibit similar behaviour after immersing in water.

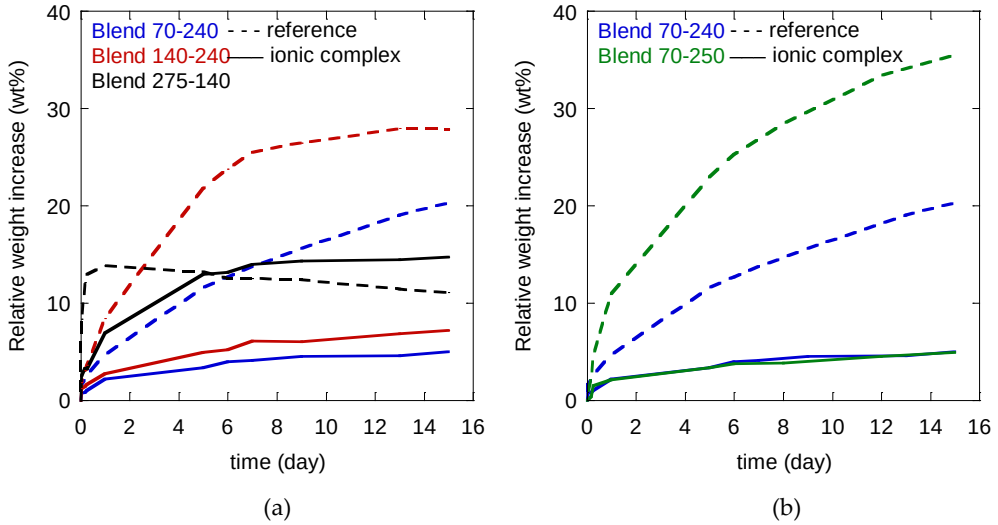

Figure 3.7. Water uptake evolution for (a) Blend 70-240, 140-240 and 275-140 and (b) Blend 70-240 and blend 70-250 polymer films at different pH´s. While reference blend films are indicated with discontinuous line, a continuous line is used for ionic complex blend films.

The reference Blends 70-240, 140-240 and 70-250 absorb water between 20 wt% and 35 wt% after 14 days immersion in water, likely due to high content of hydrophilic moieties present in the films (the sulfonate groups from NaSS). Their complement complexed materials show very low weight increase (< 8 wt%), meaning that most of the ionic species presented on the particles surface were neutralized owing to the ionic inter-particle complexes formed between the oppositely charged species. The increased contact between oppositely charged particles due to

the more efficient particle packaging probably contribute to the higher neutralization compared to the results in previous Chapter.

When comparing Blend 70-240 and 140-240 (NaSS latex varied), rather similar water uptake values were observed despite the ionic complex of Blend 140-240 contain almost doubled quantity of NaSS latex than the Blend 70-240 ionic complex. This accounts for important ionic complexation and high density ionic network creation in Blend 140-240 film, in accordance to highest reinforcement effect observed by tensile measurements (Figure 3.6 and Table 3.5).

Blend 275-140 shows higher water penetration within the reference blend during the first hours than in the complex material. Nevertheless, after two weeks of immersion, both blend films present similar water absorption. The poorest water resistance, probably is owed to the high amount of free sulfonate groups (uncomplexed NaSS), as similar behaviour was noticed in the NaSS stabilized BA/MMA films previously.[13]

By comparing Blends 70-240 and 70-250 (9 μC cm^{-2} for 240 nm DMAEMA and 19 μC cm^{-2} for 250 nm DMAEMA, respectively), while no difference was detected for complexed materials, clear effect of the surface charge density and the neat charge on water penetration for the reference blends was observed. This is another demonstration that the efficient ionic complexation in Blend 70-250 occurred, resulting in the largest effect in water sensitivity decrease between reference and ionic complex (water uptake dropped from 35% to 5%).

It is important to remark that after the water uptake experiments all the films lost weight due to solubilisation of some species and their diffusion out of the films. Figure 3.8 presents the quantities of the weight loss in each of the studied films. It may be deduced that although dialyzed latex were employed for these blends, the presence of polymer chains with higher molecular weight than the membrane cut-off (12 – 14 kDa) might be responsible for the observed weight loss. For Blends 70-240, 70-250, 140-240 and 275-140, the amount of material lost was lower than 1 wt% (with respect to the initial dry weight as explain in Appendix II). As seen in Figure 3.8, the reference materials lost more weight than the respective ionic complexes. It might be due to two reasons, either a change of the water solubility of the oligomers due to ionic complexation between them, or, the established ionic complexed network prevented their diffusion towards the water phase. Nevertheless, whatever of these two phenomena happen, the presence of ionic complexed materials increased the stability of coatings contributing to the environmental impact, reducing the leakage into environment.

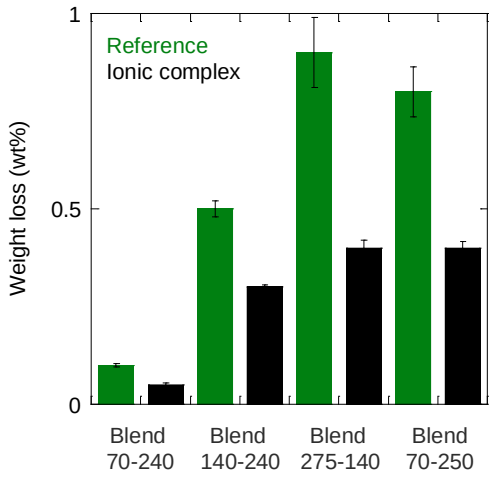

Figure 3.8. Weight loss (wt%) for the reference and ionic complex materials of the Blend 70-240, 140-240, 275-140 and 70-250.

3.4. Conclusions

The main aim of this work was to examine the packaging effect (increasing contact) between particles (more efficient particle packaging) by blending oppositely charged latexes with different average particle size on the ionic inter-particle complexation and therefore, on the final performance of the waterborne polymer film.

Charged polymer dispersions were synthesis by batch and semibatch emulsion copolymerization processes using a typical coating formulation BA/MMA (50/50 wt%). Six type of latexes were employed, three latex containing NaSS anionic monomer with an average particle size of 70 nm, 140 nm and 275 nm and another three latex containing DMAEMA with an average particle size of 140 nm, 240 nm and 250 nm.

Four different blends were performed (Blend 70-240, 70-250, 140-240 and 275-140) at two pH´s.

Visually, transparent and homogeneous films were observed. In AFM micrographs, a homogeneous distribution of large/small particles for both set of blends (reference and ionic complex materials) was seen when films surface was studied. On the other hand, ionic complex materials showed smaller neat NaSS polymer areas than in the reference films, which means the distribution of the particles within the film was affected by pH, providing more probability for ionic complexation to happen. Furthermore, while the particles kept their spherical morphology in the surface of the reference material, this pure morphology is lost in the ionic complex material.

Almost all ionic complex materials presented improved mechanical properties compared to their respective reference films, except Blend 275-140, for which the reference and ionic complex materials behaved quite similar. The observed trends indicated that the behaviour of the ionic complex was affected not only by the size of the blended latexes, but as well by their surface charge densities and the particle distribution and packing.

Regarding the water sensitivity, similar trends as for mechanical properties were observed. Nevertheless, while the reference latexes absorbed large water amounts in correspondence to the amount of ionic species presented (especially sulfonate functionalities that were in ionic form), the ionic complexes presented important drop in water absorption, probably due to the neutralization effect of the ions during ionic bonding. Interestingly, the reference materials

seemed to lose more weight than the respective ionic complexed materials after drying the immersed films in water, likely due to the lack of ionic structures that might act as a physical barrier to polymer chains diffusion.

Thus, it was demonstrated that by simple achieving more efficient particle packaging, the increased contact between large/small particles might contribute to increase the ionic bonding points reinforcing the inter-particle complexes as seen in the tensile test and water uptake test.

3.5. References

(1) Tzitzinou, A.; Keddie, J. L.; Geurts, J. M.; Peters, A. C. I. A.; Satguru, R. Film Formation of Latex Blends with Bimodal Particle Size Distributions: Consideration of Particle Deformability and Continuity of the Dispersed Phase. *Macromolecules* **2000**, *33* (7), 2695–2708. https://doi.org/10.1021/ma991372z.

(2) Colombini, D.; Hassander, H.; Karlsson, O. J.; Maurer, F. H. J. Influence of the Particle Size and Particle Size Ratio on the Morphology and Viscoelastic Properties of Bimodal Hard/Soft Latex Blends. *Macromolecules* **2004**, *37* (18), 6865–6873. https://doi.org/10.1021/ma030455j.

(3) Gauthier, C.; Guyot, A.; Perez, J.; Sindt, O. Film Formation and Mechanical Behavior of Polymer Latices. *ACS Symp. Ser.* **1996**, *648* (1), 163–178. https://doi.org/10.1021/bk-1996-0648.ch010.

(4) Feng, J.; Odrobina, E.; Winnik, M. A. Effect of Hard Polymer Filler Particles on Polymer Diffusion in a Low-Tg Latex Film. *Macromolecules* **1998**, *31* (16), 5290–5299. https://doi.org/10.1021/ma980117w.

(5) Feng, J.; Winnik, M. A.; Shivers, R. R.; Clubb, B. Polymer Blend Latex Films: Morphology and Transparency. *Macromolecules* **1995**, *28* (23), 7671–7682. https://doi.org/10.1021/ma00127a013.

(6) Robeson, L. M.; Vratsanos, M. S. Mechanical Characterization of Vinyl Acetate Based Emulsion Polymer Blends. *Macromolar Symp.* **2000**, *155*, 117–138.

(7) Peters, A. C. I. A.; Overbeek, G. C.; Buckmann, A. J. P.; Padget, J. C.; Annable, T. Bimodal Dispersions in Coatings Applications. *Prog. Org. Coatings* **1996**, *29*, 183–194.

(8) Eckersley, S. T.; Helmer, B. J. Mechanistic Considerations of Particle Size Effects on Film Properties of Hard/Soft Latex Blends. *J. Coatings Technol.* **1997**, *69* (864), 97–107. https://doi.org/10.1007/bf02696096.

(9) Kusy, R. P. Influence of Particle Size Ratio on the Continuity of Aggregates. *J. Appl. Phys.* **1977**, *48* (12), 5301–5305. https://doi.org/10.1063/1.323560.

(10) Pérez, B. T.; Tomovska, R. Comparison of Microwave Vs . Conventional Heating Polymerizations and Possible MW Applications in Polymers, Polymat and University of the Basque Country (EHU/UPV), 2021.

(11) González, E.; Barandiaran, M. J.; Paulis, M. Isolation of the Effect of the Hairy Layer Length on the Mechanical Properties of Waterborne Coatings. *Prog. Org. Coatings* **2015**, *88*, 137–143. https://doi.org/10.1016/j.porgcoat.2015.06.027.

(12) González, I.; Asua, J. M.; Leiza, J. R. The Role of Methyl Methacrylate on Branching and Gel Formation in the Emulsion Copolymerization of BA/MMA. *Polymer (Guildf).* **2007**, *48* (9), 2542–2547. https://doi.org/10.1016/j.polymer.2007.03.015.

(13) Bilgin, S.; Tomovska, R.; Asua, J. M. Effect of Ionic Monomer Concentration on Latex and Film Properties for Surfactant-Free High Solids Content Polymer Dispersions. *Eur. Polym. J.* **2017**, *93*, 480–494. https://doi.org/10.1016/j.eurpolymj.2017.06.029.

(14) González, E.; Paulis, M.; Barandiaran, M. J. Effect of Controlled Length Acrylic Acid-Based Electrosteric Stabilizers on Latex Film Properties. *Eur. Polym. J.* **2014**, *59*, 122–128. https://doi.org/10.1016/j.eurpolymj.2014.07.023.

(15) Argaiz, M.; Ruipérez, F.; Aguirre, M.; Tomovska, R. Ionic Inter-Particle Complexation Effect on the Performance of Waterborne Coatings. *Polymers (Basel).* **2021**, *13* (18), 1–18. https://doi.org/10.3390/polym13183098.

Chapter 4. Ionic complexation of particles charged by using ionic monomers with two charges per molecule

4.1. Introduction

In the first Chapters of this manuscript, it has been shown that not only the mechanical resistance of the polymeric films was increased by ionic bonding between particles, producing stiffer films without important loss of flexibility, but also the water penetration within the polymeric films was considerably hindered. By exploring the process of polymer chains interdifussion using FRET analysis, it was found that the established ionic complexation between the particles reduced significantly the interdiffusion process of polymer chains. By improving the possibility for creation of ionic bonding between the particles combining small and large oppositely charged particles, the reinforcement of the polymer film was enhanced.

These results suggest that, by further promotion of ionic interactions, the performance of the waterborne coatings might be enhanced even more. A possible approach is to multiply the ionic bonds between the particles by increasing the charge density on the particles' surface. Nevertheless, further increase of the quantity of functional monomers is challenging for their incorporation (due to their high water solubility) and it increases importantly the water

sensitivity of the coating films. A possible solution to this problem can be to increase the charge density without increasing the quantity of functional monomers using functional monomers that contain more than one charge per molecule.

Therefore, this Chapter is focused on multiplying the ionic bonds between oppositely charged particles in polymer blend, in which the charges were provided by incorporation of ionic monomers with two charges per molecule. For this purpose, IA (Figure 4.1a) was used as anionic monomer, whereas DABCO (Figure 4.1b) was selected as the cationic one. They were copolymerized with BA/MMA (50/50 wt ratio) main monomers as in the previous Chapters.

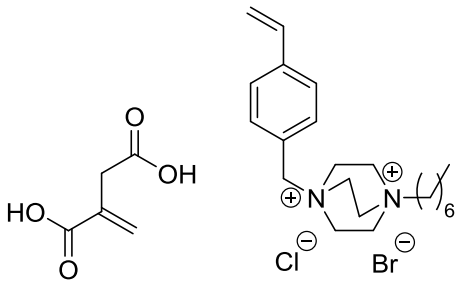

(a) (b)

Figure 4.1. Chemical structure of (a) itaconic acid anionic monomer and (b) styrenic DABCO cationic monomer.

The incorporation of the doubly charged monomers will be a key point to enable the study of the ionic bonding effect on the film performance. Incorporation of IA monomer onto BA/MMA polymer particles by emulsion polymerization has been scarcely studied. For instance, Oliveira et al. reported the emulsion copolymerization of BA and MMA in presence of IA.[1,2] They reported that higher IA content negatively affected the polymerization rate, number of particles,

coagulum formation, wet scrub and water resistance. However, its chemical structure made this monomer interest for this work. On the other hand, the solution homopolymerization and the copolymerization of DABCO cationic monomer with BA by free radical polymerization in dimethyl sulfoxide (DMSO) solvent has been recently reported.[3] Up to our best knowledge, there is nothing reported on incorporation of DABCO onto BA/MMA particles, neither its copolymerization with (meth)acrylic monomers in emulsion polymerization.

4.2. Experimental part

4.2.1. Materials

The materials are given in Appendix I.

4.2.2. DABCO monomer synthesis and characterization

The cationic monomer DABCO is not commercially available, so prior to polymerization reaction, DABCO was synthesized, following the procedure reported by Zhang et al.[3] as found in Appendix V. Later, the hydrophilicity of DABCO monomer was studied to design the proper polymerization process for incorporating this specie as described in Appendix V.

4.2.3. Synthesis of ionically charged dispersions

Ionically charged waterborne polymer dispersions were synthesized by a two-step seeded semibatch emulsion polymerization process. A typical acrylic formulation, 50/50 BA/MMA was used and IA and DABCO functional monomers were selected to give the ionic character to the

latexes. In this work, in order to incorporate functional monomers into BA/MMA, the synthetic procedure followed in Chapter 2 was used, however, this time the use of ionic surfactant was necessary to obtain stable latexes (sodium dodecyl sulfate, SDS and dodecyltrimethylammonium bromide, DTAB).

In the first step, a seed with 50/50 BA/MMA at 10% s.c. for anionically charged system and 20% for cationic one was prepared. Formulations for the seed synthesis of anionically and cationically charged waterborne dispersions are shown in Appendix I, Table I.4. The desire amount of seed was loaded for the second part of the polymerizations employing BA/MMA, 1/1, by weight. While 1% relative to the main monomers (BA and MMA) of IA was used for anionically charged dispersion, two different concentration of DABCO ionic monomer were used 1% and 1.8%. Upon achieving the desire temperature, 60 °C, the compounds were fed in three streams: initiator redox couple aqueous solutions (FF7/TBHP) and a preemulsion containing BA, MMA, functional monomers and the respective surfactant reaching final solids content of 40%. After the feeding period (180 minutes), the system was allowed to react for one more hour. The formulations are presented in Appendix I, Table I.5 and the schematic view of the processes is illustrated in Scheme 4.1. These polymer dispersions were named as IA1 (when 1 wbm% IA was used), DABCO1 (when using 1 wbm% DABCO) and DABCO1.8 (when employing 1.8% DABCO).

	Initial charge	Feeding	Initial charge	Feeding
IA1	BA/MMA/IA Surfactant	1. FF7 2. TBHP	Seed (10% s.c.)	1. BA/MMA 2. FF7IA/ Surfactant 3. TBHP

t_0 — 1st step — 2nd step — t_{final}

	Initial charge	Feeding	Initial charge	Feeding
DABCO1 **DABCO1.8**	BA/MMA/ DABCO/ Surfactant	1. FF7 2. TBHP	Seed (20% s.c.)	1. BA/MMA 2. FF7/DABCO Surfactant 3. TBHP

Scheme 4.1. Schematic view of the latex synthesis procedures.

4.2.4. Latex characterization

The conversion was measured gravimetrically and the average particle size of the latexes was analysed by DLS. The gel fraction was measured by Soxhlet extraction, using THF solvent. The molar masses of the soluble fraction of polymers was determined by SEC/GPC. Incorporation of functional monomers, surface charge density and ionic monomer fraction participating in the formation of water-soluble species were determined by titration. A detailed description of the characterization methods is provided in Appendix II.

4.2.5. Blends and film formation of oppositely charged dispersions

The main characteristic of IA is its pH dependency owing to its two pKas, $pKa_1 = 3.85$ and $pKa_2 = 5.45$,[1] while DABCO does not present any pKa value, due to the presence of the two quaternary ammonium groups. This means that when the pH of the blend is below 3.8, the IA

molecules are in their molecular form preventing the ionic interactions (the blends prepared at this pH will be called reference material), whereas when the pH is higher than 5.5, anionic groups will be formed favouring the ionic complexation between the carboxylic groups presented in IA and the quaternary ammonium groups of the DABCO unit (this will be called complex material).

In order to ensure that the species contributing to the ionic bonding were coming from the functional monomers, the latexes were dialyzed against water to remove the water-soluble species and ionic surfactants from the waterborne dispersions. For this purpose, Spectra-Por®4 membranes (M_w cut-off 12,000-14,000 Da) were employed. Conductivity of water was followed until a value around 2 $\mu S\ cm^{-1}$ was reached, which corresponds to the deionized water conductivity.

The blends were prepared by mixing both dialyzed latexes based on the equal number of opposite charges. Firstly, 1% ionic monomer (IA1 and DABCO1) containing latexes were used. As the incorporation of the DABCO into polymer particles is lower than the incorporation of IA (Table 4.4), more amount of DABCO containing latex was added to the blends in order to obtain equal number of oppositely charge species.

In order to increase the ionic bonding effect, blends were also performed between IA1 and DABCO1.8 containing dispersions since both latexes showed similar average particle size and surface charge density (Table 4.3 and Table 4.4). A summary of the prepared blends is shown in Table 4.1. Blends were named as Blend C indicating that the blends were performed considering

the surface charge density. The numbers refer to the concentration of each latex used (IA containing latex-DABCO containing latex).

Table 4.1. Summary of the performed blends between IA and DABCO containing latex based on their surface charge density parameter.

	Latex (mL)	
	Blend C1-1	**Blend C1-1.8**
IA1	3	5
DABCO1	5	-
DABCO1.8	-	5

Unfortunately, despite of the addition of buffers (formic acid and citric acid/sodium phosphate) into the IA containing latex in order to decrease the pH and ensure the deprotonated state of carboxylic groups, instantaneous aggregation was obtained immediately after adding the cationic latex.

To prevent premature coagulation of oppositely charged polymer particles during blending, sterically protective polymeric species as polyvinylpyrrolidone (PVP), polyvinyl alcohol (PVOH) and pluronic F-108 were employed as physically absorbing protective polymers onto the IA and DABCO polymer particles.

Blend C1-1 and Blend C1-1.8 (Table 4.1) were prepared at two different pHs. At pH> 5.5, at which all the species are in their ionic state (ionic complex material) and at pH< 3.9, where no ionic interactions were expected, as IA would be in its molecular state (reference material). As pH of both polymer dispersions was 7 (the reason will be described in Results and discussion

section), no buffer was employed for the ionic blend preparation, while phosphoric acid (sodium) buffer was used for the reference blend preparation to decrease the pH.

The blend dispersions were mixed for two hours before casting into silicon molds. It should be mentioned that the pH of the dispersions was controlled during the mixing time. Furthermore, the original latexes containing either IA or DABCO were also individually mixed with the selected protective specie and dried in order to examine their final performance. These polymer films were named as IA1, DABCO1 and DABCO1.8.

4.2.6. Polymer film characterization

The mechanical properties of the polymer films were measured by tensile tests and the water sensitivity of polymer films was analysed in terms of water uptake test. The detailed description of these methods is provided in Appendix II.

4.3. Results and discussion

Because DABCO cationic monomer is not available commercially, before the charged latexes synthesis, it was synthesised following reported approach.[3] The chemical structure of the purified DABCO monomer was confirmed by ^{1}H-NMR analysis (Appendix V, Figure V.1). The reaction yield was around 70%, which was in agreement with Zhang et al.[3] Moreover, the partition of the monomer between the aqueous phase and BA/MMA monomers was studied, indicating that the monomer was highly hydrophilic. Owing to the similarities with NaSS monomer in terms of hydrophilicity, the polymerization procedure of copolymerization of ionic

monomer with BA/MMA developed by Sevilay et al.[4] was employed in this work to incorporate DABCO onto BA/MMA particles. These results are described in Appendix V.

4.3.1. Characteristics of the charged polymer dispersions

The cationically and anionically charged latexes were synthesized in a two-step seeded semibatch emulsion polymerization process, during which in the first step a seed latex was prepared used afterwards to synthesize the final charged dispersions in a semibatch process. Table 4.2 summarizes the conversion and the particles of the seed latexes. Almost complete conversion was obtained at the end of the polymerization for both dispersions, reaching values above 97%. Average particle size of IA containing latex was 83 nm, and 105 nm for the DABCO one.

Table 4.2. A summary of the conversion and average particle size for the seed latexes.

Seed latex	Conversion (%)	dp (nm)
IA	98	83 ± 1
DABCO	97	105 ± 2

The kinetics of the second stage of the polymerizations carried out using two different functional monomers and different concentrations in case of DABCO are presented in Figure 4.2a. In all the cases, the instantaneous conversion along the reactions was above 95% (Table 4.3), confirming low monomer concentration in the reactor, which is a condition to eliminate the effect of reactivity ratios of the monomers on the copolymer composition and to decrease the

possibility of new particles creation due to secondary nucleation. Although there are some works in the literature stating that the presence of functional monomers as IA can slow down the polymerization[1], in this study no similar effect was observed. Regarding the particle size (Table 4.3) it can be seen that final particle size of 155 nm was achieved for IA1 latex, whereas an average particle size of 156 and 158 nm was obtained for DABCO1 and DABCO1.8, respectively. As it can be seen in Figure 4.2b, where the theoretical and experimental evolution of particle size are shown, they were similar along the reactions.

Table 4.3. Final conversion and average particle size for each of the latexes.

Latex	Conversion (%)	dp (nm)
IA1	98	155 ± 1
DABCO1	97	156 ± 2
DABCO1.8	97	158 ± 2

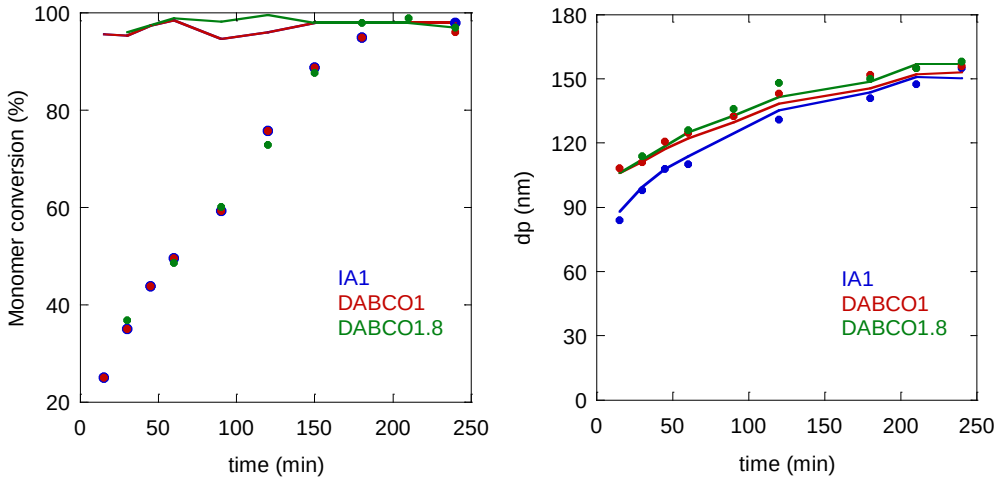

(a) (b)

Figure 4.2. Time evolution of (a) overall (dots) and instantaneous (continuous lines) monomer conversions; and (b) experimental (dots) and theoretical (continuous lines) particle size of anionically and cationically charged latexes.

The surface charge characteristics of the polymer latexes are presented in Table 4.4. Even though higher DABCO monomer incorporation (40-45 wt% functional monomer) than for IA1 (35% functional monomer) was obtained, DABCO latex presents lower surface charge density. This is based on the fact that the functional monomers' content was calculated in ionic monomer wt%, while there is an important difference of functional monomers' molar masses (IA monomer, 430 g mol^{-1} and DABCO 130 g mol^{-1}).

The surface incorporation of DABCO slightly increased with monomer concentration in the formulation (from 1 wbm% to 1.8 wbm%) and thus, the surface charge density was almost doubled (from 6 μC cm^{-2} for DABCO1 to 10 μC cm^{-2} for DABCO1.8). Higher DABCO

incorporation did not affect the kinetics, particle size evolution and the final particle size of cationic latexes, likely because the reaction was carried out under monomer starved conditions.

As expected, due to the hydrophilicity of the functional monomers, relatively high fraction of ionic monomer participated in the formation of water-soluble species, above 30% respect to the initial functional monomer content, for the three latexes (Table 4.4).

Table 4.4. Surface incorporation of ionic monomer and the fraction of ionic monomer contributing to the water-soluble species for anionically and cationically charged particles.

Latex	Surface incorporation (ionic monomer %)	Surface charge density ($\mu C\ cm^{-2}$)	Fraction of ionic monomer in water - soluble species (ionic monomer %)
IA1	35 ± 1	13 ± 1	30 ± 8
DABCO1	40 ± 6	6 ± 1	34 ± 3
DABCO1.8	45 ± 3	10 ± 1	31 ± 5

The polymer microstructure was analysed by determining the insoluble part of the polymer in THF by Soxhlet extraction (gel content) and the molar mass of the soluble part of the polymer. As observed in Table 4.5, IA and DABCO containing latexes present a significant amount of insoluble polymer, above 48%. Both, the presence of ionic species in the polymer chains and the formation of a physical gel might contribute to the formation of THF insoluble polymer.[4,5] The molar masses were in the expected range considering the emulsion polymerization process (Table 4.5). As expected, the molar mass decreases for higher gel fractions, since higher

molecular weight chains were incorporated into the gel. The polydispersity index values were in range of the ones normally obtained in BA/MMA emulsion polymerizations.

Table 4.5. THF insoluble polymer fraction, molar mass of the soluble part measured by GPC for anionically and cationically charged particles.

Latex	Gel content (%)	M_w (kDa)	Đ
IA1	48 ± 1	346 ± 45	2.4 ± 0.3
DABCO1	55 ± 1	316 ± 16	2.4 ± 0.2
DABCO1.8	50 ± 2	340 ± 30	2.5 ± 0.4

4.3.2. Polymer blend films performance

Formic acid and citric acid/sodium phosphate buffers were used to control pH during blending of IA and DABCO latexes. Even though the pH was kept bellow pKas of IA (5.45 and 3.85) during blending to keep carboxylic groups (-COOH) protonated, the blends coagulated instantaneously. There are few possible causes behind this behaviour. High ionic strength in these dispersions, affected further by the buffer addition might induced massive coagulation. On the other hand, it is difficult to ensure complete neutralization of -COOH groups in IA, which additionally may establish H-bonding with the quaternary ammonium groups of DABCO and might synergistically lead towards instantaneous coagulation.

To avoid this instantaneous aggregation, water-soluble polymeric/non-ionic surfactants were employed as steric obstacle between the particles, with an idea of postponing the ionic interaction and to have sufficient time to prepare the films before coagulation. A recent work in

the literature showed that among other surfactants, pluronic F-108 presents good performance, providing stability to the dispersions when blending oppositely charged polymer particles.[6] Hueckel et al. synthetized charge particles using ionic initiators with a final solids content of 5% and the effect of absorbing different protective polymers named pluronic family (F-38, F-68, F-127 and F-108) onto polymer particles was examined theoretically and experimentally. These protective polymers behave as non-ionic surfactant. Pluronic family surfactants are composed of triblock copolymers poly(ethylene oxide)-block-poly(propylene oxide)-block-poly(ethylene oxide) (PEO-PPO-PEO). The polymer architecture comprises an anchoring block of PPO and a variable spacer block of PEO. In these species, polymer brush length decreases from F108 to F38. It was demonstrated that, when used very diluted polymer dispersions (5 wt%) employing these polymeric stabilizers with equal or higher length (L) than the Debye length (λ_D) of particles, overlapping of the double layers between adjacent particles is prevented, ensuring stable oppositely charged dispersions. On the contrary, a polymeric stabilizer with a shorter L than the λ_D led to unstable blends, owing to the overlapping of the double layers. A schematic view is illustrated in Figure 4.3. It is also important to remark that when the length of λ_D is equal or similar to L, the repulsion from the protective specie and the electrostatic attraction are nicely balanced to establish strong ionic bonds. Herein, it was checked if this approach will be valid in a case of highly concentrated dispersions (30% s.c.), in which maintaining sufficient distance between the oppositely charged particles is challenging.

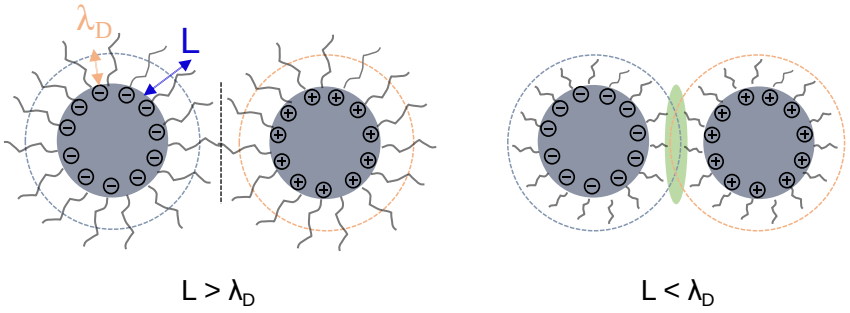

Figure 4.3. Schematic representation of the adsorption of the polymeric/non-ionic stabilizers onto the polymer particles.[6]

Moreover, different protective polymeric species were implemented, such as PVP and PVOH, based on previous good experience in waterborne composite systems stabilization, where often opposite charges in the different phases are present.[7] From the pluronic family, the highest chain length pluronic F-108 specie was adsorbed onto the surface of dialyzed charged polymer particles in a concentration range of 3% - 40% based on total polymer (wbp%), followed by blending, as illustrated in Figure 4.4.

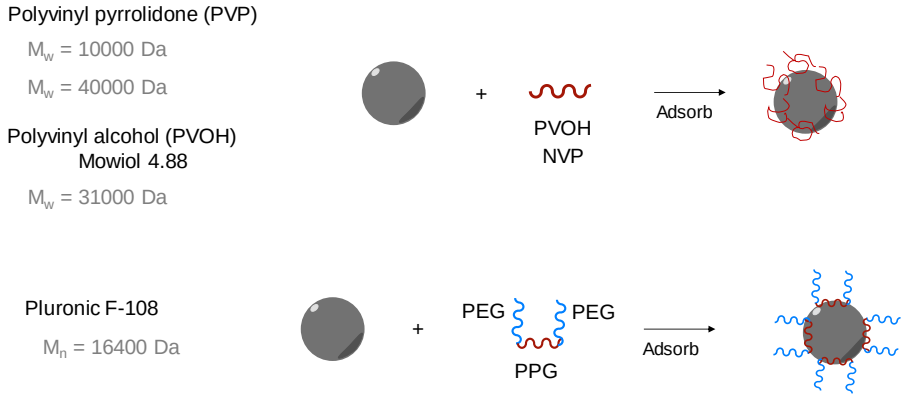

Figure 4.4. Schematic representation of the adsorption of the polymeric/non-ionic stabilizers onto the polymer particles.

It is important to optimize the amount of these species, as their incorporation affects negatively the final properties of the material as poorer water and mechanical resistance.[8–10] Unfortunately, PVP and PVOH in all concentration studied were not able to provide even temporal colloidal stability to the ionic blends. Even though both contain hydrophilic moieties pendant from the hydrophobic backbone, they do not have sufficient amphiphilic character as that of pluronic F-108 provided by the different blocks. The phase behaviour of this block-co-polymer allows adsorption of hydrophobic PPO segment of pluronic F-108 onto polymer particle surface, whereas the PEO hydrophilic blocks pare extended in water, forming denser shell around the particles. Pluronic F-108 in different concentrations (1 - 30 wbp%) was added in dialyzed latexes, which afterwards were mixed to create the blends (Blend C1-1 and Blend C1-1.8). In the case of Blend C1-1, 10 wbp% pluronic F-108 provided the most stable dispersion. Unfortunately, no stable blend dispersion was achieved for any of the studied concentrations in case of Blend C1-1.8, even at as high polymer concentration as 30 wbp%. The polymers addition increased the pH of the blend dispersion from acidic to neutral, which caused deprotonation of -COOH groups of IA containing particles. Taking into account the high charge density, this incited instantaneous coagulation.

The ionic interactions, therefore, were studied for Blend C1-1 (IA1 – DABCO1), in which pluronic F-108 was used to postpone the ionic bonding, leaving sufficient time to mix well the oppositely charged particles. After pluronic F-108 addition, the pH of the polymer dispersions were changed from 3-4 to 7, at which all functionalities were expected to be in their ionic form. Thus, no buffer was used to prepare the ionic complex material, whereas phosphoric acid

(sodium) buffer was used to decrease the pH of the IA latex bellow pH <3.8 to maintain the carboxylic functionalities protonated for preparation of the reference blend. The original polymer latexes synthesized using IA and DABCO functional monomers, and their blend dispersions obtained at different pHs (Blend C1-1, reference and ionic complex materials) were casted and dried. All of them gave rise to homogeneous and transparent films, except the reference Blend C1-1 that presented lower transparency, as shown in Figure 4.5, indicating that the particles kept their borders within the film. Probably the interdiffusion of polymer chains across the particles boundaries was suppressed due to formation of a thicker ionomer phase with higher T_g, formed by the carboxylic acid groups (-COOH) and cations after neutralization at pH <3.8, and therefore, providing resistance to diffusion across it.[11]

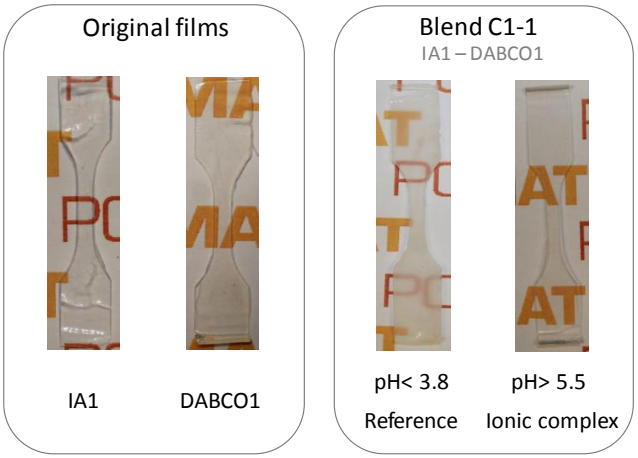

Figure 4.5. Appearance of the individual polymers (IA1 and DABCO1) and the blend C1-1 films at different pH´s (reference and ionic complex).

The polymer films surface for Blend C1-1 (reference and ionic complex) was examined by AFM. Figure 4.6 shows a representative AFM phase images of Blend C1-1. According to both set

of images, in reference materials there are neat areas of each polymer type, referring the light brown particles as stiffer to cationic material, and dark brown particles to anionic less stiff (as shown latter in Table 4.6). The complexed material presented in Figure 4.6b presents efficient homogenization of the particles due to ionic bonding.

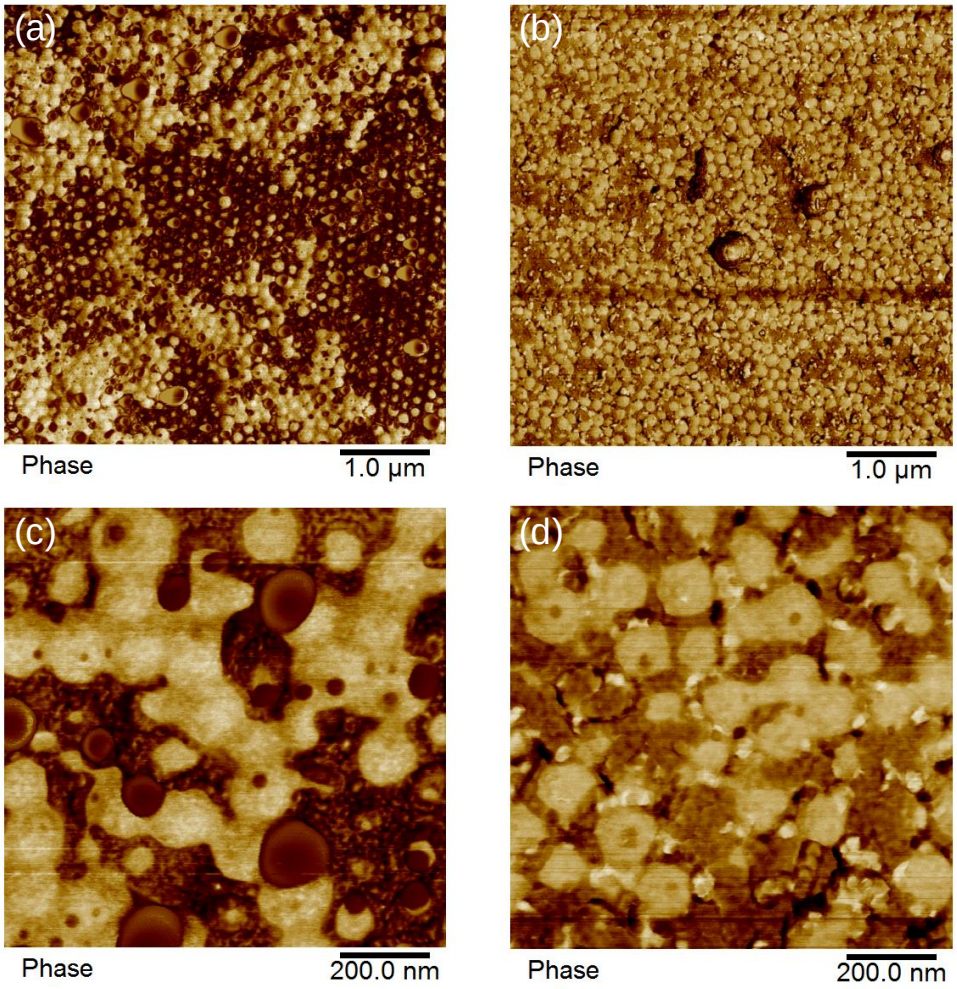

Figure 4.6. AFM air-film interface phase images for Blend C1-1 at 5 and 1 μm scale and at different pH´s. (a) and (c) refers to the reference material, while (b) and (d) refers to the ionic complex one.

The tensile properties of the films are shown in Figure 4.7 and Table 4.6, where the reference and ionic complex blends were compared to the original IA1 and DABCO1 individual polymer films with the addition of pluronic F-108.

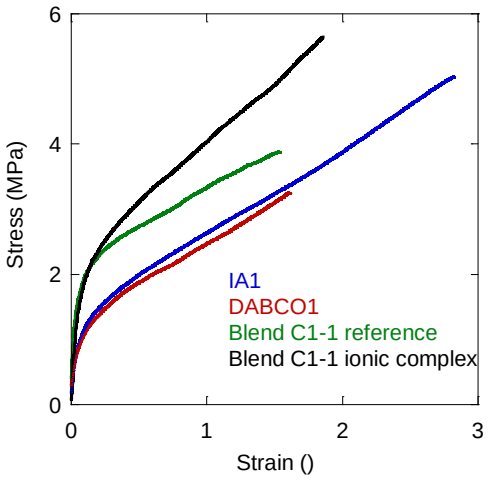

Figure 4.7. Mechanical properties of individual polymer films (IA and DABCO) and their blends (Blend C1-1, reference and ionic complex) obtained at different pH.

Table 4.6. Parameters of the original polymer films and Blend C1-1 films related to the stress-strain plots represented in Figure 4.7.

Sample		Young modulus (MPa)	Elongation at break	Ultimate strength (MPa)	Toughness (MPa)
IA1		13 ± 2	2.8 ± 0.6	5.1 ± 0.1	8.7 ± 1.1
DABCO1		16 ± 1	1.5 ± 0.6	3.3 ± 0.6	3.5 ± 0.6
Blend C1-1	Reference	30 ± 3	1.3 ± 0.2	3.3 ± 0.4	3.4 ± 0.9
	Ionic complex	28 ± 2	2.0 ± 0.1	5.9 ± 0.4	7.9 ± 0.9

As it can be seen in Figure 4.7, DABCO1 film showed slightly higher Young modulus than IA1 film, as DABCO units added rigidity to the chains due to the aromatic ring in the structure.

Nonetheless, higher elongation at break, ultimate strength and toughness values were obtained for the film containing IA, which could be attributed to the dimerization of carboxylic acid moieties on the polymer chains, as reported previously.[12]

Regarding the Blend C1-1 films, an increase in the Young modulus was observed for both, the reference and the ionic complex materials from 13 to 24 MPa. Considering lack of ionic complexation in the reference blend material, this result is rather surprising. Likely, this enhancement can be related to two effects, the carboxylic acid dimers formation and the higher T_g of BA/MMA chains rich in ionic functionalities. In the case of the Blend C1-1 ionic complex, the mechanical properties are further improved with respect to both individual films (IA1 and DABCO1) and the reference blend. Similar elastic moduli were obtained for both blends, reference and ionic complex. Nevertheless, higher ultimate strength and toughness were observed for ionic complex (5.9 MPa and 7.9 MPa, respectively) than for reference material (3.3 MPa and 3.4 MPa, respectively). The observed improvement of the films stiffness is much more important than in all previous studies, in which the functional monomers contained single ion per molecule. This means that indeed the functionalization in this study of two charges per molecules ensures creation of denser ionic network.

As already mentioned in previous chapters, most of the waterborne latex formulations contain ionic groups either to enhance latex stabilization or to introduce additional functionality. However, the presence of these ionic species shows an impact on the coating's water sensitivity.[4,13] To determine how the ionic bonding affect the water sensitivity of Blends C1-1,

both films reference and ionic complex were immersed in water for 14 days. The water uptake of the films was determined. Figure 4.8a. shows the film weight evolution upon water absorption during 14 days, while Figure 4.8b illustrates zoomed area of the initial water uptake period (two days), in order to show the film behaviour after initial immersion in water.

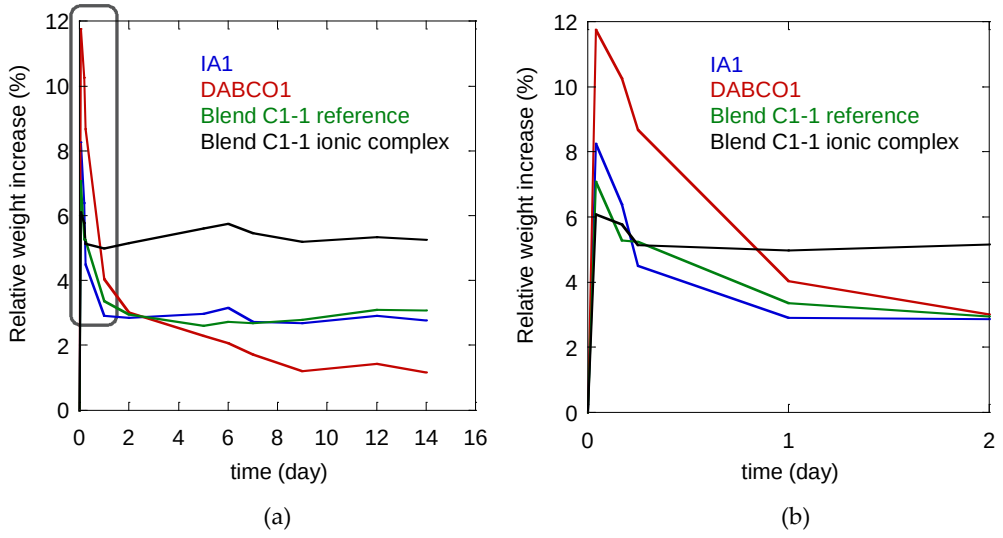

Figure 4.8. Water resistance evolution of original polymer films (IA1 and DABCO1) and their blends (C1-1, reference and ionic complex) performed at different pH during (a) 14 days of water immersion and (b) zoomed area of the initial water uptake period (2 days).

As observed, the individual IA1 and DABCO1 films showed high water uptake during the first hours, followed by a weight loss of the immersed films. The presence of ionic species along with the water-soluble polymer pluronic F-108 chains in both IA1 and DABCO1 containing films are the main cause of the observed higher water sensitivity (> 10 wt% and > 8 wt%, respectively) than for the blends. It is worth mentioning that even so, these values are importantly lower than the water uptake of BA/MMA films (50% s.c.), stabilized with conventional surfactant, usually

higher than 15 wt%.[4,13] This is likely due to chemical incorporation of the functional monomer IA and DABCO onto BA/MMA particles, which prevent migration of stabilizing units and formation of hydrophilic pockets that rise the water sensitivity in case for conventional surfactants.[4] Regarding Blend C1-1 films (reference and ionic complex), even lower water absorption was observed, likely due to the lower quantity of ionic species in case of the reference and the neutralization of the free ionic species during the ionic complexation.

The water adsorption is relatively fast and finished approximately in 2 h, after which, all films (individual and blends) lost weight, likely due to solubilization of pluronic F-108 and its diffusion in the water. After, the weight of the films remain constant, with exception of DABCO1 individual film that continue losing weight until all added pluronic-F-108 was extracted from the film. A possible explanation for the different DABCO1 behaviour might be in the established interaction of pluronic F-108 with all the films that contain carboxylic acid groups (IA1 film, blends C1-1 reference and ionic complex) throughout H-bonding and lack of this interaction within DABCO1 film.

On the other hand, the weight loss of the films during immersion in water is much lower in the ionic complex C1-1 film (0.8 wt%) than in all other films (Figure 4.8). This result indicates that the pluronic F-108 polymer chains were captured within the ionic complex film and the ionic network prevented its leaching from the film. This evidence can be very useful for preventing the leaching of surfactants from waterborne films into environment. This was further investigated by measuring the weight loss of the material after water immersion.

Films were dried and weighted before and after the immersion in water in order to determine the weight loss of the materials. The weight loss (wt%) is referred to the initial weight of the films and the results are presented in Figure 4.9.

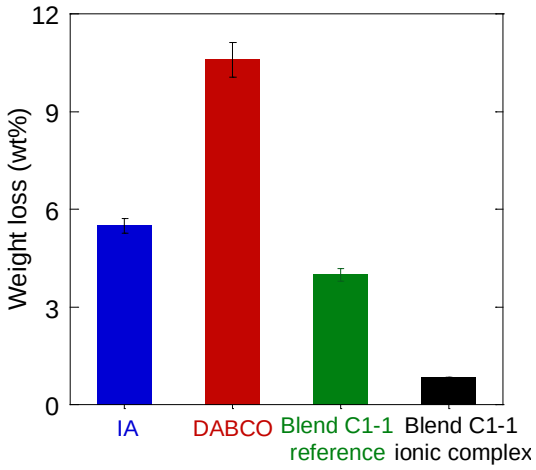

Figure 4.9. Weight loss (wt%) values after water uptake experiments for original films (IA and DABCO) and polymer blend films (reference and ionic complex).

As it can be seen, the films containing the functional monomers IA and DABCO (IA1 and DABCO1 films) and the Blend C1-1 reference materials lost more weight than the Blend C1-1 ionic complex probably owed to the physical obstacles formed as already mentioned.

4.4. Conclusions

In this work, the effect of established denser ionic complexation introducing ionic functional monomers containing two ionic groups per molecule within the BA/MMA polymer chains, IA and DABCO more precisely has been studied.

Pluronic F-108 non-ionic surfactant was employed with the idea of postponing the ionic complexation during blends preparation. Pluronic F-108 afforded preparation of stable dispersion only in case of Blend C1-1 (IA1 – DABCO1) when added 10% to the dispersion. Blend C1-1 was prepared at two different pHs; at pH< 3.8, where IA species should be in their molecular state and therefore ionic complexation is avoided (reference material) and at pH> 6, where all the species should be in their ionic state expecting the formation of the ionic complexes (ionic complex material).

Mechanical strength and water resistance of the individual (IA1 and DABCO1) and Blend C1-1 (reference and ionic complex) polymer films were investigated. DABCO1 film showed slightly higher Young modulus than IA1 film, as DABCO units added rigidity to the chains due to the aromatic ring in the structure. Nevertheless, higher elongation at break, ultimate strength and toughness values were obtained for the film containing IA (IA1 film), probably owed to the dimerization of carboxylic acid moieties on the polymer chains. Regarding the Blend C1-1 films, stiffer material was achieved of both reference and the ionic complex materials. The enhancement of the Young modulus of the reference blend material can be related to the carboxylic acid dimers formation and the distribution of stiffer polymer chains containing ionic monomer units with higher T_g within the polymer blend matrix. In the case of the C1-1 ionic complex, the mechanical properties are further improved with respect to both individual films (IA and DABCO) and the Blend C1-1 reference, which is probably related to the formation of strong ionic complexes. The effect of the ionic complexation was observed in water uptake test, where ionic complex material prevented pluronic F-108 polymeric stabilizer leaching from the

film to the water phase, while this encapsulation effect of polymeric stabilizer was not seen for IA1, DABCO1 and Blend C1-1 reference films, which presented important water adsorption and afterwards loss of weight due to diffusion of pluronic F-108 from the polymer film to aqueous solution in which the film was immersed.

The presented inter-particle complex between deprotonated carboxylic groups of IA and quaternary ammonium units from DABCO containing latexes open an interesting route for reinforcing polymer films cast from water-based polymers.

4.5. References

(1) Oliveira, M. P.; Giordani, D. S.; Santos, A. M. The Role of Itaconic and Fumaric Acid in the Emulsion Copolymerization of Methyl Methacrylate and N-Butyl Acrylate. Eur. Polym. J. 2006, 42 (5), 1196–1205. https://doi.org/10.1016/j.eurpolymj.2005.11.016.

(2) Oliveira, M. P.; Silva, C. R. Copolymerization of Styrene and N-Butyl Acrylate with Itaconic Acid: Influence of Carboxylic Groups Distribution on Performance of Decorative Paints. Lat. Am. Appl. Res. 2013, 43 (4), 337–343.

(3) Zhang, K.; Drummey, K. J.; Moon, N. G.; Chiang, W. D.; Long, T. E. Styrenic DABCO Salt-Containing Monomers for the Synthesis of Novel Charged Polymers. Polym. Chem. 2016, 7 (20), 3370–3374. https://doi.org/10.1039/c6py00426a.

(4) Bilgin, S.; Tomovska, R.; Asua, J. M. Effect of Ionic Monomer Concentration on Latex and Film Properties for Surfactant-Free High Solids Content Polymer Dispersions. Eur. Polym. J. 2017, 93, 480–494. https://doi.org/10.1016/j.eurpolymj.2017.06.029.

(5) Lee, D. I. The Effects of Latex Coalescence and Interfacial Crosslinking on the Mechanical Properties of Latex Films. Polymer (Guildf). 2005, 46 (4 SPEC. ISS.), 1287–1293. https://doi.org/10.1016/j.polymer.2004.11.054.

(6) Hueckel, T.; Hocky, G. M.; Palacci, J.; Sacanna, S. Ionic Solids from Common Colloids. Nature 2020, 580 (7804), 487–490. https://doi.org/10.1038/s41586-020-2205-0.

(7) Arzac, A.; Leal, G. P.; de la Cal, J. C.; Tomovska, R. Water-Borne Polymer/Graphene Nanocomposites. Macromol. Mater. Eng. 2017, 302 (1), 1–30. https://doi.org/10.1002/mame.201600315.

(8) Agarwal, N.; Farris, R. J. Water Absorption by Acrylic-Based Latex Blend Films And. 1998, 1407–1419.

(9) Butler, L. N.; Fellows, C. M.; Gilbert, R. G. Effect of Surfactant Systems on the Water Sensitivity of Latex Films. J. Appl. Polym. Sci. 2004, 92 (3), 1813–1823. https://doi.org/10.1002/app.20150.

(10) Butler, L. N.; Fellows, C. M.; Gilbert, R. G. Effect of Surfactants Used for Binder Synthesis on the Properties of Latex Paints. 2006, 53 (2005), 112–118. https://doi.org/10.1016/j.porgcoat.2005.02.001.

(11) Keddie, J. L.; Routh, A. F. Fundamental of Latex Film Formation; Springer laboratory: Netherlands, 2010.

(12) Voogt, B.; Huinink, H. P.; Erich, S. J. F.; Scheerder, J.; Venema, P.; Keddie, J. L.; Adan, O. C. G. Film Formation of High Tg Latex Using Hydroplasticization: Explanations from NMR Relaxometry. Langmuir 2019, 35 (38), 12418–12427. https://doi.org/10.1021/acs.langmuir.9b01353.

(13) Jiménez, N.; Ballard, N.; Asua, J. M. Hydrogen Bond-Directed Formation of Stiff Polymer Films Using Naturally Occurring Polyphenols. Macromolecules 2019, 52 (24), 9724–9734. https://doi.org/10.1021/acs.macromol.9b01694.

Chapter 5. Synthesis and ionic complexation study of emulsifier-free cationic (meth)acrylic latexes, stabilized by cationic monomer with two charges per molecule

5.1. Introduction

As already mentioned in Chapter 1, colloidal stabilization of waterborne dispersions using anionic monomers has been widely studied in the literature,[1–5] while lower attention has been paid to cationically charged polymer dispersions.[6] Production of cationic polymer particles for biomedical applications has recently emerged[6] together with the biocide ability of these species against microbial activity.[7–10] However, during the last years, attention has been also focused on the potential use of cationic latex as stain blocking primer coatings for tannin or markers bleeding.[11]

As pointed out in the Introduction of the manuscript, most of the stable cationic latexes were synthetized adding positively charged monomers and using cationic initiators at lower solids content than 25%.[12–20] All of these studies exclusively were performed using different cationic monomers with one charge per molecule.

Cationic monomers addition to waterborne (meth)acrylic particles can provide good colloidal stability during synthesis if incorporated in high amount, nevertheless, in such case the latex stability[18,21] and polymer film water sensitivity are negatively affected.[21] A possible way to increase the number of charges onto polymer particles without increasing extensively the quantity of the ionic monomer, could be using ionic monomers that contain more than one charge per molecule. In this work, this possibility was investigated, by using DABCO cationic monomer, which contains two charges per molecule. This monomer was already copolymerized with BA/MMA in Chapter 4, in which for comparison purposes cationic emulsifier was added in the formulation, too. Herein, emulsifier-free emulsion polymerization was carried out copolymerizing DABCO with BA and MMA.

A portfolio of cationic latexes were produced by varying the cationic monomer content in a range of 1 – 5 mol% based on main monomers (mbm%, BA/MMA) in the emulsifier-free seeded semicontinuous emulsion polymerization with a final solids content of 40%. First, the influence of DABCO monomer amount on polymerization kinetics, particle size and polymer microstructure was investigated, whereas in the second part, the influence of cationic monomer concentration on the final performance of the polymer films was studied. Finally, blends between emulsifier-free NaSS containing latex and DABCO one were performed in order to study the influence of the ionic complexation on the final performance of the polymer films.

5.2. Experimental part

5.2.1. Materials

The materials are given in Appendix I.

5.2.2. DABCO monomer synthesis and characteristics

DABCO cationic monomer is not commercially available, thus, this monomer was synthesized following the procedure reported by Zhang et al.[22] as described in Appendix V. The partitioning of DABCO monomer between water and organic phase (BA/MMA) was examined by mixing DABCO monomer, water and BA/MMA in different ratios. After phase separation, the content of DABCO in each phase was analysed by H^1-NMR. The procedure is explained in detail in Appendix V.

5.2.3. Synthesis of emulsifier free waterborne dispersions using doubly charged cationic monomer

Cationically charged aqueous polymer dispersions were synthetized by seeded semi-continuous emulsion polymerization process. Initially, a seed was synthetized using the formulation shown in Table 5.1. BA/MMA (50/50 wt%) and DABCO monomer with content of 1 mbm% at 10% s.c. DABCO was charged into the reactor and stirred for 20 minutes under N_2 atmosphere at 200 rpm. Once the temperature was increased to 70 °C, aqueous solution of initiator (AIBA) was added as a shot and it was left to react for 90 minutes.

Table 5.1. Formulation employed for the synthesis of the seed latex.

Compound (wt%)	Initial charge	Shot
BA	5	
MMA	5	
DABCO	1[a]	
AIBA		0.25[a]
H_2O	80	10

[a]mol based on main monomers (BA/MMA) (mbm%)

This seed was used in the seeded semibatch emulsion copolymerization of BA/MMA in ratio of 1/1, by weight. DABCO content was varied from 1 to 5 mbm% in this second step. The reactor was loaded with appropriate amount of seed (30%). Upon achieving 70 °C, initiator aqueous solution (AIBA) was added as a shot, whereas the monomers were fed in two streams: a preemulsion containing BA and MMA, and an aqueous solution of DABCO monomer. After the feeding period (180 minutes), the system was allowed to react for one hour. The final solids content was 40%. The formulation employed for the synthesis of the cationic latex is presented in Table 5.2.

Table 5.2. Formulation used for the synthesis of cationically charged polymer dispersions.

Compound (wt%)	Initial charge	Stream 1	Stream 2	Shot
Seed	30			
BA		18.5		
MMA		18.5		
DABCO			1-5[a]	
AIBA				0.25[a]
H_2O			28	5

[a]mol based on main monomers (BA/MMA) (mbm%)

These polymer dispersions were named as DABCO1 (when 1 mbm% DABCO was used), DABCO3 (when using 3 mbm%) and DABCO5 (when employing 5 mbm%).

5.2.4. Latex characterization

Monomer conversion was studied gravimetrically and coagulum amount was calculated based on the total monomer. The average particle size and the particle size distribution (PSD) were determined by Capillary Hydrodynamic Fractionation (CHDF) chromatography. The morphology of latex particles was studied by means of Transmission Electron Microscopy (TEM) technique. Zeta potential was measured in a Zetasizer Nano Z (Malvern instruments). Incorporation and the surface charge density was measured by titration analysis. The gel fraction, which is defined as the insoluble fraction of polymer in THF, was measured by Soxhlet and SEC/GPC determined the molar mass of the soluble part after the Soxhlet extraction. A detailed description of all characterization methods is provided in Appendix II.

5.2.5. Blending of emulsifier-free NaSS and DABCO containing latexes

Both latexes used in this work were synthesized without emulsifiers and this time blends were prepared using dialyzed and non-dialyzed latexes. On the one hand, the practical use of these blends was examined avoiding the dialysis process. Nevertheless, as the effect of the ionic network might be screened owed to the presence of water-soluble species, dialyzed latexes were also used. In both type of blends (non-dialyzed and dialyzed), oppositely charged latexes with different particle sizes were blended in order to ensure more efficient particle packaging, and therefore increase the ionic bonding points. For this purpose, the Kusy model described in Chapter 3 was employed. Three type of blends were prepared as summarized in Table 5.3. Blends were named indicating the particle size of each latex used (the first number refers to the latex containing NaSS while the second number to the latex containing DABCO).

Table 5.3. Summary of the prepared blends.

Latex	Blend 275-171	Blend 275-180	Blend 275-100
275 nm NaSS[a]	56%	54%	68%
100 nm DABCO seed	-	-	32%
180 nm DABCO[b]	-	46%	-
171 nm DABCO[c]	44%	-	-

[a]In Chapter 2 indicated as NaSS1.
[b]In Chapter 5 indicated as DABCO1.
[c]In Chapter 5 indicated as DABCO3.

As previously described, NaSS shows relatively low pKa (around 1), while DABCO compound is pH independent owing to the presence of the quaternary ammonium groups. This

means that NaSS and DABCO species will be in their ionic state in the whole pH range, limiting the preparation of oppositely charged dispersions. Thus, as described in Chapter 4, the addition of a polymer protective specie to prevent the premature complexation during blending was performed. For that aim, pluronic F-108 (triblock copolymer specie, composed of PPO-PEO-PPO) was employed again in this work. Nevertheless, it is important to point out that the presence of a surfactant will surely affect the performance of the polymer film, as shown in Chapter 4.

Before blending, pluronic F-108 was absorbed onto the two polymer particles' dispersions separately. For this purpose, this specie was added to the anionically charged dispersions in a range between 1% – 10% based on total polymer (wbp%), allowing the dispersion to mix for one hour. The same procedure was followed for the cationically charged polymer particles. In a second step, these latexes were blended in order to study the effect of the different concentrations used. As reference materials, individual NaSS and DABCO containing dispersions were used after pluronic F-108 surfactant was added in each. Thus, three sample sets were prepared as summarized in Table 5.4.

Table 5.4. Summary of the prepared films.

Sample set	**Reference**		**Blend**[a]
	NaSS	DABCO	
1	275 nm NaSS	171 nm DABCO	275-171
2	275 nm NaSS	180 nm DABCO	275-180
3	275 nm NaSS	100 nm DABCO seed	275-100

[a]Blends described in Table 5.3.

The references and the blends were casted into silicon molds and dried during 7 days at 23 ± 2 °C and 55 ± 5 % relative humidity.

5.2.6. Polymer film characterization

On the one hand, the morphology of the polymer films was examined by TEM technique. On the other hand, The thermal characterization of the blend polymer films was carried out by differential scanning calorimetry (DSC), the mechanical properties of the polymer films were measured by tensile tests and the water resistance of the polymer films was examined in terms of water uptake test. The detailed description of these methods is provided in Appendix II.

5.3. Results and discussion

The chemical structure of the purified DABCO monomer was analysed by ^{1}H-NMR as shown in Appendix V, Figure V.1 and the structure was successfully confirmed. As mentioned in Chapter 4, the reaction yield was around 70%. When analysing the distribution of DABCO monomer between the water and organic phase (BA/MMA), the results confirmed that DABCO monomer was highly hydrophilic as described in Appendix V.

5.3.1. Characteristics of the seed and the cationic latexes

In Table 5.5 the main properties of the seed are presented. To demonstrate the reproducibility of the seed synthesis, three experiments were performed, and the average characteristics of the three polymerizations are presented in Table 5.5.

Table 5.5. Seed latex characteristics.

Seed latex	
Conversion (%)	99
dp_{CHDF} (nm)	100 ± 2
Surface incorporation (DABCO %)[a]	28 ± 2
Surface charge density (μC cm^{-2})	7 ± 1

[a]Incorporation was calculated based on DABCO monomer.

High monomer conversion of 99% was obtained, giving rise to a final average particle size of 100 nm and relatively narrow distribution of particle sizes (Figure 5.1), as determined by CHDF. However, a shoulder at around 50 nm was observed, which might be an artefact. In order to proof that there were not 50 nm particles in the seed, the sample was analysed by TEM. A representative TEM image shown in Figure 5.2 presents that most of the particles have similar size of around 100 nm and that there is not any other particle population around 50 nm. Incorporation of DABCO into this seed latex was around 30%, achieving a surface charge density of 7 μC cm^{-2}.

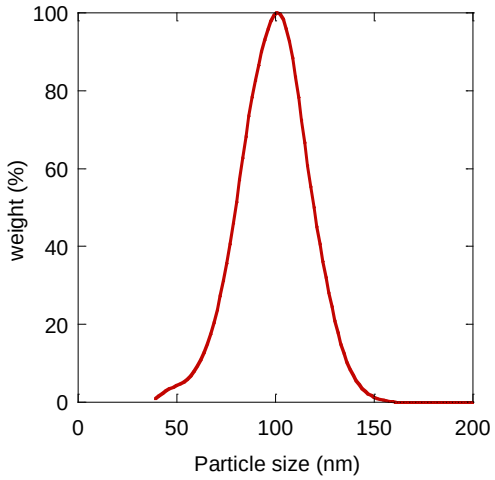

Figure 5.1. Particle size distribution (PSD) of the seed latex.

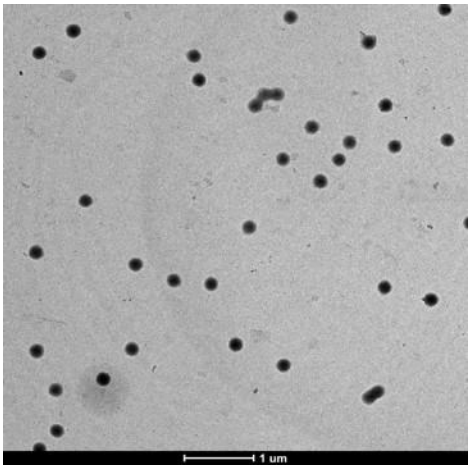

Figure 5.2. TEM images of Seed 1 latex at X6500 magnification.

Using the seed, the second stage emulsifier-free polymerization was performed to reach polymer latexes with 40% s.c by changing DABCO concentration (1, 3 and 5 mol% with respect to main monomers). The final conversion, coagulum amount and zeta potential values are presented in Table 5.6.

Table 5.6. Conversion, coagulum amount and zeta potential obtained for the three polymerizations.

Latex	Conversion (%)	dp_{CHDF}	Zeta potential (mV)	Coagulum amount (%)
DABCO1	95	180	52 ± 1	3
DABCO3	97	171	53 ± 1	4
DABCO5	97	169	52 ± 1	5

High monomer conversions were achieved for all DABCO concentration. Interestingly, very similar particle sizes were obtained, independently of the DABCO quantity employed, indicating high colloidal stability of the systems even at DABCO1, as shown by the high zeta potential values. According to the well-known Deryaguin–Landau–Ver-wey–Overbeek theory, a balance between attractive Van der Waals forces and the electrostatic repulsion governs the stability of the colloidal systems.[23,24] The magnitude of the zeta potential is a key indicator of the stability of the colloidal systems. Greater values than 30 mV lead to a stable system, while lower values can lead to agglomeration.[25] Thus, the values measured for DABCO containing dispersions (Table 5.6) indicate a great stability of the three systems (after removed coagulum).

Despite this, up to 5% of coagulum was found in the latexes, the quantity of which increased with DABCO amount, likely due to the high ionic strength in the dispersions. It should be mentioned that DABCO monomer is hydroscopic, meaning that increasing this monomer concentration, higher experimental error might be found when conversion and coagulum amount was analysed gravimetrically.

The kinetic curves of the polymerization processes of BA/MMA/DABCO for different DABCO concentrations are presented in Figure 5.3 (full dots), showing again independence on the quantity of DABCO monomer used. The polymerization is rather slow, when compared with NaSS emulsifier-free BA/MMA polymerizations,[26] probably due to slow incorporation of the cationic monomer in BA/MMA chains, thus, late creation of stabilizing units in the system. In Figure 5.3, the instantaneous monomer conversion curves (continuous lines) are as well shown, presenting that during most of the polymerization processes, the monomer concentration in the reactor was low, even though at DABCO1 where a small quantity of continuous monomer accumulation can also be seen, indicating that the polymerization rate was lower than monomer feeding rates. A small decrease in the instantaneous conversion (from 93% to 88%) can be observed at around 100 min for DABCO3 and DABCO5 latexes, which might be related to the monomer accumulation during the semibatch process.

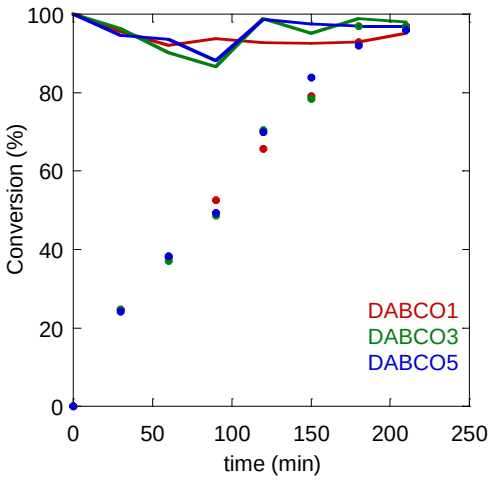

Figure 5.3. Conversion evolution of latexes containing different DABCO cationic monomer concentration. Continuous line represents the instantaneous conversion, while the dots the overall conversion.

Nevertheless, when the samples were analysed by CHDF, as observed in Figure 5.4 and Table 5.6, the final average particle size and the particle size distribution (PSD) of the cationic latexes, present dependence on the quantity of DABCO. Figure 5.4 reveals that the PSD were shifted towards the lower particle sizes for DABCO3 and DABCO5 with respect to that of DABCO1, and that this fraction of smaller particles increased with DABCO concentration. The average particle size decreased slightly, too, indicating that indeed there was more stabilizing species created at higher DABCO content, even though the effect is small. Probably this is a result of two contradictory effects of DABCO concentration: increasing quantity of stabilizing units and enhanced ionic strength in the dispersions[27] that decrease the colloidal stability. In the three cases (DABCO1, DABCO3 and DABCO5) a relatively narrow partial size distribution was achieved, with an average particle size of 180 nm, 171 nm and 169 nm, respectively. These results were in agreement with the similar particles sizes observed in TEM images (Figure 5.5).

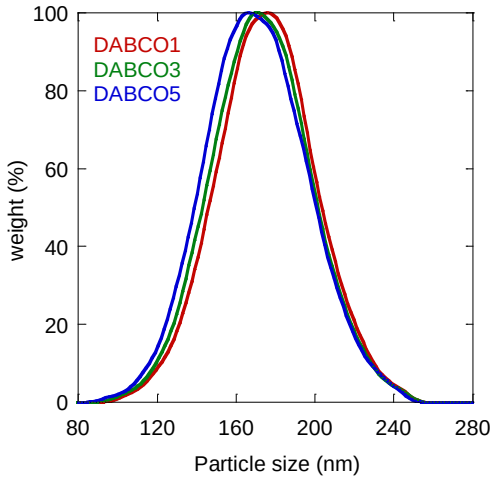

Figure 5.4. Particle size distribution (PSD) of the three latexes containing different content of DABCO.

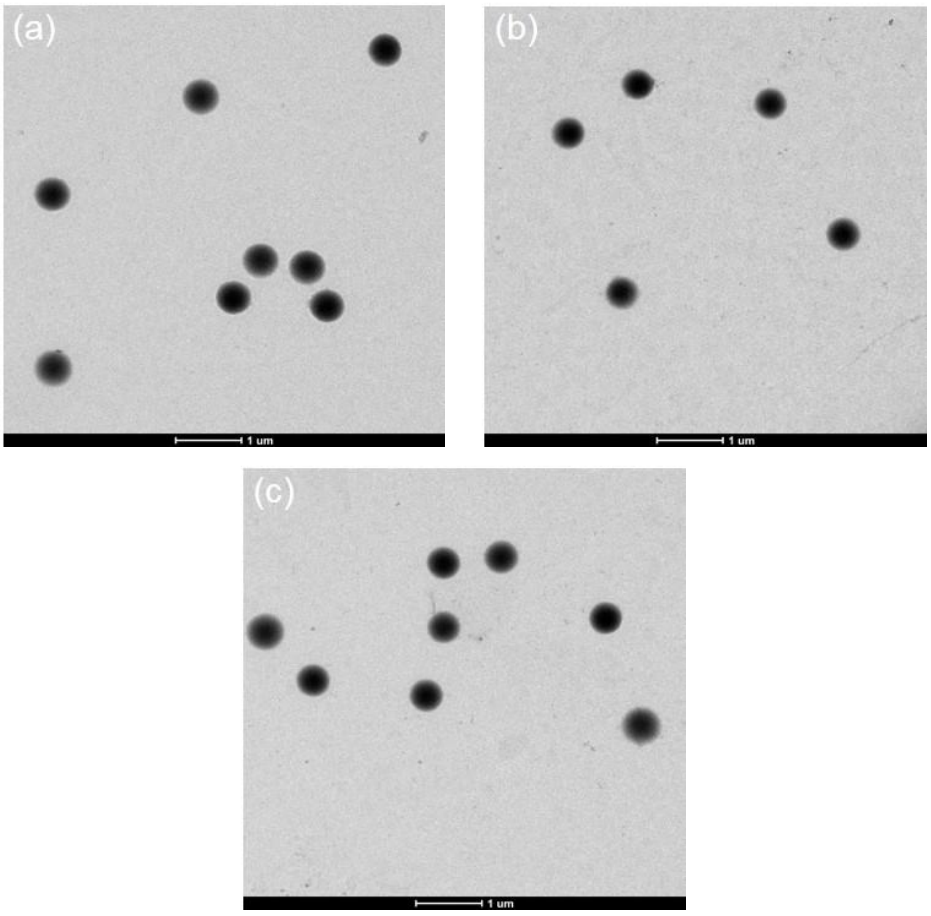

Figure 5.5. TEM images of (a) DABCO1, (b) DABCO3 and (c) DABCO5 latex at X6500 magnification.

Table 5.7 summarizes the incorporation and the surface charge density values for each of the latexes. There is contribution of two components to the cationically charge species onto particle surface, the one coming from the functional monomer DABCO and the other from the cationic initiator AIBA. Owing to the much lower amount of AIBA (0.25 mbm%) in comparison to the DABCO monomer content (from 1 to 5 mbm%), AIBA contribution was neglected and the

incorporation was calculated based on the DABCO content. The incorporation of DABCO increased with its concentration likely due to the fact that, at higher ionic strength in the dispersions, the adsorption of the ionic species is shifted towards the polymer particles. This effect was already observed for ionic monomers[27] (NaSS) and conventional surfactants[28] (sodium dodecyl sulfate, SDS). Accordingly, the surface charge density increased also with DABCO content, from 24 μC cm^{-2} to 180 μC cm^{-2}.

Table 5.7. Surface incorporation for emulsifier-free DABCO latexes.

Latex	Surface incorporation (DABCO %)[a]	Surface charge density (μC cm^{-2})
DABCO1	25 ± 1	24 ± 1
DABCO3	42 ± 1	77 ± 2
DABCO5	62 ± 1	180 ± 5

[a]Incorporation was calculated based on DABCO monomer.

The polymer microstructure was analysed by measuring the insoluble part of the polymer latexes in THF (gel content) and the molar mass of the soluble part by GPC (Table 5.8). The insoluble polymer amount was higher than expected, above 74% for the three cases. It is known, that for the copolymerization of BA/MMA (50/50 wt%) using KPS initiator and ABEX2005 surfactant under starve conditions, the insoluble polymer fraction is lower than 10%, owed to the lower reactivity of MAA terminated chains for H-abstraction, the absence of abstractable hydrogens in MMA units and the fact that MMA radicals terminated by disproportionation.[29] It seems that the presence of cationic species contributes to the insolubility of the polymer chains into THF. The insoluble fraction increased with the DABCO content, confirming its higher

incorporation onto BA/MMA particles. The molar masses of the soluble polymer fraction also increased with DABCO concentration, oppositely than in BA/MMA polymer particles stabilized with conventional anionic surfactants. This is another indication that the gel content is not related to the microstructure of the polymer, but to the solubility of DABCO containing polymer chains.

Table 5.8. Gel content, molar mass of the soluble part measured by GPC for DABCO containing latexes.

Latex	Gel content (%)	Mw (kDa)	Đ
DABCO1	74 ± 1	310 ± 30	2.4
DABCO3	78 ± 1	430 ± 20	2.3
DABCO5	83 ± 3	466 ± 40	2.7

5.3.2. Polymer blend film performance

In Figure 5.6, the photos of the polymer films containing different DABCO concentrations are shown (DABCO1, DABCO3 and DABCO5). By increasing DABCO concentration, the transparency of the films decreased. The lack of transparency indicates that complete coalescence of polymer particles into continuous films was not achieved. In order to get a better insight of the system, the morphology of these films was examined by TEM technique.

Figure 5.6. Appearance of the polymer films containing different DABCO cationic monomer concentration.

As seen in Figure 5.7, where the TEM images of the cross-section of the polymer films are shown, a honeycomb structure of deformed particles was formed within the film, which was even more evidenced increasing DABCO content. Polymer chains interpenetration was hindered by the hard DABCO rich polymer that formed a shell around the BA/MMA copolymer core, acting as a barrier against particle coalescence. Moreover, by increasing DABCO content in the film, this network might be stronger, causing drop in the film transparency (Figure 5.6). This in in line with the retardation effect produced by functional groups on polymer diffusion reported in the literature for -COOH[30] or -NaSS.[27]

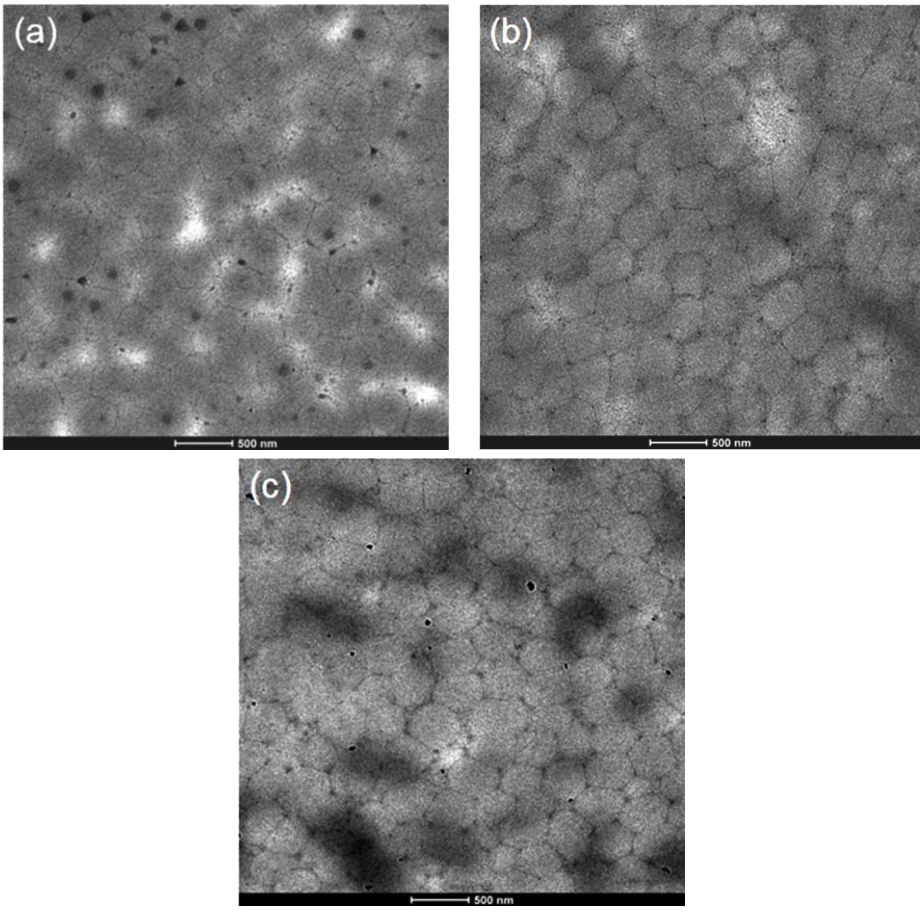

Figure 5.7. TEM images of film cross-section: (a) DABCO1, (b) DABCO3 and (c) DABCO5 films at X11500 magnification.

The T_g of the polymer films was not affected by DABCO content as the values were between 16-17 °C.

The stress-strain behaviour of the polymer films containing different content of DABCO is shown in Figure 5.8 and the mechanical parameters related to the stress-strain curves are summarized in Table 5.9. Clearly, by increasing DABCO concentration, higher Young´s modulus

was obtained, likely due to the reinforcing network formed by the DABCO reach polymer chains that became thicker for higher DABCO content, producing mechanical percolation. These results are in line with previously reported systems, where the honeycomb structure formed was responsible for the drastic differences observed in elastic modulus.[27,31] Furthermore, an increase in the ultimate strength and toughness was observed with increasing DABCO amount, resulting in stiffer and tougher materials without any drop in the elongation at break.

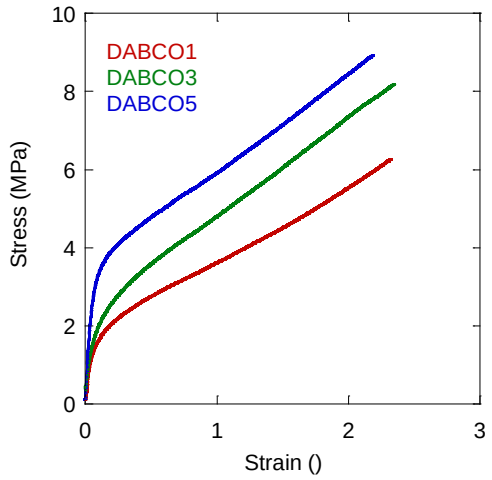

Figure 5.8. The stress -strain curves for films containing different DABCO concentration.

Table 5.9. The mechanical properties of the four polymer blend films.

	Young´s modulus (MPa)	Elongation at break	Ultimate strength (MPa)	Toughness (MPa)
DABCO1	18 ± 2	2.2 ± 0.4	6.1 ± 0.7	8.5 ± 1.6
DABCO3	23 ± 1	2.3 ± 0.2	8.6 ± 0.4	12.4 ± 1.3
DABCO5	46 ± 6	2.2 ± 0.7	8.9 ± 0.2	13.3 ± 1.2

Waterborne coatings containing ionic functional groups are strongly susceptible to durability issues pertaining to poor water resistance. It was demonstrated that water absorption of a cationic film containing methacrylate ethyl trimethyl ammonium chloride (DMC) increased with DMC concentration.[21] Therefore, DABCO containing films were immersed in water to investigate their water resistance (Figure 5.9). As expected, the water absorption increased sharply when the concentration of DABCO was increased from 1 to 5 mbm% (from 5 wt% to 45 wt%, respectively) during the first days likely due to the higher DABCO concentration in the system. However, after two days, all the films with different DABCO concentrations present the saturation behaviour; no more water absorption was evidenced. Furthermore, the small drop of weight observed in DABCO5 is probably due to solubilization of the soluble oligomers present as water-soluble species in the water phase.

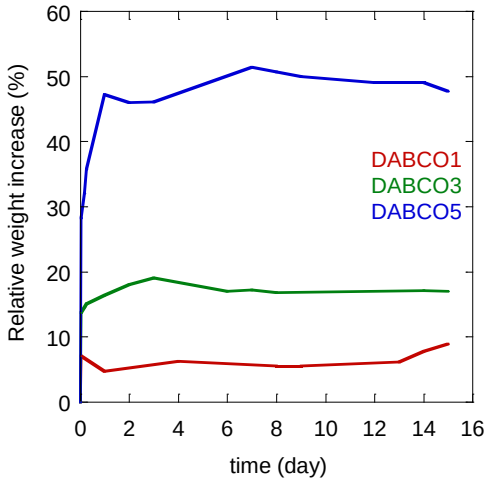

Figure 5.9. Water uptake for films containing different DABCO concentration.

5.3.3. Blending of emulsifier-free NaSS anionic and DABCO cationic polymer dispersions

The present cationic latexes were blended with previously prepared NaSS containing latex (indicated as NaSS1 in Chapter 2 and its characteristics are shown in Table 2.3), expecting to obtain much denser ionic complex structure and to study its effect on the properties of the blend. Two set of blends were prepared using non-dialyzed and dialyzed latexes in order to examine the possible effect of water-soluble species on the final performance of the films. After pluronic F-108 addition, stable blend dispersions were obtained for Blend 275-180 and for Blend 275-100, whereas for Blend 275-171 aggregation was observed probably due to high charge density (Table 5.7, DABCO3), thus this blend was not further studied (meaning that sample set 1 was not examined). The minimum concentration of pluronic F-108 that provided stability during blending of the oppositely charged dispersions was determined by trial-error procedure and is shown in Table 5.10.

Table 5.10. Optimal concentration of pluronic F-108 in respective blends.

Concentration (wbp%)	Blend 275-180	Blend 275-100
Pluronic F-108	10	7

One may think that when increasing the number of particles within the blend, higher amount of protective polymer content would be needed to cover the total surface area, however, the parking area (a_s) of pluronic F-108, which is affected by the hydrophilicity/hydrophobicity of the particle surface, might have an effect as well. The a_s of the surfactant refers to the area of

the polymer particles that can be covered by one mol of surfactant under saturation conditions ($m^2\ mol^{-1}$).[32] For a given surfactant, the a_s increases with hydrophilicity of the polymer particle, which can be easily varied by using different monomeric compositions.[33] As seen in Table 5.3, while the same NaSS latex was employed for the three blends (275 nm NaSS indicated as NaSS1 in Chapter 2), different DABCO containing dispersions were employed for blending. For the dispersions with higher DABCO content, likely the same pluronic F-108 concentration would cover greater surface area of the particles. That is why in the Blend 275-180, made of more hydrophilic cationic particles (surface charge density 24 $\mu C\ cm^{-2}$) higher amount of pluronic F-108 was used than in case of Blend 275-100 (surface charge density 7 $\mu C\ cm^{-2}$).

Before discussing the properties obtained for each of the blends, the neat charge in each blend was calculated (see Table 5.11). The neat charge was calculated as in Chapter 3 and details are provided in Appendix II. As already mentioned in Chapter 3, despite these calculations provide information about the total positive and negative charges involve in each blend system, this is not directly related to the established ionic bonding points between oppositely charged particles. The distribution of these charges in the polymer particle as well as the ionically charged particles distribution in the blend clearly affected the ionic interaction points.

Table 5.11. Neat charge calculation for each blend.

Blend	Latex	Charge per particle (μC particle^{-1})	Total charge in the blend (μC)	Neat charge in the blend (μC)[a]
Blend 275-180	275 nm NaSS	$3.8 \cdot 10^{-8}$	$-4.2 \cdot 10^{+6}$	$+3.5 \cdot 10^{+6}$
	180 nm DABCO	$2.3 \cdot 10^{-8}$	$+7.7 \cdot 10^{+7}$	
Blend 275-100	275 nm NaSS	$3.8 \cdot 10^{-8}$	$-5.1 \cdot 10^{+6}$	$-2.2 \cdot 10^{+6}$
	100 nm DABCO	$2.2 \cdot 10^{-9}$	$+2.9 \cdot 10^{+6}$	

[a]The positive sign refers to an excess of cationic charges, while the negative sign indicates an excess of negative charges.

In all the cases (references and blends), homogeneous and transparent polymer films were obtained. The stress-strain curves for the original films and the blends are presented in Figure 5.10 and the mechanical parameters in Table 5.12 for non-dialyzed latexes and Table 5.13 for dialyzed ones. As it can be seen, similar trend was observed for non-dialyzed and dialyzed polymer films in the two sample sets, meaning that the presence of the water- soluble species do not show strong influence, even though some differences can be appreciated.

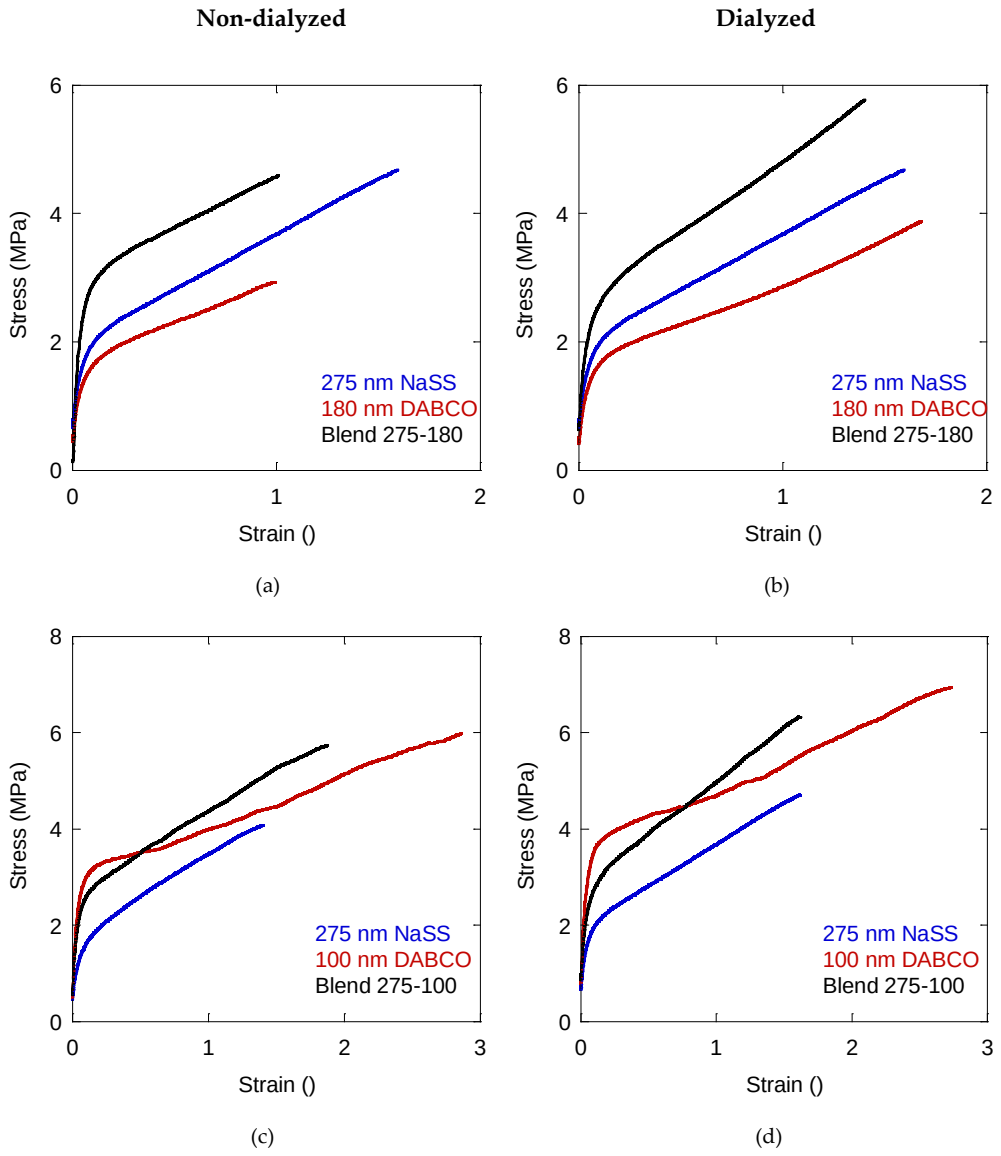

Figure 5.10. Stress-strain curves for (a) and (c) non-dialyzed and (b) and (d) dialyzed polymer films of (a) and (b) Sample set 2 and (c) and (d) Sample set 3.

Table 5.12. The mechanical properties of the non-dialyzed references and blends.

Sample set		Young´s modulus (MPa)	Elongation at break	Ultimate strength (MPa)	Toughness (MPa)
Sample set 2	275 nm NaSS	21 ± 1	1.7 ± 0.2	4.8 ± 0.5	5.7 ± 1.1
	180 nm DABCO	14 ± 2	0.9 ± 0.1	3.1 ± 0.6	2.4 ± 1.1
	Blend 275-180	28 ± 2	0.9 ± 0.2	4.4 ± 0.2	3.9 ± 0.8
Sample set 3	275 nm NaSS	17 ± 1	1.3 ± 0.2	4.0 ± 0.4	4.2 ± 0.2
	100 nm DABCO	32 ± 3	2.3 ± 0.2	5.8 ± 0.3	12.9 ± 2.8
	Blend 275-100	31 ± 4	1.7 ± 0.3	5.3 ± 0.5	6.4 ± 1.6

Table 5.13. The mechanical properties of the dialyzed references and blends.

Sample set		Young´s modulus (MPa)	Elongation at break	Ultimate strength (MPa)	Toughness (MPa)
Sample set 2	275 nm NaSS	20 ± 1	1.8 ± 0.2	4.7 ± 0.5	5.6 ± 1.1
	180 nm DABCO	19 ± 2	2.2 ± 0.2	4.4 ± 0.2	5.9 ± 0.4
	Blend 275-180	28 ± 2	1.3 ± 0.3	5.7 ± 0.4	5.8 ± 1.5
Sample set 3	275 nm NaSS	19 ± 1	1.7 ± 0.3	4.6 ± 0.4	5.4 ± 1.5
	100 nm DABCO	35 ± 3	2.5 ± 0.3	6.7 ± 0.7	17.3 ± 2.8
	Blend 275-100	31 ± 1	1.7 ± 0.2	6.6 ± 0.6	8.1 ± 0.2

Regarding the reference materials of Sample set 2, when non-dialyzed NaSS containing polymer shows enhanced mechanical properties than DABCO one in terms of Young modulus, ultimate strength, elongation at break and toughness. Nevertheless, when dialyzed NaSS containing film presented similar properties, whereas significant improvement was observed for DABCO dialyzed one. The much higher incorporation of NaSS (NaSS1, Table 2.3, Chapter 2)

leading to much lower quantity of soluble oligomers in NaSS containing film than the incorporation of DABCO1 (Table 5.7) caused the perceived difference. In the case of Sample set 3, both reference films improved the mechanical properties after removing of the water-soluble oligomers. In case of DABCO seed containing films, the enhance properties are probably owed to the better particle packaging of much smaller DABCO seed (100 nm) particles within the film.

The presence of water-soluble oligomers in Blend 275-180 provides improved stiffness, but the chains are less flexible as the elongation at break is lower. Probably, the higher content of ionic functionalities within these oligomers, which make more rigid the chains, is the reason behind this behaviour. On the other hand, this effect is almost diminished in Blend 275-100, probably because of the difference in particle size that provides improved packing of the particles and denser ionic complexation due to it and better film properties, which compensate the effect of the soluble oligomers.

Usually, when blending components showing different mechanical resistance, if no additional interactions are established, the mechanical resistance will be in between both components according to the concentration of each in the blend. Observing clear improvement of the mechanical properties of Blend 275-180, for both dialyzed and non-dialyzed polymer films (Sample set 2 in Figure 5.10 and in Table 5.12 and Table 5.13) demonstrates the positive effect of the ionic complexation established within these blend films, resulting in much stiffer and less flexible materials. Few effects may possibly cause this achievement, which was so difficult to observe in the previous works (chapters). On one hand, the difference of particle sizes between

the oppositely charged particles that improved their packing within the film, and on the other, much dense charge distribution on the surface of the particles, obviously giving rise to denser ionic network creation.

Nevertheless, Blend 275-100 (Sample set 3), for both dialyzed and non-dialyzed latexes, presents mechanical properties in-between the both references. These blends was expected to have even further improved packing than Set 2 blends, due to more important difference in particle sizes of both charged latexes. Nevertheless, the clear effect of ionic bonding cannot be appreciated in this case because of the much lower surface charge density of the cationic particles. Even the packing was improved in Sample set 3 blends, probably the established ionic complex network was less dense than in Sample set 2.

Water resistance of the polymer films results are shown in Figure 5.11.

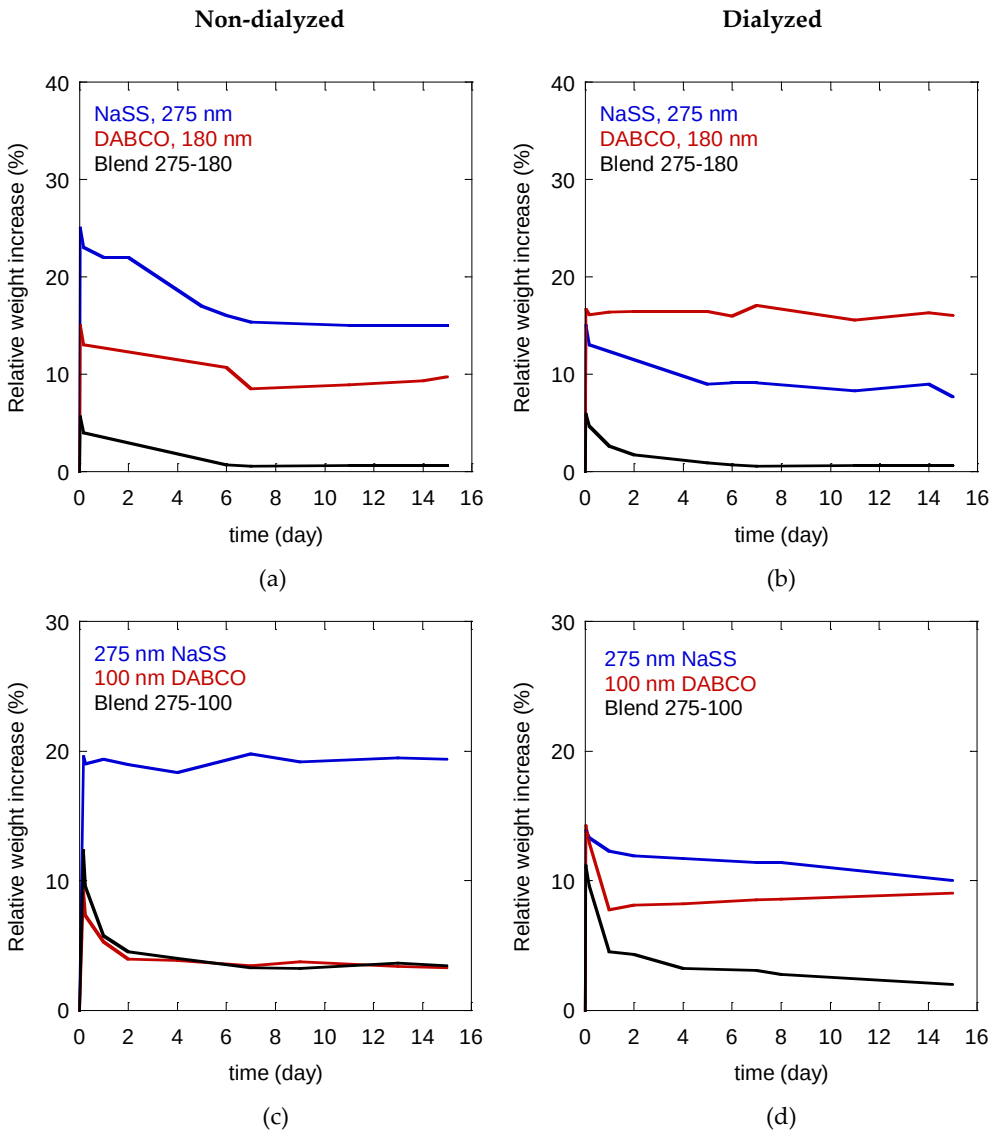

Figure 5.11. Stress-strain curves for original and blend polymer films for (a) and (c) non-dialyzed and (b) and (d) dialyzed latexes of (a) and (b) Sample set 2 and (c) and (d) Sample set 3.

The water resistance of Sample set 2 (non-dialyzed and dialyzed) was considerably improved after blending with respect to both reference materials. The ionic complexation within

Blend 275-180 resulted in very strong ionic complex network that give rise to almost completely impenetrable waterborne polymer films. The small water absorption observed initially was probably due to the presence of some water-soluble oligomers and the pluronic–F108 surfactant, which diffused from the film to water solutions, after which clearly hydrophobic films were obtained. Moreover, taking into account that water adsorption of similar BA/MMA film stabilized with conventional surfactant might be as high as 40-50 wt%,[34,35] this result presents important enhancement of this application properties of the waterborne polymer films aimed to be applied as protective coatings and paints.

Water resistance of Sample set 3 was improved only in case of dialyzed polymer films, whereas the non-dialyzed presented similar behaviour as the cationic reference. The presence of water-soluble species might screen the effect of ionic bonding. After the first hour, all the polymer films start losing weight, except the non-dialyzed NaSS film. A balance between the water absorption and the migration of the pluronic surfactant from the film might be the reason for this constant weight, whereas for non-dialyzed DABCO and Blend 275-100 films the balance shifted towards the migration of the pluronic F-108 surfactant. Even though, when blending these charged latexes with importantly different size for improved packing, both the particle packing and the surface charge density play a synergistic role in establishing the ionic complex network. The lower performance here is a clear result on the less dense network achieved in these blends.

5.4. Conclusions

This chapter investigates the possibility of producing completely emulsifier-free cationic waterborne dispersion using a homemade cationic monomer DABCO, characterized with double charge per molecule. The main idea is that, by addition of small quantity of cationic monomer to BA/MMA monomer mixture to achieve apart of colloidal stability, high surface charge density without scarifying the water resistance of the polymer film. This cationic dispersion was blended with anionic dispersion stabilized with NaSS and the effect of ionic complexation on the blend film performance was studied.

Waterborne dispersions, stabilized by DABCO cationic monomer were synthetized in the absence of emulsifier by seeded semibatch emulsion polymerization process. The final solids content was of 40% and DABCO concentration was varied from 1 mol% to 5 mol% based on main monomers (BA/MMA). Cationic latexes with high conversion (>93%), narrow particle size distribution and average particle size of around 170 nm were obtained. The polymers contain high THF insoluble fraction, probably due to the presence of cationic species in the polymer chains that make them insoluble in THF. The gel fraction, as well as the molar mass, two contradictory characteristics, were higher for higher concentration of DABCO, indicating higher DABCO incorporation onto the particles. Stiffer and less flexible, but less water resistant materials were obtained by increasing the DABCO concentration, likely due to denser reinforcing network created by the polymer chains reach in rigid DABCO reach polymer chains, as it was observed in TEM images.

Two set of blends were prepared using non-dialyzed and dialyzed DABCO and NaSS dispersions, by blending 275 nm NaSS -180 nm DABCO (Sample set 2) and 275 nm NaSS – 100 nm DABCO (Sample set 3). In order to postpone the ionic complexation that otherwise provokes immediate coagulation of the blend dispersion, pluronic F-108 surfactant was employed. No important differences in mechanical strength of the blend films were detected between non-dialyzed and dialyzed ones, meaning that the presence of water- soluble species do not show strong influence on the mechanical performance, whereas their presence affected slightly the water resistance. While clear effect of the ionic complex network was observed for the Blend 275-180 (Sample set 2), almost no effect was detected for Blend 275-100 (Sample set 3). Even though it was expected that the Sample set 3 would provide improved particle packing of the oppositely charged particles than Sample set 2 blends, obviously the surface charge density, which was much higher for Sample set 2 played a key role to establish strong and dense network.

5.5. References

(1) Bilgin, S.; Tomovska, R.; Asua, J. M. Surfactant-Free High Solids Content Polymer Dispersions. *Polymer (Guildf).* **2017**, *117*, 64–75. https://doi.org/10.1016/j.polymer.2017.04.014.

(2) Polpanich, D.; Tangboriboonrat, P.; Elaïssari, A. The Effect of Acrylic Acid Amount on the Colloidal Properties of Polystyrene Latex. *Colloid Polym. Sci.* **2005**, *284* (2), 183–191. https://doi.org/10.1007/s00396-005-1366-6.

(3) Ceska, G. W. The Effect of Carboxylic Monomers on Surfactant-free Emulsion Copolymerization. *J. Appl. Polym. Sci.* **1974**, *18* (2), 427–437. https://doi.org/10.1002/app.1974.070180210.

(4) González, I.; Mestach, D.; Leiza, J. R.; Asua, J. M. Adhesion Enhancement in Waterborne Acrylic Latex Binders Synthesized with Phosphate Methacrylate Monomers. *Prog. Org. Coatings* **2008**, *61* (1), 38–44. https://doi.org/10.1016/j.porgcoat.2007.09.012.

(5) Chimenti, S.; Vega, J. M.; García-Lecina, E.; Grande, H. J.; Paulis, M.; Leiza, J. R. In-Situ Phosphatization and Enhanced Corrosion Properties of Films Made of Phosphate Functionalized Nanoparticles. *React. Funct. Polym.* **2019**, *143* (April), 104334. https://doi.org/10.1016/j.reactfunctpolym.2019.104334.

(6) Ramos, J.; Forcada, J.; Hidalgo-Alvarez, R. Cationic Polymer Nanoparticles and Nanogels: From Synthesis to Biotechnological Applications. *Chem. Rev.* **2014**, *114* (1), 367–428. https://doi.org/10.1021/cr3002643.

(7) Muñoz-Bonilla, A.; Fernández-García, M. Polymeric Materials with Antimicrobial Activity. *Prog. Polym. Sci.* **2012**, *37* (2), 281–339. https://doi.org/10.1016/j.progpolymsci.2011.08.005.

(8) Zhang, K; Timothy, L. Dabco Containing Copolymer. Wo 2015/058137 A2, 2015.

(9) Pan, Y.; Xiao, H.; Cai, P.; Colpitts, M. Cellulose Fibers Modified with Nano-Sized Antimicrobial Polymer Latex for Pathogen Deactivation. *Carbohydr. Polym.* **2016**, *135*, 94–100. https://doi.org/10.1016/j.carbpol.2015.08.046.

(10) Fulmer, P. A.; Wynne, J. H. Development of Broad-Spectrum Antimicrobial Latex Paint Surfaces Employing Active Amphiphilic Compounds. *ACS Appl. Mater. Interfaces* **2011**, *3* (8), 2878–2884. https://doi.org/10.1021/am2005465.

(11) Rheenen, Van; Ralph, P. Cationic Latex Paint Composition, US5312863A, 1994.

(12) Twigt, F.; Piet, P.; German, A. L. Preparation and Co-Catalytic Properties of Functionalized Latices. **1991**, *27* (9), 939–945.

(13) van Streun, K. H.; Belt, W. J.; Piet, P.; German, A. L. Synthesis, Purification and Characterization of Cationic Latices Produced by the Emulsion Copolymerization of Styrene with 3-(Methacrylamidinopropyl)Trimethylammonium Chloride. *Eur. Polym. J.* **1991**, *27* (9), 931–938. https://doi.org/10.1016/0014-3057(91)90036-N.

(14) Delair, T.; Pichot, C.; Mandrand, B. Synthesis and Characterization of Cationic Latex Particles Bearing Sulfhydryl Groups and Their Use in the Immobilization of Fab Antibody Fragments. *Colloid Polym. Sci.* **1994**, *272*, 72–81.

(15) Bon, S. A. F.; Van Beek, H.; Piet, P.; German, A. L. Emulsifier-free Synthesis of Monodisperse Core–Shell Polymer Colloids Containing Chloromethyl Groups. *J. Appl. Polym. Sci.* **1995**, *58* (1), 19–29. https://doi.org/10.1002/app.1995.070580103.

(16) Xu, Z.; Yi, C.; Cheng, S.; Zhang, J. Emulsifier-Free Emulsion Copolymerization of Styrene and Butyl Acrylate with Cationic Comonomer. *J. Appl. Polym. Sci.* **1997**, No. October 1996, 1–9.

(17) Xu, Z.; Yi, C.; Lu, G.; Zhang, J.; Cheng, S. Styrene–Butyl Acrylate–N,N-Dimethyl N-ButylN-Methacrylamidino Propyl Ammonium Bromide Emulsifier–free Emulsion Copolymerization. *Polym. Int.* **1997**, *44*, 149–155.

(18) Liu, Z.; Xiao, H.; Wiseman, N. Emulsifier-Free Emulsion Copolymerization of Styrene with Quaternary Ammonium Cationic Monomers. *J. Appl. Polym. Sci.* **2000**, *76*, 1129–1140.

(19) Liu, Z.; Xiao, H. Soap-Free Emulsion Copolymerisation of Styrene with Cationic Monomer : Effect of Ethanol as a Cosolvent. **2000**, *41*, 7023–7031.

(20) Sauzedde, F.; Ganachaud, F.; Elaïssari, A.; Pichot, C. Emulsifier-Free Emulsion Copolymerization of Styrene with Two Different Amino-Containing Cationic Monomers. I. Kinetic Studies. *J. Appl. Polym. Sci.* **1997**, *65* (12), 2315–2330. https://doi.org/10.1002/(sici)1097-4628(19970919)65:12<2315::aid-app6>3.3.co;2-i.

(21) Hua, C.; Chen, K.; Wang, Z.; Guo, X. Preparation, Stability and Film Properties of Cationic Polyacrylate Latex Particles with Various Substituents on the Nitrogen Atom. *Prog. Org. Coatings* **2020**, *143* (December 2019), 105628. https://doi.org/10.1016/j.porgcoat.2020.105628.

(22) Zhang, K.; Drummey, K. J.; Moon, N. G.; Chiang, W. D.; Long, T. E. Styrenic DABCO Salt-Containing Monomers for the Synthesis of Novel Charged Polymers. *Polym. Chem.* **2016**, *7* (20), 3370–3374. https://doi.org/10.1039/c6py00426a.

(23) Tadros, T. F. *Colloid Stability, the Role of Surface Forces - Part I*; Wiley-VCH: Weinheim, 2007.

(24) Ohshima, H. *Electrical Phenomena at Interfaces and Biointerfaces. Fundamentals and Applications in Nano-, Bio-, and Environmental Sciences*; A JOHN WILEY & SONS, 2012.

(25) Dziomkina, N. V.; Hempenius, M. A.; Vancso, G. J. Synthesis of Cationic Core-Shell Latex Particles. *Eur. Polym. J.* **2006**, *42* (1), 81–91. https://doi.org/10.1016/j.eurpolymj.2005.07.015.

(26) Argaiz, M.; Ruipérez, F.; Aguirre, M.; Tomovska, R. Ionic Inter-Particle Complexation Effect on the Performance of Waterborne Coatings. *Polymers (Basel).* **2021**, *13* (18), 1–18. https://doi.org/10.3390/polym13183098.

(27) Bilgin, S.; Tomovska, R.; Asua, J. M. Effect of Ionic Monomer Concentration on Latex and Film Properties for Surfactant-Free High Solids Content Polymer Dispersions. *Eur. Polym. J.* **2017**, *93*, 480–494. https://doi.org/10.1016/j.eurpolymj.2017.06.029.

(28) Brown, W.; Zhao, J. Adsorption of Sodium Dodecyl Sulfate on Polystyrene Latex Particles Using Dynamic Light Scattering and Zeta Potential Measurements. *Macromolecules* **1993**, *26* (11), 2711–2715. https://doi.org/10.1021/ma00063a012.

(29) González, I.; Asua, J. M.; Leiza, J. R. The Role of Methyl Methacrylate on Branching and Gel Formation in the Emulsion Copolymerization of BA/MMA. *Polymer (Guildf).* **2007**, *48* (9), 2542–2547. https://doi.org/10.1016/j.polymer.2007.03.015.

(30) Park, Y. J.; Lee, D. Y.; Khew, M. C.; Ho, C. C.; Kim, J. H. Atomic Force Microscopy Study of PBMA Latex Film Formation: Effects of Carboxylated Random Copolymer. *Colloids Surfaces A Physicochem. Eng. Asp.* **1998**, *139* (1), 49–54. https://doi.org/10.1016/S0927-7757(98)00272-6.

(31) Jiménez, N.; Ballard, N.; Asua, J. M. Hydrogen Bond-Directed Formation of Stiff Polymer Films Using Naturally Occurring Polyphenols. *Macromolecules* **2019**, *52* (24), 9724–9734. https://doi.org/10.1021/acs.macromol.9b01694.

(32) Barandiaran, M. J., De la Cal, J. C., Asua, J. M. *Polymer Reaction Engineering*; J.M.Asua, Ed.; Blackwell: Oxford, 2007.

(33) Nunes, J. D. S.; Asua, J. M. Theory-Guided Strategy for Nanolatex Synthesis. *Langmuir* **2012**, *28* (19), 7333–7342. https://doi.org/10.1021/la3006647.

(34) Amalvy, J. I.; Unzué, M. J.; Schoonbrood, H. A. S.; Asua, J. M. Reactive Surfactants in Heterophase Polymerization: Colloidal Properties, Film-Water Absorption, and Surfactant Exudation. *J. Polym. Sci. Part A Polym. Chem.* **2002**, *40* (17), 2994–3000. https://doi.org/10.1002/pola.10385.

(35) Butler, L. N.; Fellows, C. M.; Gilbert, R. G. Effect of Surfactant Systems on the Water Sensitivity of Latex Films. *J. Appl. Polym. Sci.* **2004**, *92* (3), 1813–1823. https://doi.org/10.1002/app.20150.

Chapter 6. Effect of electrostatic interaction on paint performance

This work was developed in Allnex (Bergen op Zoom, The Netherlands) under the supervision of Dr. Silfredo Bohorquez.

6.1. Introduction

Improved performance of waterborne films was achieved when oppositely charged dispersions were blended, owed to the inter-particle ionic complexes formation.[1] However, the charged dispersions were dialyzed prior to blending in order to eliminate water-soluble species and conventional surfactant. The dialyzing process is not very practice from industrial point of view, besides being time consuming and expensive, due to the large amount of water needed and the high price of the specific membranes.

A possible approach to reduce the undesired effects of conventional surfactants and to decrease or eliminate the quantity of the water-soluble oligomers formed while functionalizing the particles, is the use of polymerizable emulsifiers (surfmers).[2–5] The main difference from conventional surfactants, is the presence of C=C double bonds in the structure of surfmers, which allows their copolymerizing with the main monomers. Consequently, these amphiphilic species

remain covalently bonded onto polymer particles, avoiding the desorption and migration during storage of the latex or/and film formation.[6] During the last years, various works have been published dealing with the synthesis of high solids content latexes using polymerizable surfactants.[4,7–10] Stable high solids content (60%) BA/MMA/MAA dispersions were successfully synthetized using commercial anionic surfmers, known under commercial names of Latemul PD-104 and Sipomer Cops-1.[11] Interestingly, lower amount of Latemul PD-104 polymerizable surfactant was employed compared to Dowfax 2A1 conventional surfactant to achieve stable latexes, affecting positively the water resistance of the polymer films.

Encouraged with these results that provide platform for decreasing the problems of water-soluble species creation during copolymerization of ionic monomers with (met)acrylic monomers, herein, two different polymerizable surfactants were used, both anionically charged, Hitenol AR-10 and Latemul PD-104 (see Figure 6.1). They were copolymerized with BA and MMA as main monomers by emulsion polymerization. Two sets of latexes were prepared. In the first set, the anionic charges were coming only from the polymerizable surfactants, while in the second set, an additional functional monomer, MAA, was used, which contributed to the anionic charging of the system.

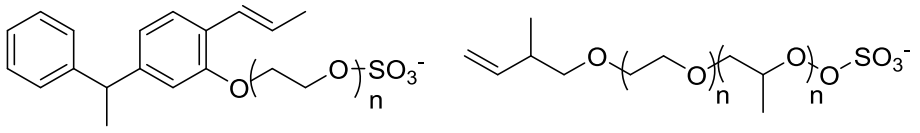

(a) (b)

Figure 6.1. Chemical structure of (a) Hitenol AR-10 and (b) Latemul PD-104.

Two lines were developed, based on these anionic latexes (Scheme 6.1). In first one, the performance of anionic latexes as binders in paint formulation was examined. In the second part of the work, commercial cationic resins from Allnex (LQUAT2-EPOXY and CATD) were blended with the anionic latexes in order to produce ionic complexation and such blends were used as binders. The main idea was to examine the effect of the ionic complexes formation on the performance and applications of the paints. Among other application properties, the effect of ionic complex towards tannin and marker resistance was investigated as the formation of this complex might act as a physical barrier avoiding the migration of markers and tannins through the paint.

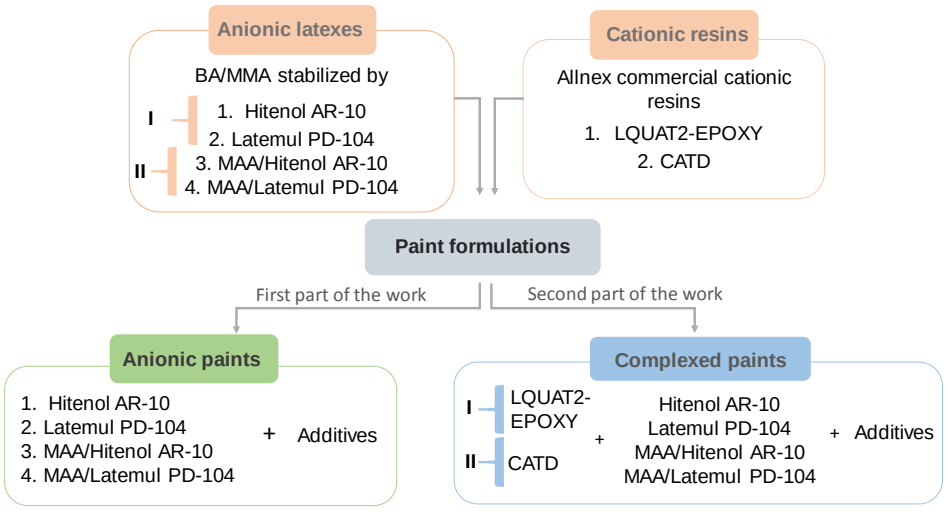

Scheme 6.1. Paints preparation scheme.

6.2. Experimental part

6.2.1. Materials

The materials are given in Appendix I.

6.2.2. Synthesis of anionically charged waterborne dispersion using polymerizable surfactants

Anionically charged aqueous polymer dispersions were synthetized by seeded semibatch emulsion polymerization process following the recipe developed by Aguirreurreta et.al.[11] While two latexes were made of BA/MMA, another two dispersions were made of BA/MMA/MAA stabilized with Hitenol AR-10 and Latemul PD-104 polymerizable surfactants. As summarized in Table 6.1, latexes were named from L1 to L4 indicating whether MAA (A) was employed in the synthesis and the type of polymerizable emulsifier used: Hitenol AR-10 (H) and Latemul PD-104 (L).

Table 6.1. Summary of the synthetized anionic waterborne dispersions.

Latex	Composition	Polymerizable emulsifier	Name
Latex 1	BA/MMA/MAA	Hitenol AR-10	L1-AH
Latex 2		Latemul PD-104	L2-AL
Latex 3	BA/MMA	Hitenol AR-10	L3-H
Latex 4		Latemul PD-104	L4-L

Initially two seeds were prepared using BA/MMA/MAA (49.5/49.5/1 wt%) at 15% solids content using conventional emulsifiers Dowfax with two different concentrations 1 wbm% and

1.5 wbm%. Formulations for these seeds are presented in Appendix I. The Seed 1 (Dowfax 1 wbm%) was used for L1-AH and L2-AL dispersions, while the Seed 2 (Dowfax 1.5 wbm%) was employed for L3-H and L4-L.

In a second step, the reactor was loaded with the desired amount of the seed and upon achieving 75 °C, the preemulsion containing BA, MMA and the polymerizable surfactant in case of L3-H and L4-H was fed, while MAA functional monomer was also added to the preemulsion for synthesis of L1-AH and L2-AL. The final solids content of all the latexes was 50 %. After the feeding period (240 minutes), the system was allowed to react for one hour more. Formulations used for the anionic latexes are represented in Appendix I, Table I.6, I.7 and I.8 and the Schematic view of these processes is illustrated in Scheme 6.2.

	Initial charge	**Feeding**	**Initial charge**	**Feeding**
L1-AH **L2-AL**	Dowfax $NaHCO_3$ Ammonia KPS	1. BA/MMA 2. MAA	Seed (15% s.c.)	1. BA/MMA/MAA 2. Polymerizable emulsifier 3. KPS
	t_0 — 1^{st} step		2^{nd} step	t_{final}
	Initial charge	Feeding	Initial charge	Feeding
L3-H **L4-L**	Dowfax $NaHCO_3$ Ammonia KPS	1. BA/MMA	Seed (20% s.c.)	1. BA/MMA 2. Polymerizable emulsifier 3. KPS

Scheme 6.2. Schematic view of the anionically charged latex synthesis procedure.

Main monomers conversion was studied gravimetrically and coagulum amount was calculated based on the total monomer. The average particle size was measured by DLS. A detailed description of the characterization methods is provided in Appendix II.

6.2.3. Paint formulation

As mentioned in Chapter 1, in general paints consists of a polymeric binder, pigments, additives and solvent.[12,13] For a practical reason, Table 6.2 summarizes the typical components of waterborne paints and their function.[12–15]

Table 6.2. Summary of the typical components of waterborne paints and their function.

	Components	Function
	Binder	Wetting of filler particles Films forming Paint adhesion on substrate
	Medium (H2O)	Particle dispersion
Pigments	**Functional filler**	Whiteness Brightness Opacity
	Extender	Space holding effect Low formulation price
Additives	**Dispersing agent**	Wetting of filler particles Avoid sedimentation
	Defoamer	Avoid foaming
	Leveling agent	Formation of a smooth uniform surface
	Thickener	Paint stabilization Ease of handing

The choice of additives in paint formulation requires a preliminary screening since the addition of an ingredient may offer antagonism response, being favourable for a given property, but non-beneficial for another. Thus, a balance is required between the additive's effects in order to optimize the coating formulation.

6.2.3.1. *Evaluation of anionic dispersions as binders*

Design of experiments (DoE) and high-throughput experimentation (HTE) combinatorial methods are valuable tools for the development of an optimal formulation. DoE is a powerful

tool for estimating the best operating conditions of a system, while HTE allows faster rates of the design experiments owing to the automation.

Coating formulation is performed following the plan of experiments given by DoE, while the experiments are carried out using the automatic Robot (SynchronXperimate: Robotic XYZ automated liquid handling systems for bench, integration and custom applications). This combination of methods was employed for the evaluation of the anionic latexes as binders. Thus, the main objective of this part of the work was to ensure the ability of anionic resins to be formulated. This is why, first of all, the original anionic latexes were applied onto glass substrates and dried for 24 hours at 5 °C in order to examine the film forming ability since it is the minimum temperature required in industry. In all cases, cracked white films were formed. A photo of the glass substrate (on top of a black card) for L1-AH film was taken as shown in Figure 6.2.

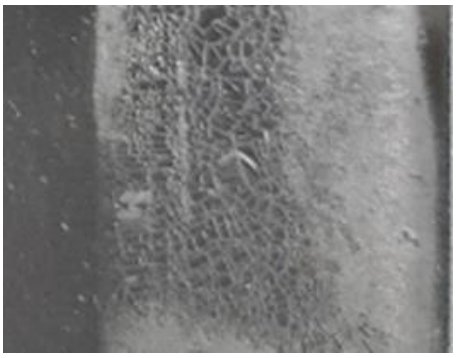

Figure 6.2. Appearance of L1-AH film after drying for 24 hour at 5 °C.

Co-solvents are widely employed in industry owing to its ability to reduce the minimum film formation temperature (MFFT), which assists the formation of a proper film. Therefore,

three of the most commonly employed co-solvents at different concentrations were selected in order to examine their effect on the film formation ability. The selected co-solvents were Butyl glycol (BG), Butyl diglycol (BdG), and Texanol (Tex). The solvent's concentration were 2, 4, 6 and 7, based on the total formulation (wt%). Films were allowed to dry for 24 hours at 5 °C, since it is the minimum temperature required in industry.

One of the anionic latexes was selected (L1-AH) to study the interaction with different defoamers and levelling agents. Surfynol 104-E and BYK-348 were chosen as leveling agents, whereas FoamStar 2292 and Additol VXW 6210N were selected as defoamers. The type of design used in DoE was Surface Response as it proffers the option of including both numerical and categorical variables. The responses measured were focused on appearance, hardness and early water resistance (EWR). Two combinations were designed based on different types and concentrations of leveling agents and defoamers, resulting in 38 experiments. Four replicate points were included in each of the sets. These experiments were performed using the Paint Robot. The formulations (Table 6.3) showing the best appearance after applying in Leneta card substrate were later used for formulating the rest of the anionic latexes (L2-AL, L3-H and L4-L).

Table 6.3. Experiments performed.

Formulation	Cosolvent (g)		Defoamer (g)	Leveling agent (g)
	Tex	BdG	Foam SI2292	Surfynol E-104
1	-	1.4	0.350	0.160
2	0.6	-	0.100	0.027

6.2.4. Selection of cationically charged waterborne dispersions as binder

Herein, Allnex commercial cationic resins, *LQUAT2 - EPOXY resin* (indicated as LQUAT2 in this work) and *CATD* resin (indicated as CATD in this manuscript) were selected for preparation of the ionic complexes with the anionic dispersions. LQUAT2 is composed of two acrylic dispersions, the first component has both tertiary amine and carboxylic acid groups attached to the acrylic backbone and the second component is composed of epoxy and hydroxylic groups, which are attached to the acrylic backbone. Quaternarization of the system occurs, once the second component reacts with LQUAT2. On the other hand, CATD resin contains quaternary ammonium compounds, meaning that it is already charged. The main difference between them is that LQUAT2 is charged during film formation, while CATD is charged in the dispersion state.

First of all, blends between the anionic latexes and cationic resins were performed in order to study the critical point of possible coagulation. For this purpose, different concentrations of the anionic resins (between 5 wbr% (weight based resin%) to 25 wbr%) were added drop by drop to the cationic resins while stirring, meaning that the cationic resin was the main component of the binder within the coating formulations. The summary of the performed blends is shown in Scheme 6.3.

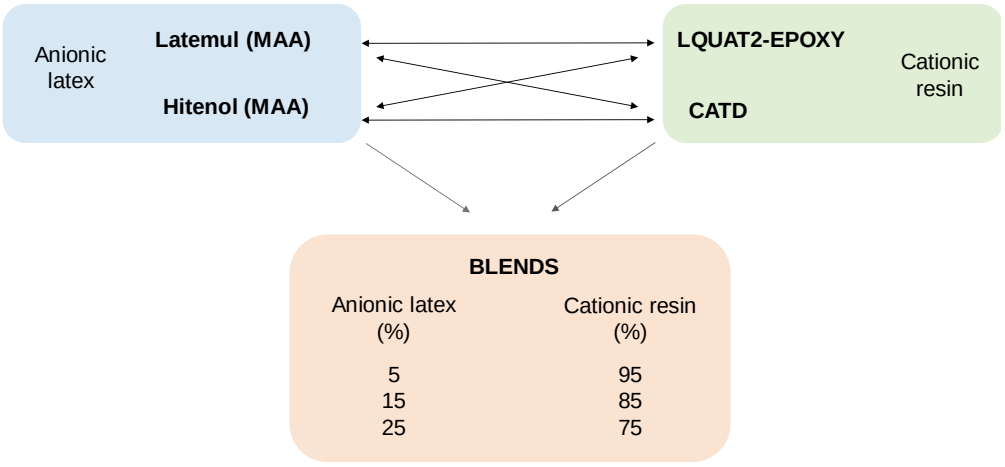

Scheme 6.3. Schematic view of performed blends.

Later, the rest of the additives were added in order to examine the effect of the established ionic complexes on the paint performance and application. Formulations developed by Allnex were. Nonetheless, it should be mentioned that formulations were different for the part where LQUAT2 was employed as cationic resin and the part where CATD was used as cationic one. In other words, the references (cationic and anionic) and the blends were formulated differently and therefore, the properties of the anionic resins may be affected from one part of the work (when LQUAT2 was used as cationic resin) to the second part (when CATD was employed as cationic one).

As reference samples, pure cationic resin (indicated as 0% during this work) and pure anionic resin (indicated as 100%) were used. Thus, samples were indicated as 0% (cationic reference), from 5% to 25% (performed blends) and 100% (anionic reference).

Blends performed using LQUAT2 were indicated as Blend 1 (LQUAT2 - L1-AH), Blend 2 (LQUAT2 - L2-AL), Blend 3 (LQUAT2 - L3-H) and Blend 4 (LQUAT2 - L4-L), whereas blends prepared employing CATD were named as Blend 6 (CATD - L1-AH), Blend 7 (CATD - L2-AL), Blend 8 (CATD - L3-H) and Blend 9 (CATD – L4-L).

Unfortunately, owing to the charged state of CATD cationic resin, tiny aggregations were observed when increasing the amount of the anionic resin in the blended system. This is why, cationic and anionic resins were formulated separately, followed by the blending of the formulated systems as described in Scheme 6.3.

One of the things that should be taken into consideration is that when mixing LQUAT2 with the anionic latexes, a competition between the carboxylic groups present in LQUAT2 and the anionic polymerizable surfactants for reacting with cationic species of LQUAT2 was expected. This means that not all the cationic species will interact with the anionic species coming from polymerizable surfactants.

6.2.5. Clear- and pigmented-coatings preparation

Clear-coats are non-pigmented coatings, meaning that pigment dispersion (mill base part) is not required. This part of the paint formulation is known as let-down and consist mainly of binder and small amount of additives (co-solvent, defoamer, thickener…). In the first part of the work (study of anionic latexes as possible binders), screening of additives at different concentrations were performed using an automatic robot as described previously. For the rest of

the work (anionic and cationic resin blends) formulations were prepared using high speed disperser (Dispermat). Once the resins were stirring, the rest of the additives were added one by one. Compounds were allowed to mix for 5 minutes at 2000 rpm.

On the other hand, pigmented-coats consist of resin, pigment, filler and small amount of additives. For this purpose, the pigment dispersion (mill base) was first prepared. The mill base compounds (dispersing agent, pigment, filler, defoamer, water) were vigorously stirred until a solid particle size below 40 μm (size accepted for primer-coats) was obtained. Grindometer instrument was employed for determining the particle size and the fineness of the mill base. The prepared mill base was added to the resin and then, the rest of the let-down additives were added while stirring in the high speed mixer (Dispemat) for 5 minutes at 2000 rpm. Pigmented-coats were formulated in the second part of the work, where anionic-cationic resin blends were employed as binders.

6.2.6. Determination of clear- and pigmented-coat performance

Clear-coats performance prepared using anionic latexes as binders was first determined by means of gloss and haze, hardness and early water resistance (EWR). The same study was carried out when the blends were employed as binders in clear-coats and pigmented paints in order to see the effect of the ionic complex formed in properties as gloss, hardness and EWR. Details of these characterization methods are provided in Appendix II.

The blocking properties of the blends containing cationic and anionic binders were also investigated. Wood is the most abundant and renewable natural resource. Photodegradation process is the major degradation pathway of wood materials and the main drawback is that the colour of the wood material changes into yellow and brown.[16] This is why, the main purpose of the primer coatings is to increase wood protection against UV light. In Paints & Coatings industry, tannin bleeding and stains are the most common problems. Tannin is a natural molecule (illustrated in Figure 6.3), that can be found in many types of wood used for construction.

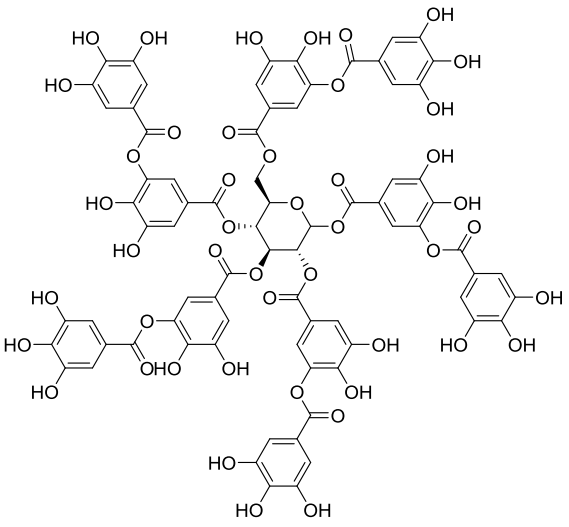

Figure 6.3. Chemical structure of tannic acids.

In contact with water, tannins which are water-soluble species, tend to migrate (bleed) into the wood substrate, causing undesirable brown or yellowish discoloration. One approach to overcome this issue is applying coatings in the wood's surface. However, the use of waterborne

coatings can still cause bleeding of tannin species during the application time. This is why manufacturers have developed a coating system that provides barrier properties as primer coatings. Primer-coats not only are used to prevent tannins migration, but also to limit or avoid migration of nicotine marks or markers/dyes through the coating/paint layers.

One of the main chemical approaches to immobilize tannins is to combine anionic carboxylated polymer dispersion with reactive pigments such as zinc oxide. As zinc oxide is the source for Zn^{2+} ions in water, these cations are able to form a water insoluble complex with the tannins. Although this method is effective in preventing tannin bleeding, it can lead to instability problems owing to the presence of multivalent metal ions or loss of stain blocking efficiency if reactive pigments interact with the anionic primer coating.[17,18] One strong alternative is the use of cationic dispersions as binders since the presence of protonated or quaternized amino-functional groups within the polymer backbone allows salt-formation with tannins, preventing the bleeding through the paint layers.[19] However, the use of cationic resin is limited due to the anionic nature of most of the paint additives used in the industry.

Regarding the markers/dyes migration, as in general they are anionic species as well, same bleeding issues as with tannins are faced. This is why developed cationic systems promote interactions with these markers/dyes preventing from bleeding through the coating layers.

Thus, as already mentioned in the introduction, the main objective of this part of the work is to examine the effect of ionic complex towards tannin and marker resistance as this complex might act as a physical barrier avoiding the migration of markers and tannins through the paint.

For this purpose, tannin and marker resistance tests were performed. These characterization methods are described bellow in order to make easier to follow this work).

6.2.6.1. *Tannin resistance*

A board of merbau wood (which is rich in tannins) was selected as a substrate for the tannin resistance test. The substrate was coated with one layer of the primer-coat using a brush and it was allowed to dry for four hours at standard conditions. The second layer of the coating was applied in half of the substrate, which means that half of the substrate was coated with one layer, while the other half was coated with two layers. The second layer was let to dry for 4 hours. Finally, a white top-coat, with no tannin blocking properties, was applied. A representation of the followed method is illustrated in Figure 6.4.

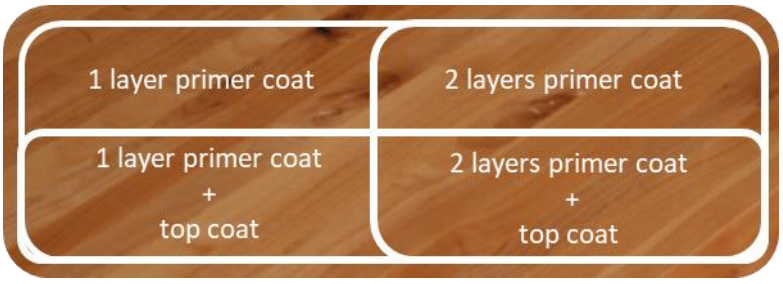

Figure 6.4. Tannin resistant test method.

6.2.6.2. *Marker resistance*

For the marker resistance test, acrylic wall paint was applied onto Leneta card substrate allowing the paint to dry for 24 hours. Markers and chemicals were applied onto the dry paint letting them dry for 24 hours (Figure 6.5a). The selected markers/chemicals list is the following

one: 1) blue waterborne marker, 2) black waterborne marker, 3) red waterborne marker, 4) blue marker based on alcohol, 5) basacid red dye (1% in water), 6) red wine, 7) betadine, 8) blue seal ink,9) coffee and 10) black permanent marker.

Dried markers were first washed with water in order to eliminate them. After, a primer coating was applied (Figure 6.5b) and it was allowed to dry before applying the white top-coat, which did not present blocking properties (Figure 6.5c). The next day, bleeding of the markers through the coatings layers was visually checked.

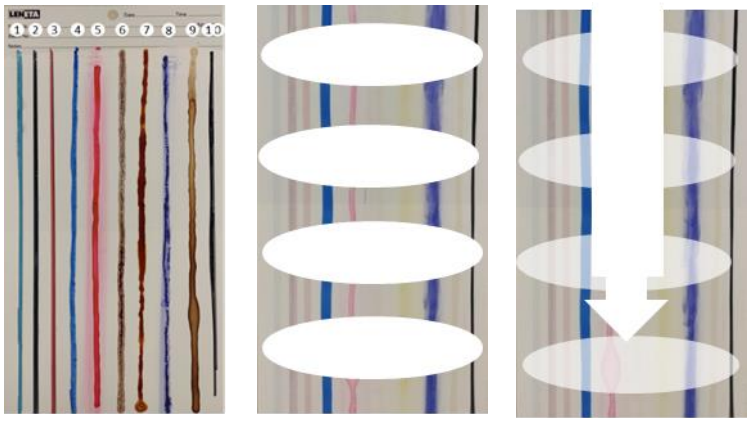

(a) (b) (c)

Figure 6.5. Marker resistance test procedure: (a) 10 markers/chemicals, (b) primer-coats and (c) white top-coat application.

6.3. Results and discussion

6.3.1. Characteristics of the anionically charged latexes

The anionically charged dispersions were synthesized by seeded semibatch emulsion polymerization. Two different seed latexes were synthesized for that aim, using different amount of Dowfax, Seed 1 (Dowfax 1 wbm%) and Seed 2 (Dowfax 1.5 wbm%). The conversion and particle sizes are presented in Table 6.4. Almost full conversion was obtained at the end of the polymerizations, obtaining an average particle size of 95 nm for Seed 1 and 75 nm for Seed 2.

Table 6.4. Seed latex characteristics.

Latex	Conversion (%)	dp_{DLS} (nm)
Seed 1	99	95 ± 5
Seed 2	98	75 ± 2

High solids content, anionically charged dispersions using polymerizable surfactants were produced in the second step of emulsion polymerization, in which Seed 1 was grew to synthesize L1-AH and L2-AL dispersions based on BA/MMA/MAA, while Seed 2 was used in the synthesis of L3-H and L4-L based on BA/MMA. Table 6.5 summarizes the main characteristics of these latexes.

Table 6.5. Conversion, average particle size, coagulum amount and final pH obtained for each of the polymerizations.

Latex	Conversion (%)	dp_{DLS} (nm)	Coagulum amount (%)	pH
L1-AH	98	230	-	Acidic
L2-AL	99	310	2	Basic
L3-H	97	215	1	Acidic
L4-L	96	215	3	Acidic

High instantaneous conversions were measured for all the cases from 60 minutes on, as shown in Figure 6.6a.

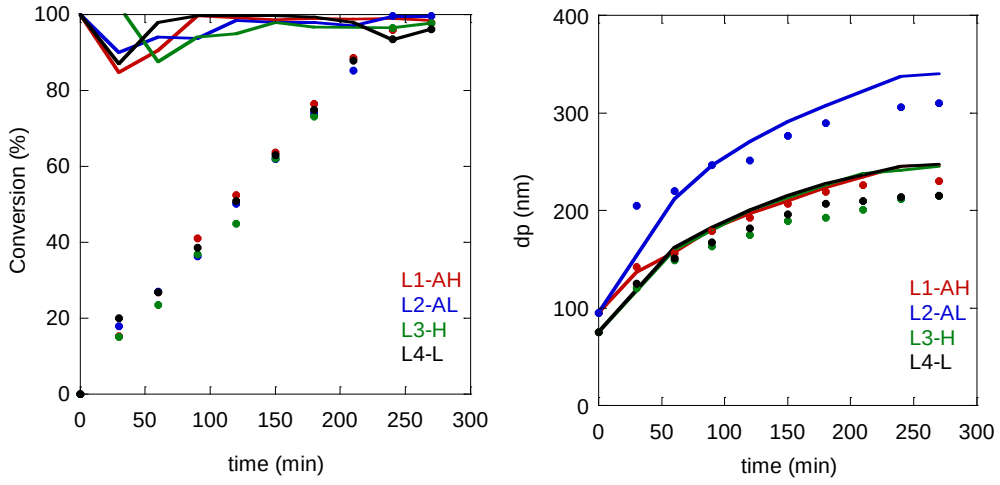

(a) (b)

Figure 6.6. Time evolution of (a) monomer conversion and (b) particle size for anionically and cationically charged latexes. Continuous line represents (a) the instantaneous conversion and (b) the theoretical particle size, while (a) the dots the overall conversion and (b) the experimental particle size.

Nevertheless, at the beginning of the semicontinuous process, monomer was accumulated in the system, probably because the feeding rate was faster than the monomer consumption rate.

Despite of it, the final conversions were high in all the cases as it is shown in Figure 6.6a. Moreover, no significant effect of polymerizable surfactant type nor of the functional monomer addition (MAA) on the reaction rate was observed. The evolution of the particle size is presented in Figure 6.6b. As it can be seen, the particle size evolution was very similar for L1-AH, L3-H and L4-L dispersions, while higher particle size was obtained for L2-AL, which is likely due to the different synthesis approach employed in the last case, in which lower quantity of the seed was used.[11] Theoretical and experimental particle size evolution were compared, as shown in Figure 6.6b to get information on the colloidal stability and secondary nucleation in the studied systems. The theoretical and experimental particle size values for L1-AH were similar along the reaction, indicating a colloidally stable system and low extent of secondary nucleation. For the other latexes, the theoretical values of the average particle size were slightly higher than experimental one, indicating certain extent of creation of new particles. The less stable system seemed to be L2-AL, showing particle coalescence in the initial period and more pronounced secondary nucleation.[8]

Stable latexes were obtained in all the cases, however, small amount of coagulum was measured at the end of the process for L2-AL, L3-H and L4-L latexes (see Table 6.5). The final pH of the latexes synthesized under basic conditions (L2-AL) was around 7.5 whereas the pH was around 3 for the latexes synthesized under acidic conditions (L1-AH, L3-H and L4-L), as summarized in Table 6.5.

6.3.2. Evaluation of anionically charged dispersion as binder

The anionically charged dispersions were used as binders to formulate clear-coatings. Three different solvents were used, as mentioned, to improve film formation from the anionic dispersions, BG, BdG and Tex. Cracked and transparent films were formed when BG was used, even at high concentrations, while in case of BdG, surface defects were not observed when adding 7 wt%. Films presented very good appearance when 3 wt% Tex was employed. Therefore, these two solvents BdG and Tex at the mentioned concentration were used to prepare the clear-coatings.

However, the addition of additives into L4-L latex, caused latex destabilization. In the case in which Tex solvent was used, significant coagulation was noticed, whereas for BdG small aggregations were observed when applying onto the Leneta substrate. This means that the use of Latemul polymerizable surfactant did not provide sufficient colloidal stabilization when the co-solvent was added, whereas when Latemul was used in combination with MAA the stability of the latex was improved (L2-AL). With other latexes, stable dispersions were obtained after the addition of either BdG or Tex.

As for the rest of the additives (defoamers and leveling agents), two formulations were selected (Table 6.3) for the clear-coats preparation using the four anionic dispersions (L1-AH, L2-AL, L3-H, L4-L), from which just the first three latexes gave rise to a nice films that allowed further studies of coating performance, by means of gloss, hardness and early water resistance tests. The results are presented in Table 6.6.

Table 6.6. Clear-coats performance after 24 hours drying.

Formulation	Binder	Gloss (20°)	Haze	Hardness (s)	EWR
1	L1-AH	82.7 ± 0.1	82.5 ± 0.1	7	3
	L2-AL[a]	76.9 ± 0.9	120 ± 1.5	7	2
	L3-H*	82.1 ± 0.6	90.1 ± 0.6	6	2
	L4-L	-	-	-	-
2	L1-AH	71.5 ± 1.8	155 ± 1.8	9	5
	L2-AL	47.5 ± 1.5	260 ± 2.9	9	3
	L3-H	60 ± 2.9	280 ± 3.1	7	3
	L4-L	-	-	-	-

[a]Coating film was still sticky

According to Table 6.6, Formulation 1 coating films showed higher gloss and lower haze, and lower EWR than Formulation 2, which is likely result of the different type and quantity of the solvent used. These results indicate that BdG solvent, used in Formulation 1, presents better compatibility with the anionic resins, which moreover was added in higher amount. Therefore, it gives enough time to promote proper coalescence process during evaporation, affecting positively the final properties as it has been reported recently.[20] Nevertheless, in both formulations, lower water resistance was observed when employing L2-AL and L3-H as binders probably owed to the higher amount of water-soluble species within polymer films. The higher Hitenol-AR10 amount employed for the synthesis may be responsible for the formation of higher content of water-soluble species in case of L3-H film, whereas, in case of L2-AL probably, the higher pH might have affected the partitioning of MAA monomer during emulsion polymerization. It is well known that the partitioning of this functional monomer is determined by its pKa ($pkA_{MAA} = 4.86$[21]), meaning that at pH above its pKa, the disassociated form of the acid

monomer will exhibit a negative charge making it more polar and therefore, more attractive to the polar water molecules of the water phase than in its undisassociated state. Thus, by increasing the pH of the dispersion, the MAA monomer would prefer to copolymerized in the aqueous phase producing higher content of water-soluble oligomers.[22,23] As L2-AL latex was synthetized under basic conditions (Table 6.5), the formation of water-soluble species was favoured. Consequently, during the film formation process these water-soluble species remain trapped within the film favouring the formation of hydrophilic pockets or aggregates within the film.

The time evolution of the coating hardness are presented in Figure 6.7, investigated during 7 days after the films were cast. Hardness was measured the first, the third, the sixth and the seventh day of the drying period. As expected, the coating films presented increased hardness during drying, because of the solvent evaporation and film formation process. Interestingly, the coating of Formulation 1 showed higher values than for Formulation 2. As already mentioned, on the one hand the greater compatibility of the polymer and on the other hand the slower evaporation of BdG, promoting proper coalescence process before evaporating, might affect positively the final performance.[20]

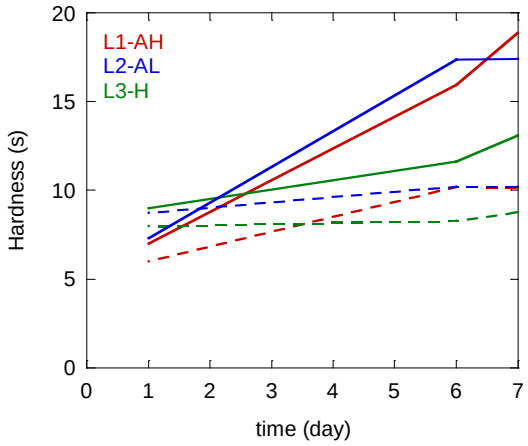

Figure 6.7. Coating film hardness evolution for one week. Continuous line (-) is referred to Formulation 1 and discontinuous line (--) is referred to Formulation 2.

These results confirm the possibility of using the resins L1-AH, L2-AL and L3-H as binders for coating formulations.

6.3.3. Use of blends of LQUAT2 cationic resin with anionic latexes as binders

The blend dispersions were prepared by mixing anionic and cationic dispersions with the aim to establish ionic inter-particle complexes and to study their effect on the performance of the coatings. For that aim, the LQUAT 2 cationic resin was combined with the four anionic dispersions (L1-AH, L2-AL, L3-H and L4-L). The anionic dispersions were added in 5%, 15% and 25% to the cationic one.

Blend dispersions were stable until 25 wt% of anionic resin was added. The rest of the additives to form the clear-coats and pigmented paints were later added to the blend resin. The

performance (gloss, hardness and EWR) and application properties (tannin and marker resistance) of clear- and pigmented-coats when using blend binders that can produce ionic bonding were deeply analysed as shown in the following paragraphs.

Analyses of clear-coat coatings were first performed. All the blends presented similar gloss values, and tannin and marker resistance, nevertheless, for simplicity, only a representative blend Blend 1 (LQUAT2 – L1-AH) is presented in this chapter, while the results for the other blends are summarized in Appendix VI, more precisely in Figure VI.1, Figure VI.2 and Figure VI.3.

6.3.3.1. *Clear-coats based on LQUAT2 cationic resin blends with anionic resins*

Figure 6.8 presents the gloss values at 20° and 60° for the clear-coats casted from Blend 1 (LQUAT2 – L1-AH) and dried at ambient temperature, compared with the reference one (0% and 100%). There is no effect of the composition of the binder on the gloss of the clear-coats. The eventual ionic bonding within the blends did not affect the gloss values, as they are in between these of the references.

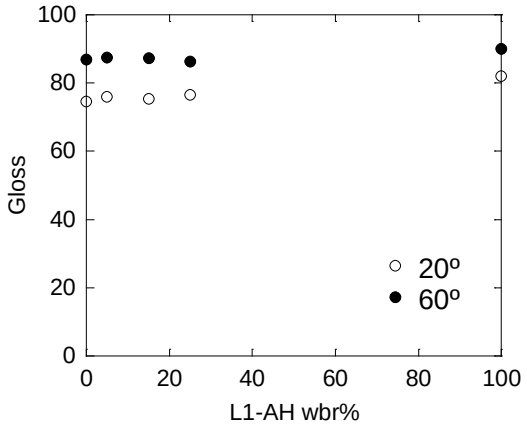

Figure 6.8. Gloss values for references and Blend 1 (LQUAT2 – L1-AH) containing from 5 to 25 wbar% of L1-AH.

The hardness of the paint films was affected by the composition of the binders. For the four blends, the hardness values after 7 drying days are shown in Figure 6.9.

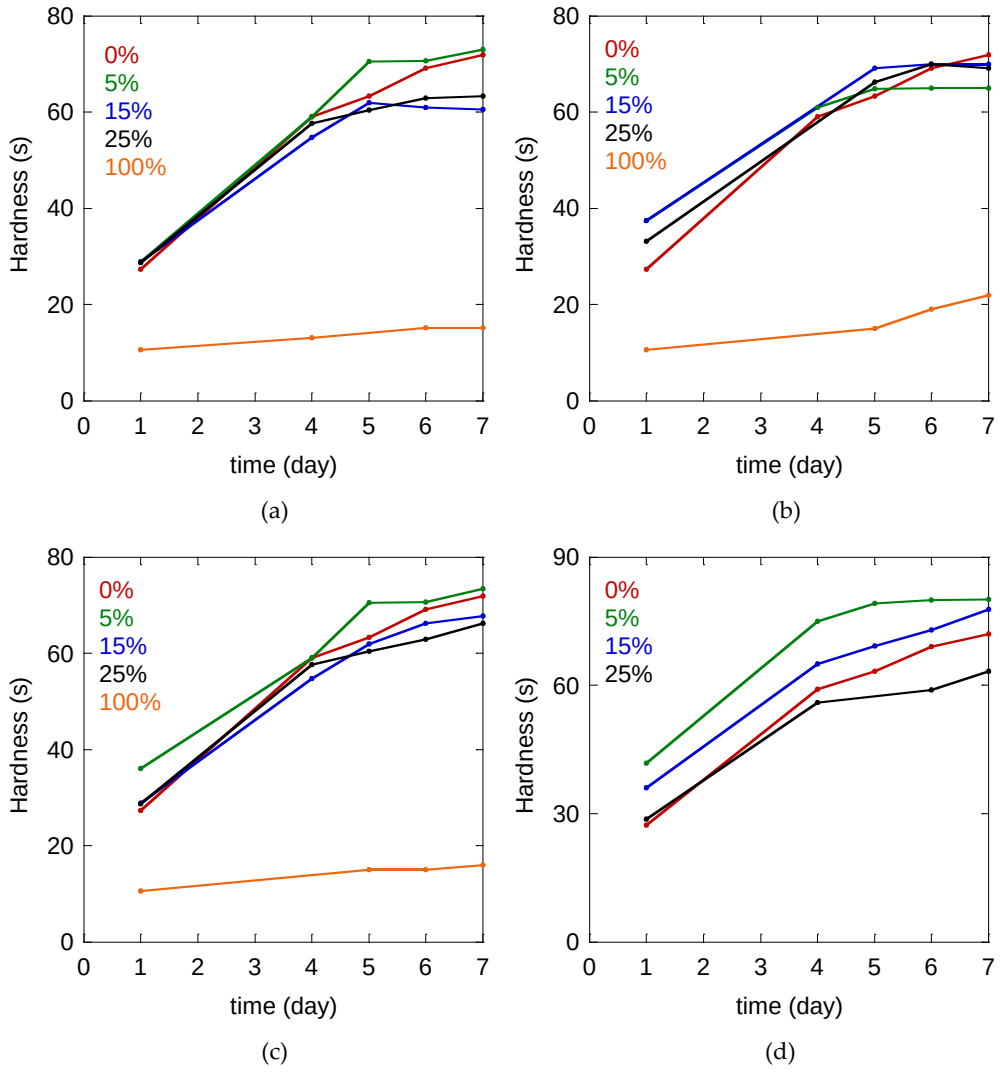

Figure 6.9. Hardness values for references and blends containing from 5 to 25 wbar% of (a) Blend 1 (LQUAT2 - L1-AH), (b) Blend 2 ((LQUAT2 – L2-AL), (c) Blend 3 (LQUAT2 – L3-H) and (d) Blend 3 (LQUAT2 – L4-L).

As it can be seen, the cationic reference material (0%) was much harder than the anionic reference one (100%). This introduces a kind of screening of the effect of ionic interactions, as

eventual improvement from the ionic complexation can be compensated by the negative effect of the low hardness of the anionic polymers.

For the case of Blend 1 (LQUAT2 – L1-AH), Blend 2 (LQUAT2 – L2-AL) and Blend 3 (LQUAT2 – L3-H), cationic reference and blend films showed similar hardness. Tiny improvements can be observed for Blend 1 (LQUAT2 – L1-AH) and Blend 3 (LQUAT2 – L3-H) when 5% anionic resin was added. Interestingly, Blend 4 (LQUAT2 – L4-L) exhibited increase in hardness to 80 s for blends containing 5% and 15% anionic resin with respect to 70 s, for hardness of the cationic reference. This increase after addition of the latex with lower mechanical resistance is likely due to ionic bonding established between the anionic and cationic resins and indicated that the ionic bonding effect was higher than the drop of hardness due to the addition of the anionic resin. Surprisingly, further increase of anionic resin content into the blend (25%) in Blend 4 (LQUAT2 – L4-L) dropped the hardness to 63 s. In this case, it is probable that the drop of the hardness due to mixing with the anionic resistance was higher than the effect of the ionic bonding. For the clear-coat based on L4-L anionic resin, the hardness could not be determined. Nevertheless, considering that L4-L resin was made of BA/MMA (50/50 wt%) as the other anionic resins, similar hardness might be expected, meaning that the observed improvements in the blends were likely related to the ionic bonding structures.

EWR of the references and blend coating films was measured during first drying day. Poor resistance was observed within the first hour. Nevertheless, films were slightly recovered after the first hour. No effect of eventual ionic bonding was visually detected in the blend samples,

probably owed to two effects. On the one hand, the performed qualitative test might not allow detecting the expected small differences and on the other hand, the low ionic neutralization degree might not be high enough for preventing water penetration.

The blocking properties to tannins and markers of the blends were also investigated. All of the blends presented very similar resistance to tannins and for simplicity reasons, only a representative image of Blend 1 (LQUAT2 – L1-AH) for the three concentrations of anionic resin 5%, 15% and 25%) is shown in Figure 6.10, where the tannins resistance of the reference coats are shown, too. The resistance to tannins of the other blends are presented in Figure VI.2 in the Appendix VI. Optically, there was not differences between references and blend primer-coats. This is why, the colour measurements of the top-coated areas were done in a quantitative way using a colorimeter in order to eliminate the subjectivity and determine exactly the tannin resistance of the samples. The CIELAB colour space (L*a*b*) was defined by the International Commission on Illumination in 1976 and expresses the colour through parameter "L", indicating the level of light or dark, parameter "a" referring to the redness or greenness, and parameter "b", determining yellowness or blueness.[24] During this work, b parameter was analysed after application of two clear-coat layers over the merbau wood panels, over which a layer of white coating without tannin resistance capacity was added. As b values will increase with increasing yellowish, values close to zero are the desired ones for the tannin resistance result.

According to Figure 6.10, when the first primer clear-coat layer was applied to the wood panels, discoloration was reduced, as b parameter was lower for all coatings including the references.

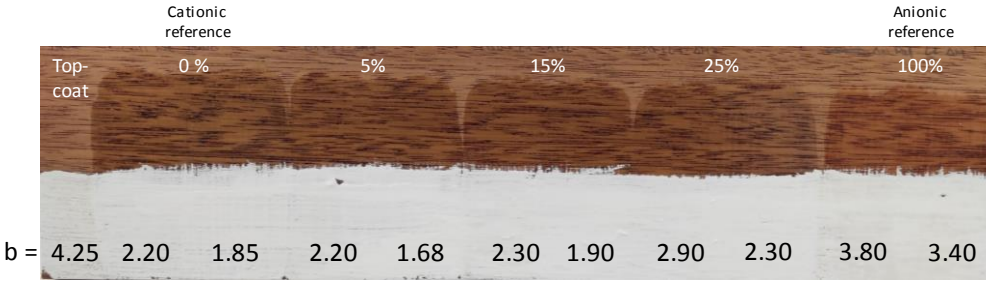

Figure 6.10. Resistance to tannins test of reference films and Blend 1 (LQUAT2 – L1-AH) films with different content of anionic resin (5, 15 and 25 wbar%)

Parameter b is 4.25 for the uncoated panel, and much lower for all coated ones (represented by the left value of b parameter for each coating). This means that primer coatings blocked the tannins migration onto the top-coat layer. The effect was much stronger when the second clear-coat layer was applied (the right values of b-parameter). The cationic reference exhibited lower b values (< 2.2) than the anionic one (< 3.4), since cationic binder forms a salt complex with tannins preventing their migration. For Blend 1 (LQUAT2 – L1-AH), no important differences were detected between the blends containing 5% (b = 1.68) and 15% (b = 1.9) anionic resin with respect to the cationic reference (b = 1.85), beside the much higher b-value of the added anionic reference. This result is likely an effect of the ionic bonding that might encapsulated the tannins within the film dropping their migration. Further increase of the fraction of anionic resin in the blend to 25% resulted in increasing the b-parameter value (2.3). Here the second effect of

addition of component with lower blocking properties is likely much stronger than the ionic bonding effect. As shown in Figure VI.2 in the Appendix VI, for the other blends similar values of b parameter were obtained for all quantities of anionic resin (5%, 15% and 25%). Taking into account the higher b values of the anionic reference, this result indicate that indeed the ionic bonding contribute to decreased migration of tannins.

The performance of the coatings to prevent markers bleeding was visually examined after application of a layer of primer clear-coat, over which a white coating that do not prevent the marker bleeding was added. The results for the representative Blend 1 (LQUAT2 – L1-AH) are shown in Figure 6.11.

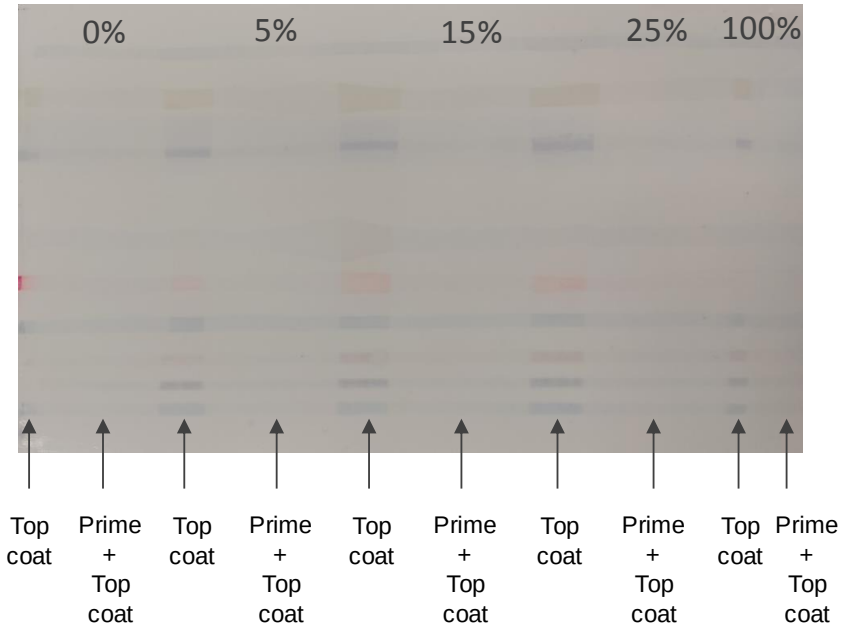

Figure 6.11. Marker resistance test for references and Blend 1 (LQUAT2 – L1-AH) with different amount of anionic resin (5, 15 and 25 wbar%) primer-coats.

As seen, in the areas where the primer-coat was not applied, migration of markers was observed, indicating that all primer coats including the references and the blends prevented successfully the marker migrations. Visually no differences were detected between cationic (0%) and anionic (100%) references and the blends. As mentioned, in case of cationic reference a salt complex formed prevented the marker migrations nevertheless, obviously in case of anionic reference interactions with the markers occurred that affected positively the migrations. The difficultness to observe differences was probably owed to the qualitative test performed. Therefore, the effect of eventual ionic bonding could be even more difficult to appreciate. Similar trends were obtained for all the blends, as shown in Figure VI.3 in the Appendix VI.

6.3.3.2. *Pigmented-coatings based on LQUAT2 cationic resin blends with anionic resins*

Pigmented-coatings were prepared by addition of mill base (pigment dispersion) to the binder, followed by the addition of the other let-down additives while stirring. In this formulation, the amount of resin is considerably reduced compared to the clear-coat formulation, affecting directly the performance of the final paint, as well as the effect of the potential physical structure formed between cationic and anionic resin. In order to be easier to follow the work, pigmented samples were again indicated as 0% (cationic reference), from 5% to 25% (blends) and 100% (anionic reference).

After formulating the blends presented in Scheme 6.3, the performance by means of gloss, hardness and EWR of the pigmented-coats was studied, as well as their tannin and marker

resistance. The results of gloss, tannin and marker resistance of a representative Blend 1 (LQUAT2 – L1-AH) will be presented, owing to the similar behaviour observed for the four blends. The results of Blend 2 (LQUAT2 – L2-AL), Blend 3 (LQUAT2 – L3-H) and Blend 4 (LQUAT2 – L4-L) can be found in Appendix VI (Figure VI.4, Figure VI.5 and Figure VI.6).

The gloss of Blend 1 (LQUAT2 – L1-AH) coats at 20° and 60° (Figure 6.12) was substantially reduced with respect to the gloss of the clear-coats, likely due to the addition of pigments and fillers.[14] Taking into consideration that the gloss of both references is quite similar, it is not surprising that the blends present comparable gloss values, independently on the binder composition. Nevertheless, the effect of ionic complexation was difficult to observed, additionally affected by the complex composition of these coatings, in which the binder quantity is even lower than in clear-coats.

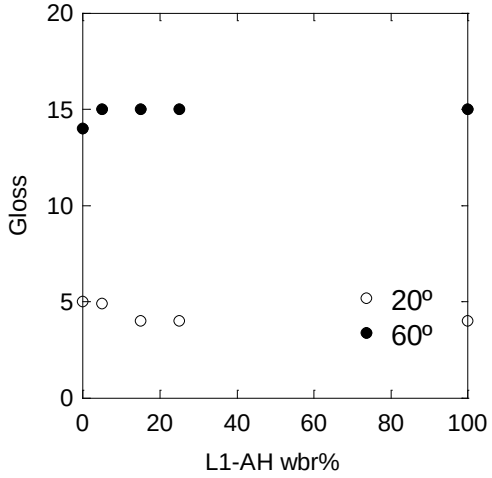

Figure 6.12. Gloss values for references and Blend 1 (LQUAT2 – L1-AH) containing different amount from 5 to 25 wbar% of L1-AH anionic resin.

Hardness of the references and the blends during one week drying is represented in Figure 6.13.

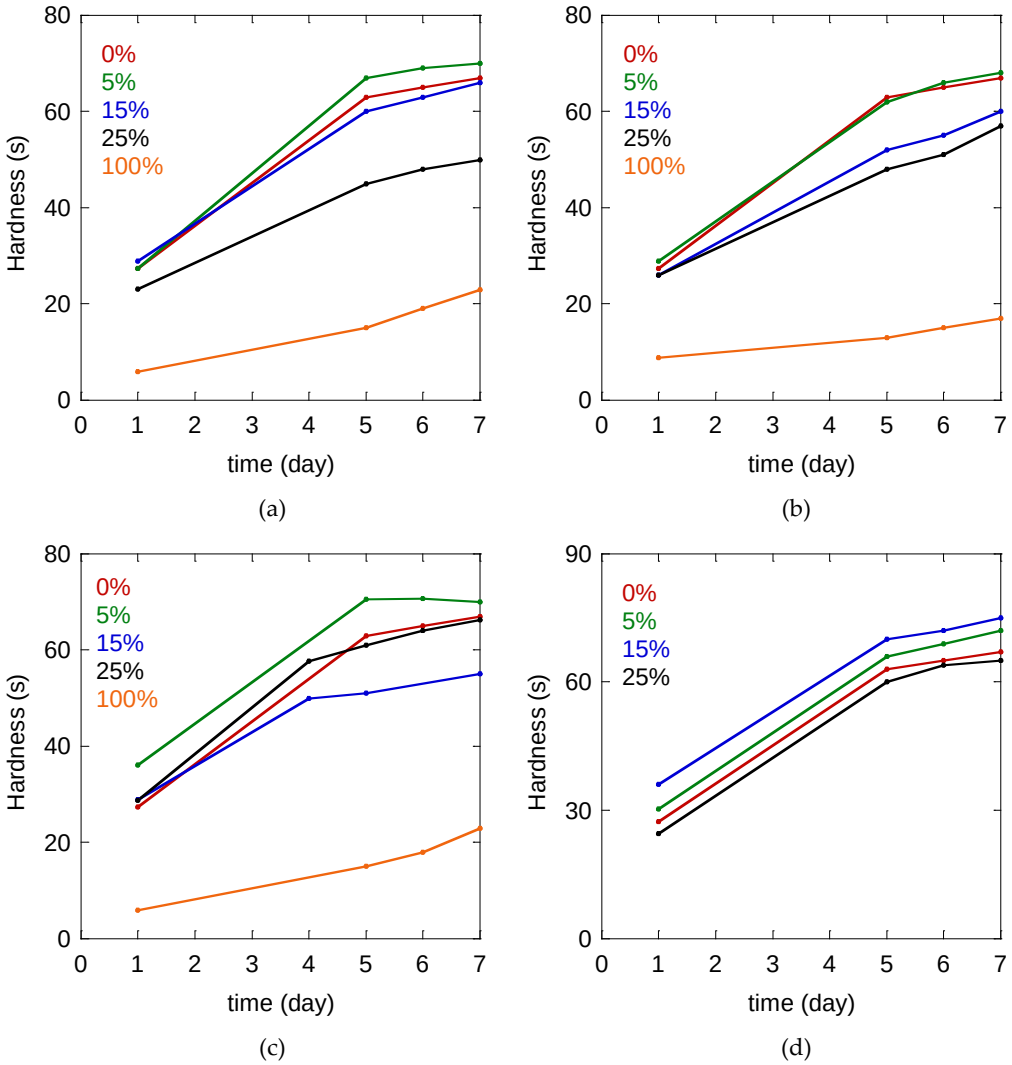

Figure 6.13. Hardness values after 7 drying days for the references and the blends containing from 5 to 25 wbar% for (a) Blend 1 (LQUAT2 - L1-AH), (b) Blend 2 ((LQUAT2 – L2-AL), (c) Blend 3 (LQUAT2 – L3-H) and (d) Blend 3 (LQUAT2 – L4-L).

Similar trend as for the clear-coats was observed for the pigmented-coats, too. As seen, while anionic reference material was softer than the cationic one, not all the blends were in between the references as one might expect after blending two components with different properties. Regarding Blend 1 (LQUAT2 – L1-AH) and Blend 3 (LQUAT2 – L3-H) tiny improvement was detected when 5% of the anionic resin was added likely related to the effect of the ionic bonding, however as already mentioned, addition of higher content of the soft anionic resin might screened the effect of ionic bonding. On the other hand, Blend 3 (LQUAT2 – L3-H) and Blend 4 (LQUAT2 – L4-L) exhibited even harder materials when 5% and 15% anionic resin was added, while greater content of soft material within the blends shifted the balance towards a worse performance despite the ionic bonding.

EWR of the references and the blends was examined during first drying day. Owing to the pigmentation, visual evaluation of these samples was even more complex. On a first sight, these films seemed to have improved resistance with respect to the clear-coats. Nevertheless, no effect of the ionic bonding was visually detected in the blend samples, likely owed to the complex formulation made of multiple components with different hydrophilicity that screen the effect of the complexation.

The results of the tannin resistance test are illustrated in Figure 6.14, for the sample Blend 1(LQUAT 2 – L1-AH). The performance of the other blends is shown in Appendix VI in Figure VI.5.

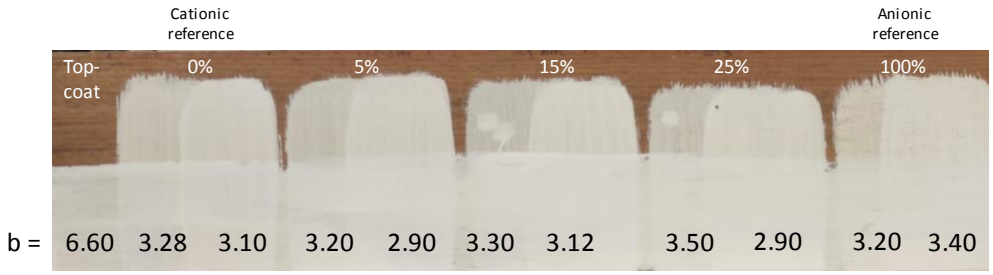

Figure 6.14. Tannin resistance test for references and Blend 1 with different content of anionic resin (5-25 wbar%) in pigmented-coats.

In merbau wood panels, high b values were measured in the area where just the white top-coat without blocking properties was applied. Even though the pigmented-coats showed higher b values than the clear-coats, the use of a primer-coating still cause a drop in the b parameter. The lower amount of polymer binder presented in the pigmented-coats, affected the tannin resistance, so the blocking of tannin migration was lower than in clear-coats. In case of Blend 1 and Blend 4 the anionic reference exhibits even slightly lower b values (around 3.28; 3.40) compared to the cationic ones (around 3.20; 3.40) likely owed to the H-bond structure formed between the sulfonate groups ($R{-}SO_3^-$) from anionic resins and the hydroxyl groups ($R-OH$) from the tannins that prevent their migration through the paint.[25] This effect was not detected in Blend 2 and Blend 3. Regarding the ionic complexes, no important differences were detected between references and complexes since similar b values (around 3) were obtained, meaning that the eventual ionic bonding might not be enough to compensate the worse performance of anionic reference when added to a good performance paint (the cationic reference one), although some blends show slight lower b values. The responsible of keeping or even lowering the b values within the blends might be the contribution of three effects: established ionic bonds might

capture the tannins, not bonded cations might create salt complexes and the free anions may create H-bonding.

Marker resistance test for Blend 1 is shown in Figure 6.15, whereas the rest of the blends' results are shown in Appendix VI, in Figure VI.6.

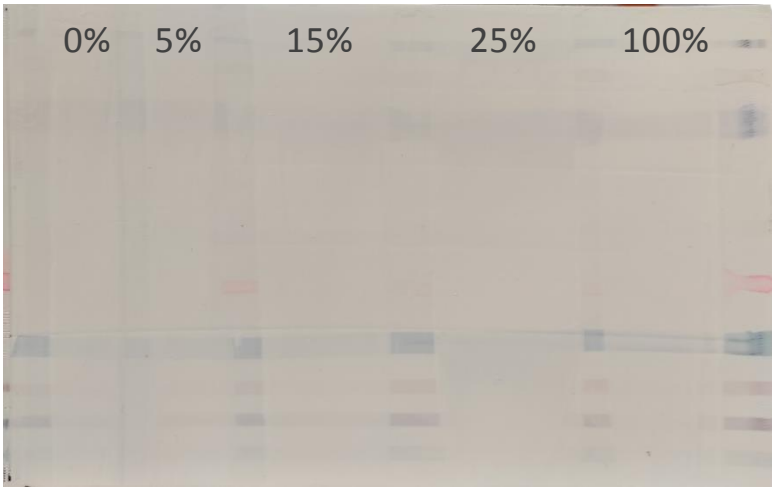

Figure 6.15. Markers bleeding test for references and Blend 1 (LQUAT2 – L1-AH) pigmented-coats.

Similarly as for the clear-coats, in the pigmented-coatings the areas where just the white top-coat was applied, markers bleeding was clearly observed. Although the use of primer coats prevented marker migration, no differences were noticed between the cationic reference (0%), the different blends and the anionic reference (100%), as it can be observed in Figure 6.15.

6.3.4. Use of blends of CATD cationic resin with anionic latexes as binders

As mentioned in the experimental section of this Chapter, owing to the charged state of the CATD cationic resin, tiny aggregations were observed when adding 25% of the anionic resin into the cationic one. This is why, the cationic and anionic resins were formulated separately and blended afterwards. Unfortunately, the addition of formulation components caused L4-L latex destabilization and therefore this anionic reference could not be formulated. The blends of the formulated systems were performed between CATD formulated cationic resin and L1-AH, L2-AL and L3-H formulated anionic systems, as described in Scheme 6.3.

Surprisingly, no aggregations were visually detected when anionic formulated system was added into the cationic one, except when 25% of the anionic one was added, where tiny aggregations were observed when it was applied onto the Leneta card. Therefore, the performance (gloss and haze, hardness and EWR) and the effect of the blends in the already mentioned applications (tannin and marker resistance) was studied for clear and pigmented systems. As previously, in this part of the work too, gloss, tannin and marker resistance results of one of the blends (Blend 5, CATD - L1-AH) will be presented owing to similarities between the three blends. The results of Blend 6 (CATD – L2-AL) and Blend 7 (CATD – L3-H) can be found in Appendix VI (Figures VI.7, VI.8, VI.9, VI.10, VI.11 and VI.12).

6.3.4.1. *Clear-coats based on CATD cationic resin blends with anionic resins*

As clearly observed in Figure 6.16, glossy films were obtained, although values decreased with increasing the anionic resin amount, which is in agreement with the low gloss value of anionic reference. Thus, the drop observed in gloss might be attributed to the addition of the anionic resins to the blends, indicating that the ionic bonding did not affected gloss properties.

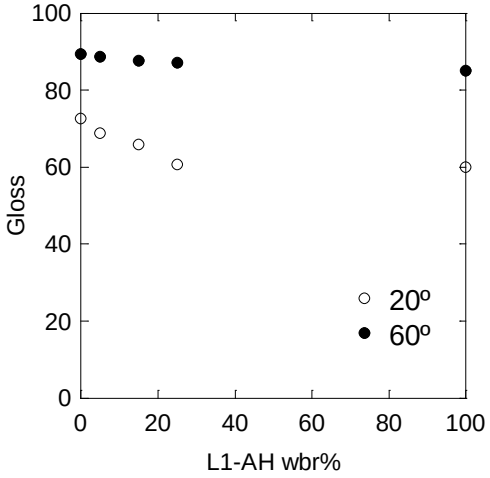

Figure 6.16. Gloss results for reference and Blend 5 (CATD – L1-AH) containing from 5 to 25 wbar% of L1-AH anionic resin.

The results for the hardness of the films investigated during one week drying period are presented in Figure 6.17.

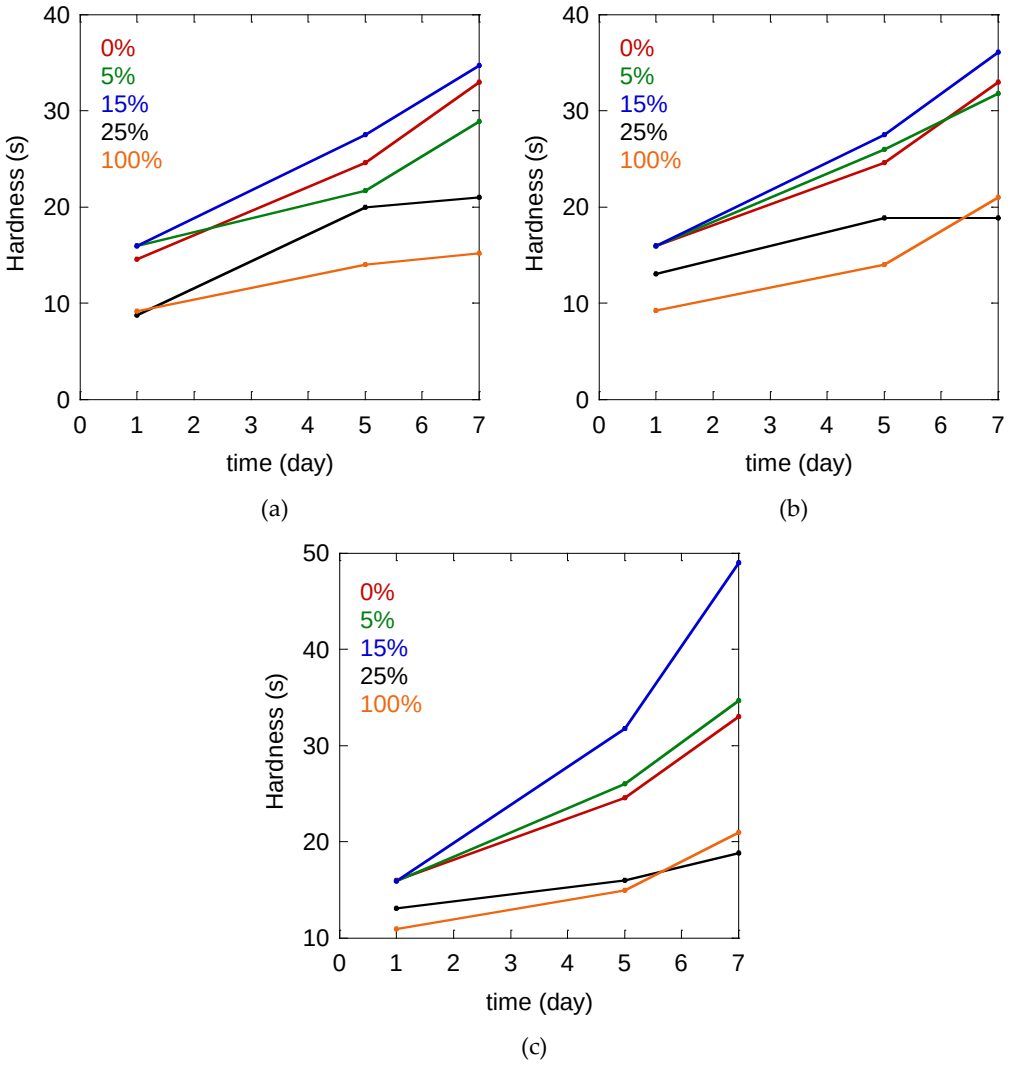

Figure 6.17. Hardness values for the references and the blends containing from 5 to 25 wbar% for (a) Blend 1 (LQUAT2 - L1-AH), (b) Blend 2 (LQUAT2 – L2-AL), (c) Blend 3 (LQUAT2 – L3-H) and (d) Blend 3 (LQUAT2 – L4-L).

As seen in Figure 6.17, cationic reference material (0%) is clearly harder than the anionic one (100%). Therefore, as already mentioned, one might expect that blending of two components

with different properties will result in a material with properties in between these two components. However, as observed in Figure 6.17, clear differences were appreciated between the cationic reference and the blends, likely due to the ionic bonding effect. Regarding the Blend 5 and Blend 6, addition of 5% of anionic resin seemed to be insufficient to detect the effect of ionic bonding on the hardness of the blend, while slightly harder materials were achieved for Blend 7, meaning that ionic bonding points could have increased, being enough for achieving a harder material. In the three cases, blends containing 15% of the anionic resin exhibited higher values than the cationic reference. Surprisingly, this blend material was even stronger for Blend 7 (CATD – L3-H). The reason of these improvements is probably related to the ionic structure formed, which may be strong enough to shift the effect of adding higher content of soft material. On the other hand, the drop in hardness when the highest concentration of anionic resin (25%) was used in the three blends is probably owed to the small aggregations formed (observed visually in the Leneta card), which affected the film quality.

Water resistance of the references and blends was evaluated during first drying day, showing good water resistance during the first hour. However, the water resistance decreased with time (from second hour on). Recovery of the films was not completed after one hour. The same test was again performed during the second drying day, showing enhanced water resistance of the films during the first hours. This means that after 1 drying day the co-solvent might not be completed evaporated, affecting negatively the performance of the coating. The recovery of these coating films was within 5 minutes. Nevertheless, no differences could be

observed between references and blends. Considering that the performed test was qualitative, it did not allow detecting of small differences between the reference and blend coatings.

As mentioned in the section in which LQUAT2 was used, brown-yellowish discoloration of the merbau wood was clearly limited when the primer coating was applied before the white top-coat. In the present case of blends made with CATD, the results of resistance to tannin migration are presented in Figure 6.18.

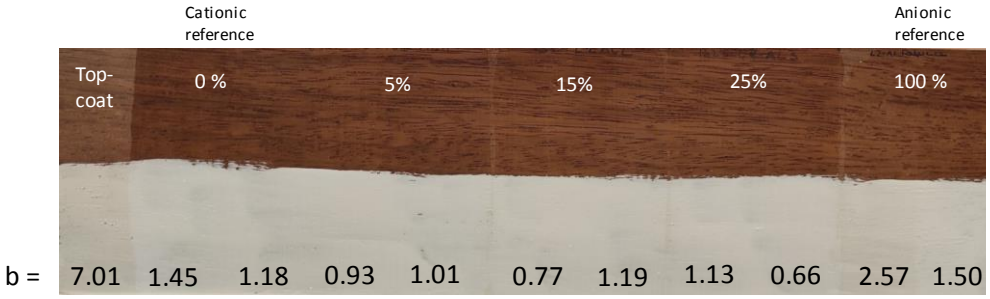

Figure 6.18. Tannin resistance test of the films prepared with reference resins and cationic-anionic resin Blend 5 with different content of L1-AH anionic resin (5-25%).

It can be seen that, discoloration of these merbau panels decreased drastically when one layer of the cationic reference and the blends was applied as primer coatings (b values around 1). However, anionic reference's coats (formulated with anionic resins) exhibited poorer blocking efficiency (b values > 2.57) likely owing to the anionic character of tannins. Cationic reference primer coat (0% case) and the blends coats presented similar barrier properties (b values < 1.5).

Application of two layers had a direct effect on the anionic reference films since b values decreased even more (b> 1.5). This decrease could be explained considering the established H-

bonding between the sulfonate groups from anionic resins and OH groups from the tannins, decreasing their migration.[25] Despite the effect of H-bonding, b values are still higher than the ones for cationic and blend materials. Nevertheless, similar values were kept for the cationic reference and blends coats (compared to one layer).

When comparing the cationic reference and blends, the b values are rather similar, without specific effect of the quantity of the anionic resin added. Combination of two effects might be responsible for this behaviour, producing a kind of synergy. On the one hand, the formation of the ionic structures that led to the formation of a physical barrier preventing from their migration, and on the other hand, the formation of a salt complex of free quaternized amino-functional groups within the polymer backbone with tannins.

Despite the small aggregations detected when 25% of anionic resin was added to the three blends, still free quaternized amino-functional groups can form a salt complex with tannins preventing from tannin migration. However, these results should be handled carefully owed to the small aggregations observed.

The resistant to marker migration of the clear-coats formed from the blends of CATD/anionic resins binders are presented in Figure 6.19. Markers bleed through the white top-coat, where no blocking coatings were applied, while this migration seemed to be blocked in the areas where primer coatings (cationic reference, blends and anionic reference) were employed. Visually no differences were detected between the cationic and anionic references. As already mentioned, the qualitative test could have not detected the small differences.

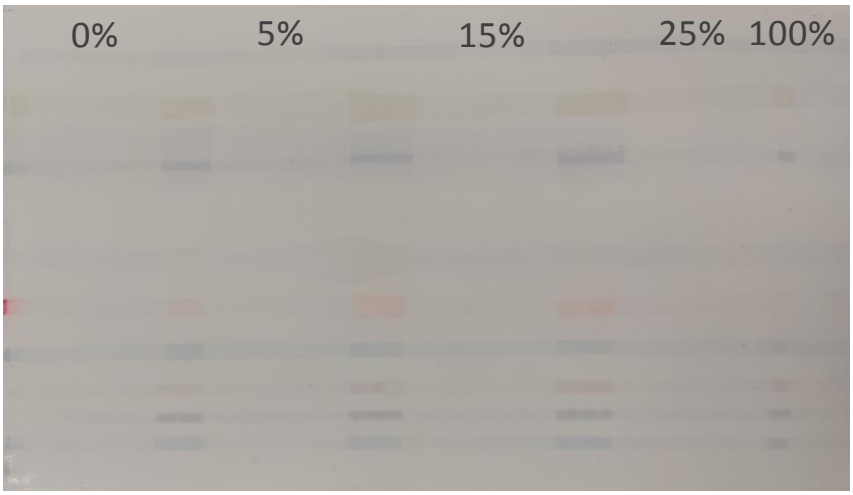

Figure 6.19. Marker resistance test for references and Blend 5 (CATD – L1-AH) containing from 5 to 25 wbar% of L1-AH.

6.3.4.2. *Pigmented-coatings based on CATD cationic resin blends with anionic resins*

As mentioned previously, cationic and anionic resins were formulated separately and blended afterwards. Unlike the clear-coatings, in the pigmented systems no aggregations were observed at high concentration of the anionic systems (25%). The lack of this effect in clear-coats indicates that the pigment or the filler, which moreover are used in much higher amount than other additives, are creating interactions with the resin, postponing the instantaneous aggregations at high concentration (25%) of the anionic system.

As in the previous cases, coatings were investigated by means of gloss, hardness and early water resistance. The summary of the performed blends is shown in Scheme 6.3. Moreover, paint application performance by means of tannin and marker resistance test was also performed. As for the clear-coat, gloss, tannin and marker resistance results of one of the blends (Blend 5, CATD

– L1-AH) will be presented owing to similarities between the four blends. The results of Blend 6 (CATD – L2-AL) and Blend 7 (CATD – L3-H) can be found in Appendix VI (Figures VI.10, VI.11 and VI.12).

As expected, gloss values decreased sharply with the addition of fillers (Figure 6.20) with respect to the corresponding clear-coats. In this case, cationic (0%) and anionic (100%) references showed similar gloss values. The blends values were in between the both references as expected.

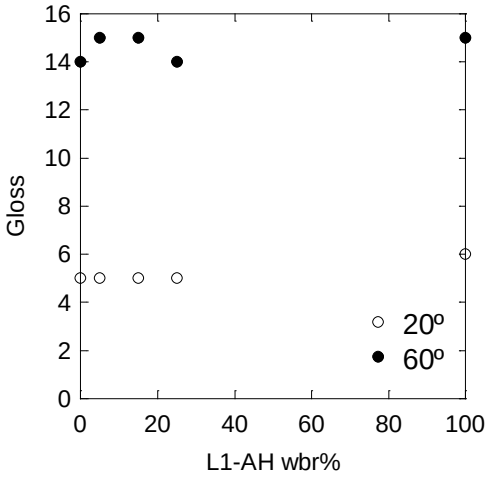

Figure 6.20. Gloss results for references and Blend 5 (CATD – L1-AH) containing from 5 to 25 wbr% of L1-AH anionic resin.

Hardness values during 7 drying days is presented in Figure 6.21.

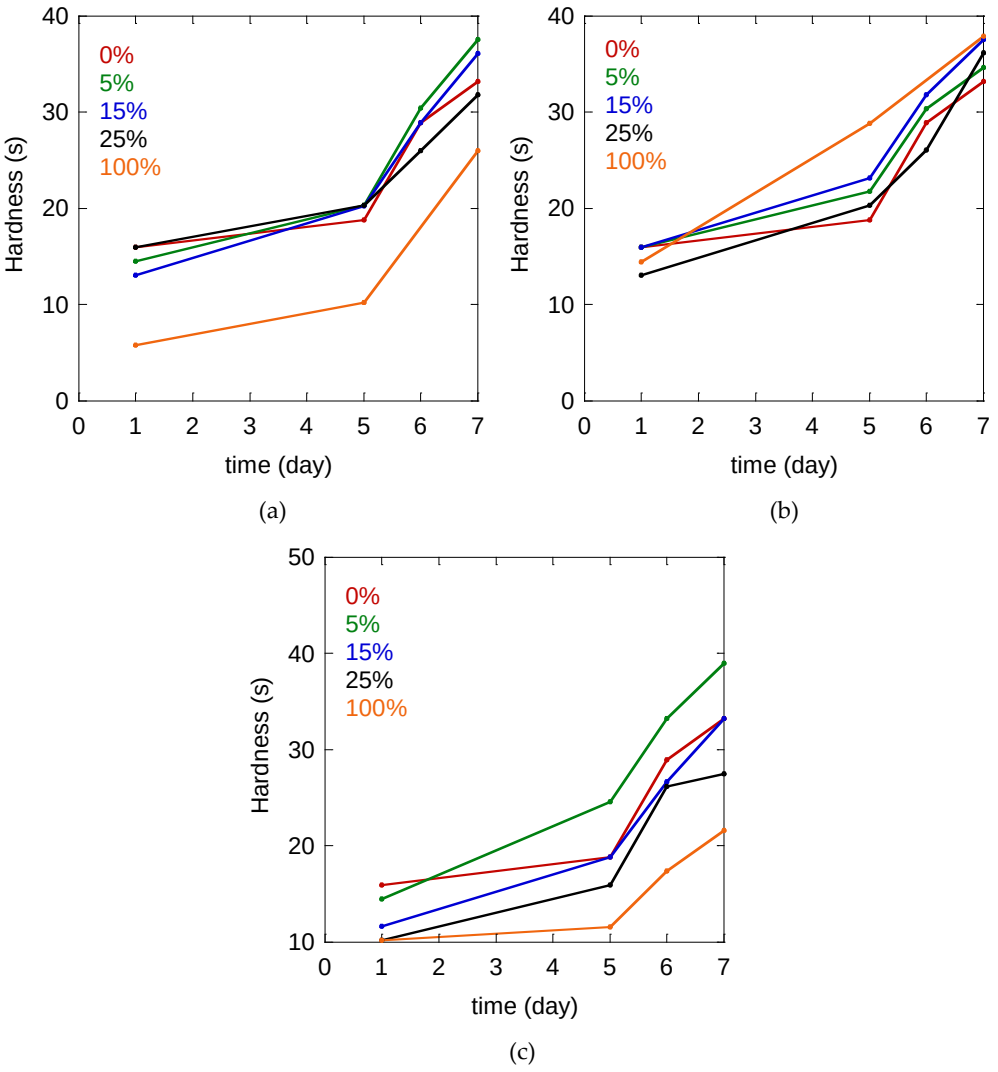

Figure 6.21. Hardness after one drying week for the references and the blends containing from 5 to 25 wbar% for (a) Blend 5 (CATD - L1-AH), (b) Blend 6 (CATD – L2-AL) and (c) Blend 7 (CATD – L3-H).

Cationic reference material was harder than the anionic one, except when L2-AL resin was used as binder. This behaviour was unexpected and different than in all the systems studied in the present work. Furthermore, as already mentioned, the formulation employed for the

references and blends in this part of the work differ from the formulation used in the part where the effect of LQUAT when blending with anionic latexes was studied. Therefore, anionic resins might show different performance when formulated.

According to Figure 6.21, addition of 5% of the anionic resin in all the blends, improved the hardness, being the effect the strongest for L3-H in Blend 7. With respect to L1-AH and L2-AL, the particle size of this anionic resin was smaller. According to the previous experience, the smaller particle size might provide improved contact with the cationic particles establishing higher number of ionic bonds. Nevertheless, while in case of L1-AH and L2-AL, the hardness enhancement of Blend 5 and Blend 6 was kept for 15% anionic resin, in case of Blend 7, it decreased to the level of the cationic reference. The reason might be within the softener effect of the anionic resins, which already dominates over the effect of ionic bonding. This effect also appears in case of all CATD blends when 25% anionic resin was added to the blends.

EWR of the reference and blend films was examined during first drying day. Owing to the white colour of the film, visual evaluation of these samples was not as easy as for the clear-coats' systems. The whitening grad was measured using a rating with numbers from 1 to 5 as summarized in Appendix II, Figure II.5. Early water resistance of 4/5 was noted after 6 hours. No visible differences were detected between the references and the blends.

The results of tannin migration test are presented in Figure 6.22. High b values were detected for the areas where just white top-coat was applied, while this value decreased where primer-coats were applied, meaning limited migration of tannins. Anionic reference coats

exhibited lower b values than the cationic ones (1.32-1.36 versus 2.35-2.25), which means that the anionic paint as well decreased the tannins migration. A possible scenario of this outstanding performance of the anionic paint might be that the anionic particles could establish interactions with compounds from the mill base (pigment, filler…). As already mentioned for clear-coats, the stablished H-bonds between the sulfonate groups from anionic resins and OH groups from the tannins might prevent their migration through the paint would contribute as well.[25] Regarding the blends' b values, they are in between the both references (between 1.32 and 3.20) for Blend 5 and Blend 7, while Blend 6 shows lower b values for all amounts of anionic resin added in the blend. There are three different effects within the blends that will contribute to improve tannins resistance: established ionic bonds will capture the tannins, not bonded cations will create sat complexes and the free anions will create H-bonding. Nevertheless, from the results available it is difficult to distinguish which of these effects would be dominant in each of the blends.

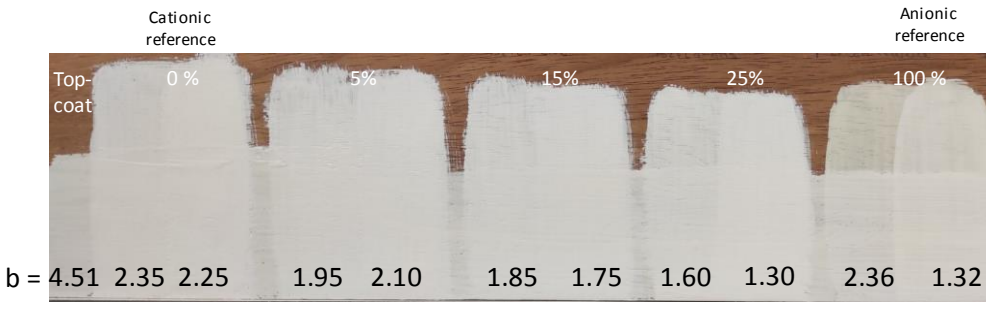

Figure 6.22. Tannin bleeding test for references and Blend 5 performed adding from 5 to 25 wbr% of L1-AH anionic resin.

Marker resistance of the reference and blend materials for Blend 5 (CATD – L1-AH) is shown in Figure 6.23. The migration of markers can be visually observed in areas where just the

white top-coat was applied, while this bleeding was prevented when primer coats were first applied. No visual differences between the performance of the different films was detected probably owed to the qualitative test performed.

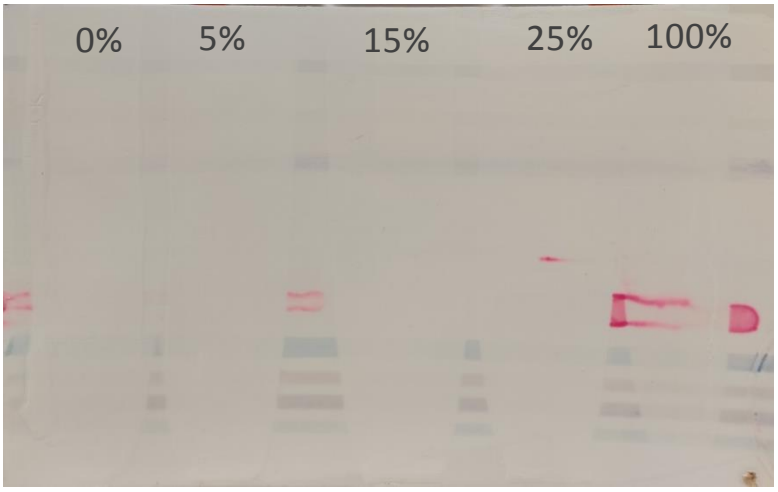

Figure 6.23. Markers bleeding test for references and Blend 5 containing from 5 to 25 wbar%.

6.4. Conclusions

In the first part of the work, four different anionic resins containing anionically charged polymer particles were synthetized using BA and MMA as main monomers. In one of the two sets, the charges were provided by the polymerizable surfactants (Hitenol AR-10 and Latemul P-104), while in the second set also from MAA functional monomer. The ability of the coatings to form a film was studied using these anionic resins as binders, from which clear-coats were prepared. However, the performance of the latex containing just Latemul PD-108 as stabilizer (L4-L) could not be studied since the addition of additives destabilized the system. The

performance of the rest of anionic resins were similar being soft (maximum of 20 s in Koning) and showing poor water resistance probably owed to the higher amount of water-soluble species within polymer films, except when L1-AH was employed. Despite the performance of anionic resins, the possibility of using L1-AH, L2-AL and L3-H anionic resins as binders was successfully confirmed.

In the second part of the work, two cationic resins were selected from Allnex: LQUAT2 and CATD to blend them with the anionic resins and to use them as binders for coating formulation. The effect of ionic structure on paint performance as gloss, hardness and early water resistance, followed by the investigation in tannin and marker resistance was studied. As a general trend, the performance of the blends were similar to the ones observed for cationic and anionic references, except for hardness. With respect to hardness, cationic resin presented much better performance than anionic resin. Nevertheless, when blended, the resulting coatings were harder, likely to the effect of ionic bonding. Unfortunately, this behaviour was not general as some blends show lower performance than cationic materials likely due to two different effects. On the one hand, the low content of anionic resin may not be enough to form enough ionic points, and on the other hand, the excess of soft component might screen the effect of the ionic structure, shifting the balance towards a worse performance. Regarding the gloss and the EWR, the eventual ionic bonding within the blends seems to not affected these properties as they are in between both references. With respect to the blocking properties of the blends, in most of the cases similar ability to prevent the migration as one of the references (cationic), which presents better properties, was achieved. There are three different effects within the blends that might

have contributed to keep similar b values as the cationic paint: established ionic bonds may have captured the tannins, the not bonded cations might have created sat complexes and the free anions could have created an H-bonding structure.

This work demonstrates the advantages of preparing blend paints, even when soft and hard components were mixed probably owed to the ionic structure formed.

6.5. References

(1) Argaiz, M.; Ruipérez, F.; Aguirre, M.; Tomovska, R. Ionic Inter-Particle Complexation Effect on the Performance of Waterborne Coatings. *Polymers (Basel).* **2021**, *13* (18), 1–18. https://doi.org/10.3390/polym13183098.

(2) Unzué, M. J.; Schoonbrood, H. A. S.; Asua, J. M.; Goñi, A. M.; Sherrington, D. C.; Stähler, K.; Goebel, K. H.; Tauer, K.; Sjöberg, M.; Holmberg, K. Reactive Surfactants in Heterophase Polymerization. VI. Synthesis and Screening of Polymerizable Surfactants (Surfmers) with Varying Reactivity in High Solids Styrene-Butyl Acrylate-Acrylic Acid Emulsion Polymerization. *J. Appl. Polym. Sci.* **1997**, *66* (9), 1803–1820. https://doi.org/10.1002/(sici)1097-4628(19971128)66:9<1803::aid-app20>3.0.co;2-u.

(3) Schoonbrood, H. A. S.; Unzué, M. J.; Beck, O. J.; Asua, J. M.; Goñi, A. M.; Sherrington, D. C. Reactive Surfactants in Heterophase Polymerization. 7. Emulsion Copolymerization Mechanism Involving Three Anionic Polymerizable Surfactants (Surfmers) with Styrene-Butyl Acrylate-Acrylic Acid. *Macromolecules* **1997**, *30* (20), 6024–6033. https://doi.org/10.1021/ma9701447.

(4) Aramendia, E.; Barandiaran, M. J.; Grade, J.; Blease, T.; Asua, J. M. Polymerization of High-Solids-Content Acrylic Latexes Using a Nonionic Polymerizable Surfactant. *J. Polym. Sci. Part A Polym. Chem.* **2002**, *40* (10), 1552–1559. https://doi.org/10.1002/pola.10236.

(5) Schoonbrood, H. A. S.; Asua, J. M. Reactive Surfactants in Heterophase Polymerization. 9. Optimum Surfmer Behavior in Emulsion Polymerization. *Macromolecules* **1997**, *30* (20), 6034–6041. https://doi.org/10.1021/ma9701494.

(6) Aguirreurreta, Z.; de la Cal, J. C.; Leiza, J. R. Anionic Polymerizable Surfactants and Stabilizers in Emulsion Polymerization: A Comparative Study. *Macromol. React. Eng.* **2017**, *11* (1), 1–10. https://doi.org/10.1002/mren.201600033.

(7) Aramendia, E.; Barandiaran, M. J.; De La Cal, J. C.; Grade, J.; Blease, T.; Asua, J. M. Incorporation of a New Alkenyl-Based Nonionic Surfmer into Acrylic Latexes. *J. Polym. Sci. Part A Polym. Chem.* **2004**, *42* (17), 4202–4211. https://doi.org/10.1002/pola.20259.

(8) Aguirreurreta, Z.; Dimmer, J. A.; Willerich, I.; Leiza, J. R.; de la Cal, J. C. Improving the Properties of Water-Borne Pressure Sensitive Adhesives by Using Non-Migratory Surfactants. *Int. J. Adhes. Adhes.* **2016**, *70*, 287–296. https://doi.org/10.1016/j.ijadhadh.2016.07.011.

(9) Lu, D.; Huang, H.; Shen, L.; Xie, J.; Guan, R. Nonionic Polymerizable Emulsifier in High-Solids-Content Acrylate Emulsion Polymerization. *J. Wuhan Univ. Technol. Sci. Ed.* **2012**, *27* (5), 924–930. https://doi.org/10.1007/s11595-012-0575-3.

(10) Xu, X. J.; Goh, H. L.; Siow, K. S.; Gan, L. M. Synthesis of Polymerizable Anionic Surfactants and Their Emulsion Copolymerization with Styrene. *Langmuir* **2001**, *17* (20), 6077–6085. https://doi.org/10.1021/la010364k.

(11) Aguirreurreta, Z.; de la Cal, J. C.; Leiza, J. R. Preparation of High Solids Content Waterborne Acrylic Coatings Using Polymerizable Surfactants to Improve Water Sensitivity. *Prog. Org. Coatings* **2017**, *112* (December 2016), 200–209. https://doi.org/10.1016/j.porgcoat.2017.06.028.

(12) Karger-Kocsis, J. *Paints, Coatings and Solvents*; 1994; Vol. 51. https://doi.org/10.1016/0266-3538(94)90094-9.

(13) Müller, B.; Poth, U. *Coatings Formulation: An International Textbook*; Vincentz Network: Hannover, Germany, 2011.

(14) Alvarez, V.; Paulis, M. Effect of Acrylic Binder Type and Calcium Carbonate Filler Amount on the Properties of Paint-like Blends. *Prog. Org. Coatings* **2017**, *112* (May), 210–218. https://doi.org/10.1016/j.porgcoat.2017.07.023.

(15) Heilen, W. *Additives for Waterborne Coatings*; 2014.

(16) Cogulet, A.; Blanchet, P.; Landry, V. Wood Degradation under UV Irradiation: A Lignin Characterization. *J. Photochem. Photobiol. B Biol.* **2016**, *158*, 184–191. https://doi.org/10.1016/j.jphotobiol.2016.02.030.

(17) Sataloff, R. T.; Johns, M. M.; Kost, K. M. 04829610 A2, 1992.

(18) Klljn, A; Twene, D; Mestach, D. Stain Blocking Waterborne Coating Composition. WO2005071023A1, 2004.

(19) Van Rheenen, P. and C. C.-S. Cationic Latex Coatings, 1994.

(20) Chen, Q.; Scheerder, J.; de Vos, K.; Tak, R. Influence of Cosolvent Retention on Film Formation and Surface Mechanical Properties of Water Based Acrylic Coatings by Atomic Force Microscopy. *Prog. Org. Coatings* **2017**, *102*, 231–238. https://doi.org/10.1016/j.porgcoat.2016.10.018.

(21) Fisher, S.; Kunin, R. Effect of Cross-Linking on the Properties of Carboxylic Polymers. I. Apparent Dissociation Constants of Acrylic and Methacrylic Acid Polymers. *J. Phys. Chem.* **1956**, *60* (8), 1030–1032. https://doi.org/10.1021/j150542a003.

(22) Shoaf, G. L.; Poehlein, G. W. Solution and Emulsion Polymerization with Partially Neutralized Methacrylic Acid. *J. Appl. Polym. Sci.* **1991**, *42* (5), 1239–1257. https://doi.org/10.1002/app.1991.070420507.

(23) Dos Santos, A. M.; Mckenna, T. F.; Guillot, J. Emulsion Copolymerization of Styrene and N-Butyl Acrylate in Presence of Acrylic and Methacrylic Acids: Effect of PH on Kinetics and Carboxyl Group Distribution. *J. Appl. Polym. Sci.* **1997**, *65* (12), 2343–2355. https://doi.org/10.1002/(SICI)1097-4628(19970919)65:12<2343::AID-APP8<3.0.CO;2-9.

(24) Becerir, B. Color Concept in Textiles: A Review. *J. Text. Eng. Fash. Technol.* **2017**, *1* (6), 240–244. https://doi.org/10.15406/jteft.2017.01.00039.

(25) Balasubramani, K.; Muthiah, P. T.; Lynch, D. E. R22(8) Motifs in Aminopyrimidine Sulfonate/ Carboxylate Interactions: Crystal Structures of Pyrimethaminium Benzenesulfonate Monohydrate (2:2:1) and 2-Amino-4,6-Dimethylpyrimidinium Sulfosalicylate Dihydrate (4:2:2). *Chem. Cent. J.* **2007**, *1* (1), 1–10. https://doi.org/10.1186/1752-153X-1-28.

Chapter 7. | Conclusions

This PhD thesis aims to introduce ionic complexation during film formation from waterborne polymer dispersions (latexes) in order to improve the performance of waterborne coatings. For this purpose, ionically charged polymer particles made of a typical coating formulation BA/MMA in 50/50 weight ratio with small amounts of functional ionic monomers, containing either one charge or two charges per molecule were synthesized by batch and semibatch emulsion copolymerization processes, followed by blending anionic and cationic polymer dispersions with the aim of establishing ionic bonding between the oppositely charged waterborne particles.

In a light of the fact that ionic complexation within polymer dispersions have rarely been studied, in Chapter 1, a comprehensive state-of-the art is presented related to the synthesis of anionically and cationically charged latexes using ionic monomers. The reported works demonstrated that by employing functional monomers, the latexes exhibit improve colloidal stability as well as enhance mechanical performance of the polymer films. However, clearly, the presence of these species increased the water sensitivity of the materials, which will be one of the main challenges of this work, expected to be substantially increased by the complexation reactions.

In Chapter 2, ionically charged polymer particles with similar sizes were prepared employing functional monomers containing one charge per molecule, either NaSS or DMAEMA. The blends were prepared varying two parameters: surface charge density and number of particles. As pKa of DMAEMA is about 7.5, all the blends were prepared at two different pHs. At pH< 7.5 ionic complexed films were prepared (ionic complex material), while at pH> 7.5 no ionic interactions happen, allowing the preparation of reference films (reference material). Despite that the overall level of chain interdiffusion degree decreased for ionic complex material (as seen by FRET technique), when blending oppositely charged polymer dispersions, modest improved of mechanical properties was achieved in all studied combinations, while the reference blend presented enhanced polymer chain mobility, but lower mechanical performance. This means that although polymer chains diffusion is affected when ionic network is formed within the film, the established inter-particle force was enough to observe slight improvement of the mechanical properties compared to the reference materials. Regarding the water resistance of the materials, as a general trend the reference blends prepared at pH> 7.5 showed higher water absorption than the ionic complex materials (pH< 7.5), likely due to the neutralization of the ionic species in the last.

In Chapter 3, denser ionic network was achieved owed to the more efficient particle packaging reached by blending oppositely charged particles with different sizes that contributed to increase the probability of the ionic complexation. Ionically charged polymer dispersions were synthesized using NaSS and DMAEMA functional monomers. Blending was performed employing oppositely charged polymer particles with different sizes and at two different pHs

(for the ionic complex and the reference materials). As a general behaviour, almost all ionic complexed materials showed improved mechanical properties compared to their respective reference films. The observed trends indicated that the ionic complex materials were affected not only by the size of the blended latexes, but as well by their surface charge densities and the particle distribution and packing. Similarly, the water uptake results showed that the reference films adsorbed larger content of water compared to the ionic complex films, likely due to the neutralization of ions occurred during the complexation. Thus, it was demonstrated that by more efficient particle packaging, the increased contact between large/small particles contribute to the increase of the ionic bonding points, reinforcing the inter-particle complexes as seen in the tensile test and water uptake tests.

In Chapter 4, further improvement of the film properties was achieved, owed to the even denser ionic network reached by introducing functional monomers containing two charges per molecule within the BA/MMA polymer chains. These ionically charged dispersions were prepared employing small contents of anionic IA (commercial monomer) and cationic DABCO (synthesized for that aim in this work) monomers. Due to very high charge density, immediate coagulation occurred when these dispersions were blended. With the idea of postponing the ionic complexation during blends preparation, and therefore to avoid the fast coagulation when blending, pluronic F-108 polymeric non-ionic surfactants was successfully adsorbed onto the surface of the polymer particles. Regardless of it, the stable dispersion was obtained only in case of blending dispersions containing 1% of IA (IA1) and 1% of DABCO (DABCO1), when 10 wbp% pluronic F-108 was added to each of the dispersions before blending. It was prepared at two

different pHs; at pH< 3.8, giving rise to reference material and at pH> 6 for ionic complex material. Regarding the mechanical properties, the ionic complex material was much stiffer than the reference blend and the bare films (IA1 and DABCO1), due to the established ionic complex network. Surprisingly, the reference blend film was stiffer than the individual IA1 and DABCO1 films, indicating that during blending some interactions between both particle types affected the film properties. The enhancement in the Young modulus of the reference blend material was related to the carboxylic acid dimers formation of IA containing chains and the distribution of stiffer, ionic containing chains with higher T_g in higher concentration within the polymer blend than in individual films. Strong effect of the ionic complexation was observed in water uptake results. While the ionic complexed network prevented pluronic F-108 chains leaching from the film to the water phase, this encapsulation effect of polymeric stabilizer was not observed in IA, DABCO and reference blend films. Thus, it was shown that the denser ionic network achieved by introducing functional monomers containing two charges per molecule contribute to increase the ionic bonding points for reinforcing the inter-particle complexes.

In Chapter 5, the possibility of producing and complexing emulsifier-free cationic waterborne dispersions using a homemade cationic monomer DABCO, characterized with two charges per molecule was investigated. Waterborne dispersions, stabilized by DABCO cationic monomer were synthetized in the absence of emulsifier by seeded semibatch emulsion polymerization process. The final solid content was of 40% and DABCO concentration was varied from 1 to 5 mbm%. Cationic latexes with high conversion (> 93%), narrow particle size distribution and average particle size between 171-180 nm were obtained. Stiffer and less

flexible, but less water resistant materials were obtained by increasing the DABCO concentration, likely due to denser reinforcing network created by the polymer chains rich in rigid DABCO, as it was observed in TEM images. Afterwards, the ionic complexation of emulsifier-free DABCO dispersions with emulsifier-free NaSS was studied. Two sets of blends were prepared using non-dialyzed and dialyzed DABCO and NaSS dispersions, by blending 275 nm NaSS - 180 nm DABCO (Blend 275-180,Sample set 2) and 275 nm NaSS - 100 nm DABCO (Blend 275-100, Sample set 3). Pluronic F-108 surfactant was employed to avoid immediate coagulation of the blends. While clear effect of the ionic complex network was observed for the Blend 275-180 (Sample set 2), almost no effect was detected for Blend 275-100 (Sample set 3). Even though it was expected that the Sample set 3 would provide improved particle packing of the oppositely charged particles than Sample set 2 blends, obviously the surface charge density, which was much higher for Sample set 2 played a key role to establish strong and dense network. No important differences in mechanical strength of the blend films were detected between non-dialyzed and dialyzed ones, meaning that the presence of water- soluble species do not show strong influence on the mechanical performance, whereas their presence affected slightly the water resistance.

In Chapter 6 anionic latexes were synthetized using two types of polymerizable surfactants (Latemul PD-104 and Hitenil AR-10), with and without addition of MAA functional monomer, resulting in four anionic latexes (L1-AH, L2-AL, L3-H and L4-L). The idea was to blend these anionic latexes with commercial cationic ones and to use these blends in coatings application. In the first part of Chapter 6, the possibility of using L1-AH, L2-AL and L3-H anionic resins as

binders to formulate clear-coats was successfully confirmed, despite the low performance of the anionic resins. In the second part, the ionic complexation effect on paint performance when employing cationic and anionic resins blend as binders in the formulation was investigated. For that aim 5%, 15% and 25% of anionic resin was added to the cationic one to prepare the blends.

As a general trend, slight enhancement of mechanical resistance with lower water sensibility was observed, while the other paints properties were not affected compared to the reference materials for lower content of the anionic resin in the blend (5% and 15%). When the anionic resin fraction was further increased, this resulted in slow decreasing of the mechanical properties. Two different and contradictory effects were responsible for this behaviour, ionic bonding that improve the properties and mixing effect of hard (cationic resin) and soft (anionic resin) materials. When the effect of ionic bonding is higher than the mixing effect, improved performance of the blends was noticed. In opposite case, when higher quantity of anionic resin was added (25%), the mixing effect overwhelmed the ionic complex effect, and the films in such case presented decreased performance. Regarding the gloss and the EWR, the ionic bonding within the blends seems to have not affected these properties as they are in between both references. With respect to the blocking properties of the blends, investigated by means of tannins and marker migration tests, in most of the cases similar ability to prevent tannin migration was achieved. This effect was similar for the cationic resin and all of the blends. There are three different effects within the blends that might have contributed to this result: established ionic bonds may have captured the tannins, the not bonded cations might have created salt complexes and the free anions could have created H-bonding structures.

This work has shown that the ionic complexation might be a useful tool towards improved performance of the waterborne coating if sufficiently dense ionic network is established and if immediate coagulation of the oppositely ionic charged particles is avoided.

7.1. Future Perspectives

There are some aspects of this work that could be further developed. From a research point of view, it might be interesting to deeply examine the ionic bonding effect when blending hard/soft components with different particles sizes.

During this thesis, most efforts have been devoted to understand the effect of ionic complexation when blending two dispersions containing oppositely charged particles. For this reason, there are some aspects of this study that could be further developed in order to be industrially more applicable. The possibility of producing a latex containing both functional monomers, anionic and cationic one, with similar surface charge density in order to investigate not only the effect of ionic complex on the final properties, but also the storage time of this kind of dispersions.

From the application point of view, the possible use of latexes containing oppositely charged particles blends as binders was confirmed, but it may be particularly important to study if the trends observed when blending soft and hard components are also observed, or even improved when employing oppositely charged particles with similar performance. Another

interesting topic would be the development of paints with binders containing hard/soft polymers with different particle sizes.

Appendix I. Materials and synthesis processes

I.1. Materials

Technical grade monomers n-butyl acrylate (BA, Quimidroga), methyl methacrylate (MMA, Quimidroga), methacrylic acid (MAA, Sigma-Aldrich), sodium styrene sulfonate (NaSS, Sigma Aldrich), 2-(dimethylamino)ethyl methacrylate (DMAEMA, Aldrich) and Itaconic acid (IA, sigma Aldrich) were used as monomers. 1,4-diazabicyclo[2.2.2]octane (DABCO, Sigma Aldrich), 1-bromohexane (Sigma Aldrich), ethyl acetate ($C_4H_8O_2$), 4-vinylbenzyl chloride (90%, Sigma Aldrich) and acetonitrile (CH_3CN, Sigma Aldrich) were used for DABCO monomer synthesis.

Disponil AFX 2075 (BASF) non-ionic emulsifier, sodium dodecyl sulfate (SDS, Sigma Aldrich) and dodecyltrimethylammonium bromide (DTAB, Sigma-Aldrich) were used as received. Latemul PD-104 and Hitenol AR-10 polymerizable surfactants. The initiator tert-butyl hydroperoxide (TBHP, 70 wt% aqueous solution, Luperox Sigma Aldrich), ascorbic acid (AsAc, purity ≥ 99%, Panreac), Bruggolit 7 (FF7, Bruggemann Chemical), potassium persulfate (KPS, Sigma Aldrich) and 2,2'-azobis(2-methylpropionamidine) dihydrochloride (AIBA, Sigma-Aldrich) were also used as received. Hydroquinone (Fluka) was used to stop the polymerization reaction in the samples withdrawn from the reactor. Technical grade tetrahydrofuran (THF,

Scharlab) and High-performance liquid chromatography grade THF (Scharlab) were used for soxhlet extraction and Size Exclusion Chromatography (SEC) measurements, respectively. Hhydrochloric acid (HCl, 37%, Sigma Aldrich) was used to decrease the pH of DMAEMA and IA charge dispersions to later perform the titration analysis and sodium hydroxide (NaOH, Panreac) was employed for the titration of both latexes. DABCO cationically charge dispersion was titrated using silver nitrate ($AgNO_3$, Sigma Aldrich). Ammonium hydroxide solution (28% NH_3 in water, Sigma-Aldrich), sodium phosphate monobasic (Sigma-Aldrich), sodium phosphate dibasic (Sigma-Aldrich), formic acid and citric acid/sodium phosphate were all used for buffer preparations.

(9-phenanthryl) methyl methacrylate (Phe-MMA, Toronto Research Chemical) and [1-(4-nitrophenyl)-2-pyrrolidinmentyl]-acrylate (NNP-A, Sigma-Aldrich) were employed as donor and acceptor pair to carried out FRET analysis.

Clear- (let-down formulation) and pigmented-coat (let-down and mill base) were prepared as follow. For the let-down part, Butyl glycol (BG), Butyl digycol (BdG) and Texanol (Tex) were employed as co-solvents. Surfynol CT-111 (Evonik) and BYX-348 as levealing agents. Foamstar SI 2292 and Additol VXW 6210N (Allnex) as defoamers.

Two different paints application tests were carried out. On the one hand, tannin bleeding test was carried out using merbau wood panels. On the other hand, marker resistance test was done using Leneta card, white paint and 10 markers/compounds (blue, red and black waterborne

markers, blue alcohol based marker, black permanent marker, sabacid red dye (1% in water)), red wine, betadine, blue seal ink and coffee (1 g coffee/25 g water) were used.

I.2. Synthesis processes

Ionically charged latexes were synthesized by either batch or semibatch process. The polymerizations were carried out in a 1 or 2 L glass jacketed reactor fitted with a reflux condenser, sampling device, N_2 inlet, thermocouple and a steal anchor type stirrer rotating at 200 rpm. The temperature and the inlet flow rates of the semibatch feeds were controlled by an automatic control system (Camile TG, CRW Automation Solutions). The scheme of the polymerization set up is presented in Figure I.1. The samples were withdrawn at regular intervals from the reactor and the polymerization was short-stopped with hydroquinone.

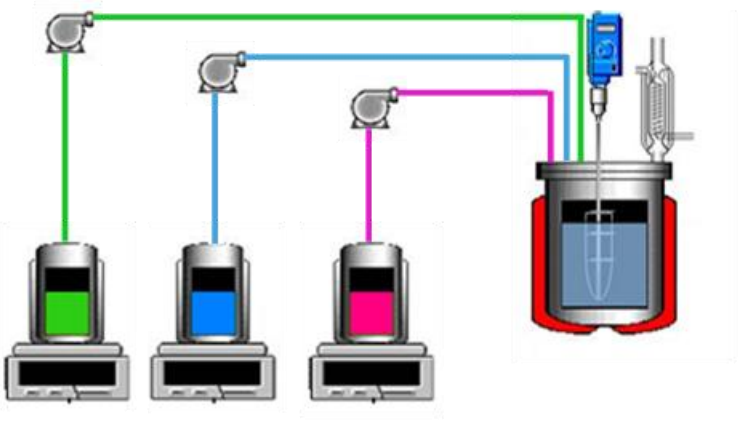

Figure I.1. Scheme of the reaction set up.

In the following Tables, formulations used during this work are summarized. Formulations for Table I.1 and

Table I**.2** were used in Chapter 2 and Chapter 3. The recipe shown in Table I.3 was used in Chapter 3.

Table I.**4** and Table I.5 were employed in Chapter 4. Finally, formulations for Chapter 6 are described in

Table **I.6**, Table I.7 and Table I.8.

Table I.1. Seed formulations for NaSS and DMAEMA containing latex.

Compound (wt%)	Initial charge		Stream 1		Stream 2		Stream 3	
	NaSS	DMAEMA	NaSS	DMAEMA	NaSS	DMAEMA	NaSS	DMAEMA
BA	5	-	-	10	-	-	-	-
MMA	5	-	-	10	-	-	-	-
F.M[a]	2[b]	-		-	-		-	3[b]
Disponil AFX2075	-	4[b]	-	-	-	-	-	-
TBHP	-	-	0.5[b]	-	-	1[b]	-	-
AsAc	-	-		-	0.5[b]	-	-	1[b]
H_2O	70	60	10	-	10	10	-	10

[a]NaSS and DMAEMA
[b]weight based on main monomers (BA/MMA) (wbm%)

Table I.2. Seeded semibatch formulations for NaSS and DMAEMA containing latex.

Compound (wt%)	Initial charge		Stream 1		Stream 2		Stream 3	
	NaSS	DMAEMA	NaSS	DMAEMA	NaSS	DMAEMA	NaSS	DMAEMA
Seed	39	44	-	-	-	-	-	-
BA	-	-	23	20	-	-	-	-
MMA	-	-	23	20	-	-	-	-
F.M[a]	-	-	-	-	-	-	1-3[b]	1-3[b]
Disponil AFX2075	-	-	-	-	-	-	-	4[b]
TBHP	-	-	-	-	0.5[b]	0.2[b]	-	0.2[b]
AsAc	-	-	-	-	-	-	0.5[a]	-
H_2O	-	-	-	-	5	8	10	8

[a]NaSS and DMAEMA
[b]weight based on main monomers (BA/MMA) (wbm%)

Table I.3. Seed formulations for 70 nm NaSS containing latex.

Compound (wt%)	Initial charge
BA	15
MMA	15
NaSS	2[a]
SDS	1[a]
KPS	0.5[a]
H_2O	70

[a]weight based on main monomers (BA/MMA) (wbm%)

Table I.4. Seed formulations for IA and DABCO containing latex.

Compound (wt%)	Initial charge		Stream 1		Stream 2	
	IA	DABCO	IA	DABCO	IA	DABCO
BA	5	10	-	-	-	-
MMA	5	10	-	-	-	-
F.M[a]	2[b]	2*	-	-	-	
Emulsifier	1.5[b]	1.5[b]	-	-	-	-
TBHP	-	-	0.15[b]	-	-	0.15[b]
FF7	-	-	-	0.15[b]	0.15[b]	-
H_2O	70	60	10	-	10	10

[a]IA and DABCO

[b]weight based on main monomers (BA/MMA) (wbm%)

Table I.5. Seeded semibatch formulations for IA and DABCO containing latex.

Compound (wt%)	Initial charge		Stream 1		Stream 2		Stream 3	
	IA	DABCO	IA	DABCO	IA	DABCO	IA	DABCO
Seed	40	50	-	-	-	-	-	-
BA	-	-	18	15	-	-	-	-
MMA	-	-	18	15	-	-	-	-
F.M[a]	-	-	-	-	1[b]	1-2.5[b]	-	-
Emulsifier	-	-	-	-	1.5[b]	1.5[b]	-	-
TBHP	-	-	-	-	-	-	0.15[b]	0.15[b]
FF7	-	-	-	-	0.15[b]	0.15[b]	-	-
H_2O	-	-	-	-	12	10	12	10

[a]IA and DABCO

[b]weight based on main monomers (BA/MMA) (wbm%)

Table I.6. Seed latex for L1-AH, L2-AL, L3-H and L4-L latex.

Compound (wt%)	Initial charge (%wt)	Stream 1 (%wt)
BA	-	7.4
MMA	-	7.4
MAA	-	0.2
Dowfax	1-1.5[a]	-
$NaHCO_3$	0.2[a]	-
Ammonia	1[a]	-
KPS	0.5[a]	-
H_2O	85	-

[a]weight based on main monomers (BA/MMA) (wbm%)

Table I.7. Seeded semibatch formulations for L1-AH and L2-AL latex.

Compound (wt%)	Initial charge		Stream 1	
	L1-AH	L2-AL	L1-AH	L2-AL
Seed 1 (dp= 95 nm)	19.6	8.4	-	-
BA	-	-	23.7	24.3
MMA	-	-	23.7	24.3
MAA	-	-	1[b]	1[b]
Ammonia	-	-	-	1[b]
Polymerizable emulsifier[a]	-	-	1[b]	-
KPS	0.5[b]	0.5[b]	-	-
H_2O	15	43	18	-

[a]Hitenol AR-10 and Latemul PD-104
[b]weight based on main monomers (BA/MMA) (wbm%)

Table I.8. Seeded semibatch formulations for L3-H and L4-L latex.

Compound (wt%)	Initial charge	Stream 1
Seed 2 (dp=75 nm)	5.8	-
BA	-	24.6
MMA	-	24.6
Polymerizable emulsifier[a]	-	2-2.4[b,c]
KPS	0.5[b]	-
H_2O	31	14

[a]Hitenol AR-10 and Latemul PD-104
[b]weight based on main monomers (BA/MMA) (wbm%)
[c]2 wbm% Hitenol AR-10 and 2.4 wbm% Latemul PD-104

Appendix II. Characterization methods

II.1. Monomer characterization methods

II.1.1. Nuclear Magnetic Resonance (NMR)

The ^{1}H-NMR measurements were performed on a Bruker AVANCE 400 MHz spectrometers. On the one hand, DABCO monomer was examined using dimethylformamide (DMF) as solvent, and on the other hand, while DMF solvent was used for the monomer phase study, deuterium oxide (D_2O) solvent was employed for analysing the water phase using the WATERGATE pulse sequence for suppression of the signal from water, was employed for analysing water phase. The samples were prepared adding a small amount of DABCO monomer and dissolving in 600 μL of DMF, whereas 300 μL of the monomer phase and water phase were mixed with 300 μL DMF and D_2O, respectively, as external standards.

II.2. Latex characterization methods

II.2.1. Monomer conversion

Monomer conversion was determined by gravimetry. The instantaneous conversion, X_{inst}, was defined as the amount of polymer in the reactor divided by the total amount of monomer

and polymer in the reactor. The global conversion, X_{glob}, was the amount of polymer in the reactor divided by the amount of monomer plus the amount of polymer in the formulation.

II.2.2. Coagulum amount

The amount of coagulum was measured by filtering the latex through a 85 μm nylon mesh and drying the retained amount. The results are presented as the weight of the coagulum with respect to the total weight of solids in the formulation.

II.2.3. Average particle size and particle size distribution (PSD)

II.2.3.1. *Dynamic Light Scattering (DLS)*

Particle sizes were measured by dynamic light scattering (DLS) in a Zetasizer Nano Z (Malvern instruments). Samples were prepared by diluting a fraction of latex with deionized water. The equipment was operating at 25 °C and a run consisted in 2 minutes of temperature equilibration. The reported values were the Z-average of three repeated measurements.

II.2.3.2. *Capillary Hydrodynamic Fractionation Chromatography (CHDF)*

Average particle size and particle size distribution (PSD) in Chapter 5 was determined using capillary hydrodynamic fractionation (CHDF) technique. A CHDF-3000 (Matec Applied Science) was used with an operating flow of 1.4 mL min^{-1} at 35 °C and detector wavelength at 220 nm. The carrier fluid was 1X-GR500 (Matec). The samples were diluted to 0.5% s.c. using the carrier fluid and the samples were analysed using the Matec software v.2.3.

II.2.3.3. *Number of particles (N_p)*

Polymer particle sizes were measured by DLS using a Malvern Zetasizer Nano ZS (laser: 4mw, He-Ne, λ=633 nm, angle 173°). The equipment determines the particle size by measuring the rate of fluctuations in light intensity scattered by particles as they diffuse through a fluid.

Samples were prepared by diluting a fraction of the latex with deionized water. The analyses were carried out at 25 °C and each run consisted in 1 minute of temperature equilibration followed by 2 size measurements per sample.

Results obtained from DLS were used to determine the number of particles (N_p). Np was determined following equation II.3.

$$N_p = \frac{V_p}{V_t} = \frac{6(W_{pol}/\rho_{pol})X}{\pi {d_p}^3} \quad \text{(eq. II.3)}$$

In this case, W_{pol} corresponds to the amount of polymer (g) at each time, and it was calculated from the monomer conversion (X). ρ_{polym} refers to the polymer density (1.11 g cm^{-3}) and d_p to the average particle size. N_p involved some uncertainty because the third power of d_p was used in their calculation.

II.2.4. Gel fraction

The gel content by definition is the fraction of polymer that is not soluble in a good common solvent such as THF. The gel fraction was determined by Soxhlet extraction.

To measure the gel content glass fibre square pads (CEM) were used as backing. A few drops of latex were placed on the filter (filter weight = W_0) and dried at 62 °C overnight. The filter together with the dried polymer was weighed (W_2) and a continuous extraction with THF under reflux in the Soxhlet for 24 hours was done afterwards (Figure II.1). After this, the wet filter was dried overnight. Finally, the weight of the dry sample was taken (W_3). Gel content was calculated as the ratio between the weight of the insoluble polymer fraction and that of the initial sample, as equation II.4 shows.

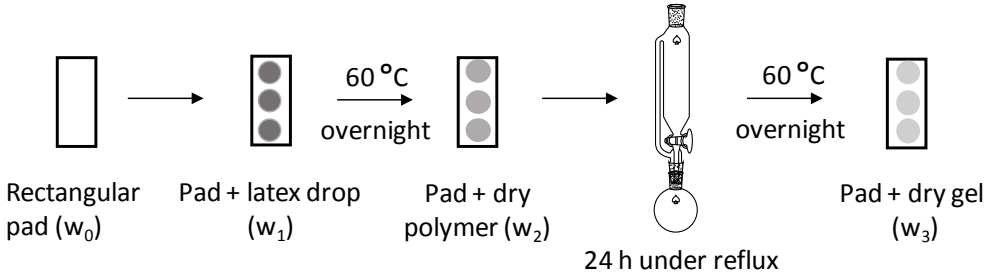

Figure II.1. Scheme of Soxhlet extraction method for gel content measurements.

$$\text{Gel content (\%)} = \frac{W_3 - W_0}{W_2 - W_0}\,100 \quad \text{(eq. II.4)}$$

II.2.5. Sol molar mass

The molar mass of the soluble fraction (obtained by Soxhlet extraction) was determined by SEC/GPC. The samples taken out from the Soxhlet were first dried, redisolved in THF to achieve a concentration of about 0.1% (g ml^{-1}) and filtered (polyamide Φ=45 μm) before injection into the SEC instrument. The set up consisted of a pump (LC-20A, Shimadzu), an autosampler (Waters 717), a differential refractometer (Waters 2410) and three columns in series (Styragel HR2, HR4

and HR6, with pore sizes ranging from 10^2 to 10^6 Å). Chromatograms were obtained at 35 °C using THF flow rate of 1 mL min^{-1}. The equipment was calibrated using polystyrene standards (5^{th} order universal calibration) and therefore, the molecular weight was referred to PS.

II.2.6. Functional monomer incorporation and surface charge density

Incorporation and surface charge density were analysed by titration of the dialyzed latexes. These latexes were diluted to 2.5 wt% solids content and dialyzed against ultrapure water by using Spectra-Por®4 membranes (Mw cut-off 12,000-14,000 Da) until constant conductivity.

As for NaSS containing polymer dispersions, the dialyzed latexes were pass through a Dowex Marathon MSC cation exchange resin in order to substitute Na^+ of the sulfonate groups by titratable H^+, while DMAEMA and IA latexes pH was reduce to 2. These samples were titrated conductimetrically using Metrohm 718 stat titrino equipment against 5mM NaOH. On the other hand, DABCO containing latex were titrated against 0.1 M $AgNO_3$.

Ionic monomer incorporation (%) was calculated based on the initial mol added to the system as seed in equation II.6.

$$\text{Surface incorporation (ionic monomer \%)} = \frac{n_{neutralized}}{n_{initial}} 100 \quad \text{(eq. II.6)}$$

where $n_{neutralized}$ is the number of moles of NaOH or $AgNO_3$ require to neutralized the functional groups of the latex and $n_{initial}$ is the number of moles added at the beginning for the polymerization reaction.

The surface charge density (σ) was calculated according to the following equation II.7:

$$\sigma = \frac{Fn\rho R}{3w} \quad \text{(eq. II.7)}$$

where F is the faraday constant, n is the number of moles of NaOH or $AgNO_3$ require to neutralize functional groups of the latex, ϱ is the colloid´s density and R is the radius of the latex spheres and w is the fraction of the solids content of the latex.

II.2.7. Fraction of ionic monomer in the formation of water-soluble species

The fraction of ionic monomer participating in the formation of water-soluble species was calculated based on the initial ionic monomer. The diluted latexes (12.5 wt% solids content) were centrifuged at 13000 rpm for 3 hours at 4 °C. The serum parts were carefully taken with a syringe and NaSS containing serum part were passed through a Dowex Marathon MSC cation exchange resin in order to substitute Na^+ of the sulfonate groups by titratable H^+, while DMAEMA and IA serum parts pH were reduced to 2. These samples were titrated conductimetrically using Metrohm 718 stat titrino equipment against 5mM NaOH for NaSS, DMAEMA and IA containing serums and against 0.1 M $AgNO_3$ for DABCO ones.

II.3. Calculations for the neat charge in the blends

The neat charge was was determined in Chapter 3 and Chapter 5 for the blends and the calculations used can be found in the following paragraphs.

First, the surface charge per particle (μC particle^{-1}) was calculated as shown in equation II.9 using the area of the sphere (equation II.8) and the surface charge density values (from equation II.7).

$$A_{sphere} = 4\pi r^2 \quad \text{(eq. II.8)}$$

where r is the radious of the latex particle

$$Charge\ per\ particle\ (\mu C\ particle^{-1}) = A_{sphere}\ \sigma \quad \text{(eq. II.9)}$$

Total charge in the blend (equation II.10) was calculated using the result of the equation II.9 and the number of particles (Np) determined in equation II.3. Finally, the difference between the cationic and anionic species was calculated to obtain the neat charge in the blend.

$$Total\ charge\ in\ the\ blend\ (\mu C) = \frac{charge}{particle} N_p \quad \text{(eq.II.10)}$$

II.4. Polymer film characterization methods

II.4.1. Differential Scanning Calorimetry (DSC)

The glass transition temperature (T_g) was determined by Differential Scanning Calorimeter (DSC) (DSC, Q1000, TA instruments). The films were dried at control conditions and 3-5 mg of samples, which were placed into aluminium hermetic pans, were first heated to 150 °C with a heating rate of 10 °C min^{-1} and kept isothermal for 2 minutes. Then, they were cooled down to -70 °C with a cooling rate of 50 °C min^{-1} and kept isothermal for 2 minutes. The second heating run was carried out at 10 °C min^{-1} to determine the T_g of the polymers.

II.4.2. Tensile test

Tensile test measurements were performed in an universal testing machine, TA.HD plus Texture Analyser under control conditions (23 ± 2 °C and 55 ± 5% relative humidity) applying a crosshead speed of 25 mm min^{-1} to an approximate 0.6 mm film. Films with 0.6 mm thickness were prepared by casting latex into silicon moulds and letting dried for 7 days under control conditions (23 ± 2 °C and 55 ± 5% relative humidity). At least five specimen per sample were analysed and the average values are reported. The reproducibility of the samples was good.

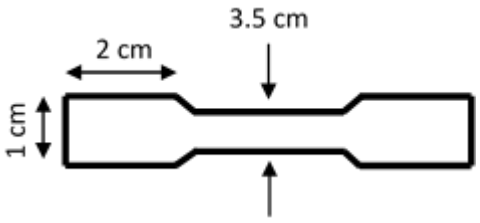

Figure II. 2. Dimensions of the probed employed for the mechanical properties measurements.

II.4.3. Fluorescence Resonance Energy Transfer (FRET)

Fluorescence decay profiles were measured by Time Correlated Single Photon Counting (TCSPC) measurements carried out using Fluoromax-4 spectrofluorometer (Horiba Jobin Yvon) equipped with a single photon counting controller (Fluorohub, Horiba, Jobin-Yvon) and a pulse diode light source NanoLED emitting at 300 nm. Emission from the sample was detected at 360 nm. Each measurement was continued until 10000 counts were acquired in the maximum channel. DAS6 Fluorescence decay analysis software was applied for analysis of time domain fluorescence lifetimes.

II.4.4. Water uptake

In order to evaluate the water resistance films with 0.6 mm thickness were prepared by casting latex into silicone molds and dried at 23 ± 2 °C and 55 ± 5 % of relative humidity during 7 days until a constant weight was achieved. Each sample was weighted (w_0) before immersing in a small plastic bottle which contained 100 mL of deionized water for one month. Each sample was withdrawn from the plastic container once per day, smoothly dried with paper and weighed

(w_1). Water uptake was calculated by comparing the final weigh of each sample and the initial weigh of each sample (equation II.11).

$$Water\ uptake\ (\%) = \frac{w_1 - w_0}{w_0}\ 100 \quad \text{(eq. II.11)}$$

II.4.5. Water contact angle (WCA)

Water contact angle (WCA) measurements of each blend film were performed by placing 12 μL droplets of distilled water on the surface of the films, using a goniometer OCA 20 (Data Physics Instrument) under controlled environment (23 ± 2 °C and 55 ± 5 % of relative humidity). The data presented are the average of 15 readings.

II.4.6. Atom Force Microscopy (AFM)

The morphology of the films surface and cross-section was analysed by Atomic Force Microscopy (AFM). These measurements were performed using a Dimension ICON AFM (Bruker) operating in tapping mode. An integrated 7 nm ratio silicon tip/cantilever with a resonance frequency of 320 kHz was used performing measurements at a scan rate of 1 Hz sec^{-1} with 512 scan lines.

II.4.7. Transmission Electronic Microscopy (TEM)

The morphology of the latex particles and films cross-section of Chapter 5 was analysed by transmission electron microscopy (TEM) using a Jeol TM-1400 Plus series 120 kV electron microscope.

II.5. Clear- and pigmented-coat performance

II.5.1. Gloss and haze

In terms of visual appearance, gloss is one of the key parameters for coating formulation. Gloss is related to the ability of the surface to reflect light directly. The angle of incident is selected depending on the gloss of the coating: high gloss coatings (20°), matt coatings (85°) and semi- gloss coatings (60°). Gloss measurements may varied from polymer films to coating film owing to the addition of various additives, which might affect the stability and increase heterogeneity. Microscopy surface defects in coatings result in light scattering with low intensity causing an optical phenomenon known as haze. Haze affects the appearance quality of the surface. Figure II.3 shows two glossy-surface examples, at low haze values (top image) the reflected image appears clear, while in case of high haze (bottom image) a well non-defined image is obtained.

In this work, gloss at 20°/60° and haze of the coatings were determined using goniophotometer Rhopoint IQ (Figure II.3). Average values were calculated from five repetitions

per sample. Formulated coatings were applied onto Leneta cards using wire bars (120 μm wet film thickness) allowing to dry for 24 hours at 22 °C and 50% humidity.

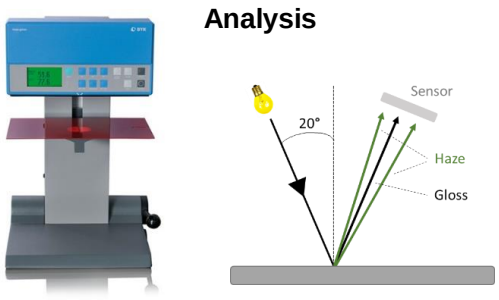

Figure II.3. Illustration of gloss and haze measurement.

II.5.2. Hardness

Hardness is defined as the resistance offered by a coating to an external mechanical action as pressure, friction or scratching.[1] Hardness was measured with Konig pendulum apparatus (Erichsen model 299/300, Figure II.4). The instrument consists of a pendulum, where two stainless steel balls are attached. The pendulum is placed onto the coated glass substrate and is set into oscillation. The stainless steel balls movement cause pressure on the coated surface and the oscillation amplitude damping defines the strength of the coating depending on its elasticity and hardness. Coating hardness is defined by the number of oscillations made by the pendulum within the specified limits of amplitude and is reported as a damping time in seconds. Formulated dispersions were applied onto glass substrates using Baker type applicator (120 μm wet film thickness) and let them dry at 22 °C and 50% of relative humidity.

Figure II.4. Representation of Konig pendulum apparatus.

II.5.3. Early Water Resistance (EWR)

In this work, the water resistance was evaluated. Formulated dispersions were applied onto Leneta cards using wire bars (120 μm wet film thickness) and they were allowed to dry for 24 hours at standard conditions (22 °C and 50% of relative humidity). Herein, the ''spot'' test was performed by depositing six drops of water on the top of the dry film in order to evaluate the damage caused by water in the substrate. The evaluation was performed every hour during 6 hours by removing the water drops with absorbent paper. The whitening grad was measured using a rating with numbers from 1 to 5 as illustrated in Figure II.5.

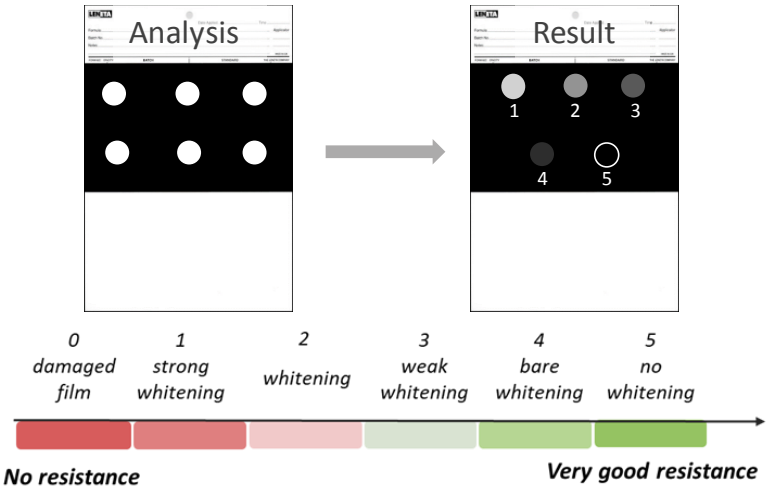

Figure II.5. Whitening graduation used for early water resistance test.

II.6. References

(1) Goldschmidt, A.; Streitberger, H.-J. *BASF Handbook Basics of Coating Technology*, Network.; Hannover, Germany, 2007.

Appendix III. Fluorescence Resonance Energy Transfer (FRET)

Over the past 20 years, the group of Prof. Winnik at University of Toronto have used FRET technique to study a variety of factors that affect the rate of polymer diffusion in latex films. FRET is refer to non-radiative transmission of energy from a donor molecule to an acceptor molecule. The donor molecule is the dye or chromophore that initially absorbs the energy and the acceptor is the chromophore to which the energy is subsequently transfer.[1,2] Hence, the energy that is captured by the donor upon its excitation is transferred to the acceptor. Although there are large different parameters that can affect FRET experiments, the distance between the donor/acceptor molecules is an important one.

The basic principle of this technique is that when polymer dispersions containing donor and acceptor labelled polymer particles are dried to form a film, the donor and acceptor labelled polymer chains are separated due to boundaries between particles. Once these polymer chains diffuse across this boundary, they bring the donor and acceptor dyes into proximity allowing the energy transfer to increase and leading to a faster decrease in the fluorescent profile. Following the rate of the decay (Figure III.1), the quantum efficiency of energy transfer (Φ_{ET}) can be calculated.

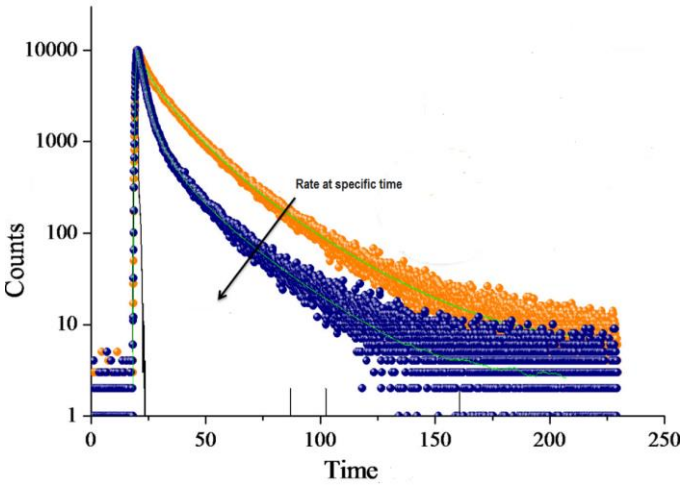

Figure III.1. Example of fluorescent decay evolution

III.1. FRET data acquisition

Fluorescence decay profile were measured by Time Correlated Single Photon Counting (TCSPC) measurements carried out using the Fluoromax-4 appartus (Horiba, Jobin-Yvon) equipped with a single photon counting controller (FluoroHub, Horiba Jobin-Yvon) and a pulsed diode light source NanoLED emiting at 300 nm. Emission from the sample was detected at 360 nm. Each measurement was continued until 10000 counts were acquired in the maximum channel.

III.2. FRET data analysis

The last step of the film formation process, where the polymer chains from neighbour particles diffuse, was monitored by measuring the energy extent between the donor and acceptor

labelled particles. In this technique, donor fluorophore, initially in its electronic excited state, might transfer energy to any nearby acceptor fluorophore through the non-radiative dipole-dipole coupling. As observed in Equation 3, the rate of energy transfer (w (t)) strongly depends on the distance between the donor and acceptor fluorophores (sixth-power relationship).[1,2]

$$w\,(t) = \frac{1}{\tau_D^0}\left(\frac{R_{F0}}{r}\right)^6 \quad \text{(eq. III.1)}$$

where τ_D^0 is the donor fluorescence lifetime in the absence of acceptors and R_{F0} refers to the Föster distance at which the energy transfer is 50% efficient. Conceptually, the Föster critical distance is the maximal separation length between the donor and acceptor labelled polymers under which energy transfer will still occur.

In the presence of isolated donor molecules, the fluorescence decay profile (I_D) is defined as the exponential decay function of time (t).[1,3]

$$I_D = Aexp\left(\frac{-t}{\tau_D^0}\right) \quad \text{(eq. III.2)}$$

where A is a constant and τ_D^0 is the lifetime of the donor in absence of the acceptor as explained above. τ_D^0 for Phe-NaSS1 labelled latex films was measured experimentally obtaining a value of 43.5 ns.

However, the energy transfer for donors and acceptors ia randomly distributed in a three dimensional space, and the donor fluorescence decay profile will have a stretch exponential form.[1,3]

$$I_D\,(t) = \exp\left(-\frac{t}{\tau_D^0}\right)\exp\left[-2\delta\left(\frac{t}{\tau_D^0}\right)^{0.5}\right] \quad \text{(eq. III.3)}$$

where δ is a constant parameter proportional to the concentration of acceptor and Föster distance.

In these experiments, each fluorescence decay profile was standardized to the unit intensity and time zero (t_0). These values were fitted to the following equation.[1,3]

$$I_D\,(t) = \exp\left(-\frac{t}{\tau_D^0}\right)\exp\left[-2\delta\left(\frac{t}{\tau_D^0}\right)^{0.5}\right] + A_2\exp\left(-\frac{t}{\tau_D^0}\right) \quad \text{(eq. III.4)}$$

where the first term corresponds to the region where the donor and acceptor molecules are mixed, while the second term refers to the unmixed region where energy transfer does not occur. A_1 and A_2 parameters were obtained from the fitting of each decay profile, while fixed values for δ (0.45) and τ_D^0 (43.5 ns) were used. The presented parameters were used to integrate I_D (t) analytically, from decay time zero to time infinity.

The quantum efficiency of energy transfer (Φ_{ET}) is defined as follows.[1,3]

$$\Phi_{ET}\,(t) = 1 - \frac{\int_0^{\infty} I_D\,(t)dt}{I_D^0\,(t)\,dt} \quad \text{(eq. III.5)}$$

where $\int_0^{\infty} I_D\,(t)dt$ refers to the integrated area under the normalized decay profile and $I_D^0\,(t)\,dt$ is defined as the donor decay profile of the film containing donor fluorescence molecule (τ_D^0)[1,3]. τ_D^0 value was experimentally defined as 43.5 ns as explained above.

$$\Phi_{ET}\,(t) = 1 - \frac{\int_0^{\infty} I_D\,(t)dt}{\tau_D^0} = 1 - \frac{area\,(t)}{\tau_D^0} \quad \text{(eq. III.6)}$$

III.3. References

(1) McPhie, P. *Principles of Fluorescence Spectroscopy, Second Ed. Joseph R. Lakowicz*; 2000; Vol. 287. https://doi.org/10.1006/abio.2000.4850.

(2) Wu, J.; Winnik, M. A.; Farwaha, R.; Rademacher, J. Effect of a Water-Soluble Polymer on Polymer Interdiffusion in P(MMA-Co-BA) Latex Films. *Macromol. Chem. Phys.* **2003**, *204* (16), 1933–1940. https://doi.org/10.1002/macp.200350060.

(3) Pinenq, P.; Winnik, M. A.; Ernst, B.; Juhué, D. Polymer Diffusion and Mechanical Properties of Films Prepared from Crosslinked Latex Particles. *J. Coatings Technol.* **2000**, *72* (903), 45–61. https://doi.org/10.1007/bf02697987.

Appendix IV. AFM air-film interface phase images for Chapter 3 surface materials

IV.1. Blend 140-240

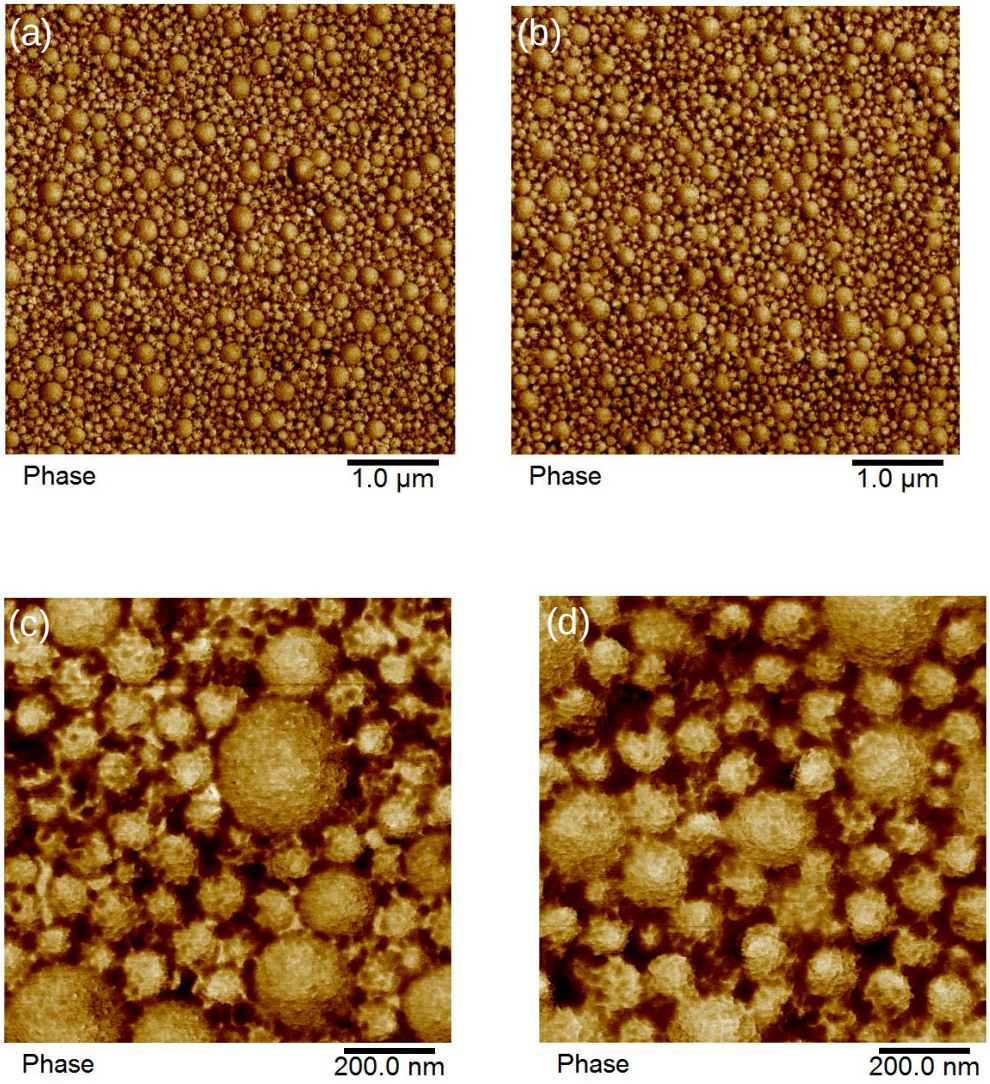

Figure IV.1. AFM air-film interface phase images for Blend 70-240 at different pH´s. (a) and (c) for reference material and (b) and (d) for ionic complex one. The materials analyzed at 5 µm scale are (a) and (b), while (c) and (d) samples were examined at 1 µm scale.

IV.2. Blend 275-140

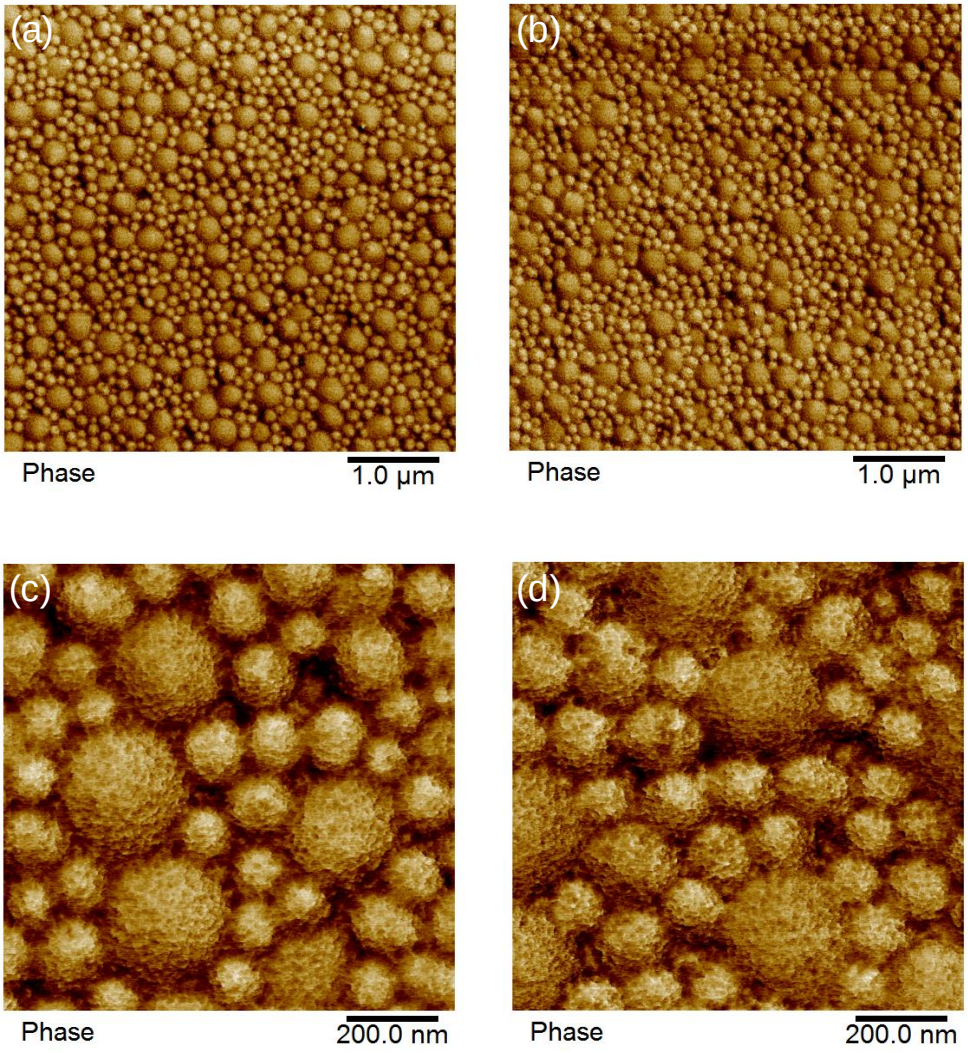

Figure IV.2. AFM air-film interface phase images for Blend 275-140 at different pH´s. (a) and (c) for reference material and (b) and (d) for ionic complex one. The materials analysed at 5 µm scale are (a) and (b), while (c) and (d) samples were examined at 1 µm scale.

IV.3. Blend 70-250

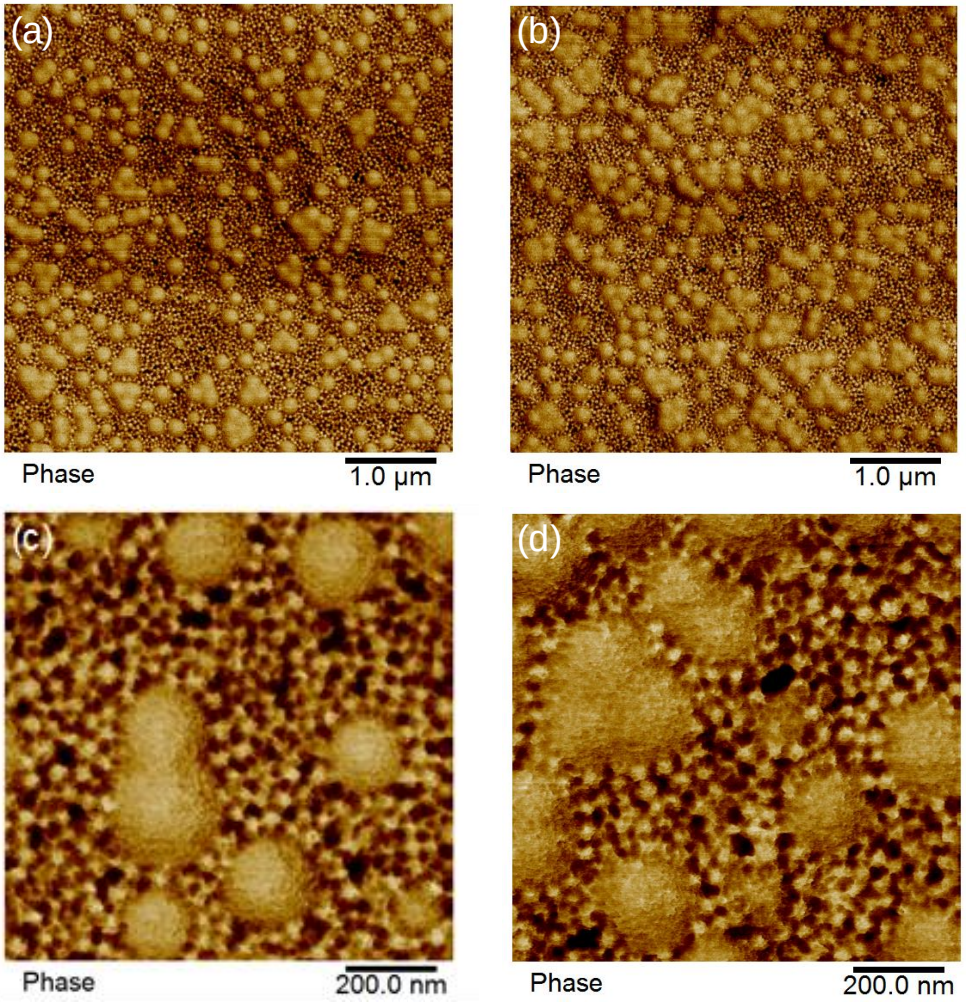

Figure IV.3. AFM air-film interface phase images for Blend 70-250 at different pH´s. (a) and (c) for reference material and (b) and (d) for ionic complex one. The materials analysed at 5 μm scale are (a) and (b), while (c) and (d) samples were examined at 1 μm scale.

IV.4. References

(1) Goldschmidt, A.; Streitberger, H.-J. *BASF Handbook Basics of Coating Technology*, Network.; Hannover, Germany, 2007.

Appendix V. DABCO monomer synthesis and characterization

V.1. Experimental part

The DABCO cationic monomer was synthetized following the method developed by Zhang et al.[1] as summarize in Scheme V.1.

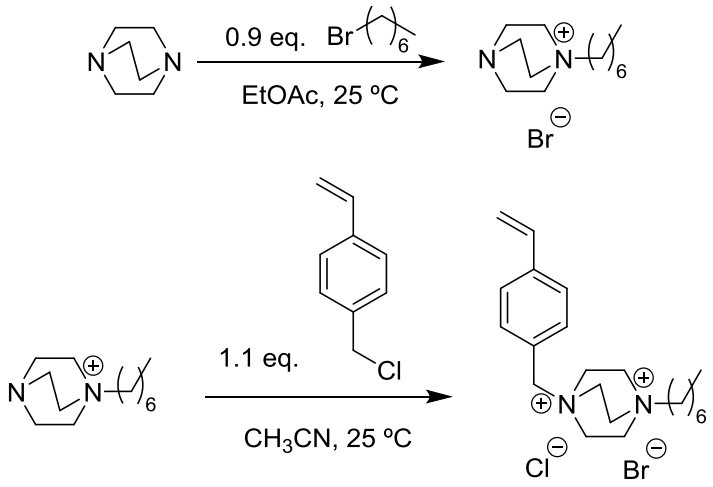

Scheme V.1. Schematic representation of the reactions for DABCO cationic monomer synthesis.

It is important to highlight that one of the essential characteristic of monomers that can polymerize through emulsion polymerization is their partial water solubility.[2] Despite Zhang et al. reported that the synthetized salt was completely soluble in water[1], herein the distribution of the synthetized cationic monomer between water and the organic phase made of BA/MMA monomers was studied. A series of mixtures where prepared as presented in Table V.1. The

mixture of water, DABCO and the BA/MMA monomers were mixed in glass bottles and one drop of a solution of 1 wt% hydroquinone was added to avoid polymerization. Each glass bottle was agitated for 3 hours at 23 °C. Once, the mixing was finished, the mixture was transfer into a separation funnel to let the two phases (organic and aqueous one) separate. Gravimetric analysis were applied to analyse the amount of DABCO in each of the phases. These results were confirmed by NMR-H^1.

Table V.1. A series of mixtures employed for determination of DABCO monomer distribution.

DABCO (g)	**H_2O (g)**	**MMA (g)**	**BA (g)**
0.0625	12.5	12.5	0
		0	12.5
		6.25	6.25
0.0925	12.5	12.5	0
		0	12.5
		6.25	6.25
0.125	12.5	12.5	0
		0	12.5
		6.25	6.25
0.250	12.5	12.5	0
		0	12.5
		6.25	6.25
0.355	12.5	12.5	0
		0	12.5
		6.25	6.25

V.2. Results and discussion

After the different synthesis and washing steps, a pure white solid material was obtained with relatively high yield (70%). The chemical structure of the purified DABCO cationic monomer was confirmed by ^{1}H-NMR spectroscopic analysis as shown in Figure V.1. Figure V.1 shows each signal in te NMR spectra with its hydrogen type on the DABCO monomer structure. The peaks assignments are the following ones: 7.65-7.57 (a-b,4H, Ha+b), 6.81 (c,1H, J1 = 10.9 Hz, J2 = 17.6 Hz, Hc), 5.98 (d,1H, J = 17.6 Hz, Hd), 5.39 (e,1H, J = 10.9 Hz, He), 4.96 (f,2H, Hf), 3.94 (g,12H, Hg), 3.52 (h,2H, Hh), 1.65 (i,2H, Hi), 1.27 (j,6H, Hj), 0.86 (k,3H, Hk).

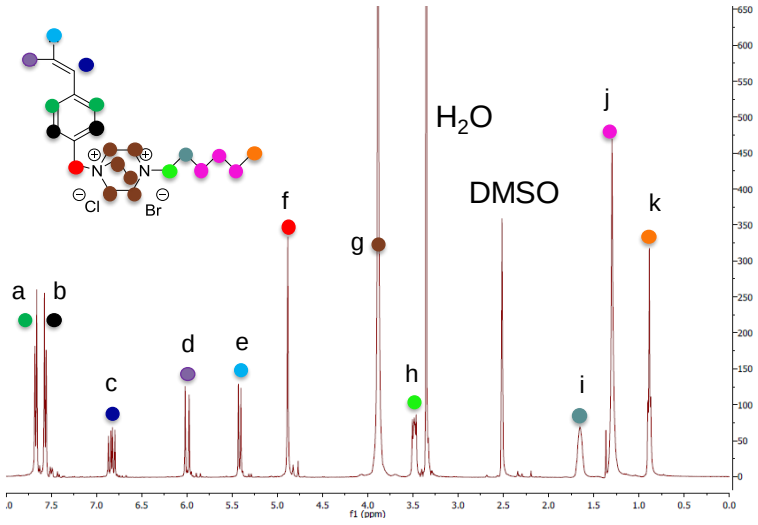

Figure V.1. ^{1}H NMR (400 MHz, d$_6$-DMSO) spectra of DABCO cationic monomer.

In order to know the partitioning of the cationic monomer in water, gravimetric analysis were performed as explained in the previous section. In total 5 different water/BA/MMA ratios were tried and it was determined that in all the mixtures more than 95% of the cationic monomer

was presented in the aqueous phase. Moreover, NMR-H[1] showed negligible signals of DABCO in the monomer phase (BA/MMA), while strong signal was observed in the aqueous phase, which is in agreement with the results obtained gravimetrically. This means that the synthesized monomer is highly hydrophilic. Owing to the similarities with NaSS in terms of hydrophilicity, DABCO was incorporated into BA/MMA following the recipe developed by Sevilay et al.[3].

V.3. References

(1) Zhang, K.; Drummey, K. J.; Moon, N. G.; Chiang, W. D.; Long, T. E. Styrenic DABCO Salt-Containing Monomers for the Synthesis of Novel Charged Polymers. *Polym. Chem.* **2016**, *7* (20), 3370–3374. https://doi.org/10.1039/c6py00426a.

(2) De la Cal, J. C.; Leiza, J. R.; Asua, J. M.; Butte, A.; Storti, G.; Morbidelli, M. *Handbookd of Polymer Reaction Engineering*; Blackwell Science Publ: Oxford (England), 2005.

(3) Bilgin, S.; Tomovska, R.; Asua, J. M. Effect of Ionic Monomer Concentration on Latex and Film Properties for Surfactant-Free High Solids Content Polymer Dispersions. *Eur. Polym. J.* **2017**, *93*, 480–494. https://doi.org/10.1016/j.eurpolymj.2017.06.029.

Appendix VI. Effect of electrostatic interaction on paint performance

VI.1. Use of blends of LQUAT2 cationic resin with anionic latexes as binders

VI.1.1. Clear-coat performance

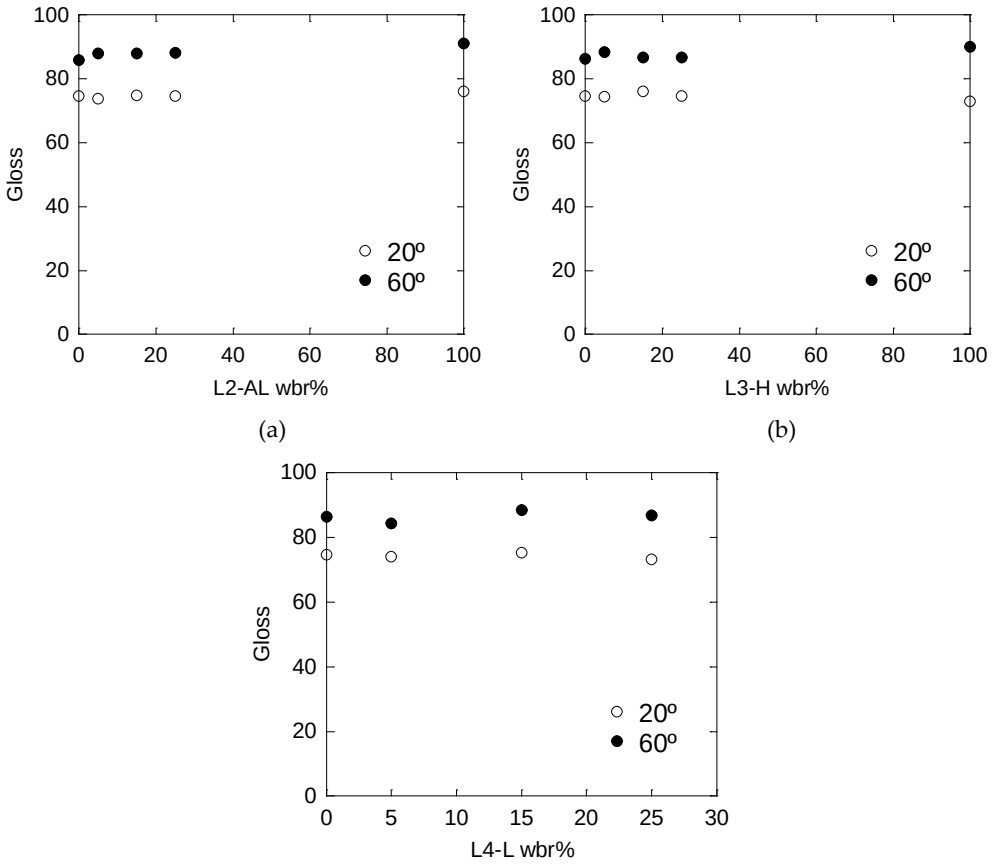

Figure VI.1. Evolution of hardness upon drying time for the references and the (a) Blend 2 (LQUAT2 – L2-AL) and (b) Blend 3 (LQUAT2 – L3-H) and (c) Blend 4 (LQUAT2 – L4-H) containing from 5 to 25 wbr% anionic resin.

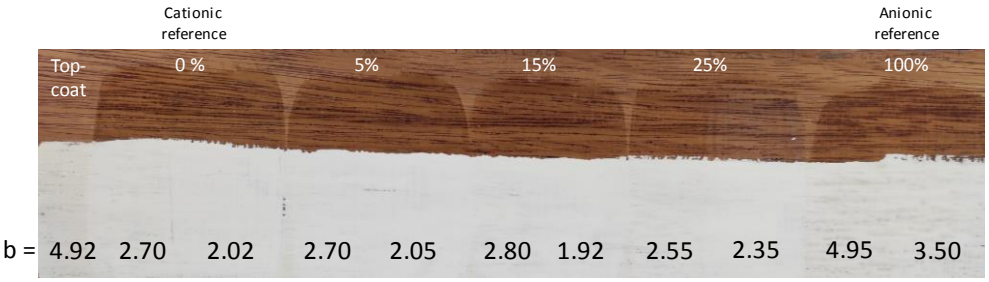

(a)

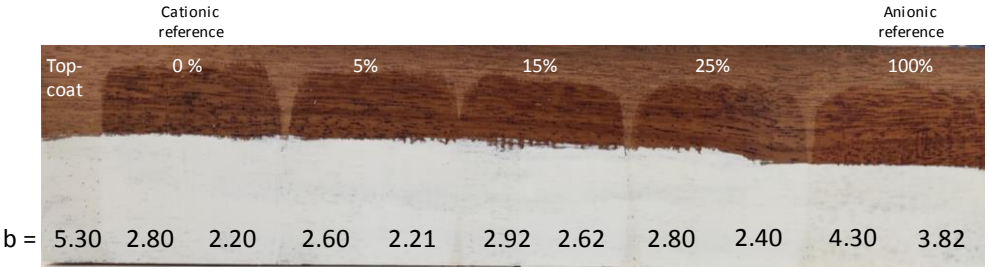

(b)

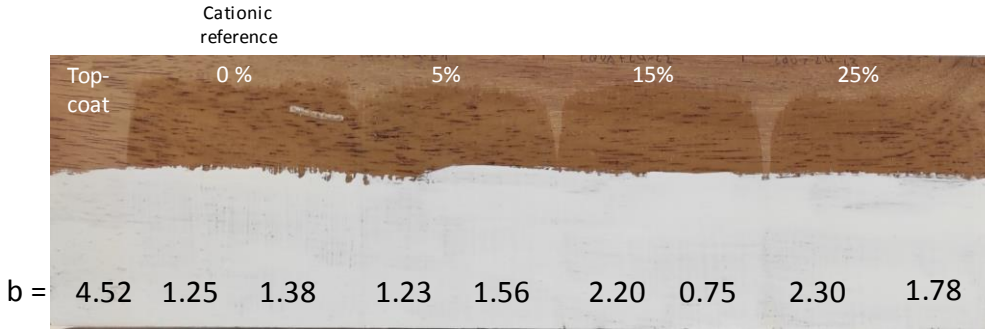

(c)

Figure VI.2. Resistance to tannins test using references and oppositely charged dispersions as binders (from 5 wbr% anionic resin to 25 wbr%). (b) Blend 2 ((LQUAT2 – L2-AL), (c) Blend 3 (LQUAT2 – L3-H) and (d) Blend 3 (LQUAT2 – L4-L).

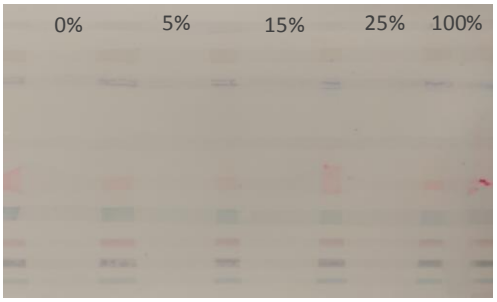

(a)

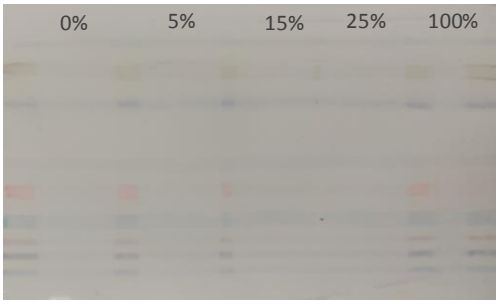

(b)

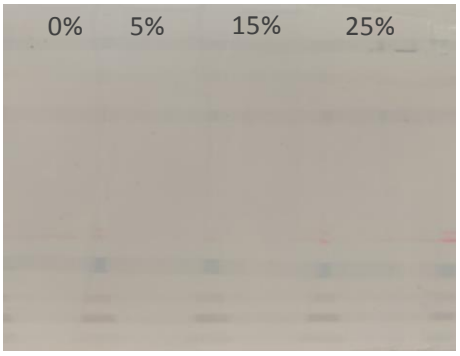

(c)

Figure VI.3. Marker resistance test for the references and the blends (from 5 wbr% anionic resin to 25 wbr%) for (b) Blend 2 ((LQUAT2 – L2-AL), (c) Blend 3 (LQUAT2 – L3-H) and (d) Blend 3 (LQUAT2 – L4-L).

VI.1.2. Pigmented-coat performance

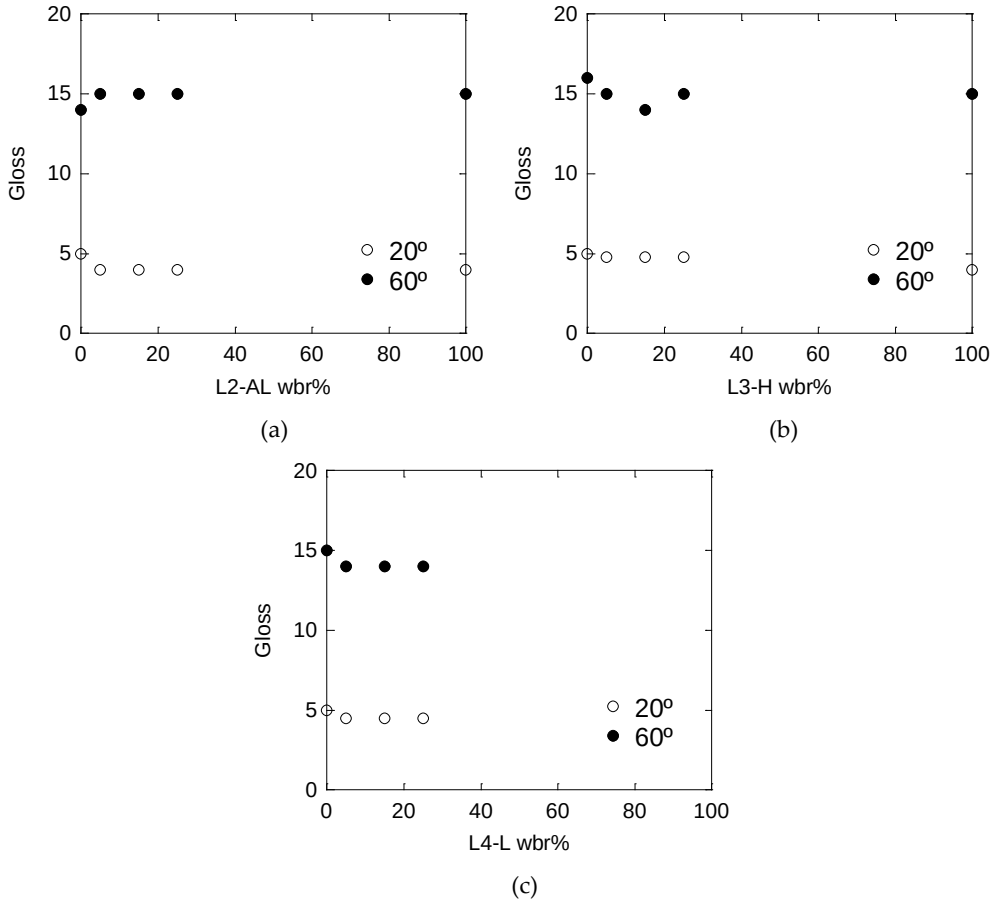

Figure VI.4. Gloss values for the references and the (b) Blend 2 (LQUAT2 – L2-AL), (c) Blend 3 (LQUAT2 – L3-H) and (c) Blend 4 (LQUAT2 – L4-L) containing from 5 to 25 wbar%.

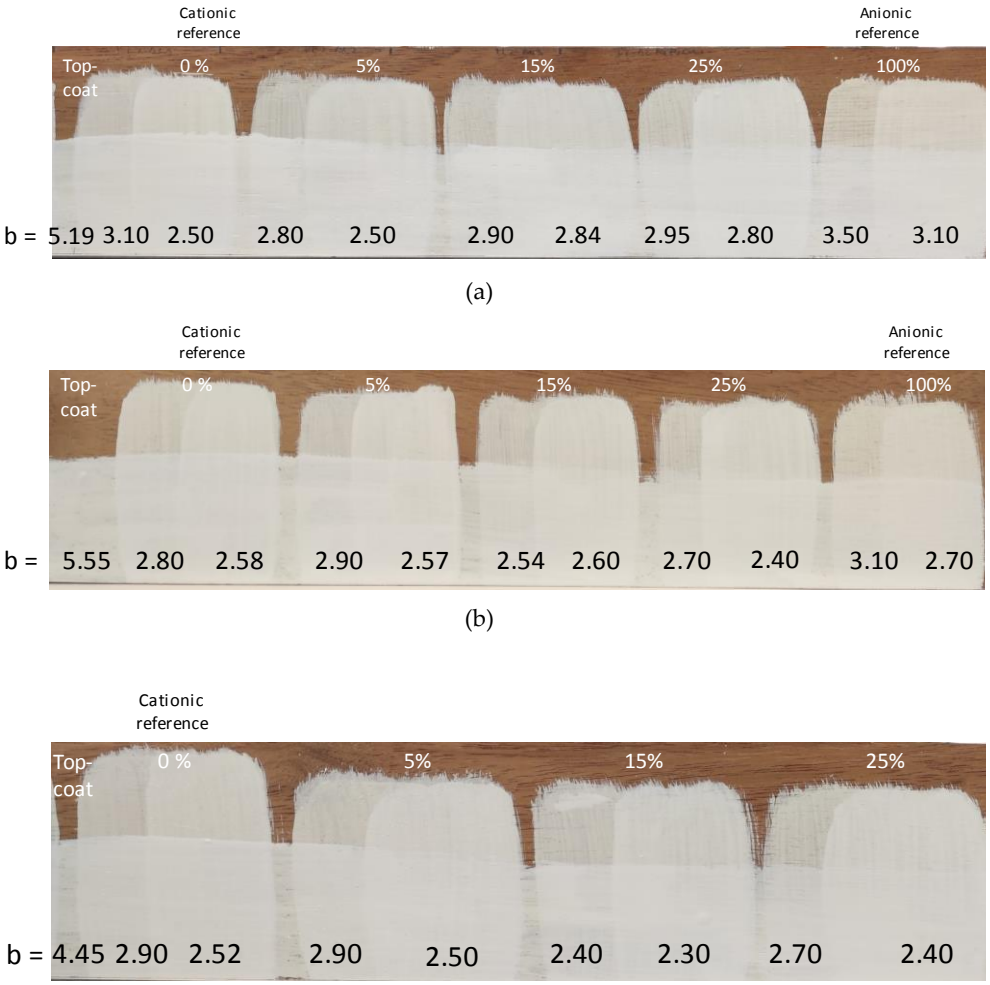

Figure VI.5. Tannin resistance test for the references and the blends (from 5 wbar% to 25 wbar%) for (b) Blend 2 (LQUAT2 – L2-AL), (c) Blend 3 (LQUAT2 – L3-H) and (d) Blend 3 (LQUAT2 – L4-L).

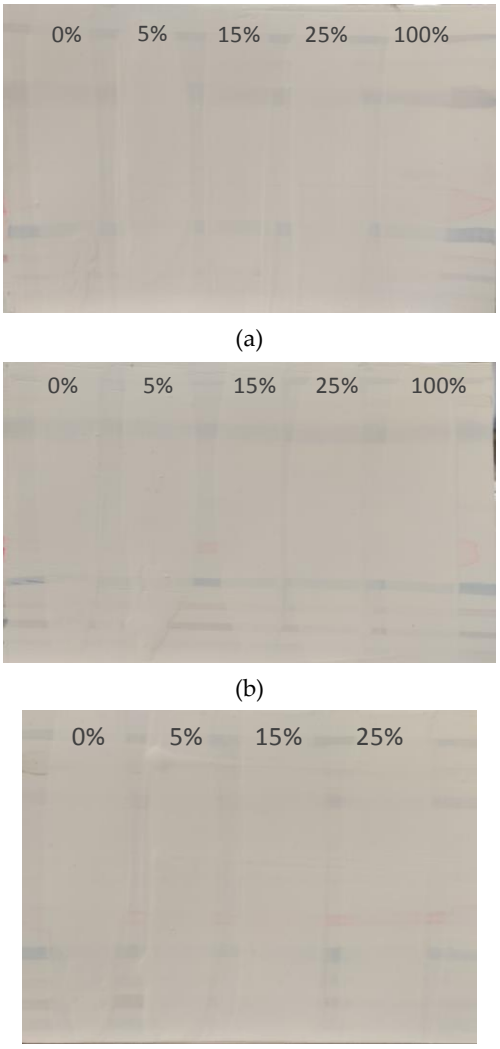

Figure VI.6. Markers bleeding test for the references and the blends containing 5-25 wbar% pigmented-coats for (b) Blend 2 ((LQUAT2 – L2-AL), (c) Blend 3 (LQUAT2 – L3-H) and (d) Blend 3 (LQUAT2 – L4-L).

VI.2. Use of blends of CATD cationic resin with anionic latexes as binders

VI.2.1. Clear-coat performance

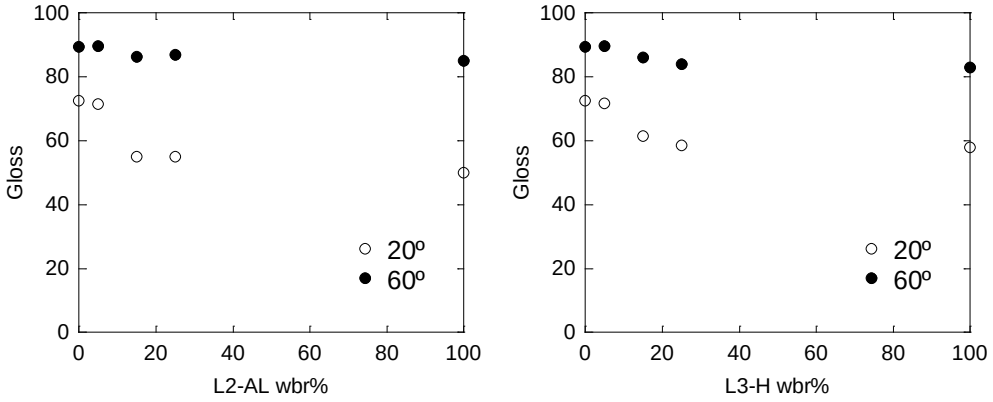

Figure VI.7. Gloss values for the references and the blends containing from 5 to 25 wbar% for (a) Blend 6 (CATD – L2-AL) and (c) Blend 7 (CATD – L3-H).

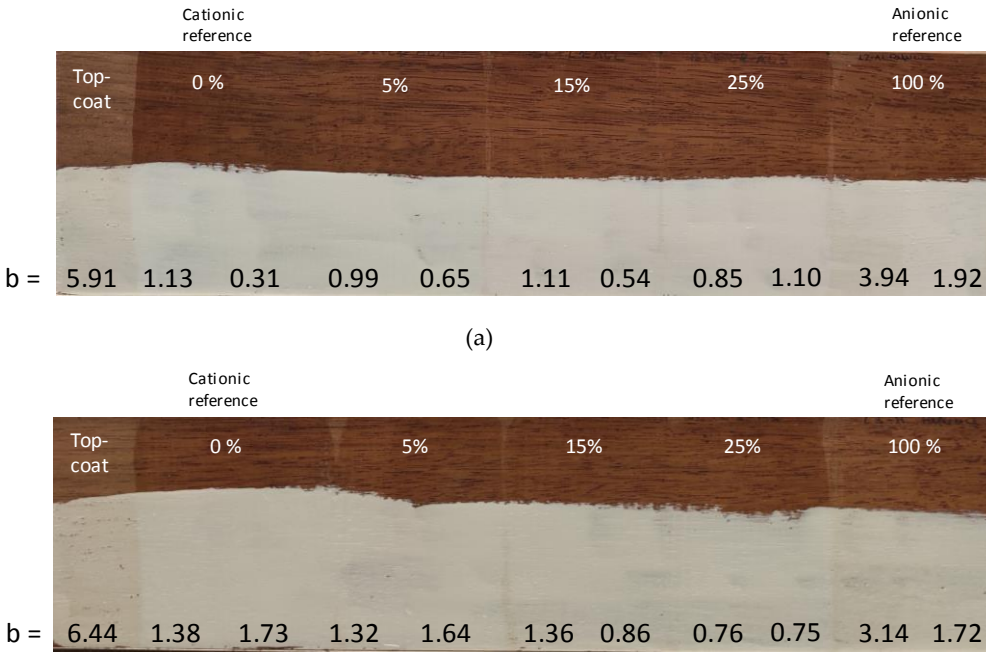

Figure VI.8. Tannin resistance test of the films prepared with the reference resins and the cationic-anionic resin blends for (b) Blend 6 (CATD– L2-AL) and (c) Blend 7 (CATD – L3-H).

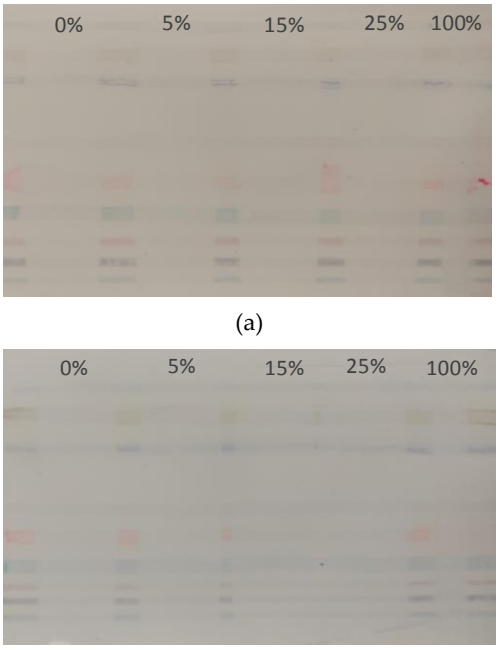

Figure VI.9. Tannin bleeding test for the references and the oppositely charged blends used as binders for (b) Blend 6 (CATD– L2-AL) and (c) Blend 7 (CATD – L3-H).

VI.2.2. Pigmented-coat performance

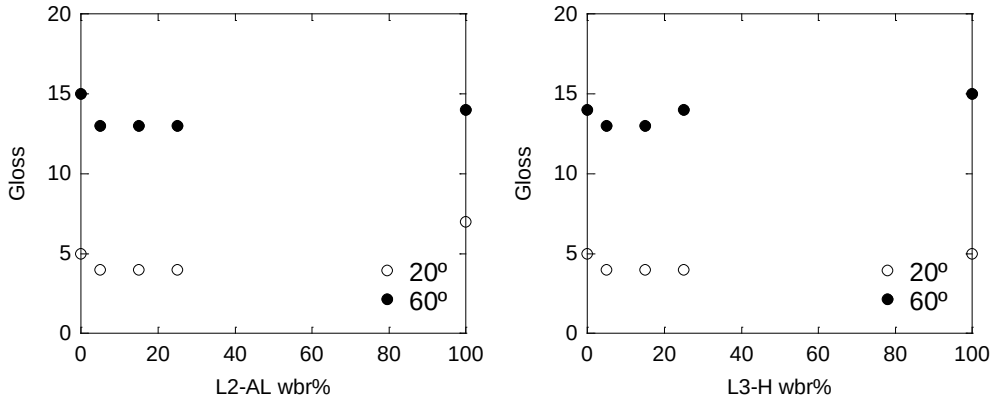

Figure VI.10. Gloss results for the references and the blends (a) Blend 6 (CATD – L2-AL) and (b) Blend 7 (CATD – L3-H) containing from 5 to 25 wbar%.

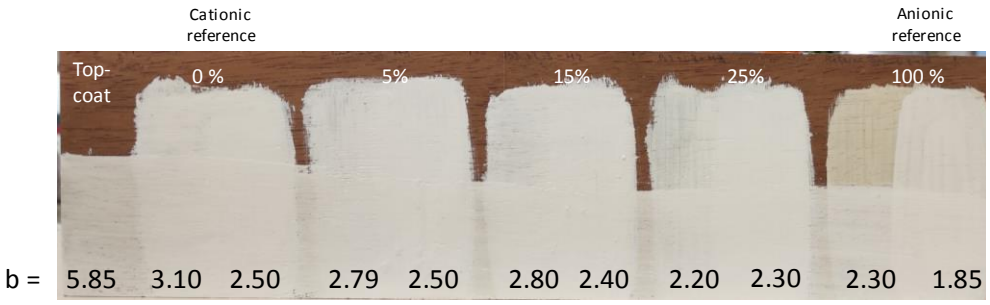

(a)

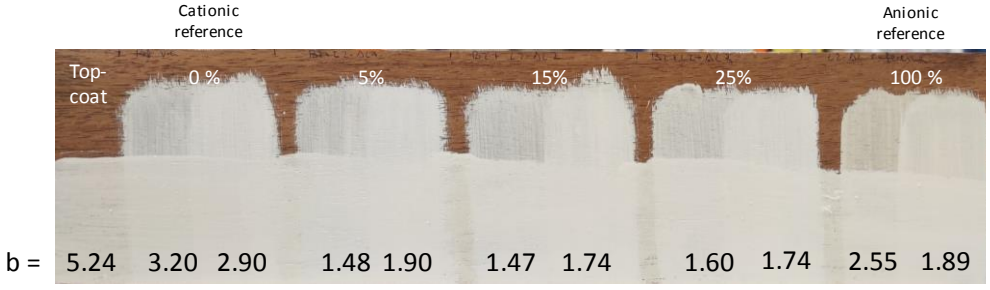

(b)

Figure VI.11. Tannin bleeding test for the references and the blends performed adding from 5 wbar% (weight based anionic resin) to 25 wbar% for (b) Blend 6 (CATD– L2-AL) and (c) Blend 7 (CATD – L3-H).

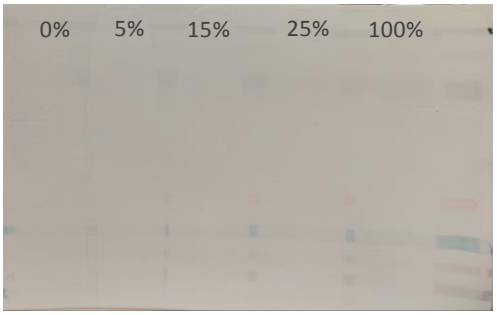

(a)

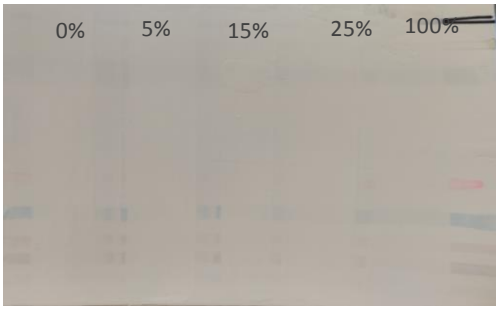

(b)

Figure VI.12. Markers bleeding test for the references and the cationic-anionic resin blends from 5 %wbar (weight based anionic resin) to 25 % for (b) Blend 6 (CATD– L2-AL) and (c) Blend 7 (CATD – L3-H).

List of Publications

Part of this thesis has been published or will be published in a near future. The list of articles that would be issued from this work is as follows (the authors list and/or article title might be changed).

- **Argaiz, M**; Aguirre, M; Tomovska, R, Ionic Inter-Particle Complexation Effect on the Performance of Waterborne Coatings, *Polymers*, **2021**.

Additionally, the scientific works performed in collaborations with the Department of Materials from Loughborough University (Leicestershire, United Kingdom) will be enumerated bellow as well.

- Tinkler, J; Scacchi, A; **Argaiz, M**; Tomovska, R; Archer, A. J; Willcock, H; Martín-Fabiani, I, Role of Particle Interactions on the Assembly of Drying Colloidal Mixtures, *Lagmuir*. Accepted
- Tingler, J. D; Scacchi, A; Kothari, H. R; Tulliver, H; **Argaiz, M**; Archer, A. J; Martín-Fabiani, I, Evaporation-driven Self-assembly of Binary and Ternary Colloidal Polymer Nanocomposites for Abrasion Resistant Applications, *Journal of Colloid & Interface Science*, **2020**, 581, 729-740.

- Dong, Y; **Argaiz, M**; He, B; Tomovska, R; Sun, T; Martín-Fabiani, I, Zinc oxide superstructures in colloidal polymer nanocomposite films: Enhanced antibacterial activity through slow drying, *ACS Applied Polymer Materials*, **2020,** 2 (2), 626-635.

Part of this work have been presented in international and national conferences.

Oral presentations

Argaiz, M.; Aguirre, M. and Tomovska, R., Study of electrostatic interaction between ionically charged polymer particles, **Oral presentation** in the *Graduated Research Seminar and the International Polymer Colloids Group Conference (GRS-IPCG) at Sentosa (*Singapore) June 21-June 28, **2019**

Argaiz, M.; Aguirre, M. and Tomovska, R., Electrostatic interaction for high performance waterborne coatings, **Oral presentation** in the *XV Congress of the GEP*, Huelva (Spain). September 24-September 27, **2018**

Argaiz, M.; Aguirre, M. and Tomovska, R., Ur fasean sintetizatutako estaldura polimerikoen hobetzea elkarrekintza elektrostatikoen bidez, **Oral presentation** in Materialen Zientzia IV Kongresua (MZT), Donostia-San Sebastián (Spain). July 2-July 3, **2018**

Argaiz, M.; Aguirre, M. and Tomovska, R., Electrostatic interaction for high performance waterborne coatings, **Oral presentation** in the *IX and X Industrial Liason Meeting* of POLYMAT, Donostia-San Sebastián (Spain). **2017-2019**

Poster presentations

Argaiz, M.; Aguirre, M. and Tomovska, R., Study of electrostatic interaction between ionically charged polymer particles, **Poster presentation** in the *Graduated Research Seminar and the International Polymer Colloids Group Conference (GRS-IPCG) at Sentosa (*Singapore) June 21-June 28, **2019**

Argaiz, M.; Aguirre, M. and Tomovska, R., Electrostatic interaction for high performance waterborne coatings, **Poster presentation** in the *Functional Polymers Workshop*, Donostia-San-Sebastián (Spain). March 19-March 21, **2018**

Argaiz, M.; Aguirre, M. and Tomovska, R., Ambient temperature non covalent curing of waterborne dispersions: Polyelectrolyte inter-polymer complexation, **Poster presentation** in 6th PhD-Workshop on Polymer Reaction Engineering, Vienna (Austria). September 8-September 10, **2017**